Analytical and Meta-heuristic Methods for Multi-objective Optimal DG Deployment in Distribution Networks Under Normal and Uncertainty Conditions

Submitted in partial fulfillment of the requirements
for the award of the degree of

Doctor of Philosophy

by

B. Kiran Babu

(Roll No. 714119)

Under the Supervision of

Dr. Sydulu Maheswarapu

Professor (HAG)

DEPARTMENT OF ELECTRICAL ENGINEERING

NATIONAL INSTITUTE OF TECHNOLOGY

WARANGAL – 506 004, TELANGANA, INDIA

August - 2020

<u>**APPROVAL SHEET**</u>

This Thesis entitled "**Analytical and Meta-heuristic Methods for Multi-objective Optimal DG Deployment in Distribution Networks Under Normal and Uncertainty Conditions**" by **B. Kiran Babu** is approved for the degree of Doctor of Philosophy

<u>**Examiners**</u>

____

____

<u>**Supervisor**</u>

Dr. Sydulu Maheswarapu
Professor, EED, NITW

<u>**Chairman**</u>

Dr. S. Srinivasa Rao
Professor & Head
Department of Electrical Engineering
NIT Warangal - 506 004 - TS - India

Date: _____________

Dedicated to
My Loving Mother
Late Smt. B. Sujanamma

DEPARTMENT OF ELECTRICAL ENGINEERING
NATIONAL INSTITUTE OF TECHNOLOGY
WARANGAL – 506 004, TELANGANA, INDIA

CERTIFICATE

This is to certify that the dissertation work entitled "**Analytical and Meta-heuristic Methods for Multi-objective Optimal DG Deployment in Distribution Networks Under Normal and Uncertainty Conditions**", which is being submitted by **Mr. B. Kiran Babu** (Roll No: 714119), is a bonafide work submitted to National Institute of Technology, Warangal in partial fulfilment of the requirement for the award of the degree of **Doctor of Philosophy** in Electrical Engineering. To the best of my knowledge, the work incorporated in this thesis has not been submitted elsewhere for the award of any degree.

Dr. Sydulu Maheswarapu
(Supervisor)
Professor
Department of Electrical Engineering
National Institute of Technology
Warangal - 506 004 - TS - India

DECLARATION

This is to certify that the work presented in the thesis entitled "**Analytical and Meta-heuristic Methods for Multi-objective Optimal DG Deployment in Distribution Networks Under Normal and Uncertainty Conditions**" is a bonafide work done by me under the supervision of **Dr. Sydulu Maheswarapu, Professor**, Department of Electrical Engineering, National Institute of Technology, Warangal, India and was not submitted elsewhere for the award of any degree.

I declare that this written submission represents my ideas in my own words and where othersideas or words have been included, I have adequately cited and referenced the original sources. I also declare that I have adhered to all principles of academic honesty and integrity and have not misrepresented or fabricated or falsified any idea/data/fact/source in my submission. I understand that any violation of the above will be a cause for disciplinary action by the Institute and can also evoke penal action from the sources which have thus not been properly cited or from whom proper permission has not been taken when needed.

B. Kiran Babu
(Roll No: 714119)

Date:
Place: NIT Warangal

ACKNOWLEDGEMENTS

It gives me immense pleasure to express my deep sense of gratitude and thanks to my supervisor **Dr. Sydulu Maheswarapu, Professor,** Department of Electrical Engineering, National Institute of Technology Warangal, for his invaluable guidance, support, and suggestions. His knowledge, suggestions, and discussions helped me to become a capable researcher. He has shown me the interesting side of this wonderful and potential research area. His encouragement helped me to overcome the difficulties encountered in my research as well in my life.

I am very much thankful to **Prof. S. Srinivasa Rao**, **Chairman of DSC & Head**, Department of Electrical Engineering for his constant encouragement, support, and cooperation.

I wish to express my sincere thanks to **Prof. N.V. Ramana Rao**, Director, NIT Warangal for his official support and encouragement

I take this privilege to thank all my Doctoral Scrutiny Committee (DSC) members, **Prof. M. Sailaja Kumari**, Department of Electrical Engineering, **Dr. S. Anuradha**, Associate Professor, Department of Electronics and Communication Engineering and **Dr. G. Siva Kumar**, Assistant Professor, Department of Electrical Engineering for their detailed review, constructive suggestions and excellent advice during the progress of this research work. I also express my sincere thanks to former DSC member, **Prof. N.V.S.N. Sarma**, Department of Electronics and Communication Engineering.

I also appreciate the encouragement and support extended by the Teaching, Non-teaching members and fraternity of Department of Electrical Engineering of NIT Warangal. They have always been cooperative and supportive.

I convey my special thanks to contemporary Research Scholars Mr. M. Kalyan Chakravarthi, Dr. K.V. Praveen Kumar, Dr. L. Suresh, Dr. Sachidananda Prasad, Dr. T. Ratna Rahul, Mr. Ankeshwarapu Sunil, Mr. P. Sumanth (NIT Nagpur) and also to Power System Engineering M.Tech Students Mr. Ankur Srivastava (2013), Mr. T. Praveen Kumar (2015), Mr. D. Ananda Babu (2017).

I convey my special thanks to Bro. B. Srinivas Reddy (Vijayawada), Bro. K. John (Hanamkonda), Bro. Allen Lovesh (Vijayawada), Sis. B. Jyothi (Vijayawada), and other spiritual leaders for their encouragement and support during the difficult periods.

I acknowledge my gratitude to Co-scholars at NIT Warangal for their moral support and technical suggestions.

I acknowledge my gratitude to all my teachers and colleagues at various places for supporting and encouraging me to complete the work.

I would like to thank my better-half Smt. B. Premalatha and children Master B. Jedidiah Kiran and Master B. Joash Kiran for their continuous support during the research period. Finally, I render my respect to all my family members (my father Sri. B. Obulapathi, my mother Late. Smt. B. Sujanamma, my brother Dr. B. Arun Babu, my sister-in-law Smt. B. Meramma, my brother Sri. B. Suneel Babu, my niece B. Suji Sharon, my nephew Master B. Gaius, my mother-in-law Smt. P. Arunamma, my brother Sri. B. Suresh Babu and his family members, and my brother Sri. G. Venkata Subbaiah and his family members) for giving me moral support and inspiration. They have motivated and helped me to complete my thesis work successfully.

B. Kiran Babu

ж

CONTENTS

SYNOPSIS

Introduction

Power Distribution Network (PDN) is an essential part of the Electrical systems which delivers the electrical power to the end users without interruptions. Today's modern PDN is more efficient than the earlier one as it has gone through several reforms in terms of physical structure and the adaptation of technology to serve its consumers in a better way. Reforms of physical structure include radial, weakly meshed, and interconnected PDN. However, the technological reforms comprise of Automated distribution systems (use of IT and Data communications), passive to active PDN (Micro grid), and Vehicle to Grid (V2G) and Grid to Vehicle (G2V).

In recent years, across the world, the integration of small-scale power generating units such as Distributed Generation (DG) into the PDN has been increased. This rampant increase of DG penetration is due to inability to meet the unexpected load growth by the conventional power plants, unpredictable fuel prices, deregulation of power systems, an increased per capita consumption of energy, depletion of fossil fuels, policy changes in the power sector, and concern for the environment. According to the report from Frost & Sullivan, the global DG capacity is expected to grow to 1182 GW by 2030 [7]. In contrast to the traditional and conventional centralized generation, Distributed Generation is a modular, decentralized, and more flexible technology that generates and delivers the electrical power to the end users with small generation units to support the power distribution networks. Based on the technology used, DGs are of two categories such as renewable and non-renewable (fossil fuel). Renewable Energy Sources (RES) include Solar Photo Voltaic (SPV), Wind Turbine (WT), Micro-hydro, and Biomass. On the other hand, the non-renewable consists of Micro Turbine (MT), Gas Turbine (GT), IC Engines, and Fuel Cell (FC).

The potential benefits offered by the DG units are reducing the real power losses, minimizing the reactive power losses, enhancement of system reliability and voltage stability, power quality improvement, reduction in investment and operating costs of distribution systems, savings in fossil fuel cost, reduction of emission costs, decreasing the emissions, and natural resources conservation. The improper allocation and sizing of DG units can result in high line losses, voltage instability, poor power quality, and protection degradation.

Optimal Deployment of DGs (ODDGs) is a planning problem where the quality of solutions (optimal location and size of DGs) is more important than the solution time. However, the time incurred for getting the optimal solution cannot be given less importance. The solution time to get the optimum values for ODDG problem depends on the planning horizon, optimizer being used, and an employed Distribution Load Flow (DLF) method. The planning horizon on long-term basis can demand more solution time as it involves the execution of several load flows and update of various optimizer steps and vice-versa. For an optimizer, the steps and time for the execution of these steps remains constant. Therefore, the solution time purely depends on the planning horizon and DLF. The DLF that offers the solution in less time can be adopted to reduce the overall solution time of ODDGs problem. Also, the optimizer which is easy to understand, implement and takes less time to produce the required results can also be selected. Therefore, in this direction, there is need to propose an efficient and fast DLF algorithm and optimizer for optimal deployment problem of DGs.

Multi-Objective Optimization

Optimization can be observed in all spheres of our real life situations from home to industry where the resources (money, man power, use of machinery, time) are optimally utilized to realize the desired outcome. Multi-objective optimization is defined as the problem of finding “a vector of decision variables which satisfies the constraints and optimize a vector function whose elements represent the objective function.” These objective functions are from the mathematical description of relevant performance criteria. Hence, the term ‘optimize’ means finding a solution which offers the values of all objective functions that are acceptable.

The multi-objective problem can be attempted in two ways: Weighted Sum Approach and Pareto Optimal Approach. In the former one, each objective function is made prioritized according to the choice of the system operator. Whereas in the later one, a best-compromised solution can be chosen from the Pareto front.

Motivation

From the literature review, it was observed that the maximum technical, economical, and environmental benefits can be obtained from the optimal deployment of DGs in the Distribution Network. In order to get the aforementioned benefits, several Analytical and Meta-heuristic techniques were proposed in the literature. However, an efficient optimization technique is required to attain global optimum value by incorporating various constraints and covering different load models under normal and uncertainty conditions. Furthermore, the optimal accommodation of DGs is a planning problem which needs the execution of large number of load flows. Therefore, an efficient Distribution Load Flow (DLF) method which works on Radial and Weakly Meshed Distribution Networks and offers solution in less execution time is preferred. The following gaps have been identified as motivation of the thesis.

- Need an efficient and fast Distribution Load Flow (DLF) method that can work for both Radial and Weakly Meshed Distribution Systems under different load models and which can go as effective tool for DG deployment problem.
- Optimal Deployment of DG (ODDG) problem can be attempted for Single objective and Multi-objective cases by proposing a new *Analytical method* to identify the potential location for the placement of DG units.
- Required to propose an analytical method for finding the optimal weights of the individual objectives in the case of Weighted Sum Multi-objective optimization problem.
- Need an effective Nature/Bio-inspired Meta-heuristic algorithm to solve the ODDG problem to attain the global optimum value.
- To account for the uncertainty associated with (i) Residential, Commercial, and Industrial loads, (ii) Wind Turbine power output, and (iii) Solar Photo Voltaic power output while solving the long-term DG deployment problem. Furthermore, required to consider the variability, seasonality, and diversity among the above realistic loads.
- To investigate the effect of *DG degradation* on Optimal placement and sizing of DG units problem for the optimization of technical, economical, and environmental issues.

Objectives of Thesis

The objectives of this thesis include:

- To propose an effective Distribution Load Flow (DLF) algorithm which addresses the solution of load flow problem of Radial and Weakly Meshed Distribution Systems on equal strength and that can be used as a powerful tool for ODDG problem.
- To focus the investigation on (i) minimization of electrical energy losses, (ii) minimization of overall node voltage deviation, (iii) maximization of overall voltage stability margin, and (iv) minimization of Energy Not Served (ENS) by placing the single DG at optimal location identified by the proposed *Branch Loss Bus Injection Index (BLBII) method* (Analytical method).
- To propose an *Analytical Hierarchy Process (AHP)* method to obtain the optimal weights of the individual objectives in the case of "Weighted Sum Multi-objective optimization problem".
- To propose new Meta-heuristic optimization algorithm "*Hybrid Multi-Verse Optimizer (HMVO)*" by combining the best features of *Space Transformation Search* (*STS*) *algorithm* and *Piecewise Linear Chaotic Map* (*PLCM*) *method* to attain the optimal values of the aforementioned objective functions.
- To propose *Multi-objective Jaya Algorithm (MOJA)* for the case of long-term optimal deployment of mixed DGs under *uncertainty environment* and also considering *DG degradation effect*. For this attempt, the following aspects are incorporated.
    - ✓ Two objective functions: (i) Maximization of Distribution Company (DISCO) profit, and (ii) Distribution Network Technical Objectives Improvement.
    - ✓ Use of Self-adaptive Polyhedral Deterministic Uncertainty Set (SPDUS) to account for uncertainty associated with realistic customer load demand, Wind Turbine (WT) power, and Solar Photo Voltaic (SPV) power.
    - ✓ To generate the synthetic data at quarterly-hour (15 minutes) time stamp required for different types of customer loads, WT, and PV resources.

Description of Research Work

In the majority of previous works, the authors have proposed Distribution Load Flow (DLF) methods for radial systems and a few for weakly meshed distribution networks.

Furthermore, the system studies were conducted only on constant power load model. A very few DLFs were tested for algorithm's robustness (different tolerances, X/R ratios, and loadings). Here, the tolerance means, difference of the maximum value of voltages ($|\Delta Vmax|$) between any two successive iterations is less than or equal to 0.0001 p.u. Hence, in order to address these shortfalls, an efficient DLF method have been proposed that works well for both Radial and Weakly meshed systems under different load models. The load models being considered were Constant Power (CP), Constant Current (CI), Constant Impedance (CZ), and combination of these three (CZIP). The applicability of the proposed DLF is tested on IEEE 33-, IEEE 69-, Taiwan Power Company (TPC) 84-, Test system of 136-, and Test system of 874 buses with radial and weakly meshed distribution systems. The results offered by the proposed DLF are compared with Current Injection Method (CIM) and concluded that proposed DLF is time efficient, robust, and divergence free over the CIM method. This part of the work was published in 13th International IEEE India Conference INDICON 2016, 16-18 Dec 2016, at IISc Banglore, India, 10.1109/INDICON.2016.7838992.

Optimal accommodation of DGs have been solved using Analytical methods with different objectives. Most of the literature focused on Single-objective and a very few on Multi-objectives. So, in this research work, new multi-objective function is formulated with: (i) minimization of electrical energy losses, (ii) minimization of overall bus voltage deviation, (iii) maximization of overall voltage stability margin, and (iv) minimization of energy not served (ENS). An *Analytical Hierarchy Process* (*AHP*) technique is proposed for finding the optimal weights for the selected objective functions as the optimization model was attempted in Weighted Sum Approach. DG unit placed at the candidate location can offer the notable improvements to the distribution systems. Hence, new analytical method, *Branch Loss Bus Injection Index* (*BLBII*) is proposed to find the optimal location for the emplacement of DG unit. Two benchmark radial systems such as IEEE 33- and INDIAN 85-bus systems have been used to demonstrate its applicability. The impact of the Single DG operating at unity power factor and 0.9 lagging power factor was analyzed. This work was published in *International Transactions on Electrical Energy Systems* journal (SCIE indexed) with vol. 29, no. 10, October 2019, e12093. https://doi.org/ 10.1002/2050-7038.12093.

Meta-heuristic techniques are more popular to solve the complex combinatorial optimization problems. To date, there are numerous meta-heuristic optimization algorithms available in the literature. The more popular meta-heuristic algorithms are Genetic Algorithm (GA), Particle Swarm Optimization (PSO), Artificial Bee Colony (ABC), Simulated Annealing (SA), Teaching-Learning-Based Optimization (TLBO), *etc*. Recently, Multi-Verse Optimization (MVO) algorithm is proposed to solve the benchmark unimodal, multi-modal, and composite problems. The basic MVO is suffering from *poor convergence* and provides the *solutions near the local optima* when applied to the real life problem like optimal DG accommodation. Hence, a hybrid version of MVO (HMVO) algorithm is proposed by combining the best features of *Space Transformation Search (STS)* and *Piecewise Linear Chaotic Map (PLCM)* algorithms. The results produced by proposed HMVO algorithm are compared with various algorithms and also previously reported works in the literature and the test results found to be superior. This work was published in *IET Generation, Transmission and Distribution* journal (Indexed in SCI) with vol. 13, no. 13, pp. 2673-2685, July 2019, DOI: 10.1049/iet-gtd.2018.5763 and a primitive portion was in *20th National Power Systems Conference (NPSC).*, 14-16 Dec. 2018. Tiruchirappalli, India, DOI: 10.1109/NPSC.2018.8771743.

Furthermore, optimal accommodation of DG units under uncertainty environment have been solved by several authors. To model the randomness of variables (load, WT power, PV output power, load growth, fuel prices), they have used Probability Distribution Function (PDF), Fuzzy approach, Point Estimation Method (PEM), and Self-adaptive Polyhedral Deterministic Uncertainty Set (SPDUS). The PDF method suffers from computational effectiveness, whereas Fuzzy needs the suitable membership function and PEM required to find the solution on interval basis. However, SPDUS needs only the mean and standard deviation of the historical data which can be easily determined from the stored data base. In this thesis, SPDUS have been adopted to create the uncertainty in load of different customers (real and reactive) and resources (Power output of WT and PV) which resulted in an uncertainty pattern that has close relevance with practical data. Furthermore, *DG degradation effect* is also considered in DG placement problem which was ignored by majority of the works in literature. Therefore, new objective function is formulated with: (i) Maximization of DISCO profit and (ii) Distribution Network Technical Objectives Improvement. Multi-objective Jaya Algorithm (MOJA) embedded with Fuzzy Decision Method, is employed to solve the DG planning problem. The potential results of MOJA are compared with Non-dominated Sorting Genetic Algorithm (NSGA-II) and found to be superior. This part of the research work has been communicated to *Energy* journal (SCI Indexed).

LIST OF FIGURES

Figure Title **Page. No**

ж

LIST OF TABLES

ж

ABBREVIATIONS

AE	Analytical Expression
AHP	Analytical Hierarchy Process
AM	Analytical Method
BCS	Best Compromised Solution
BFOA	Bacterial Foraging Optimization Algorithm
BLBII	Branch Loss Bus Injection Index
BLM	Branch Loss Matrix
BOU	Budget of Uncertainty
CABC	Chaotic Artificial Bee Colony
CHP	Combined Heat and Power
CHSFA	Combined Harmony Search Firefly Algorithm
CI	Constant Current
CIM	Current Injection method
CP	Constant Power
CPLSI	Combined Power Loss Sensitivity Index
CSOS	Chaos Symbiotic Organisms Search
CTLBO	Comprehensive Teaching Learning Based Optimization
CZ	Constant Impedance
DE	Diesel Engine
DG	Distributed Generation
DGO	Distributed Generation Owner
DISCOM	Distribution Company
DLF	Distribution Load Flow
DNO	Distribution Network Operator
DS	Data Spread
EIR	Energy Index of Reliability
ENS	Energy Not Served
FA	Fuzzy Approach
FC	Fuel Cell
FDC	Fast Decoupled method

GA	Genetic Algorithm
GA-PSO	Genetic Algorithm-Particle Swarm Optimization
GT	Gas Turbine
HIGA	Hybrid Immune Genetic Algorithm
HMVO	Hybrid Multi-Verse Optimizer
ICA	Imperialistic Competitive Algorithm
LIF	Load Index Factor
LIFM	Load Index Factor Matrix
LSF	Loss Sensitivity Factor
MCS	Monte Carlo Simulation
MOJA	Multi-objective Jaya Algorithm
MOO	Multi-Objective Optimization
MOODDG	Multi-Objective Optimal Deployment of Distribution Generation
MOTA	Multi-Objective Taguchi Approach
MT	Micro Turbine
NPDF	Normal Probability Distribution Function
NR	Newton-Raphson
NSGA-II	Non-dominated Sorting Genetic Algorithm-II
OCDE	Oppositional based Chaotic Differential Evaluation
ODDG	Optimal Deployment of Distributed Generation
PDN	Power Distribution Network
PEM	Point Estimation Method
PEV	Plug-in Electric Vehicle
PLCM	Piecewise Linear Chaotic Map
PPF	Probabilistic Power Flow
PSI	Power Stability Index
PSO	Particle Swarm Optimization
QOTLBO	Quasi-Oppositional Teaching Learning Based Optimization
RDN	Radial Distribution Network
RES	Renewable Energy Sources
RO	Robust Optimization
SA	Simulated Annealing
ShBAT	Shuffled Bat Algorithm

SPDUS	Self-adaptive Polyhedral Deterministic Uncertainty Set
SPV	Solar Photo Voltaic
SSA	Salp Swarm Algorithm
STS	Space Transformation Search
TDR	Travelling Distance Rate
TLBO	Teaching Learning Based Optimization
TOPSIS	Technique for Order of Preference by Similarity to Ideal Solution
TPC	Taiwan Power Company
VSI	Voltage Stability Index
VSM	Voltage Stability Margin
WEP	Wormhole Existence Probability
WMDN	Weakly Meshed Distribution Network
WOA	Whale Optimization Algorithm
WPDF	Weibull Probability Distribution Function
WSA	Weighted Sum Approach
WT	Wind Turbine

CHAPTER-1

Introduction

1.1 Introduction to Power Distribution Network

Power Distribution Network (PDN) typically starts from the distribution substation that is fed by one or more sub-transmission lines and ends at the meter terminal of the consumer. In other words, PDN is generally low voltage network where power flows in one direction only, from the substation to the consumer terminals. The unidirectional power flow, in addition to the extremely low statistical failures rate of equipment at low voltage levels, led various authorities throughout the world to adopt radial configuration for their distribution networks [1].

Radial networks have some advantages over the meshed networks such as lower short circuit currents and simpler switching and protecting equipment. On the other hand, the radial structure provides lower overall reliability. Therefore, to use the benefits of the radial structure, and at the same time to overcome the difficulties, distribution systems are planned and built as weakly meshed networks, but operated as radial networks.

Today's modern PDN is more efficient than the earlier one as it has gone through several reforms in terms of physical structure and the adaptation of technology to serve its consumers in a better way. Reforms of physical structure include radial, weakly meshed, and interconnected PDN. However, the technological reforms comprise of Automated distribution systems (use of IT and Data communications), passive to active PDN (Micro grid), and Vehicle to Grid (V2G) and Grid to Vehicle (G2V).

To supply the quality and uninterrupted power to the customers of Distribution Network, it should be continuously monitored, controlled, and alarmed. This involves various system studies such as distribution load flows, stability studies, security studies, short circuit studies, and state estimation studies, *etc*. Quality of supply in the context of distribution system refers to the excellence in its performance in

(i) providing continuous power supply at specified voltage and frequency.

(ii) detection and isolation of faults and restoration of service.

(iii) maintaining voltage profile and load transfer between the feeders for relief of over load.

(iv) capacitor switching on-off for voltage improvement (reactive power control).

(v) minimization of technical and commercial losses.

(vi) energy auditing and effective utilization of resources.

(vii) demand side management.

1.2 Distribution Load Flow

The operation and planning studies of a PDN require a steady state condition of the system for various load demands. The steady state operating condition of a system can be obtained from the load flow solution. Therefore, Distribution Load Flow (DLF) is a steady state solution of Distribution networks that finds the system states such as voltage magnitude and phase angle at all the buses under normal and abnormal conditions subjected to different loading scenarios, contingencies, tap changing conditions, and other situations [2].

1.2.1 Need for an effective Distribution Load Flow Method

In reality, most of the distribution networks are Radial in nature, having low reactance to resistance ratio, ill conditioned network, unbalanced operation, and suffers from the low voltage problem. The conventional load flow methods such as Newton-Raphson (NR) [3] and Fast Decoupled method (FDC) [4] have shown poor convergence due to low X/R ratio and radial characteristics of Distribution Network. However, the improved versions of these methods are developed in [5]-[6] for the system studies of the distribution networks but they are not efficient and effective. Therefore, researchers have given the special attention to develop effective load flow methods for Distribution Systems.

1.3 Distributed Generation

In recent years, across the world, the integration of small-scale power generating units such as Distributed Generation (DG) into the PDN has been increased. This rampant increase of DG penetration is due to inability to meet the unexpected load growth by the conventional power plants, enhanced system security, reduced overall costs, increased utilization of transmission and distribution network capacity, unpredictable fuel prices, deregulation of power systems, an increased per capita consumption of energy, depletion of fossil fuels, policy changes in the power sector, and concern for the environment. According to the report from Frost & Sullivan, the global DG capacity is expected to grow to 1182 GW by 2030 [7].

In contrast to the traditional and conventional centralized generation, Distributed Generation (DG) is a modular, decentralized, and more flexible technology that directly connected to the PDN where the generated power from the DG unit is consumed by the end users locally [8].

Based on the technology used, DGs are of two categories such as renewable and non-renewable (fossil fuel) energy sources. Renewable energy sources include Solar Photo Voltaic (SPV), Wind Turbine (WT), Micro-hydro, and Biomass. On the other hand, the non-renewable consists of Micro Turbine (MT), Gas Turbine (GT), IC Engines, and Fuel Cell (FC).

1.3.1 Optimal Deployment of Distributed Generation

The placement of DG units in a Distribution Systems offers several advantages. However, the amount of improvement depends on the size and location of the DG units. Integrating DG units may lead to negative impacts on a Distribution System, especially for large scale installations if they are not optimally placed. For instance, DG units may result in high voltage causing currents that exceed the line's thermal limits, harmonic problems, noticeable voltage flicker, and instability of the voltage profile of some of the customers. In addition, the bidirectional power flows can lead to voltage profile fluctuation and change the short circuit levels.

The installation of DG units is becoming more prominent in distribution systems due to their overall positive impacts on power networks. Some major advantages of integrated DG units include reduction of real power losses, minimization of reactive power losses, enhancement of system reliability and voltage stability, power quality improvement, reduction in investment and operating costs of distribution systems, savings in fossil fuel cost, reduction of emission costs, decreasing the gas emissions, and natural resources conservation. Because of these benefits, utility companies have started to change their electric infrastructure to adapt to the introduction of DG units in their Distribution Networks. In order to maximize the benefits, solution for DG deployment should be obtained using optimization methods, since installing DG units at non-optimal places and of inappropriate sizes may cause an increase in system power losses and costs. Moreover, installation of DG units is not straightforward, and thus the placement and sizing of DG units should be addressed carefully. Investigation of this optimization problem act as major motivation of the present search work.

1.4 Multi-Objective Optimization

Optimization can be observed in all spheres of our real life situations from home to industry where the resources (money, man power, use of machinery, time) are optimally utilized to realize the desired outcome. Multi-Objective Optimization (MOO) is defined as the problem of finding “a vector of decision variables which satisfies the constraints and optimize a vector function whose elements represent the objective function”. These objective functions are from the mathematical description of relevant performance criteria. Hence, the term ‘optimize’ means finding a solution which offers the values of all objective functions that are acceptable.

In general, the Multi-objective optimization problem can be represented as follows:

$$\left.\begin{array}{lll} \text{minimize} \quad f_i(x), & & (i=1,2,\ldots\ldots M), \\ \text{subjected} \quad \text{to} & & \\ & h_j(x) = 0, & (j=1,2,\ldots\ldots J), \\ & g_k(x) \le 0, & (k=1,2,\ldots\ldots K), \end{array}\right\} \tag{1.1}$$

where $f_i(x)$, $h_i(x)$, and $g_k(x)$ are the set of objective functions, equality and inequality constraints, respectively of the design vector

$$x = (x_1, x_2, \ldots\ldots\ldots x_D)^T \tag{1.2}$$

Here the components x_i of x are called *design* or *decision variables*, and they can be real continuous, discrete, or a mix of these two.

The multi-objective problem can be attempted in two ways: Weighted Sum Approach and Pareto Optimal Approach.

1.4.1 Weighted Sum Approach

In the case of Weighted Sum Approach (WSA), each objective function is made prioritized with real value according to the choice of the system operator or decision maker and then, they are aggregated to form a Single objective function. This formulated Single objective optimization function is solved to get the optimal solution subjected to the set of constraints. The mathematical form of the Weighted Sum Approach to the optimization problem is given as

$$\left.\begin{aligned} &\text{minimize} \quad \sum_{i=1}^{M} \Psi_i f_i(x), \qquad (i = 1,2,\ldots\ldots M), \\ &\text{subjected to} \\ &\qquad h_j(x) = 0, \qquad (j = 1,2,\ldots\ldots J), \\ &\qquad g_k(x) \le 0, \qquad (k = 1,2,\ldots\ldots K), \end{aligned}\right\} \tag{1.3}$$

where the weights $\Psi_1,\ \Psi_2,\ \ldots.\ \Psi_M$ are non-negative numbers with $\Psi_1 + \Psi_2 + \ldots. + \Psi_M = 1$.

1.4.2 Pareto Optimal Method

When the objective functions are in conflict and there is no optimal solution that simultaneously optimize all the objective functions, the Pareto Optimal Method can be used to solve the multi-objective optimization problem. Once the multi-objective optimization problem is solved, it offers a set of solutions which are all optimal. But user needs only one final solution. Higher level information is required to choose one best solution from the set of near optimal solutions. Often such higher level information is non-technical, qualitative, empirical, and experience driven. Therefore, in multi-objective optimization, an idealistic effort must be made in finding the set of trade-off optimal solutions by considering all objectives simultaneously. For this case, a concept of *Pareto optimal solution* is employed. The *pareto optimal solution* means that it is impossible to improve any one objective function without sacrificing on one or more of the other objective functions. The definition of *Pareto optimal solution* is given as

Pareto Optimal Solution: A feasible solution x^* is said to be a pareto solution if there is no feasible solution *x* such that

$$\left.\begin{array}{ll} f_i(x) \geq f_i(x^*), & i = 1,2,\ldots.M \quad and \\ f_j(x) > f_j(x^*) & for \quad at \quad least \quad one \quad index \quad j \end{array}\right\} \tag{1.4}$$

Pareto Optimal Set: The entire set of pareto optimal solutions is called a Pareto optimal set.

1.5 Literature Survey

Optimal Deployment of DGs (ODDGs) is a planning problem where the quality of solutions (optimal location and size of DGs) is more important than the solution time. However, the time incurred for getting the optimal solution cannot be given less importance. The solution time to get the optimum values for ODDG problem depends on the planning horizon, optimizer being used, and an employed Distribution Load Flow (DLF) method. The planning horizon on long-term basis can demand more solution time as it involves the execution of several load flows and update of various optimizer steps and vice-versa. For an optimizer, the steps and time for the execution of these steps remains constant. Therefore, the solution time purely depends on the planning horizon and DLF. The DLF that offers the solution in less time can be adopted to reduce the overall solution time of ODDGs problem. Also, the optimizer which is easy to understand, implement, and takes less time to produce the required results can also be selected. Therefore, in this direction, there is need to propose an efficient and fast DLF algorithm and optimizer for optimal deployment of DGs.

1.5.1 Distribution Load Flow Methods

The planning and efficient operation of Power Distribution Network (PDN) highly depends on the load flows, VAR control, and other preventive maintenance procedures which are taken against the faults and contingencies. Usually, load flow study is conducted to know the current status of the system and make appropriate decision for smother operation of the Distribution network. Several load flow methods have been reported in the literature to address the distribution system studies.

Aravindhababu, Ganapathy and Nayar [9] have introduced a method for Radial Distribution Systems. The proposed method utilises the network topology to construct the constant branch-to-node matrix (binary). The constructed matrix was a *sparse upper* *triangular matrix*, that can be used directly to determine the node voltages. However, the proposed method needs the proper nomenclature for the branches and nodes of a selected Distribution Network. Improper nomenclature leads to erroneous results and divergence problem especially for a bigger size system.

Mekhamer *et al.* [10] have delineated a load flow method for Radial Distribution Networks, which was of simple in nature, accurate, fast, reliable, and having low storage requirements. However, the proposed method was implemented only for Constant Power (CP) load model and is not attempted for other load models.

Ranjan and Das have proposed an iterative DLF for Radial Distribution Systems. The method was quite simple and efficient, which needs to solve a single node voltage equation related to receiving end of the each line. However, the authors have not mentioned any procedure for the calculation of phase angle of voltage magnitude [11].

Chang, Chu and Wang [12] have presented a Backward-Forward Sweep Power flow method for Radial Distributed Network. In backward sweep, Kirchhoff's Current laws and Kirchhoff's Voltage laws were used to determine the upstream bus voltages and a linear proportional principle was adapted to find the ratio of real and imaginary components of the specified voltage to the calculated voltage at substation node. In forward sweep, this calculated ratio will be used to update the node voltages of the network. The demerit of this method was that linear proportional principle is applicable only to the resistive network.

Ghosh and Sherpa [13] have introduced a method for Radial Distribution Networks. In this method, two arrays which of two dimensional in nature are used to store the information of all feeders, laterals, and sub-laterals. In the *first array*, the information related to node number of each feeder, lateral, and sub-lateral was stored, whereas in the *second array* their branch number was stored. This stored information was used to determine the effective real and reactive powers and the node voltages in *forward sweep*. The proposed method also works for the system having improper numbering for its nodes and branches but needs carefulness while storing the data. The method was also tested for different load models such as Constant Impedance (CZ), Constant Current (CI), Composite, and Exponential along with the commonly used Constant Power (CP) load model.

In [14], Nagaraju *et al*. have formulated the load flow method for Radial Network. The authors have developed a new expression to determine the voltage magnitude at each bus of the system. The performance of the method has been invested on realistic loads like residential, commercial, and industrial along with the Constant Power (CP) load model. Furthermore, the effect of load growth has also been investigated to address the system expansion problem. The applicability of this method was not tested for Weakly Meshed Distribution Networks.

Abul'Wafa [15] has proposed a load flow method for Radial Distribution Systems. In this method, two matrices, *bus-injection to branch-current* (*BIBC*) and *branch-current to bus-voltage* (*BCBV*) were formed based on the topology of the network. Multiplication of these matrices gives the node voltages. The proposed method was tested for different load models, loading conditions, tolerance levels, and X/R ratio values to validate its convergence capability. However, to form the BIBC and BCBV matrices, the receiving end nodes of the selected system should be arranged in the ascending order.

Singh and Ghose [16] have introduced two methods, Current flow based forward/backward sweep method and Power flow based forward/backward sweep method for Radial Distribution Systems. *Current flow method*: in backward step - initially a matrix with load currents and then branch currents are determined. In forward step, node voltages are determined. *Power flow based method*: in backward sweep, the matrix with each element representing the summation of total load at a node and the loss taking place ahead of that node and then convert them into branch power flows. The node voltages are determined in forward step. Both the methods require large memory to store the elements of matrices. In fact, they were sparse matrices.

Murty, Teja and Kumar [17] have introduced the similar kind of load flow methods for Radial Distribution Network as reported in [16] without formation of the load current and load power matrices. As a result, the proposed method takes less memory. However, the receiving end nodes of the selected system should be arranged in the ascending order to carry out the load flow study.

In [18], Garcia *et al.* have proposed a three phase-load flow method for unbalanced distribution systems. The method was formulated based on the current injection equations that are expressed in rectangular coordinates and was solved using NR method. The method can also be extended for weakly meshed distribution systems. However, this method was investigated only on Constant Power (CP) and Constant Impedance (CZ) load models.

Teng [19] has carried out the distribution system studies by proposing a direct method. In the proposed method, two matrices such as bus-injection to branch-current matrix (BIBC) and branch-current to bus-voltage matrix (BCBV) has been developed using network topology and then these matrices were multiplied to get the required load flow solution. The method can work effectively for both radial and meshed distribution networks. However, the proposed method requires the large memory to store the elements of the resultant matrix. Furthermore, it was validated only on the CP load model.

Chang *et al*. [20] have presented an efficient distribution load flow method for weakly meshed distributed network. Compensation method has been used to break the meshes. During the backward sweep, branch current and upstream voltages are calculated, and then a linear proportional principle was applied to calculate the ratio of specified bus voltage to calculated bus voltage. Then, this ratio was used to find the updated voltages in forward sweep. Though the method can work effectively even for large size distribution systems but demands more CPU time as it involves the decomposition process.

Teja and Kumar [21] have suggested a new and efficient Distribution Load flow method for solving the load flow problem of Radial and Meshed distribution systems. The method uses the network topology, basic circuit laws, and power summation technique to solve the load flows of the distribution system. The method works equally well for both radial and meshed systems. However, for weakly meshed distribution systems, loop impedance matrix is required to get the solution. Formation of the loop impedance matrix for the bigger size distribution system is difficult if the system has more laterals.

1.5.2 Optimal DG Deployment using Analytical Methods

A bibliographical survey on Optimal integration and planning of renewable distributed generation in the power distribution networks using analytical techniques was summarized by Ehsan and Yang [22]. In case of Analytical methods, an Analytical Expression (AE) is developed to find either DG location or DG size, and then using a search technique the corresponding optimal DG size or optimal location will be identified.

It means, if the expressions are developed to find the optimal DG location, then an effective search technique will be employed to find the optimal DG size and vice-versa.

Acharya, Mahat and Mithulananthan [23] have proposed an Analytical Expression (AE) for finding the size of DG unit to be placed at each bus to minimize the real power losses of the Radial Distribution Network (RDN). The objective function was minimization of active power losses and these losses were determined by placing the DG unit one at a time at each bus and then final values of optimal location and size of DG are identified. The method was simple, but needs the inversion of Y_{bus} to calculate the coefficients used in AE.

Aman *et al*. [24] have introduced an analytical expression for Power Stability Index (PSI) to identify the most voltage sensitive bus (candidate location for DG unit). A heuristic method has been employed to find the optimal size of DG unit by minimizing the real power losses of the system. The impact of the DG unit on voltage stability has also been investigated for different loading conditions by considering constant power load model. However, in this paper, the authors have analyzed the impact of DGs operating at unity power factor mode only, but not attempted the other power factor modes.

Murthy and Kumar [25] have suggested a method for the reduction of power losses in Radial Distribution Systems. A Combined Power Loss Sensitivity Index (CPLSI) method has been proposed to identify the appropriate location for DG unit placement. The CPLSI index was formed by combining the real power loss index and reactive power loss index. A heuristic approach has been used to find the optimal DG size. The proposed method provides the optimal results. However, it has failed in identifying the optimal DG location for the well known standard test system which is of IEEE 33-bus.

In [26], an Improved Analytical (IA) method has been presented to minimize the real power losses. AEs related to the size of different types of DG units are developed using Elgerd's Loss Formula (ELF). The authors concluded that the proposed method offers reduced losses as compared to Loss Sensitivity Factor (LSF) and Exhaustive Load Flow (ELF) methods. However, the solution time of the proposed method is high as it needs the inversion of Y_{bus}.

Hung, Mithulananthan and Bansal [27] have proposed three AEs based on (i) Elgerd's loss formula (ii) Branch current loss formula, and (iii) Branch power loss formula to find DG unit size. The energy loss minimization was taken as an objective function. DG units such as Biomass, Photo Voltaic (PV), and Wind Turbine (WT) with time varying power output nature have been considered. However, the uncertainty aspect in the power output of PV and WT was ignored. Furthermore, simple 24 hour load pattern has been used to represent one full year.

Murthy and Kumar [28] have developed an expression for Voltage Stability Index (VSI) to find optimal DG location [24]. A heuristic method has been employed to find the optimal size of DG unit by minimizing the real power losses of the system. Furthermore, investigation has also been carried out on size and location of DG unit by considering the yearly load growth. In the formulation of VSI, the load demand at i^{th}-bus was considered instead of effective load which may result in non-optimal DG locations.

Viral and Khatod [29] have suggested a new AE for the DG unit to be placed at each bus, based on the concept of *minimization of loss associated with active and reactive component of branch currents*. The aim of this investigation was the minimization of real power losses in the distribution system. The demerit of the proposed method was that it needs an additional binary matrix to find the size of the DG unit. The size of this binary matrix relies on the number of DG units to be deployed and the number of branches of the selected distribution network. The elements of the binary matrix were determined as follows: unitary value for all the lines connected between the substation bus and the bus where the DG unit was placed, else zeros. Therefore, for large size system with less number of DGs (economic point of view), the majority of the elements of binary matrix are zeros. This will result in huge memory requirement for storing the zero elements, even the role played by them is insignificant.

Kaur, Kumbhar and Sharma [30] have studied the impact of single and multiple DG units on Radial Distribution Systems in reducing the real power losses. The authors have solved the DG placement and sizing problem in two phases, namely Siting Planning Model (SPM) and Capacity Planning Model (CPM). The SPM model selects the candidate buses based on Combined Loss Sensitivity (CLS). In CPM, optimal locations and sizes are obtained by integrating Sequential Quadratic Programming (SQP) and Branch and Bound (BAB) algorithm. The authors of this paper, have investigated an Optimal Deployment of DG (ODDG) problem only for Single objective cases, but not attempted for the multi-objective case.

Elsaiah, Benidris and Mitra [31] have introduced an analytical method for optimal placement and sizing of DG units on power distribution systems for real power loss reduction. The proposed method was based on the new load flow formulation, and was a non-iterative method. A priority list based on real power loss sensitivity factors was used to determine the optimal DG locations. Sensitivity analysis has been performed to estimate the optimal size and power factor of the candidate DG units. Several assumptions have been made while developing the new load flow method that may offer an inaccurate solution for the DG placement problem.

In all the above cases of the literature review, single objective only has been considered to solve the optimal placement and sizing of DG problem. However, in [32]-[33], a multi-objective function consisting of real and reactive power loss minimization have been solved based on the Weighted Sum Approach. They developed an AE for DG size with the inclusion of adaptive weights of the objective functions. Furthermore, in [34], an additional objective function such as minimization of node voltage deviation has been considered along with the objectives of [33] for the optimal accommodation of PV unit.

Analytical techniques offers the advantage of short computing time for smaller size systems. However, when the problem size becomes large and complex, the assumptions used in order to simplify the problem may override the accuracy of the solution.

1.5.3 Optimal DG Deployment using Meta-heuristic Methods

Meta-heuristic methods initiate the optimization process with a set of random candidate solutions and improve them over the course of iterations. To solve the multi-objective Optimal Deployment of Distributed Generation (ODDG) problem of the power distribution networks, several authors have proposed numerous Meta-heuristic 'or' improved versions of Meta-heuristic/Hybrid meta-heuristic techniques. Meta-heuristic methods are capable to solve the complex real world problems where most of the Analytical methods have failed. A bibliographical survey on optimal sizing and siting techniques for distributed generation in distribution systems is summarized in [35]-[36].

Satish, Vishal and Barjeev [37] have proposed Particle Swarm Optimization (PSO) algorithm for the minimization of real power losses in Distribution systems. The impact of different types of DG units such as Type-I (injects only real power), Type-II (injects only reactive power), and Type-III (injects both real and reactive powers) have been investigated on the selected distribution systems by considering only the Constant Power (CP) load model. The investigation revealed that the optimal placement of mix of Type-I and Type-II DGs offers more loss reduction as compared to the individual DG Types. However, in the proposed work, only Single objective case was attempted, but not addressed the case of multi-objective optimization.

Shukla *et al*. [38] have suggested a Genetic Algorithm along with Loss Sensitivity Factors (GA-LSF) approach to solve the optimal deployment DG problem aiming at the minimization of real power losses. LSF and GA were used to find the optimal location and optimal size of multiple DG units, respectively. The authors have concluded that the proposed GA-LSF method took the less CPU time to converge due to the incorporation of LSF technique without sacrificing the solution accuracy. In this work, the investigation was conducted on Constant Power (CP) load model assumed with three step variation. Furthermore, the examination was carried out with the incorporation of DG units operating at unity power factor mode only.

The authors of [37]-[38] have focused only on the minimization of single objective function (real power loss). In practice, Distribution companies have to optimize more than one objective function. Therefore, a bi-objective function consisting of minimization of real power loss and voltage profile improvement has been attempted by Nekooei *et al.* [39] to solve the ODDG problem using an Improved Harmony Search algorithm. Furthermore, a *max-min* approach was merged with the proposed Improved Harmony Search Algorithm to select the best compromised solution from the Pareto front of the multi-objective function. In this work, the uncertainty associated with the load demand and DG units was not accounted in the problem formulation.

Bahram *et al*. [40] have presented a modified Imperialistic Competitive Algorithm (ICA) for the minimization of losses and maximization of overall voltage stability index. A constant power load model that increases with the step size of 1%, between 50% - 150% of the base load demand, has been considered for the investigation purpose. Based on the test results, a general expression has been developed with load variation component for finding the optimal DG size. The proposed methodology has addressed the future expansion of DG problem without considering the seasonality in the load demand.

The research work proposed by Aman *et al*. [41] has solved the DG deployment problem for the minimization of losses and maximization of overall voltage stability index using Particle Swarm Optimization (PSO) method. However, the second objective function (maximization of overall voltage stability index) was formed by combining the two indices (bus voltage stability index and line voltage stability index). Furthermore, suitable weights were assigned to the individual objective functions to develop Weighted Sum Optimization model. The proposed algorithm was attempted only on the Constant Power (CP) model and the effectiveness of the proposed approach for other different load models was not reported.

Mitra, Mallikarjuna and Singh [42] have suggested a Simulated Annealing (SA) algorithm for the optimal placement and sizing of mixed DG units (Micro Turbine and Solar Photo Voltaic) to improve the distribution network performance. Minimization of annualized depreciation cost and annual fuel cost, subjected to the Energy Index of Reliability (EIR) constraint, have been considered as the main aim of the investigation. Furthermore, they incorporated the location based DG investment cost component to analyze the impact of these DG units on the system performance. To conduct the case study, the annual historical data of load demand plus PV power was divided into four seasons, each season with 24 samples. However, the uncertainty associated with the load and PV resource was ignored in the case studies.

Injeti and Kumar [43] have addressed the optimal deployment of DG problem using a Simulated Annealing (SA) algorithm incorporating the aspect of Loss Sensitivity Factors (LSF). LSF and SA methods were used to find the optimal locations and their appropriate optimal sizes, respectively. The selected objective function was the minimization of losses and maximization of voltage stability. The SA algorithm demands a large number of iterations in order to avoid the trapping into the local optimum value.

Moradi and Abedini [44] have proposed a Genetic Algorithm-Particle Swarm Optimization (GA-PSO) method for minimization of real power losses, minimization of node voltage deviation, and maximization of voltage stability index of distribution network with Constant Power (CP) load model. The penalty function approach was employed to address the priority of objective functions. Also, in [45], [46], and [47], the Teaching Learning Based Optimization (TLBO), Quasi-Oppositional Teaching Learning Based Optimization (QOTLBO), and Chaos Symbiotic Organisms Search (CSOS) algorithm, respectively, have been used to investigate the ODDG problem by considering the objectives of [44]. In these papers, authors have implemented proposed algorithms only the DG units operating at unity power factor mode to improve the system performance.

Quadri, Bhowmick and Joshi [48] have presented a Comprehensive Teaching Learning Based Optimization (CTLBO) algorithm embedded with ε-constraints method for finding the optimal placement and size of the DG units. The objective functions which were of real power loss minimization, voltage profile enhancement, and maximization of voltage stability index have been considered to enhance the performance of the distribution network. Furthermore, the energy loss minimization problem was also attempted on the time varying CP load model. However, while investigating the ODDG problem, they have not incorporated the seasonality and uncertainty associated with the load demand.

In [49], a Whale Optimization Algorithm (WOA) has been suggested for finding the optimal location and size of DG units for multi-objectives. The multi-objectives include the real power loss minimization, voltage profile enhancement, minimization of operating cost, and maximization of voltage stability index subjected to operational equality and inequality constraints. Weighted Sum Approach was employed to account the priority of the objective functions. Here, the weights are chosen based on the experience of the system operator, which may result in the inaccurate optimal solution.

The minimization of power losses, minimization of node voltage deviation, and maximization of voltage stability margin subjected to various system operational constraints have been considered by Wanxing Sheng *et al.* [50], to accommodate the DG units using the Non-dominated Sorting Genetic Algorithm-II (NSGA-II). A Fuzzy Decision Method was employed to select the best compromised solution (BCS) from the Pareto Optimal Set. The authors concluded that the proposed method offers the optimal values compared to the other methods for the selected objective functions. However, the load model of Constant Power (CP) with multi-step variation has been considered to address the ODDG problem by ignoring the randomness in the load demand and DG power outputs.

Soroudi, Ehsan and Zareipour [51], a Hybrid Immune Genetic Algorithm (HIGA) along with the Fuzzy Satisfaction Approach have been implemented to minimize the total cost and total emissions. The total cost include the cost of electrical energy purchased from the grid, installation and operational costs of the DGs, and reinforcement cost of distribution network. The total emissions are taken from the emissions produced by the grid and DG units. A long-term dynamic planning problem (10 years) has been considered for the optimal placement and sizing of the non-renewable DG sources (MT, GT and FC). The authors have concluded that the proposed methodology can be directly used in power markets in which the Distribution Network Operator (DNO) is authorized for DG integration in addition to the network reinforcement. However, in this work, the reliability aspect was not given due attention while attempting the ODDG problem.

Mohamed and Kowsalya [52] have presented Loss Sensitivity Factor + Bacterial Foraging Optimization Algorithm (LSF+BFOA) for optimal accommodation of DG in the distribution system for minimizing power losses, operational cost (cost associated with the electrical energy purchased from the grid and DG), and improving voltage stability. LSF and BFOA were used to identify the potential locations and optimal sizes for installation of DG units. Impact of different load models like Constant Power (CP), Constant Current (CI), and Constant Impedance (CZ) and each for light load, peak load, and heavy load conditions have been analyzed to get the optimal solution for ODDG problem. However, the proposed methodology did not consider the seasonality and uncertainty of the load demand and energy sources.

Bohre, Agnihotri and Dubey [53] have conducted a comparative study on multi-objective function that includes minimization of real power loss, reactive power loss, and shift index factor, voltage profile improvement, and reliability enhancement by using Genetic Algorithm (GA) and Particle Swarm Optimization (PSO) methods. The voltage dependent load models of residential, commercial, industrial, and mix of them have been adopted for investigation. In this work, the multi DGs operating with lagging power factor mode were considered. From the test results, authors have concluded that PSO offers the significant improvement in terms of the selected objective functions as compared to GA. However, in the proposed work, only technical aspects were addressed and not focused on the environmental and economic issues.

Chandrasekhar, Sydulu and Sailaja [54] have suggested a Shuffled Bat Algorithm (ShBAT) along with Weighted Sum Approach for multi-objective optimal deployment of DG units. The multi-objective function comprise of real power loss minimization, reactive power loss minimization, node voltage deviation minimization, and line capacity reduction. The DG units such as PV, WT, FC, and MT were considered for improving the distribution system performance. Furthermore, the load growth effect is also studied for the future planning of DG units. However, in this paper, only CP load model was considered for the investigation of ODDG problem, not attempted the other load models.

In [55], a trade-off solution between maximization of profit of DG owners and minimization of Distribution Company (DISCO) operational cost, has been obtained using Multi-objective Particle Swarm Optimization (MOPSO) algorithm. The time varying constant power load model along with the annual load growth of 2% over the period of 20 years was taken into consideration to solve the optimal DG planning problem. Load profile of 24 hrs has been used to represent one full year. However, in the planning model, uncertainty associated with loads and DG's power output was not addressed in the proposed work.

Rao and Das [56] have proposed a multi-objective GA based algorithm to obtain the optimal size of DG units operating at unity and lagging power factors considering technical and economical factors of the distribution system. The technical factors include real power loss reduction, line load reduction, and voltage profile improvement and reduction of economical factors related to optimal DG investment cost. DGs which were of PV, WT, and Biomass with variable nature have been considered to address the time varying nature of constant power load by ignoring its uncertainty nature.

Mohandas, Balamurugan and Lakshminarasimman [57] have introduced a hybrid Chaotic Artificial Bee Colony (CABC) method for minimization of real power loss, reactive power loss, node voltage deviation, and line capacity along with maximization of voltage stability index. The problem was solved using Weighted Sum Approach by incorporating the user defined weights for the selected objective functions. The diversity in load model such as constant power, residential, commercial, industrial, and mix of these loads have been considered without the variability, seasonality, and uncertainty aspects of loads for optimal accommodation of DG units.

Abdi and Afshar [58] have carried out the investigation on multi-objective function that consists of minimization of cost of energy purchased from the grid, cost of real and reactive energy losses, cost of reliability, DG investment cost, and DG maintenance and operation cost using Improved Particle Swarm Optimization (IPSO) method. The optimal placement and sizing of DG units under different load models like residential, industrial, commercial, constant power, constant current, and constant impedance have been investigated. The authors have concluded that significant cost benefit can be realized when the residential load model was employed as compared to the other load models. However, in this work, the aspect of randomness corresponding to the load demand and DG units was kept aside while addressing the optimal accommodation of DG problem.

Tanwar and Khatod [59] have proposed Combined Sensitivity Index-Particle Swarm Optimization (CSI-PSO) method for minimization of active power loss, line capacity, node voltage deviation, gas emissions, and DG investment cost. The Combined Sensitivity Index (CSI) was developed based on apparent load power and voltage deviation to find the potential locations for the emplacement of DG units. The multi level constant power load model has been incorporated to obtain the optimal size of DG units such as PV, WT, and Biomass. Optimal accommodation of these DG units have shown the significant improvement of distribution system. However, in this paper, the ODDG problem has not given due attention under stochastic domain.

Meena *et al.* [60] have introduced a Multi-Objective Taguchi Approach (MOTA) embedded with Technique for Order of Preference by Similarity to Ideal Solution (TOPSIS) method for optimal integration of DG units in distribution systems. The multi-objective function includes minimization of real power loss and reactive power loss, voltage profile improvement, maximization of voltage stability margin and voltage stability index. In this work, the CP load model was considered for the investigation. The proposed method was efficient and computationally fast to provide the optimal solution. However, in the proposed work, the authors have not attempted the ODDG problem under uncertainty environment.

Tolba *et al.* [61] have presented a Salp Swarm Algorithm (SSA) along with LSF for optimal allocation and capacity of renewable (PV and WT) and non-renewable (FC) distributed generation sources on Distribution grids aiming at minimization of active power loss, DG costs, and cost of power purchase from the grid, and enhancement of voltage profile. In this paper, the authors have not accounted the uncertainty associated with PV and WT resources while solving the ODDG problem.

In [62], a trade-off solution between minimization of real power loss and Energy Not Served (ENS) has been obtained using LSF and hybrid version of TLBO-Grey Wolf

Algorithm with the incorporation of Fuzzy Satisfaction Technique. Renewable DG sources like PV and WT, operating at unity power factor and lagging power factor, have been employed to improve the distribution system performance. However, the modeling aspects related to the stochastic nature of PV and WT units were ignored in the problem formulation.

Kumar, Mandal and Chakraborty [63] have attempted a multi-objective ODDG problem with the aim of minimization of real power loss and node voltage deviation and maximization of cost of yearly energy loss saving by using Oppositional based Chaotic Differential Evaluation (OCDE) algorithm. A Fuzzy Satisfaction Method was employed to select the best compromised solution from the set of optimal solutions. Investigation with the placement of 3 DGs and 4 DGs has been conducted to improve the system performance with respect to the selected objective functions. In this paper, authors have concluded that proposed method is computationally time efficient over the established algorithms. However, the randomness associated with load demand and DG units was not addressed while solving the ODDG problem.

1.5.4 Optimal DG Deployment using Meta-heuristic Methods Under Uncertainty Environment

Renewable Energy Sources (RES) like Solar Photo Voltaic (SPV), Wind Turbine (WT), Mini hydro, Tidal, *etc*., provide the clean electrical energy. This will results in improved public health, inexhaustible energy, enhanced system reliability and resilience. However, their output power depends on the weather conditions which is intermittent in nature. Also, the load demand on the system is not constant, but varies with time and season. Therefore, while investigating the optimal deployment of DG problem of distribution systems, it is necessary to model the randomness associated with the RES and load demand. A review article on the optimal integration of renewable energy sources considering uncertainties was presented by Zubo *et al*. [64].

Zhipeng, Fushuan and Gerard [65] have proposed Monte-Carlo Simulation (MCS) embedded with GA algorithm (MCS-GA) for the minimization of (i) DG investment cost, (ii) DG operation cost, (iii) DG maintenance cost, (iv) network loss cost, and (v) capacity adequacy cost by considering the uncertainty in Plug-in Electric Vehicle (PEV), WT, PV, Fuel prices, and future Load growth. The uncertainty of these resources was modeled using Normal Probability Distribution Function (NPDF) which strongly depends on the shape index and scale index. The formulated optimization problem was solved using Monte-Carlo method, it needs large number of simulations to get the accurate solution.

Soroudi, Ehsan and Caire [66] have solved a long-term dynamic multi-objective optimal DG deployment problem for providing the maximum benefits to Distribution Network Operator (DNO) and Distributed Generation Owner (DGO) on the basis of win-win strategy. To address the formulated problem, a Hybrid Immune Genetic Algorithm (HIGA) along with Fuzzy Satisfaction Method was employed. DG units like Gas Turbine (GT), Diesel Engine (DE), Combined Heat and Power (CHP), and Wind Turbine (WT) has been considered to improve the distribution system performance. Two-Point Estimation Method (2PEM) has been used to model the uncertainties of electricity price, electric loads, and generation of Wind Turbines. However, in this paper, the authors have ignored the diversity among the load demands.

Jain, Singh and Srivastava [67] have employed a modified PSO for finding the optimal DG location and size aiming at minimization of real power loss, reactive power loss, node voltage deviation, and level of gas emission. The probabilistic nature of load and WT power was modeled using Normal distribution and Weibull distribution function, respectively. However, the seasonality and diversity among the loads were ignored while solving the optimization model.

Evangelopoulos and Georgilakis [68] have proposed a Probabilistic Power Flow (PPF)-Genetic Algorithm (GA)-based approach for minimization of (i) DG investment cost, (ii) DG operation cost, (iii) DG maintenance cost, (iv) network loss cost, and (v) capacity adequacy cost. Point Estimate Method (PEM) was employed for the solution of the involved PPF problem. The uncertainties related to the future load growth, WT generation, PV output power, the fuel costs, and the electricity prices were modelled using Normal Probability Distribution Function (NPDF). The authors have claimed that GA–PEM was seven times faster than Genetic Algorithm-Monte Carlo Simulation (GA–MCS) approach. However, in this work, the aspect of emission level was not included in the optimal planning of DG units problem.

Kayal and Chanda [69] have solved the optimal placement and sizing of stochastic natured DGs (PV and WT) problem using Weighted Aggregation PSO incorporating the Weighted Sum Method for the minimization of real power loss, maximization of voltage stability index, and improvement of network security. Furthermore, the seasonality of load and DGs has been considered while modeling the uncertainty. However, in this work, the constant power load model with time varying character was only attempted, but not focused on the realistic load models.

Kefayat, Ara and Niaki [70] have analyzed the impact of DG units on distribution system by placing them at optimal locations with appropriate sizes. The multi-objective function was formulated with the aim of minimization of real power losses, emissions produced by grid and DG, and total energy cost and maximization of voltage stability margin. To solve this multi-objective optimization model an Ant Colony Optimization (ACO) - Artificial Bee Colony (ABC) along with the Fuzzy Satisfaction Method was employed. Both dispatchable (GT and FC) and non-dispatchable (WT) DGs were adopted for the enhancement of distribution system performance. The stochastic nature of load and WT was modeled by using Normal Probability Distribution Function (NPDF) and Weibull Probability Distribution Function (WPDF), respectively. In this work, the authors have ignored the diversity feature of customers while solving the ODDG problem.

In [71], Ganguly and Dipanjan have proposed Adaptive GA with Weighted Sum Approach under Fuzzy environment aiming at minimization of loss and voltage profile improvement. In this paper, the authors have used Triangular Fuzzy membership function to model the uncertainty of both load and DG power output. However, they have not included the variability and diversity of load model in framing the problem.

Ameli *et al.* [72] have suggested a Multi-objective Particle Swarm Optimization (MOPSO) algorithm along with Fuzzy decision-making technique to find the optimal location, size and DG technology considering economic, technical, and environmental issues simultaneously subjected to various equality and inequality constraints. In this investigation, impact of Diesel Engine, Gas Turbine, Micro Turbine, Fuel Cell, and Wind Turbine have been analyzed on the Distribution Network with Constant Power (CP) load model. The ODDG problem was solved for the planning horizon of 20 years by assuming the yearly load growth of 2%. Furthermore, the uncertainty of WT was modeled using

Normal Probability Distribution Function (NPDF). However, in this paper, the authors have ignored the uncertainty aspect and diversity attribute among the different customers.

A trade-off solution between minimization of DISCO cost and maximization of DG Owners profit have been obtained using Non-dominated Sorting Genetic Algorithm - II (NSGA-II) while solving the optimal DG location and size problem in [73]. The randomness associated with load and contractual prices was modeled using the Probability Distribution Function (PDF) approach. However, in the investigation, the intermittent nature of DG units was not given due attention.

Hamid and Alireza [74] have proposed a PSO algorithm for the minimization of cost of power loss, cost of emissions, and total cost of DGs (investment+ replacement+operation and maintenance). DG units such as WT, PV, and FC were chosen to place at the optimal locations with their appropriate sizes to enhance the performance of DS. The stochastic nature of the load demand, WT, and PV was modeled based on the forecasted values and noise generated from the white noise block available in the MATLAB software. From the test results, authors have concluded that after installation of renewable energy resources, emissions remarkably reduced more than 80%. This work also has not analysed the impact of the mix of realistic loads.

Kanwar *et al*. [75] have solved the long-term mixed DG deployment problem under uncertainty environment using Improved PSO meta-heuristic method to maximize the profit of DISCO. A Self-adaptive Polyhedral Deterministic Uncertainty Set (SPDUS) has been proposed to account the intermittence nature of both load and DGs. Furthermore, in this work, the diversity, variability, and seasonality of the various customers (residential, commercial, and industrial) were considered but the uncertainty associated with reactive power load of the customers and the operation of DGs at other than unity power factor were not given attention in the problem formulation.

Jeddi *et al.* [76] have suggested a Combined Harmony Search Firefly Algorithm (CHSFA) for Distributed Energy Resources (DER) planning in distribution network. The aim of the study was maximization of the profit of DN companies by increasing income and reducing costs. Load uncertainty was considered in the proposed planning model and the Robust Optimization (RO) approach was employed to cope with the uncertainty. The developed methodology was illustrated using real-world voltage-dependent load models, including residential, commercial, and industrial types. In this work, the uncertainty in the yearly load increment was accounted for different type of loads while attempting the ODDG problem. Their work has not cover the irregularity associated with load and DGs on hourly basis.

1.6 Motivation

From the above literature review, it was observed that the maximum technical, economical, and environmental benefits can be obtained from the optimal deployment of DGs in the Distribution Network. In order to get the aforementioned benefits, several Analytical and Meta-heuristic techniques were proposed in the literature. However, an efficient optimization technique is required to attain global optimum value by incorporating various constraints and covering different load models under normal and uncertainty conditions. Furthermore, the optimal accommodation of DGs is a planning problem which needs the execution of large number of load flows. Therefore, an efficient Distribution Load Flow (DLF) method which works on Radial and Weakly Meshed Distribution Networks and offers solution in less execution time can be preferred. The following gaps have been identified as motivation of the thesis.

- Need an efficient and fast Distribution Load Flow (DLF) method that can work for both Radial and Weakly Meshed DS under different load models and which can go as effective tool for DG deployment problem.
- Optimal Deployment of DG (ODDG) problem can be attempted for Single objective and Multi-objective cases by proposing a new *Analytical method* to identify the potential location for the placement of DG units.
- Need an effective Nature/Bio-inspired Meta-heuristic algorithm to solve the ODDG problem to attain the global optimum value.

- Required to propose an analytical method for finding the optimal weights of the individual objectives in the case of Weighted Sum Multi-objective optimization problem.
- To account for the uncertainty associated with (i) Residential, Commercial, and Industrial loads, (ii) Wind Turbine power output, and (iii) Solar Photo Voltaic power output while solving the long-term DG deployment problem. Furthermore, required to consider the variability, seasonality, and diversity among the above realistic loads.
- To investigate the effect of *DG degradation* on Optimal placement and sizing of DG units problem for the optimization of technical, economical, and environmental objective functions.

1.7 Objectives of Thesis

The objectives of this thesis include:

- To propose an effective Distribution Load Flow (DLF) algorithm which addresses the solution of load flow problem of Radial and Weakly Meshed Distribution Systems on equal strength and that can be used as a powerful tool for ODDG problem.
- To focus the investigation on (i) minimization of electrical energy losses, (ii) minimization of overall node voltage deviation, (iii) maximization of overall voltage stability margin, and (iv) minimization of Energy Not Served (ENS) by placing the single DG at optimal location identified by the proposed *Branch Loss Bus Injection Index (BLBII) method* (Analytical method).
- To propose an *Analytical Hierarchy Process (AHP)* method to obtain the optimal weights of the individual objectives in the case of "Weighted Sum Multi-objective optimization problem".
- To propose new Meta-heuristic optimization algorithm "*Hybrid Multi-Verse Optimizer (HMVO)*" by combining the best features of *Space Transformation Search* (*STS*) *algorithm* and *Piecewise Linear Chaotic Map* (*PLCM*) *method* to attain the optimal values of the aforementioned objective functions.
- To propose *Multi-objective Jaya Algorithm (MOJA)* for the case of long-term optimal deployment of mixed DGs under *uncertainty environment* and also considering *DG degradation effect*. For this attempt, the following aspects are incorporated.

- ✓ Two objective functions: (i) Maximization of DISCO profit, and (ii) Distribution Network Technical Objectives Improvement.
- ✓ Use of Self-adaptive Polyhedral Deterministic Uncertainty Set (SPDUS) to account for uncertainty associated with realistic customer load demand, Wind Turbine (WT) power, and Solar Photo Voltaic (SPV) power.
- ✓ To generate the synthetic data at quarterly-hour (15 minutes) time stamp required for different types of customer loads, WT, and PV resources.

1.8 Thesis Organization

The thesis is organized into six chapters and presented as follows;

The **first chapter** presents the detailed literature survey, key issues, and motivation for the research work carried out in the area of "Optimal deployment of DGs in Distribution System." In this chapter, an in-depth literature review is carried out on optimal planning of DGs using Analytical and Meta-heuristic methods. Furthermore, literature review is also carried out on Distribution Load Flow (DLF) methods. The objectives, motivation of the thesis, and chapter wise summary are also outlined.

Second chapter reports "an efficient power flow method for Distribution System Studies under various load models." This newly proposed DLF method works on equal strength for both Radial and Weakly Meshed Distribution Systems. The applicability of the proposed DLF is investigated on various load models like Constant Power (CP), Constant Current (CI), Constant Impedance (CZ), and combination of these load models. Furthermore, the robustness of the algorithm is tested for different tolerance values, loading conditions, and various X/R ratios. The investigation conducted on five test systems (IEEE 33-, IEEE 69-, TPC 84-, 136-, and 874 bus) operating under Radial and Weakly Meshed mode conditions could reveal that the proposed DLF is superior over the Current Injection Method (CIM).

Third chapter delineates the "multi-objective optimal accommodation of DG unit using Analytical method." A new multi-objective problem was formulated with: (i) minimization of electrical energy losses, (ii) minimization of overall bus voltage deviation, (iii) maximization of overall voltage stability margin, and (iv) minimization of Energy Not Served (ENS). The optimal values for these objective functions can be attained only when the DG unit is placed at candidate location. Hence, an analytical method called, *Branch Loss Bus Injection Index* (*BLBII*) is proposed to find the optimal location for the emplacement of DG unit. Furthermore, an unique *Analytical Hierarchy Process* (*AHP*) approach has been proposed to estimate the optimal weights for the individual objectives of the multi-objective function as the optimization problem was solved using Weighted Sum Approach. The case studies are conducted on IEEE 33- and INDIAN 85- bus benchmark Radial Test Systems. The impact of Single DG unit operating at unity and 0.9 lagging power factor has been analyzed. From the simulation results, it is concluded that the DG unit operated with lagging power factor mode offers the optimum results compared to the results of base case and unity power factor mode of operation.

Fourth chapter presents the "multi-objective optimal DG deployment using Hybrid Multi-Verse Optimization (HMVO) method." The basic Multi-Verse Optimization (MVO) approach is originated from the three concepts of cosmology: white hole, black hole, and wormhole. The mathematical models of these three concepts are used to perform the exploration, exploration, and exploitation /local search, respectively. As the basic MVO exhibits the poor convergence, the hybrid version of MVO (HMVO) is developed by combining the best features of Space Transformation Search (STS) and Piecewise Linear Chaotic Map (PLCM) algorithms. The objectives which were considered in the *Chapter - 3* have been used while solving the DG deployment problem. The case studies are carried out on IEEE 33- and INDIAN 85 bus Radial Test Systems under two scenarios: (i) three DGs operating at unity power factor condition, and (ii) three DGs operating at 0.9 lagging power factor condition. The investigation reveals that the proposed HMVO algorithm outperforms the various algorithms attempted for comparison purpose and the already published works in the literature, in terms of quality solutions, objective values, and convergence characteristics. Furthermore, the superiority of HMVO is also established through the statistical analysis.

Fifth chapter covers the "Long-term optimal planning of mixed DG units considering uncertainty and DG degradation effect." The uncertainty on quarter-hour (15 minutes) time stamp basis is modelled for residential, commercial, and industrial customer loads and WT and PV power outputs using Self-adaptive Polyhedral Deterministic Uncertainty Set (SPDUS) method. Furthermore, the DG degradation effect is also considered in planning problem. The *Multi-Objective Jaya Algorithm* (*MOJA*) has been used to solve the formulated multi-objective problem comprising of (i) Maximization of DISCO profit, and (ii) Distribution Network Technical Objectives Improvement. The case studies carried out on modified IEEE 33-bus Radial Test System concluded that *MOJA* provides optimal solutions over the NSGA-II algorithm. Furthermore, it is observed that DG placement with degradation effect earns more profit than without degradation effect.

Finally, **Sixth chapter** highlights the various conclusions drawn at different stages of the work, the significant contribution of research work, and provides scope for further research in this area.

The list of Research publications of the present work, References, and APPENDIX 1-8 are also reported at the end of this Thesis.

Total description of the present research work is presented in Figure 1.1 in the form of a flow chart for ready reference.

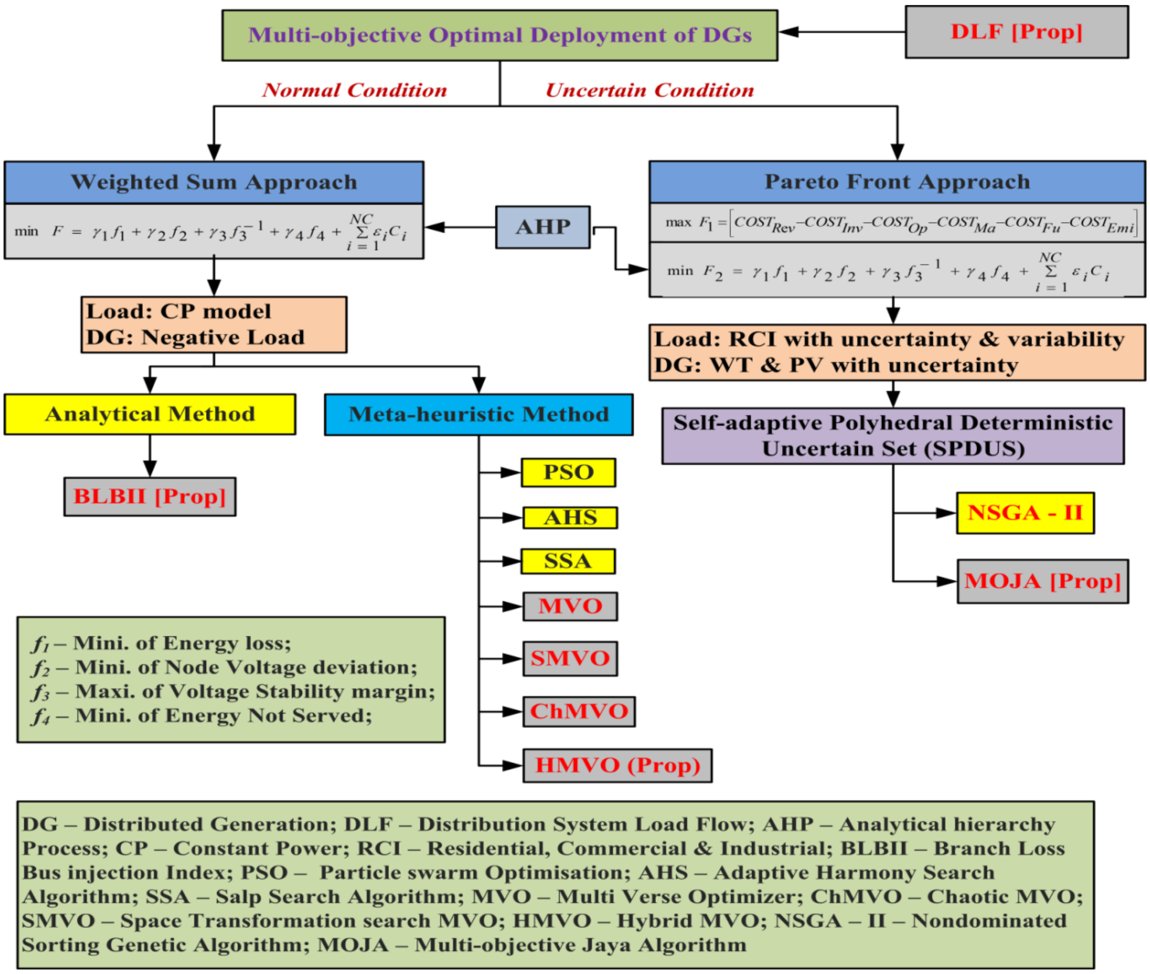

Figure 1.1 Flow chart for organization of research work

CHAPTER-2

An effective Distribution Load Flow Method for Radial and Weakly Meshed Power Distribution Networks

2.1 Introduction

In reality, most of the distribution networks are radial in nature, having low reactance to resistance ratio (X/R ratio), suffering from the low voltages and unbalanced operation. The conventional Load Flow methods like Gauss Seidel (GS), Newton-Raphson (NR), and Fast Decoupled (FDC) have failed to converge due to low X/R ratio and radial nature of distribution systems [9]-[11], [13]. In view of this, special attention has been paid for solving such networks. In this connection, various efficient Distribution Load Flow (DLF) algorithms have been proposed in the literature [9]-[21]. However, majority of the algorithms were developed for Radial Distribution Networks (RDN) [9]-[17], but a few for Weakly Meshed Distribution Networks (WMDN) [18]-[21]. Furthermore, they have not demonstrated the applicability of the algorithms for different load models, loading conditions, tolerance levels, and ill condition cases. In fact, an algorithm is said to be more stable if it offers a solution without divergence problem for all the above aspects.

Therefore, there is a need for an effective algorithm which addresses the solution of load flow problem of Radial and Weakly Meshed Distribution System on equal strength. In this Chapter, a simple but fast and efficient Distribution Load Flow (DLF) algorithm is proposed which can work effectively for both Radial Distribution Network (RDN) and Weakly Meshed Distribution Network (WMDN) subjected to different situations.

2.2 Mathematical model of Proposed Distribution Load Flow Method

An efficient power flow method is developed for the system studies of Radial and Weakly Meshed Distribution Networks on equal strength by making use of the new voltage variables e_1, e_2,.....e_N (defined in Eq. (2.1)) and the concept of building up algorithm [77] for determining network matrix. In this section, primarily the mathematical model for Radial Distribution Network (RDN) is presented and later it is extended to Weakly Meshed Distribution Network (WMDN).

2.2.1 For Radial Power Distribution Networks

For system studies, Radial distribution system is represented as balanced equivalent single phase network. Line shunt capacitance at distribution voltage level is very small and it is ignored in the modelling of the distribution line. A simple 6-bus Radial Distribution Network [19] is shown in Figure 2.1.

In this representation, the proposed new voltages e_1, e_2, e_3, e_4, e_5, and e_6 are illustrated as shown in Figure 2.1 and they are defined as in Eq. (2.1).

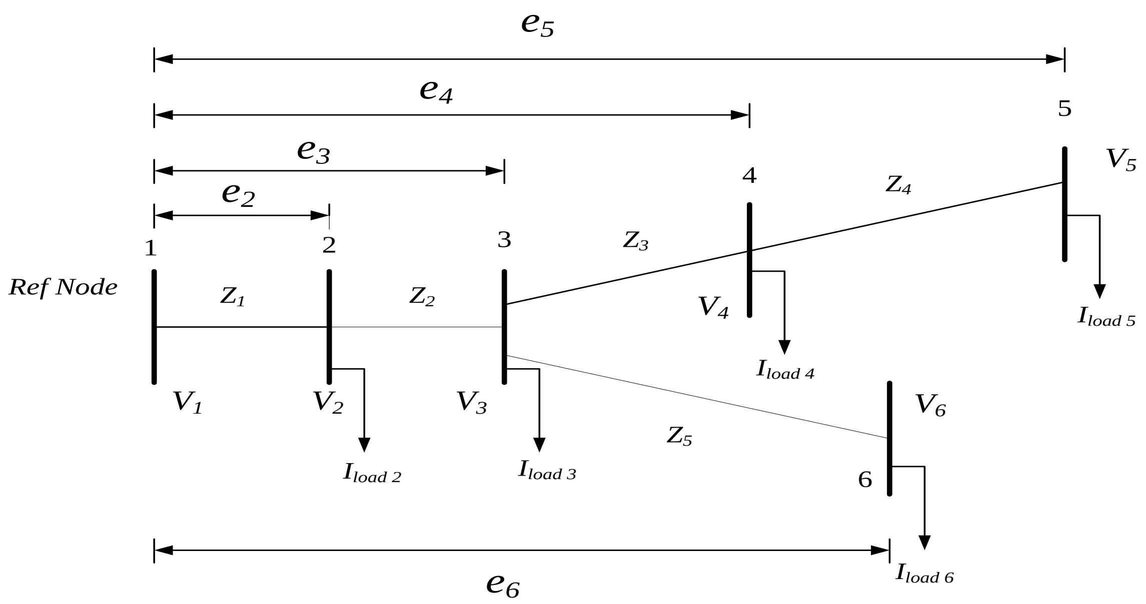

Figure 2.1 Simple 6-bus Radial Distribution Network

$$\left.\begin{aligned} e_1 &= V_1 - V_1 = 0; \\ e_2 &= V_2 - V_1; \\ e_3 &= V_3 - V_1; \\ e_4 &= V_4 - V_1; \\ e_5 &= V_5 - V_1 \text{ and} \\ e_6 &= V_6 - V_1 \end{aligned}\right\} \qquad (2.1)$$

where V_1, V_2, V_3, V_4, V_5 and V_6 are the complex bus voltages.

These e_1 to e_6 are representing the voltage deviations of the complex bus voltages with respect to source node or reference node voltage V_1. It may be noted that e_1 turns out to be zero as node 1 is taken as reference node. The currents flowing through various line elements can easily be written as below in Eq. (2.2).

$$\left.\begin{aligned}
I_{Z1} &= I_{load2} + I_{load3} + I_{load4} + I_{load5} + I_{load6};\\
I_{Z2} &= I_{load3} + I_{load4} + I_{load5} + I_{load6};\\
I_{Z3} &= I_{load4} + I_{load5};\\
I_{Z4} &= I_{load5};\\
I_{Z5} &= I_{load6}
\end{aligned}\right\} \tag{2.2}$$

Then, the e_2, e_3, e_4, e_5, and e_6 can be written as in Eq. (2.3).

$$\left.\begin{aligned}
e_2 &= -Z_1 I_{Z1};\\
e_3 &= -Z_1 I_{Z1} - Z_2 I_{Z2};\\
e_4 &= -Z_1 I_{Z1} - Z_2 I_{Z2} - Z_3 I_{Z3}\\
e_5 &= -Z_1 I_{Z1} - Z_2 I_{Z2} - Z_3 I_{Z3} - Z_4 I_{Z4};\\
e_6 &= -Z_1 I_{Z1} - Z_2 I_{Z2} - Z_5 I_{Z5}
\end{aligned}\right\} \tag{2.3}$$

Substituting the values of I_Z from Eq. (2.2) in Eq. (2.3), the Eq. (2.4) can be written as below:

$$\begin{bmatrix} e_2\\ e_3\\ e_4\\ e_5\\ e_6 \end{bmatrix}_{(5X1)} = -\begin{bmatrix}
Z_1 & Z_1 & Z_1 & Z_1 & Z_1\\
Z_1 & Z_1+Z_2 & Z_1+Z_2 & Z_1+Z_2 & Z_1+Z_2\\
Z_1 & Z_1+Z_2 & Z_1+Z_2+Z_3 & Z_1+Z_2+Z_3 & Z_1+Z_2\\
Z_1 & Z_1+Z_2 & Z_1+Z_2+Z_3 & Z_1+Z_2+Z_3+Z_4 & Z_1+Z_2\\
Z_1 & Z_1+Z_2 & Z_1+Z_2 & Z_1+Z_2 & Z_1+Z_2+Z_5
\end{bmatrix}_{(5)X(5)} \begin{bmatrix} I_{load\,2}\\ I_{load\,3}\\ I_{load\,4}\\ I_{load\,5}\\ I_{load\,6} \end{bmatrix}_{(5X1)} \tag{2.4}$$

The given complex power load at i^{th}-bus is $S_{load\,i} = P_{load\,i} + jQ_{load\,i}$, $i = 2$ to N (i.e. $N = 6$), can be converted into equivalent load currents $I_{load\,i}$ given in Eq. (2.5).

$$I_{load\,i} = (S_{load\,i} / V_i)^*, \quad i = 2 \text{ to } N \tag{2.5}$$

It may be recall that for any multiport network, currents entering ports are taken as positive and they act as current injections at various buses.

At this stage, the above load currents are modified as current injections ($I_{inj\ i}$) at the buses of the network and they are given by Eq. (2.6).

$$I_{inj\ i} = - I_{load\ i}\ ; \quad i = 2 \text{ to } N \tag{2.6}$$

Then, $I_{inj\ i}$ can be further modified as below Eq. (2.7) if a generating unit is available at i^{th}- node.

$$I_{inj\ i} = I_{gen\ i} - I_{load\ i} \tag{2.7}$$

Then, $I_{inj\ i} = (S_{inj\ i} / V_i)^*\ ; \quad i = 2 \text{ to } N$

$$= (\{(P_{gen\ i} - P_{load\ i}) + j (Q_{gen\ i} - Q_{load\ i})\} / V_i)^*,$$

For a Radial Distribution System without generating units case, the $I_{inj\ i} = - I_{load\ i}$ can be used at each bus.

Finally, the matrix form for e_2 to e_6 can be written as:

$$\begin{bmatrix} e_2 \\ e_3 \\ e_4 \\ e_5 \\ e_6 \end{bmatrix}_{(5X1)} = \begin{bmatrix} \\ \\ \textit{Network Matrix, } Z \\ \\ \\ \end{bmatrix}_{(5)X(5)} \begin{bmatrix} I_{inj\ 2} \\ I_{inj\ 3} \\ I_{inj\ 4} \\ I_{inj\ 5} \\ I_{inj\ 6} \end{bmatrix}_{(5X1)} \tag{2.8}$$

The Eq. (2.8) can be extended to N bus system and may be written in compact form as below.

$$[e_i]_{(N-1)X1} = [Z]_{(N-1)X(N-1)} [I_{inj\ i}]_{(N-1)X1} \quad ; \quad i = 2 \text{ to } N \tag{2.9}$$

Where $[e_i]_{(N-1)x1} = [V_i - V_1]_{(N-1)x1}$ (2.10)

The Radial or Weakly Meshed Distribution Network will have negligible shunt capacitance and hence the network matrix [Z] can be formed by using the popular *Building up algorithm* ‘or’ *Step-by-Step algorithm* [77] considering the addition of *an uncoupled branch* or *uncoupled link*. In radial distribution system, only uncoupled case is observed. The set of equations related to addition of *uncoupled branch* is as below [77].

APPENDIX - 7 reports the relevant information of Z_{bus} formation using *Step-by-Step algorithm* [77]. For addition of *an uncoupled* α^{th} *branch* with primitive impedance $z_{\alpha\alpha}$ having the nodes *p* and *q*:

Impedance matrix, [*Z*] =

0	0	0
0	Z_{old}	Z_{iq}
0	Z_{qi}	Z_{qq}

If p or q ≠ reference node, then

$$\left.\begin{array}{ll} Z_{qi} = Z_{pi} & \text{for off-diagonal elements} \\ Z_{qq} = Z_{pq} + z_{\alpha\alpha} & \text{for diagonal elements} \end{array}\right\} \quad (2.11)$$

If p = reference node, then

$$\left.\begin{array}{ll} Z_{qi} = Z_{pi} = 0 & \text{for off-diagonal elements} \\ Z_{qq} = z_{\alpha\alpha} & \text{for diagonal elements} \end{array}\right\} \quad (2.12)$$

These equations are very simple due to the fact that the elements in radial distribution system are uncoupled. Once network matrix [*Z*] is formed, it remains constant for the selected distribution network. *Due to symmetry, the* Z_{iq} *can be taken from* Z_{qi}*. Further, the calculation of* Z_{qi} *or* Z_{qq} *is not causing any computational burden as they don't need any multiplication or division. Hence, there is a huge reduction in the CPU time requirement even for large size system.*

The load flow solution can be obtained by *simple matrix multiplication of constant network matrix [Z]* with *current injection vector*. This product offers the voltage deviation vector $[e_i]_{(N-1)X1}$. This voltage deviation vector is used to update the bus voltage vector at each iteration as below.

$$V_i = V_1 + e_i \quad ; \qquad i = 2 \text{ to } N \qquad (2.13)$$

The proposed approach can easily be extended for Weakly Meshed Distribution Networks. Several of the existing load flow techniques for distribution networks do not have the ability to address the Weakly Meshed Network problems though they perform satisfactorily for Radial Distribution Systems.

The proposed algorithm exhibits credible convergence due to the following reasons:

(i) [Z] matrix is a constant matrix. Once it is formed for a given distribution network structure, it remains constant for all the required iterations leading to low CPU burden.

(ii) [Z] matrix is a full matrix with non-zero elements. Any change in load current at bus-*i* can be automatically accounted for each e_i of all the buses with appropriate coefficient of [Z] matrix. This aspect of simultaneous correction in e_i for any possible change in load current at bus-*i* can help in exhibiting faster convergence.

2.2.2 For Weakly Meshed Power Distribution Networks

To improve the reliability and provide better voltage regulation, Weakly Meshed Distribution Networks are created by closing the Tie-line switches. A simple 6-bus Weakly Meshed Distribution Network [19] is created by closing a Tie-line between bus-5 and bus-6 and is shown in Figure 2.2.

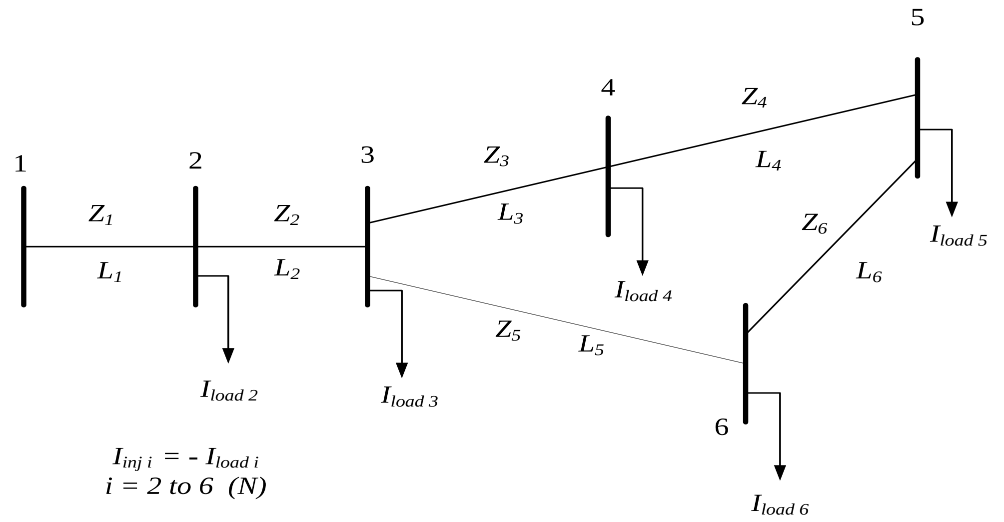

Figure 2.2 Simple 6-bus Weakly Meshed Distribution Network

The addition of a line L_6 between bus-5 and bus-6 will create the loop containing the line numbers $L_3, L_4, L_5,$ and L_6. In this case also, the network matrix [*Z*] can be formed by using the *building up algorithm* considering addition of an *uncoupled link* [77]. The relevant equations related to addition of an *uncoupled link* are given below [77].

For addition of *an uncoupled* α^{th} *link* with primitive impedance $z_{\alpha\alpha}$ between p – q buses:

Impedance matrix, [*Z*] =

0	0	0
0	Z_{old}	Z_{il}
0	Z_{li}	Z_{ll}

Where '*l*' is fictitious node [77].

If p or q $\neq$ reference node, then

$$\left.\begin{aligned} Z_{li} &= Z_{pi} - Z_{qi} && \text{for off-diagonal elements} \\ Z_{ll} &= Z_{pl} - Z_{ql} + z_{\alpha\alpha} && \text{for diagonal elements} \end{aligned}\right\} \tag{2.14}$$

If p = reference node, then

$$\left.\begin{aligned} Z_{li} &= -Z_{qi} && \text{for off-diagonal elements} \\ Z_{ll} &= -Z_{ql} + z_{\alpha\alpha} && \text{for diagonal elements} \end{aligned}\right\} \tag{2.15}$$

It may be noted from the above equations, that elements corresponding to new fictitious node '*l*' can easily be obtained without much computational burden. Then, the fictitious node '*l*' can be eliminated and the resulting new elements of [*Z*] matrix are [77]:

$$Z_{ij\ new} = Z_{ij\ old} - \frac{Z_{il} Z_{lj}}{Z_{ll}} \tag{2.16}$$

The above aspect can be used if any further mesh is created by closing another Tie-line switch. This approach is very effective as it does not involve any approximations or assumptions in building up [Z] matrix for addition of new loops. Once the constant [*Z*] matrix for weakly meshed network is made available, the iterative process for calculating voltage deviation vector [e] remains similar to the previous case and algorithm would be identical in both the cases.

2.3 Load modeling

Load modeling is essential in distribution system analysis, planning and control. Power Distribution Network (PDN) loads are characterized by voltage sensitivity. As the voltage available at the load point changes, the behaviour of the electrical load is also changes. Therefore, in order to get the precise results, the loads must be modeled as accurately as possible. Some of the standard load models which are being used for the distribution system studies are of the following nature [15]:

Constant Power (CP)	:	The real and reactive power consumed by the load remains constant irrespective of the voltage changes at its terminal point.
Constant Current (CI)	:	The current drawn by the load remains constant and independent of the voltage changes.
Constant Impedance (CZ)	:	The impedance is treated constant for all the voltage changes.
Composite load (CZIP)	:	The combination of CP, CI, and CZ loads.

The general expression for the above load models is shown below [15].

$$P = P_o\left(a_0 + a_1 V + a_2 V^2\right)\ ;\quad Q = Q_o\left(b_0 + b_1 V + b_2 V^2\right) \tag{2.17}$$

where P_0 and Q_0 are nominal real and reactive powers, respectively and V is the bus voltage. For all the loads, the equations corresponding to P and Q are constrained as below.

$$a_0 + a_1 + a_2 = 1.0\ ;\quad b_0 + b_1 + b_2 = 1.0 \tag{2.18}$$

The values of constants used in Eq. (2.18) are different for various load models and are given in Table 2.1 [15].

Table 2.1 Numerical Values of the Constants for different Load models [15]

Type of Load	Value of '*a*'	Value of '*b*'
CP	$a_0 = 1;\ a_1 = 0; a_2 = 0$	$b_0 = 1;\ b_1 = 0;\ b_2 = 0$
CI	$a_0 = 0;\ a_1 = 1; a_2 = 0$	$b_0 = 0;\ b_1 = 1;\ b_2 = 0$
CZ	$a_0 = 0;\ a_1 = 0; a_2 = 1$	$b_0 = 0;\ b_1 = 0;\ b_2 = 1$
CZIP	$a_0 = 0.4;\ a_1 = 0.3; a_2 = 0.3$	$b_0 = 0.4;\ b_1 = 0.3;\ b_2 = 0.3$

2.4 Steps for the implementation of Proposed Distribution Load Flow Method and Flow Chart

To determine the voltage magnitude and phase angle at each bus of Radial Distribution and Weakly Meshed Distribution Networks, the proposed algorithm can be summarized in the following steps:

Step 1: // Read the Data of Distribution Network //

(i) N = Number of buses of the selected Distributed Network.

(ii) NL = Number of lines in the system.

(iii) Impedance of each line: $Z_k = R_k + j\ X_k$; k = 1 to NL.

(iv) Complex load demand at each bus: $S_{load,\ i} = P_{load,i} + j\ Q_{load,i}$; i = 2 to N

(v) Convergence value, Epsilon (ε) = 0.0001 p.u.

(vi) Maximum number of iterations: *Itermax*

Step 2: Build the *constant network matrix* [Z], using Eqs. (2.11) – (2.12) for Radial Distribution Network (RDN) and Eqs. (2.14) – (2.16) for Weakly Meshed Distribution Network (WMDN).

Step 3: Assume $V_i = 1 + j\ 0$ p.u at all buses and also store them in $V_{old\ i}$.

Step 4: Select the load model from Eqs. (2.17) – (2.18). Compute equivalent current injections $I_{inj\ i}$, at all the buses except reference bus -1 using Eq. (2.7).

Step 5: Set iteration count, *iter* = 1 and Set $|\ \Delta V\max\ | = 0$.

Step 6: Determine the voltage deviation vector, $[e_i]_{(N-1)X1}$, i = 2 to N using Eq. (2.9).

Step 7: Update the bus voltages, $V_i = V_1 + e_i$, i = 2 to N.

Step 8: Calculate, $\Delta V_i = V_i - V_{old\ i}$, $i=2$ *to* N and $|\Delta V\text{max}|$.

Step 9: Test for convergence: if $|\Delta V\text{max}| \leq \varepsilon$ go to **Step 12**.

Step 10: Otherwise, recalculate the $I_{inj\ i}$ vector using Eq. (2.7). Set $V_{old\ i} = V_i$, i = 2 to N.

Step 11: Advance iteration count: $iter = iter + 1$.

If ($iter \geq Itermax$) Go to **Step 13**.

else

Set $|\Delta V\text{max}| = 0$ then Go to **Step 6**.

Step 12: Problem converged in '*iter*' iterations. Print the load flow results and **STOP**.

Step 13: Problem not converged in '*Itermax*' iterations. **STOP**.

For better understanding, the algorithm steps of the proposed DLF algorithm are shown in Figure 2.3.

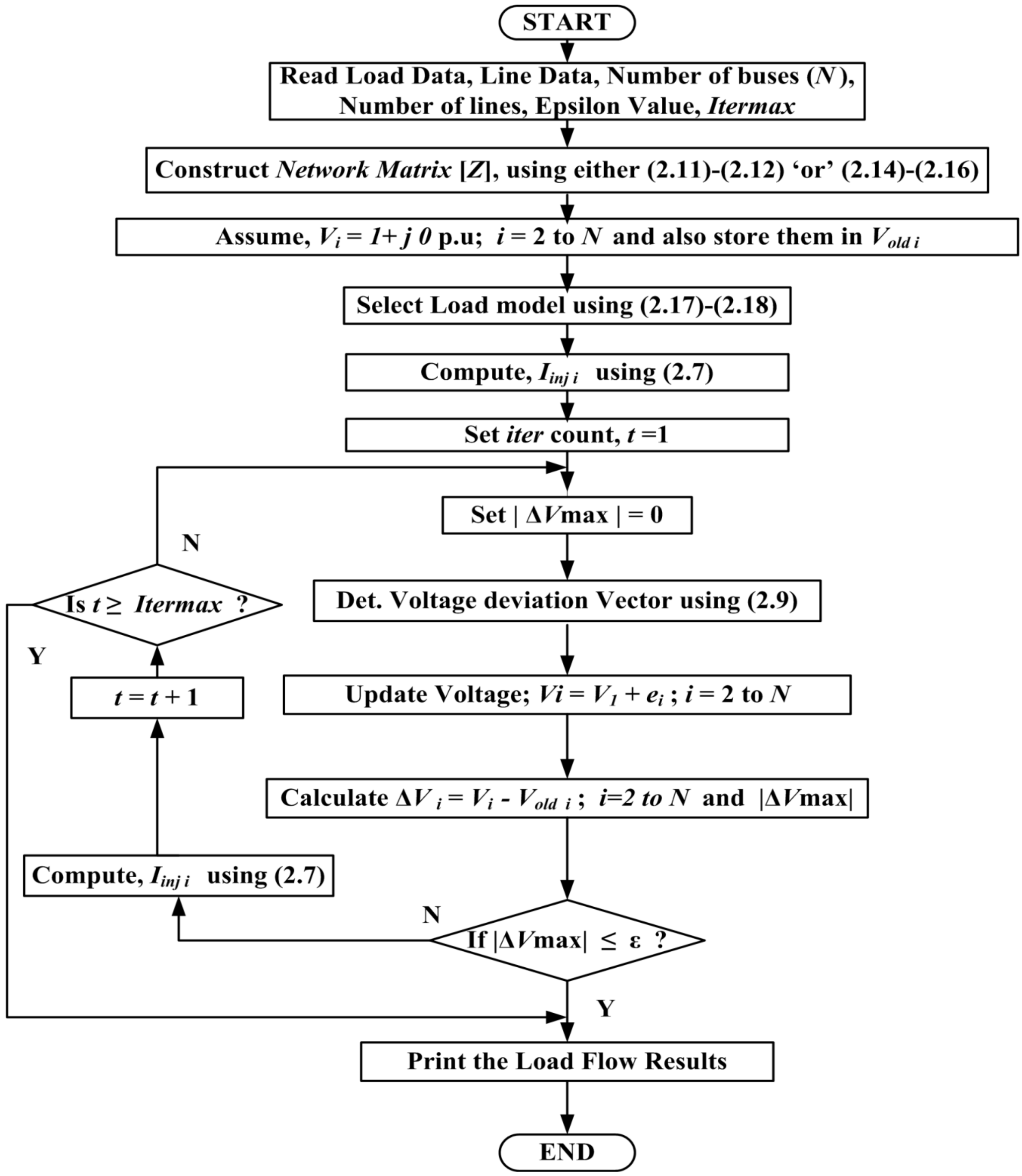

Figure 2.3 Flow chart of the Proposed Distribution Load Flow algorithm

2.5 Test Systems

The applicability and strength of the proposed DLF method are demonstrated on *five test systems* ranged from small to large size Distribution Networks. Description of these test systems is given below.

2.5.1 Description of IEEE 33-bus Test System

IEEE 33 bus, 12.66 kV, 100 kVA, 33 nodes, 32 lines (for Radial), and 37 lines (for Weakly Meshed System which includes 5 Tie-lines) of distribution system is considered as a first test case. The line data and bus data of this test system are reported in APPENDIX-1 [78]. The network total real and reactive power loads are 3715 kW and 2300 kVAR, respectively.

2.5.2 Description of IEEE 69-bus Test System

In second test case, IEEE 69 bus, 12.66 kV, 100 kVA, 69 nodes, 68 lines (for Radial system), and 73 lines (for WMDN which includes 5 Tie-lines) of distribution system is employed. The data related of this system is given in APPENDIX-2 [79]. The network total real and reactive power loads are 3801.89 kW and 2694.10 kVAR, respectively.

2.5.3 Description of TPC 84-bus Test System

As a third test case, a practical low voltage distribution network of Taiwan Power Company (TPC) 84 bus, 11.4 kV, 100 kVA, 84 nodes, 83 lines (for Radial), and 96 lines (for WMDN consisting of 13 Tie-lines) is considered. The relevant data of this test system is available in APPENDIX-3 [80]. The network total real and reactive power loads are 28350 kW and 20700 kVAR, respectively.

2.5.4 Description of 136-bus Test System

As a fourth test case, 136 bus, 13.8 kV, 100 kVA, 135 lines (for Radial), and 156 lines (for WMDN with 21 Tie-lines) of distribution network is adopted. It is a real distribution system in a medium size city of Brazil. The data of this system can be found in APPENDIX-5 [81]. The network total real and reactive power loads are 18312.81 kW and 7930.26 kVAR, respectively.

2.5.5 Description of 874-bus Test System

As a fifth test case, 874 bus, 130.8 kV, 100 kVA, 873 lines (for Radial), and 900 lines (for WMDN with 27 Tie-lines) of distribution network is considered. The data of this system is reported in APPENDIX-6 [81]. The network total real and reactive power loads are 124871.61 kW and 75262.22 kVAR, respectively.

2.6 Simulation Results and Discussion

The proposed Distribution Load Flow (DLF) method and Current Injection Method (CIM) [18] are coded in MATLAB environment and tested on Windows 8.1 based HP Laptop with Intel Core i3 CPU, 1.8GHz, and 4GB RAM. The two load flow algorithms (Proposed DLF and CIM) are implemented on five benchmark distribution systems (IEEE 33-, IEEE 69-, TPC 84-, 136-, and 874 bus) for both Radial and Weakly Meshed conditions. Furthermore, the impact of the various *voltage dependent load models* such as *Constant Power* (*CP*), *Constant Current* (*CI*), *Constant Impedance* (*CZ*), and *Composite Load* (*CZIP*) is investigated to observe the voltage profile and power loss of the selected distribution systems operating in Radial mode and simulated Weakly Meshed mode. The proposed DLF method is said to be converged if the difference of the maximum value of voltages ($|\Delta Vmax|$) between any two successive iterations is less than or equal to 0.0001 p.u.

2.6.1 Impact of different Load models on Radial Distribution Networks

For *Radial condition*, the test results offered by the proposed DLF and CIM [18] approaches are reported in Tables: 2.2 to 2.6. These tables compare the voltage magnitudes of the test systems for different load models like CP, CI, CZ, and CZIP. Furthermore, for all the test cases, the voltage magnitude at the initial buses starting from 1 to 10 and the buses at sag end of the test systems are shown in the tables. However, for each load model the complete voltage profile of all buses is depicted in the Figures: 2.4 to 2.8. From the tables 2.2-2.6, it may be pointed out that the results of the proposed method are closely matched with the results of CIM method [18]. Thus, it validates the simulation results of the proposed method.

Table 2.2 Comparison of voltage magnitudes of IEEE 33-bus *RDN* for different Load models

Bus No.	CP Load		CI Load		CZ Load		CZIP Load	
	CIM [18]	PM	CIM [18]	PM	CIM [18]	PM	CIM [18]	PM
	Voltage (p.u.)	Voltage (p.u.)	Voltage (p.u.)	Voltage (p.u.)	Voltage (p.u.)	Voltage (p.u.)	Voltage (p.u.)	Voltage (p.u.)
1	1.0000	1.0000	1.0000	1.0000	1.0000	1.0000	1.0000	1.0000
2	0.9970	0.9970	0.9972	0.9972	0.9973	0.9973	0.9972	0.9972
3	0.9828	0.9828	0.9839	0.9839	0.9847	0.9847	0.9838	0.9838
4	0.9753	0.9753	0.9769	0.9770	0.9782	0.9782	0.9768	0.9768
5	0.9679	0.9679	0.9701	0.9701	0.9718	0.9718	0.9698	0.9699
6	0.9494	0.9494	0.9530	0.9531	0.9559	0.9560	0.9526	0.9527
7	0.9459	0.9459	0.9498	0.9499	0.9528	0.9530	0.9493	0.9494
8	0.9322	0.9323	0.9373	0.9374	0.9412	0.9414	0.9367	0.9368
9	0.9259	0.9259	0.9315	0.9316	0.9359	0.9361	0.9309	0.9310
10	0.9200	0.9200	0.9261	0.9263	0.9310	0.9311	0.9255	0.9256
11	0.9192	0.9192	0.9253	0.9255	0.9302	0.9304	0.9247	0.9248
12	0.9177	0.9177	0.9240	0.9241	0.9290	0.9291	0.9233	0.9234
13	0.9115	0.9115	0.9184	0.9185	0.9238	0.9240	0.9176	0.9177
14	0.9092	0.9092	0.9163	0.9164	0.9219	0.9221	0.9155	0.9156
15	0.9078	0.9078	0.9150	0.9151	0.9207	0.9209	0.9142	0.9143
16	0.9064	0.9064	0.9138	0.9139	0.9196	0.9198	0.9129	0.9130
17	0.9043	0.9043	0.9119	0.9121	0.9179	0.9181	0.9110	0.9112
18	0.9037	0.9037	0.9113	0.9115	0.9173	0.9176	0.9105	0.9106
19	0.9964	0.9964	0.9967	0.9967	0.9968	0.9968	0.9966	0.9966
20	0.9929	0.9929	0.9931	0.9931	0.9933	0.9933	0.9931	0.9931
21	0.9922	0.9922	0.9924	0.9924	0.9926	0.9926	0.9924	0.9924
22	0.9915	0.9915	0.9918	0.9918	0.9920	0.9920	0.9918	0.9918
23	0.9793	0.9793	0.9804	0.9804	0.9813	0.9814	0.9803	0.9803
24	0.9726	0.9726	0.9739	0.9740	0.9750	0.9751	0.9738	0.9738
25	0.9693	0.9693	0.9707	0.9707	0.9719	0.9719	0.9706	0.9706
26	0.9475	0.9475	0.9512	0.9513	0.9542	0.9543	0.9508	0.9509
27	0.9449	0.9449	0.9489	0.9489	0.9520	0.9521	0.9484	0.9485
28	0.9335	0.9335	0.9383	0.9384	0.9422	0.9423	0.9378	0.9379
29	0.9253	0.9253	0.9308	0.9309	0.9351	0.9353	0.9302	0.9302
30	0.9217	0.9217	0.9275	0.9276	0.9321	0.9323	0.9269	0.9269
31	0.9176	0.9176	0.9237	0.9238	0.9286	0.9287	0.9230	0.9231
32	0.9166	0.9166	0.9228	0.9229	0.9278	0.9279	0.9222	0.9222
33	0.9164	0.9164	0.9226	0.9227	0.9275	0.9277	0.9219	0.9220

CIM = Current Injection Method; PM = Proposed Method

Table 2.3 Comparison of voltage magnitudes of IEEE 69-bus *RDN* for different Load models

Bus No.	CP Load		CI Load		CZ Load		CZIP Load	
	CIM [18]	PM	CIM [18]	PM	CIM [18]	PM	CIM [18]	PM
	Voltage (p.u.)	Voltage (p.u.)	Voltage (p.u.)	Voltage (p.u.)	Voltage (p.u.)	Voltage (p.u.)	Voltage (p.u.)	Voltage (p.u.)
1	1.0000	1.0000	1.0000	1.0000	1.0000	1.0000	1.0000	1.0000
2	1.0000	1.0000	1.0000	1.0000	1.0000	1.0000	1.0000	1.0000
3	0.9999	0.9999	0.9999	0.9999	0.9999	0.9999	0.9999	0.9999
4	0.9998	0.9998	0.9998	0.9998	0.9999	0.9999	0.9998	0.9998
5	0.9990	0.9990	0.9991	0.9991	0.9991	0.9991	0.9991	0.9991
6	0.9901	0.9901	0.9908	0.9908	0.9913	0.9913	0.9907	0.9907
7	0.9808	0.9808	0.9821	0.9821	0.9831	0.9832	0.9819	0.9820
8	0.9786	0.9786	0.9800	0.9801	0.9812	0.9812	0.9799	0.9799
9	0.9774	0.9774	0.9790	0.9790	0.9802	0.9802	0.9788	0.9788
10	0.9724	0.9724	0.9742	0.9742	0.9755	0.9756	0.9740	0.9740
26	0.9564	0.9564	0.9587	0.9588	0.9607	0.9608	0.9585	0.9585
27	0.9563	0.9563	0.9587	0.9588	0.9607	0.9608	0.9585	0.9585
28	0.9999	0.9999	0.9999	0.9999	0.9999	0.9999	0.9999	0.9999
29	0.9999	0.9999	0.9999	0.9999	0.9999	0.9999	0.9999	0.9999
44	0.9985	0.9985	0.9985	0.9985	0.9985	0.9985	0.9985	0.9985
45	0.9984	0.9984	0.9984	0.9984	0.9984	0.9984	0.9984	0.9984
46	0.9984	0.9984	0.9984	0.9984	0.9984	0.9984	0.9984	0.9984
47	0.9998	0.9998	0.9998	0.9998	0.9998	0.9998	0.9998	0.9998
48	0.9985	0.9985	0.9986	0.9986	0.9986	0.9986	0.9986	0.9986
49	0.9947	0.9947	0.9947	0.9947	0.9948	0.9948	0.9947	0.9947
50	0.9942	0.9942	0.9942	0.9942	0.9942	0.9943	0.9942	0.9942
51	0.9785	0.9785	0.9800	0.9800	0.9811	0.9812	0.9798	0.9799
52	0.9785	0.9785	0.9800	0.9800	0.9811	0.9812	0.9798	0.9798
53	0.9747	0.9747	0.9764	0.9765	0.9778	0.9779	0.9762	0.9763
54	0.9714	0.9714	0.9735	0.9735	0.9751	0.9752	0.9732	0.9733
55	0.9669	0.9669	0.9694	0.9694	0.9713	0.9714	0.9691	0.9692
56	0.9626	0.9626	0.9654	0.9655	0.9676	0.9677	0.9651	0.9651
64	0.9098	0.9098	0.9172	0.9175	0.9230	0.9236	0.9164	0.9167
65	0.9092	0.9092	0.9167	0.9170	0.9226	0.9232	0.9158	0.9161
66	0.9713	0.9713	0.9730	0.9731	0.9744	0.9745	0.9728	0.9729
67	0.9713	0.9713	0.9730	0.9731	0.9744	0.9745	0.9728	0.9729
68	0.9679	0.9679	0.9697	0.9698	0.9713	0.9713	0.9695	0.9696
69	0.9679	0.9679	0.9697	0.9698	0.9713	0.9713	0.9695	0.9696

CIM = Current Injection Method; PM = Proposed Method

Table 2.4 Comparison of voltage magnitudes of TPC 84-bus *RDN* for different Load models

Bus No.	CP Load		CI Load		CZ Load		CZIP Load	
	CIM [18]	PM	CIM [18]	PM	CIM [18]	PM	CIM [18]	PM
	Voltage (p.u.)	Voltage (p.u.)	Voltage (p.u.)	Voltage (p.u.)	Voltage (p.u.)	Voltage (p.u.)	Voltage (p.u.)	Voltage (p.u.)
1	1.0000	1.0000	1.0000	1.0000	1.0000	1.0000	1.0000	1.0000
2	0.9810	0.9810	0.9823	0.9828	0.9833	0.9842	0.9821	0.9826
3	0.9665	0.9665	0.9687	0.9695	0.9705	0.9720	0.9685	0.9691
4	0.9506	0.9506	0.9539	0.9550	0.9566	0.9586	0.9535	0.9545
5	0.9450	0.9450	0.9486	0.9498	0.9517	0.9538	0.9482	0.9493
6	0.9336	0.9336	0.9381	0.9395	0.9417	0.9443	0.9376	0.9388
7	0.9316	0.9316	0.9362	0.9377	0.9400	0.9427	0.9357	0.9370
8	0.9300	0.9300	0.9347	0.9362	0.9386	0.9414	0.9342	0.9356
9	0.9294	0.9294	0.9342	0.9357	0.9381	0.9409	0.9336	0.9350
10	0.9285	0.9285	0.9333	0.9349	0.9373	0.9401	0.9328	0.9342
12	0.9959	0.9959	0.9960	0.9960	0.9961	0.9961	0.9960	0.9960
24	0.9651	0.9651	0.9662	0.9665	0.9671	0.9678	0.9661	0.9664
25	0.9651	0.9651	0.9661	0.9664	0.9670	0.9677	0.9660	0.9663
26	0.9966	0.9966	0.9966	0.9967	0.9967	0.9968	0.9966	0.9967
27	0.9921	0.9921	0.9923	0.9923	0.9924	0.9925	0.9923	0.9923
40	0.9612	0.9612	0.9624	0.9627	0.9636	0.9641	0.9623	0.9626
41	0.9611	0.9611	0.9624	0.9627	0.9635	0.9641	0.9622	0.9625
42	0.9603	0.9603	0.9615	0.9618	0.9627	0.9633	0.9614	0.9617
43	0.9601	0.9601	0.9613	0.9617	0.9625	0.9631	0.9612	0.9615
44	0.9985	0.9985	0.9985	0.9985	0.9985	0.9985	0.9985	0.9985
55	0.9670	0.9670	0.9680	0.9685	0.9690	0.9700	0.9679	0.9684
56	0.9666	0.9666	0.9677	0.9682	0.9686	0.9696	0.9676	0.9680
57	0.9909	0.9909	0.9912	0.9913	0.9915	0.9917	0.9912	0.9913
64	0.9677	0.9677	0.9687	0.9690	0.9696	0.9703	0.9686	0.9689
65	0.9675	0.9675	0.9685	0.9689	0.9694	0.9701	0.9684	0.9687
66	0.9961	0.9961	0.9963	0.9964	0.9965	0.9966	0.9963	0.9964
73	0.9488	0.9488	0.9514	0.9525	0.9536	0.9556	0.9511	0.9521
74	0.9863	0.9863	0.9866	0.9867	0.9868	0.9871	0.9866	0.9867
80	0.9576	0.9576	0.9595	0.9605	0.9612	0.9631	0.9593	0.9602
81	0.9544	0.9544	0.9565	0.9576	0.9583	0.9604	0.9562	0.9572
82	0.9517	0.9517	0.9539	0.9551	0.9559	0.9580	0.9537	0.9547
83	0.9508	0.9508	0.9530	0.9542	0.9550	0.9572	0.9528	0.9538
84	0.9479	0.9479	0.9503	0.9515	0.9524	0.9546	0.9500	0.9511

CIM = Current Injection Method; PM = Proposed Method

Table 2.5 Comparison of voltage magnitudes of 136-bus *RDN* for different Load models

Bus No.	CP Load		CI Load		CZ Load		CZIP Load	
	CIM [18]	**PM**	**CIM [18]**	**PM**	**CIM [18]**	**PM**	**CIM [18]**	**PM**
	Voltage (p.u.)	Voltage (p.u.)	Voltage (p.u.)	Voltage (p.u.)	Voltage (p.u.)	Voltage (p.u.)	Voltage (p.u.)	Voltage (p.u.)
1	1.0000	1.0000	1.0000	1.0000	1.0000	1.0000	1.0000	1.0000
2	0.9910	0.9910	0.9912	0.9914	0.9914	0.9918	0.9912	0.9914
3	0.9909	0.9909	0.9912	0.9914	0.9914	0.9918	0.9911	0.9913
4	0.9850	0.9850	0.9854	0.9857	0.9858	0.9864	0.9854	0.9857
5	0.9824	0.9824	0.9829	0.9833	0.9833	0.9841	0.9828	0.9832
6	0.9785	0.9785	0.9791	0.9796	0.9796	0.9806	0.9790	0.9795
7	0.9750	0.9750	0.9757	0.9762	0.9763	0.9774	0.9756	0.9761
8	0.9747	0.9747	0.9754	0.9760	0.9760	0.9771	0.9753	0.9758
9	0.9743	0.9743	0.9749	0.9755	0.9756	0.9767	0.9749	0.9754
10	0.9738	0.9738	0.9745	0.9751	0.9752	0.9763	0.9745	0.9750
17	0.9716	0.9716	0.9723	0.9729	0.9730	0.9742	0.9722	0.9728
18	0.9913	0.9913	0.9915	0.9916	0.9917	0.9920	0.9915	0.9916
34	0.9733	0.9733	0.9739	0.9743	0.9746	0.9753	0.9739	0.9742
37	0.9733	0.9733	0.9740	0.9744	0.9746	0.9754	0.9739	0.9743
38	0.9729	0.9729	0.9736	0.9740	0.9742	0.9750	0.9735	0.9738
40	0.9909	0.9909	0.9910	0.9912	0.9912	0.9915	0.9910	0.9912
62	0.9737	0.9737	0.9743	0.9747	0.9749	0.9757	0.9743	0.9746
64	0.9999	0.9999	0.9999	0.9999	0.9999	0.9999	0.9999	0.9999
65	0.9955	0.9955	0.9956	0.9957	0.9957	0.9958	0.9956	0.9957
75	0.9771	0.9771	0.9775	0.9779	0.9780	0.9786	0.9775	0.9778
76	0.9998	0.9998	0.9998	0.9998	0.9998	0.9998	0.9998	0.9998
84	0.9720	0.9720	0.9727	0.9732	0.9734	0.9742	0.9726	0.9730
85	0.9711	0.9711	0.9718	0.9723	0.9725	0.9734	0.9717	0.9721
86	0.9997	0.9997	0.9997	0.9997	0.9997	0.9997	0.9997	0.9997
87	0.9873	0.9873	0.9875	0.9877	0.9878	0.9882	0.9875	0.9877
97	0.9734	0.9734	0.9739	0.9744	0.9745	0.9754	0.9739	0.9743
100	0.9997	0.9997	0.9997	0.9997	0.9997	0.9997	0.9997	0.9997
101	0.9939	0.9939	0.9943	0.9945	0.9946	0.9951	0.9942	0.9944
117	0.9307	0.9307	0.9352	0.9382	0.9388	0.9445	0.9347	0.9374
118	0.9307	0.9307	0.9352	0.9382	0.9388	0.9445	0.9347	0.9374
122	0.9997	0.9997	0.9997	0.9997	0.9997	0.9998	0.9997	0.9997
123	0.9848	0.9848	0.9851	0.9853	0.9854	0.9858	0.9851	0.9853
136	0.9734	0.9734	0.9740	0.9744	0.9746	0.9753	0.9739	0.9743

CIM = Current Injection Method; PM = Proposed Method

Table 2.6 Comparison of voltage magnitudes of 874-bus *RDN* for different Load models

Bus No.	CP Load		CI Load		CZ Load		CZIP Load	
	CIM [18]	**PM**	**CIM [18]**	**PM**	**CIM [18]**	**PM**	**CIM [18]**	**PM**
	Voltage (p.u.)	Voltage (p.u.)	Voltage (p.u.)	Voltage (p.u.)	Voltage (p.u.)	Voltage (p.u.)	Voltage (p.u.)	Voltage (p.u.)
1	1.0000	1.0000	1.0000	1.0000	1.0000	1.0000	1.0000	1.0000
2	0.9994	0.9994	0.9994	0.9994	0.9994	0.9994	0.9994	0.9994
3	0.9994	0.9994	0.9994	0.9994	0.9994	0.9994	0.9994	0.9994
4	0.9990	0.9990	0.9990	0.9990	0.9990	0.9990	0.9990	0.9990
5	0.9988	0.9988	0.9988	0.9988	0.9988	0.9988	0.9988	0.9988
6	0.9986	0.9986	0.9986	0.9986	0.9986	0.9986	0.9986	0.9986
7	0.9983	0.9983	0.9983	0.9983	0.9983	0.9983	0.9983	0.9983
8	0.9981	0.9981	0.9981	0.9981	0.9981	0.9981	0.9981	0.9981
9	0.9980	0.9980	0.9980	0.9980	0.9980	0.9980	0.9980	0.9980
10	0.9977	0.9977	0.9977	0.9977	0.9977	0.9977	0.9977	0.9977
91	0.9998	0.9998	0.9998	0.9998	0.9998	0.9999	0.9998	0.9998
176	0.9861	0.9861	0.9863	0.9863	0.9864	0.9865	0.9863	0.9863
178	0.9979	0.9979	0.9979	0.9980	0.9980	0.9980	0.9979	0.9979
179	0.9977	0.9977	0.9977	0.9977	0.9977	0.9977	0.9977	0.9977
291	0.9891	0.9891	0.9892	0.9892	0.9893	0.9893	0.9891	0.9892
292	0.9947	0.9947	0.9948	0.9948	0.9948	0.9948	0.9948	0.9948
312	0.9890	0.9890	0.9892	0.9892	0.9893	0.9893	0.9891	0.9892
346	0.9992	0.9992	0.9992	0.9992	0.9992	0.9992	0.9992	0.9992
461	0.9863	0.9863	0.9864	0.9865	0.9866	0.9866	0.9864	0.9864
462	0.9995	0.9995	0.9995	0.9995	0.9995	0.9995	0.9995	0.9995
463	0.9994	0.9994	0.9994	0.9994	0.9994	0.9994	0.9994	0.9994
643	0.9562	0.9562	0.9579	0.9579	0.9593	0.9594	0.9577	0.9577
644	0.9561	0.9561	0.9578	0.9578	0.9593	0.9593	0.9576	0.9576
651	0.9968	0.9968	0.9969	0.9969	0.9970	0.9970	0.9969	0.9969
695	0.9561	0.9561	0.9578	0.9578	0.9593	0.9593	0.9576	0.9576
702	0.9943	0.9943	0.9945	0.9945	0.9946	0.9946	0.9945	0.9945
703	0.9940	0.9940	0.9942	0.9942	0.9943	0.9943	0.9941	0.9941
744	0.9561	0.9561	0.9578	0.9578	0.9593	0.9593	0.9576	0.9576
820	0.9999	0.9999	0.9999	0.9999	0.9999	0.9999	0.9999	0.9999
821	0.9997	0.9997	0.9997	0.9997	0.9997	0.9997	0.9997	0.9997
873	0.9962	0.9962	0.9962	0.9962	0.9962	0.9962	0.9962	0.9962
874	0.9961	0.9961	0.9961	0.9962	0.9962	0.9962	0.9961	0.9961

CIM = Current Injection Method; PM = Proposed Method

The voltage profiles of the five *RDS* tests systems for different load models are shown in the Figures: 2.4 to 2.8. From these figures, it may be pointed out that the voltage profile for the CZ load model is significantly high as compared to the other load models. Also, it is observed that the CP load model has resulted in least voltage profile. This is mainly due to the variation of power with respect to the voltage magnitude. For CZ load model, power varies with the square of the voltage magnitude and for CI load model power varies directly with the voltage magnitude but in CP load model power does not vary with the changes in voltage magnitude. Therefore, the voltage profile of CI load model lies between CZ and CP load models.

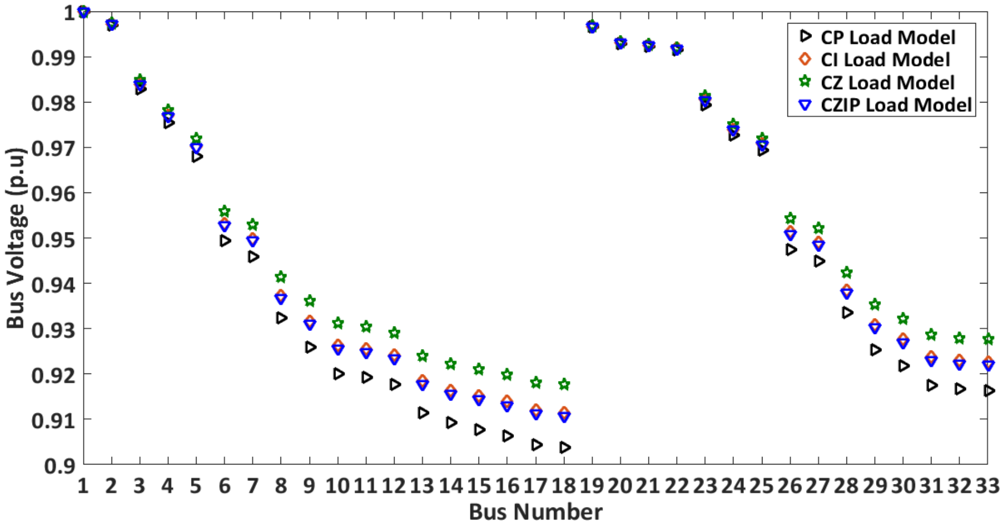

Figure 2.4 Voltage profile of the IEEE 33-bus *RDN* for different Load models

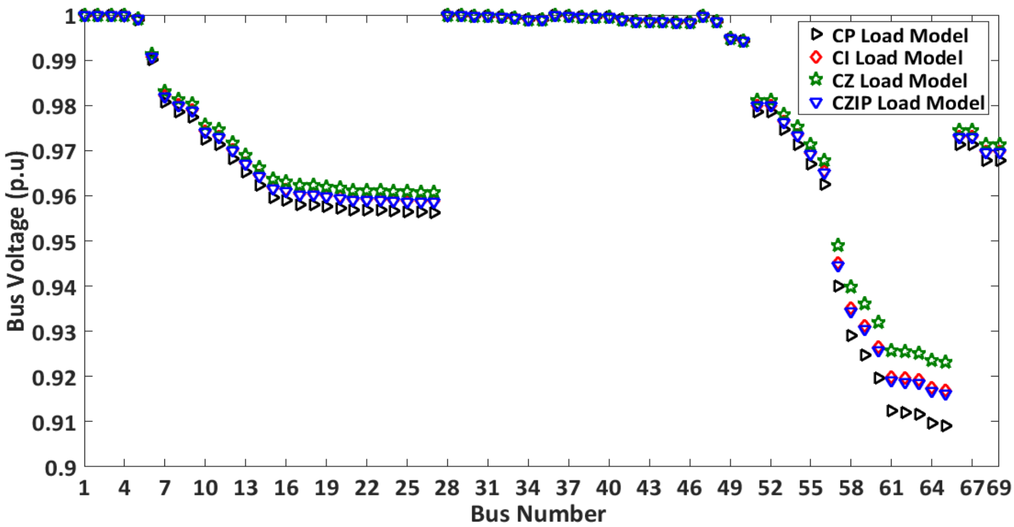

Figure 2.5 Voltage profile of the IEEE 69-bus *RDN* for different Load models

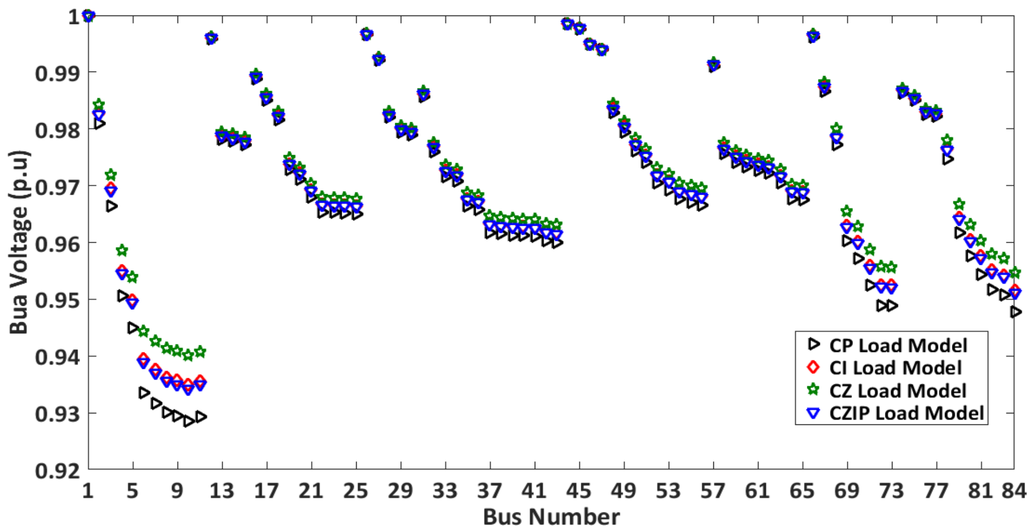

Figure 2.6 Voltage profile of the TPC 84-bus *RDN* for different Load models

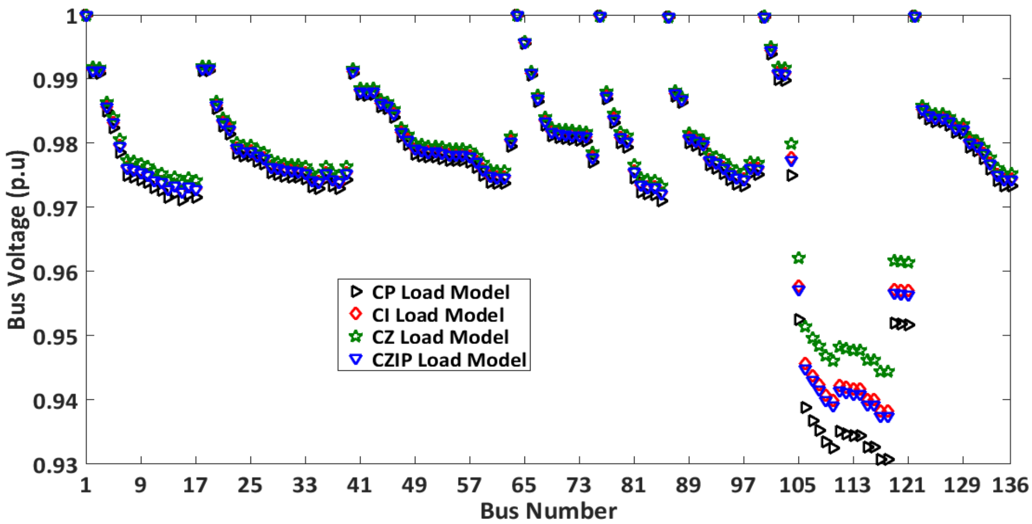

Figure 2.7 Voltage profile of the 136-bus *RDN* for different Load models

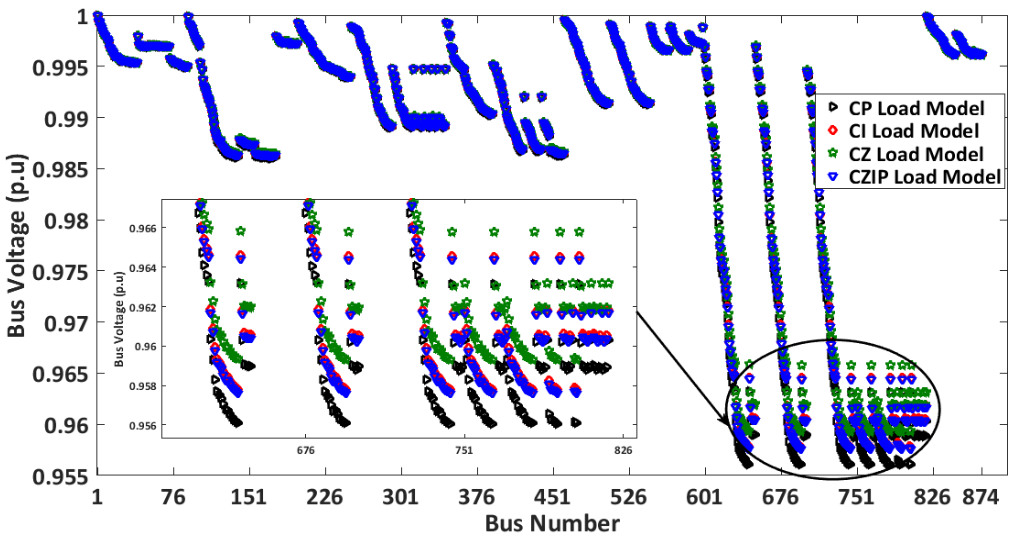

Figure 2.8 Voltage profile of the 874-bus *RDN* for different Load models

Table 2.7 to 2.11 shows the test results provided by the proposed and CIM [18] methods. The tables compare the real power loss, reactive power loss, and minimum voltage magnitude for different load models. From these tables, it is observed that the results of the proposed method are very near to the results of CIM method. Thus, it validates the simulation results of the proposed method. Furthermore, it is observed that the system with CZ load model have the low values of real and reactive power losses and a better value for the minimum node voltage as compared to the other models. This is mainly due to the variation of power with the square of the voltage magnitude.

Table 2.7 Comparison of real & reactive power losses and minimum voltage magnitude for different Load models of IEEE 33-bus *RDN*

Type of Load	**CIM [18]**			**PM**		
	Ploss (kW)	**Qloss (kVAR)**	**Vmin @ bus**	**Ploss (kW)**	**Qloss (kVAR)**	**Vmin @ bus**
CP	210.99	143.98	0.9038@18	210.98	143.02	0.9037@18
CI	182.49	123.36	0.9113@18	182.18	123.17	0.9115@18
CZ	161.19	108.71	0.9173@18	160.73	108.42	0.9176@18
CZIP	185.60	125.51	0.9105@18	185.33	125.34	0.9106@18

CIM = Current Injection Method; PM = Proposed Method

Table 2.8 Comparison of real & reactive power losses and minimum voltage magnitude for different Load models of IEEE 69-bus *RDN*

Type of Load	**CIM [18]**			**PM**		
	Ploss (kW)	**Qloss (kVAR)**	**Vmin @ bus**	**Ploss (kW)**	**Qloss (kVAR)**	**Vmin @ bus**
CP	224.96	102.14	0.9092@65	224.93	102.13	0.9091@65
CI	191.46	87.78	0.9167@65	191.46	87.78	0.9170@65
CZ	167.13	77.31	0.9226@65	167.29	77.38	0.9231@65
CZIP	195.13	89.35	0.9158@65	195.07	89.33	0.9161@65

CIM = Current Injection Method; PM = Proposed Method

Table 2.9 Comparison of real & reactive power losses and minimum voltage magnitude for different Load models of TPC 84-bus *RDN*

Type of Load	CIM [18]			PM		
	Ploss (kW)	Qloss (kVAR)	Vmin @ bus	Ploss (kW)	Qloss (kVAR)	Vmin @ bus
CP	531.99	1374.32	0.9285@10	531.97	1374.28	0.9285@10
CI	488.63	1261.54	0.9333@10	488.64	1261.56	0.9348@10
CZ	452.79	1168.27	0.9373@10	454.08	1171.72	0.9401@10
CZIP	493.24	1273.52	0.9328@10	492.88	1272.56	0.9341@10

CIM = Current Injection Method; PM = Proposed Method

Table 2.10 Comparison of real & reactive power losses and minimum voltage magnitude for different Load models of 136-bus *RDN*

Type of Load	CIM [18]			PM		
	Ploss (kW)	Qloss (kVAR)	Vmin @ bus	Ploss (kW)	Qloss (kVAR)	Vmin @ bus
CP	320.26	702.65	0.9307@117 & 118	320.25	702.62	0.9307@117 & 118
CI	297.20	651.78	0.9352@117 & 118	297.20	651.79	0.9382@117 & 118
CZ	277.98	609.44	0.9388@117 & 118	279.28	612.34	0.9444@117 & 118
CZIP	299.64	657.17	0.9347@117 & 118	299.28	656.35	0.9374@117 & 118

CIM = Current Injection Method; PM = Proposed Method

Table 2.11 Comparison of real & reactive power losses and minimum voltage magnitude for different Load models of 874-bus *RDN*

Type of Load	CIM [18]			PM		
	Ploss (kW)	Qloss (kVAR)	Vmin @ bus	Ploss (kW)	Qloss (kVAR)	Vmin @ bus
CP	1502.74	1404.40	0.9561@764	1502.62	1404.30	0.9560@764
CI	1419.68	1332.37	0.9578@764	1419.69	1332.37	0.9577@764
CZ	1347.40	1269.47	0.9593@764	1347.58	1269.61	0.9593@764
CZIP	1428.42	1339.95	0.9576@764	1428.40	1339.92	0.9576@764

CIM = Current Injection Method; PM = Proposed Method

2.6.2 Impact of different Load models on Weakly Meshed Distribution Networks

The distribution network is often operated in the Weakly Meshed mode to have the reduced power losses, better voltage profile, enhanced service reliability, *etc*. Certainly, the weakly meshed network provides the more benefits as compared to the radial network. Therefore, the simulations are also carried out on weakly meshed network by closing the Tie-lines of the network. Many of the available algorithms are not suitable for Weakly Meshed Distribution Systems. The strength of the proposed DLF method is to be examined on the Weakly Meshed Distribution Systems.

For *Weakly meshed condition*, the simulation results provided by the proposed DLF and Current Injection Method (CIM) [18] approaches are presented in Tables: 2.12 to 2.16. These tables compare the voltage magnitudes of the test systems for different load models. Furthermore, for all the test cases, the voltage magnitude at the initial buses starting from 1 to 10 and the buses at the sag end of the test systems are shown in the tables. However, for each load model the complete voltage profile of all buses is depicted in the Figures 2.9 to 2.13. From the tables 2.12-2.16, it may be pointed out that the results of the proposed method are closely matched with the results of CIM method [18]. This establishes the strength of the proposed DLF method for Weakly Meshed Distribution Systems, without any reduction in accuracy level.

The voltage profiles of the five *WMDN* test systems for different load models are shown in the Figures: 2.9 to 2.13. From these figures, it may be observed that the voltage profile for the CZ load model is significantly high as compared to the other load models. Further, as expected the voltage magnitudes of *WMDN* are significantly more as compared to the *RDN* due to the presence of the loop currents in appropriate direction of the network elements.

Tables 2.17 to 2.21 show the test results of real power loss, reactive power loss and minimum voltage magnitude experienced for different load models. These results indicate that the complex losses are perfectly matching with the results of CIM method. Furthermore, it is observed that the system with CZ load model have resulted in the low values of real and reactive power losses and improved value for 'minimum node voltage' as compared to the other models.

Table 2.12 Comparison of voltage magnitudes of IEEE 33-bus *WMDN* for different Load models

Bus No.	CP Load		CI Load		CZ Load		CZIP Load	
	CIM [18]	**PM**	**CIM [18]**	**PM**	**CIM [18]**	**PM**	**CIM [18]**	**PM**
	Voltage (p.u.)	Voltage (p.u.)	Voltage (p.u.)	Voltage (p.u.)	Voltage (p.u.)	Voltage (p.u.)	Voltage (p.u.)	Voltage (p.u.)
1	1.0000	1.0000	1.0000	1.0000	1.0000	1.0000	1.0000	1.0000
2	0.9971	0.9971	0.9972	0.9972	0.9973	0.9973	0.9972	0.9972
3	0.9863	0.9863	0.9868	0.9868	0.9872	0.9872	0.9868	0.9868
4	0.9827	0.9827	0.9833	0.9833	0.9838	0.9838	0.9832	0.9832
5	0.9793	0.9793	0.9800	0.9800	0.9807	0.9807	0.9800	0.9800
6	0.9714	0.9714	0.9724	0.9724	0.9733	0.9734	0.9723	0.9723
7	0.9705	0.9705	0.9715	0.9716	0.9725	0.9725	0.9714	0.9714
8	0.9682	0.9683	0.9694	0.9694	0.9704	0.9704	0.9693	0.9693
9	0.9651	0.9651	0.9664	0.9664	0.9675	0.9675	0.9662	0.9662
10	0.9647	0.9647	0.9660	0.9660	0.9671	0.9672	0.9659	0.9659
11	0.9647	0.9647	0.9660	0.9660	0.9671	0.9672	0.9659	0.9659
12	0.9649	0.9649	0.9662	0.9662	0.9673	0.9673	0.9660	0.9660
13	0.9615	0.9615	0.9629	0.9630	0.9642	0.9642	0.9628	0.9628
14	0.9603	0.9603	0.9618	0.9618	0.9631	0.9631	0.9616	0.9617
15	0.9600	0.9600	0.9615	0.9615	0.9628	0.9628	0.9613	0.9613
16	0.9582	0.9583	0.9598	0.9598	0.9612	0.9613	0.9596	0.9597
17	0.9548	0.9549	0.9566	0.9566	0.9581	0.9582	0.9564	0.9564
18	0.9538	0.9538	0.9556	0.9556	0.9572	0.9572	0.9554	0.9554
19	0.9953	0.9953	0.9955	0.9955	0.9956	0.9956	0.9954	0.9954
20	0.9804	0.9804	0.9811	0.9811	0.9817	0.9817	0.9810	0.9810
21	0.9763	0.9763	0.9771	0.9771	0.9778	0.9779	0.9770	0.9770
22	0.9725	0.9725	0.9735	0.9735	0.9743	0.9744	0.9734	0.9734
23	0.9808	0.9808	0.9815	0.9815	0.9821	0.9821	0.9814	0.9814
24	0.9701	0.9701	0.9712	0.9712	0.9721	0.9722	0.9711	0.9711
25	0.9628	0.9628	0.9641	0.9641	0.9654	0.9654	0.9640	0.9640
26	0.9704	0.9704	0.9715	0.9715	0.9724	0.9724	0.9713	0.9714
27	0.9691	0.9691	0.9702	0.9702	0.9712	0.9712	0.9701	0.9701
28	0.9638	0.9638	0.9652	0.9652	0.9664	0.9664	0.9650	0.9650
29	0.9603	0.9603	0.9617	0.9618	0.9631	0.9631	0.9616	0.9616
30	0.9570	0.9570	0.9586	0.9587	0.9601	0.9601	0.9585	0.9585
31	0.9538	0.9538	0.9556	0.9556	0.9572	0.9572	0.9554	0.9554
32	0.9532	0.9532	0.9550	0.9550	0.9566	0.9567	0.9548	0.9548
33	0.9534	0.9534	0.9552	0.9552	0.9568	0.9568	0.9550	0.9550

CIM = Current Injection Method; PM = Proposed Method

Table 2.13 Comparison of voltage magnitudes of IEEE 69-bus *WMDN* for different Load models

Bus No.	CP Load		CI Load		CZ Load		CZIP Load	
	CIM [18]	PM	CIM [18]	PM	CIM [18]	PM	CIM [18]	PM
	Voltage (p.u.)	Voltage (p.u.)	Voltage (p.u.)	Voltage (p.u.)	Voltage (p.u.)	Voltage (p.u.)	Voltage (p.u.)	Voltage (p.u.)
1	1.0000	1.0000	1.0000	1.0000	1.0000	1.0000	1.0000	1.0000
2	1.0000	1.0000	1.0000	1.0000	1.0000	1.0000	1.0000	1.0000
3	0.9999	0.9999	0.9999	0.9999	0.9999	0.9999	0.9999	0.9999
4	0.9999	0.9999	0.9999	0.9999	0.9999	0.9999	0.9999	0.9999
5	0.9995	0.9995	0.9995	0.9995	0.9996	0.9996	0.9995	0.9995
6	0.9955	0.9955	0.9957	0.9957	0.9958	0.9958	0.9956	0.9956
7	0.9914	0.9914	0.9916	0.9916	0.9918	0.9918	0.9916	0.9916
8	0.9904	0.9904	0.9907	0.9907	0.9909	0.9909	0.9906	0.9906
9	0.9900	0.9900	0.9902	0.9902	0.9904	0.9904	0.9902	0.9902
10	0.9867	0.9867	0.9870	0.9870	0.9873	0.9873	0.9870	0.9870
26	0.9734	0.9734	0.9742	0.9742	0.9749	0.9749	0.9741	0.9741
27	0.9729	0.9729	0.9736	0.9736	0.9743	0.9743	0.9735	0.9735
28	0.9999	0.9999	0.9999	0.9999	0.9999	0.9999	0.9999	0.9999
29	0.9999	0.9999	0.9999	0.9999	0.9999	0.9999	0.9999	0.9999
44	0.9872	0.9872	0.9875	0.9875	0.9878	0.9878	0.9875	0.9875
45	0.9865	0.9865	0.9868	0.9868	0.9871	0.9871	0.9868	0.9868
46	0.9865	0.9865	0.9868	0.9868	0.9871	0.9871	0.9868	0.9868
47	0.9998	0.9998	0.9998	0.9998	0.9998	0.9998	0.9998	0.9998
48	0.9972	0.9972	0.9972	0.9972	0.9973	0.9973	0.9972	0.9972
49	0.9888	0.9888	0.9891	0.9891	0.9893	0.9893	0.9890	0.9891
50	0.9870	0.9870	0.9873	0.9873	0.9876	0.9876	0.9873	0.9873
51	0.9904	0.9904	0.9906	0.9906	0.9908	0.9908	0.9906	0.9906
52	0.9904	0.9904	0.9906	0.9906	0.9908	0.9908	0.9906	0.9906
53	0.9891	0.9891	0.9894	0.9894	0.9896	0.9896	0.9893	0.9893
54	0.9881	0.9881	0.9884	0.9884	0.9887	0.9887	0.9884	0.9884
55	0.9867	0.9867	0.9871	0.9871	0.9874	0.9874	0.9870	0.9870
56	0.9855	0.9855	0.9858	0.9858	0.9862	0.9862	0.9858	0.9858
64	0.9662	0.9662	0.9672	0.9672	0.9681	0.9681	0.9671	0.9671
65	0.9693	0.9693	0.9702	0.9702	0.9710	0.9710	0.9701	0.9701
66	0.9859	0.9859	0.9862	0.9862	0.9866	0.9866	0.9862	0.9862
67	0.9859	0.9859	0.9862	0.9862	0.9865	0.9866	0.9862	0.9862
68	0.9829	0.9829	0.9833	0.9833	0.9837	0.9837	0.9833	0.9833
69	0.9829	0.9829	0.9833	0.9833	0.9837	0.9837	0.9833	0.9833

CIM = Current Injection Method; PM = Proposed Method

Table 2.14 Comparison of voltage magnitudes of TPC 84-bus *WMDN* for different Load models

Bus No.	CP Load		CI Load		CZ Load		CZIP Load	
	CIM [18]	**PM**	**CIM [18]**	**PM**	**CIM [18]**	**PM**	**CIM [18]**	**PM**
	Voltage (p.u.)	Voltage (p.u.)	Voltage (p.u.)	Voltage (p.u.)	Voltage (p.u.)	Voltage (p.u.)	Voltage (p.u.)	Voltage (p.u.)
1	1.0000	1.0000	1.0000	1.0000	1.0000	1.0000	1.0000	1.0000
2	0.9879	0.9879	0.9884	0.9886	0.9888	0.9893	0.9883	0.9885
3	0.9785	0.9785	0.9794	0.9798	0.9801	0.9808	0.9793	0.9796
4	0.9684	0.9684	0.9697	0.9702	0.9708	0.9718	0.9695	0.9700
5	0.9650	0.9650	0.9664	0.9670	0.9677	0.9687	0.9663	0.9668
6	0.9587	0.9587	0.9604	0.9610	0.9618	0.9631	0.9602	0.9608
7	0.9576	0.9576	0.9593	0.9600	0.9609	0.9621	0.9592	0.9598
8	0.9573	0.9573	0.9591	0.9597	0.9606	0.9619	0.9589	0.9595
9	0.9567	0.9567	0.9585	0.9592	0.9600	0.9613	0.9583	0.9589
10	0.9559	0.9559	0.9577	0.9584	0.9592	0.9606	0.9575	0.9581
12	0.9955	0.9955	0.9956	0.9956	0.9957	0.9958	0.9956	0.9956
24	0.9622	0.9622	0.9634	0.9638	0.9645	0.9653	0.9633	0.9637
25	0.9621	0.9621	0.9633	0.9638	0.9644	0.9653	0.9632	0.9636
26	0.9954	0.9954	0.9955	0.9956	0.9956	0.9957	0.9955	0.9956
27	0.9894	0.9894	0.9897	0.9898	0.9899	0.9901	0.9897	0.9897
40	0.9780	0.9780	0.9785	0.9786	0.9789	0.9792	0.9784	0.9786
41	0.9776	0.9776	0.9781	0.9783	0.9785	0.9788	0.9781	0.9782
42	0.9772	0.9772	0.9777	0.9778	0.9781	0.9784	0.9776	0.9778
43	0.9773	0.9773	0.9778	0.9780	0.9783	0.9785	0.9778	0.9779
44	0.9963	0.9963	0.9964	0.9964	0.9964	0.9965	0.9964	0.9964
55	0.9591	0.9591	0.9607	0.9614	0.9622	0.9634	0.9606	0.9612
56	0.9587	0.9587	0.9604	0.9610	0.9618	0.9631	0.9602	0.9608
57	0.9870	0.9870	0.9875	0.9878	0.9880	0.9885	0.9875	0.9877
64	0.9592	0.9592	0.9608	0.9614	0.9622	0.9635	0.9606	0.9612
65	0.9593	0.9593	0.9609	0.9616	0.9624	0.9636	0.9608	0.9614
66	0.9975	0.9975	0.9975	0.9976	0.9976	0.9977	0.9975	0.9976
73	0.9677	0.9677	0.9687	0.9690	0.9696	0.9702	0.9686	0.9689
74	0.9827	0.9827	0.9831	0.9833	0.9836	0.9839	0.9831	0.9833
80	0.9653	0.9653	0.9665	0.9670	0.9675	0.9685	0.9663	0.9668
81	0.9638	0.9638	0.9650	0.9655	0.9661	0.9671	0.9649	0.9653
82	0.9628	0.9628	0.9640	0.9645	0.9651	0.9661	0.9639	0.9643
83	0.9630	0.9630	0.9642	0.9647	0.9653	0.9662	0.9641	0.9645
84	0.9640	0.9640	0.9652	0.9656	0.9662	0.9670	0.9651	0.9654

CIM = Current Injection Method; PM = Proposed Method

Table 2.15 Comparison of voltage magnitudes of 136-bus *WMDN* for different Load models

Bus No.	CP Load		CI Load		CZ Load		CZIP Load	
	CIM [18]	**PM**	**CIM [18]**	**PM**	**CIM [18]**	**PM**	**CIM [18]**	**PM**
	Voltage (p.u.)	Voltage (p.u.)	Voltage (p.u.)	Voltage (p.u.)	Voltage (p.u.)	Voltage (p.u.)	Voltage (p.u.)	Voltage (p.u.)
1	1.0000	1.0000	1.0000	1.0000	1.0000	1.0000	1.0000	1.0000
2	0.9912	0.9912	0.9914	0.9916	0.9916	0.9920	0.9914	0.9916
3	0.9912	0.9912	0.9914	0.9916	0.9916	0.9919	0.9914	0.9915
4	0.9854	0.9854	0.9858	0.9861	0.9861	0.9867	0.9857	0.9860
5	0.9829	0.9829	0.9833	0.9837	0.9837	0.9844	0.9833	0.9836
6	0.9791	0.9791	0.9796	0.9801	0.9801	0.9809	0.9796	0.9800
7	0.9757	0.9757	0.9763	0.9768	0.9769	0.9778	0.9762	0.9767
8	0.9753	0.9753	0.9759	0.9764	0.9765	0.9775	0.9759	0.9763
9	0.9750	0.9750	0.9757	0.9762	0.9763	0.9772	0.9756	0.9761
10	0.9751	0.9751	0.9757	0.9762	0.9763	0.9772	0.9756	0.9761
17	0.9726	0.9726	0.9733	0.9738	0.9739	0.9749	0.9732	0.9736
18	0.9903	0.9903	0.9905	0.9907	0.9908	0.9911	0.9905	0.9907
34	0.9712	0.9712	0.9719	0.9724	0.9726	0.9736	0.9718	0.9723
37	0.9715	0.9715	0.9722	0.9727	0.9729	0.9739	0.9721	0.9726
38	0.9710	0.9710	0.9718	0.9723	0.9725	0.9735	0.9717	0.9722
40	0.9887	0.9887	0.9890	0.9893	0.9893	0.9897	0.9890	0.9892
62	0.9699	0.9699	0.9707	0.9713	0.9715	0.9725	0.9707	0.9711
64	0.9998	0.9998	0.9998	0.9998	0.9998	0.9998	0.9998	0.9998
65	0.9939	0.9939	0.9941	0.9942	0.9942	0.9944	0.9940	0.9941
75	0.9719	0.9719	0.9726	0.9731	0.9733	0.9742	0.9725	0.9730
76	0.9998	0.9998	0.9998	0.9998	0.9998	0.9998	0.9998	0.9998
84	0.9730	0.9730	0.9737	0.9742	0.9744	0.9753	0.9737	0.9741
85	0.9726	0.9726	0.9733	0.9738	0.9740	0.9750	0.9733	0.9737
86	0.9997	0.9997	0.9997	0.9997	0.9997	0.9997	0.9997	0.9997
87	0.9886	0.9886	0.9888	0.9890	0.9890	0.9894	0.9888	0.9890
97	0.9741	0.9741	0.9748	0.9753	0.9754	0.9764	0.9747	0.9752
100	0.9998	0.9998	0.9998	0.9998	0.9998	0.9998	0.9998	0.9998
101	0.9958	0.9958	0.9959	0.9960	0.9960	0.9961	0.9959	0.9959
117	0.9652	0.9652	0.9662	0.9668	0.9671	0.9682	0.9661	0.9666
118	0.9652	0.9652	0.9662	0.9668	0.9671	0.9682	0.9661	0.9666
122	0.9998	0.9998	0.9998	0.9998	0.9998	0.9998	0.9998	0.9998
123	0.9867	0.9867	0.9870	0.9873	0.9873	0.9878	0.9870	0.9872
136	0.9729	0.9729	0.9736	0.9741	0.9743	0.9752	0.9735	0.9740

CIM = Current Injection Method; PM = Proposed Method

Table 2.16 Comparison of voltage magnitudes of 874-bus *WMDN* for different Load models

Bus No.	CP Load		CI Load		CZ Load		CZIP Load	
	CIM [18]	**PM**	**CIM [18]**	**PM**	**CIM [18]**	**PM**	**CIM [18]**	**PM**
	Voltage (p.u.)	Voltage (p.u.)	Voltage (p.u.)	Voltage (p.u.)	Voltage (p.u.)	Voltage (p.u.)	Voltage (p.u.)	Voltage (p.u.)
1	1.0000	1.0000	1.0000	1.0000	1.0000	1.0000	1.0000	1.0000
2	0.9994	0.9994	0.9994	0.9994	0.9994	0.9994	0.9994	0.9994
3	0.9993	0.9993	0.9994	0.9994	0.9994	0.9994	0.9994	0.9994
4	0.9989	0.9989	0.9989	0.9989	0.9989	0.9989	0.9989	0.9989
5	0.9988	0.9988	0.9988	0.9988	0.9988	0.9988	0.9988	0.9988
6	0.9984	0.9984	0.9984	0.9984	0.9985	0.9985	0.9984	0.9984
7	0.9981	0.9981	0.9981	0.9981	0.9981	0.9981	0.9981	0.9981
8	0.9979	0.9979	0.9979	0.9979	0.9979	0.9979	0.9979	0.9979
9	0.9978	0.9978	0.9978	0.9978	0.9978	0.9978	0.9978	0.9978
10	0.9975	0.9975	0.9975	0.9975	0.9975	0.9975	0.9975	0.9975
91	0.9996	0.9996	0.9997	0.9997	0.9997	0.9997	0.9997	0.9997
176	0.9942	0.9942	0.9942	0.9942	0.9942	0.9942	0.9942	0.9942
178	0.9969	0.9969	0.9969	0.9969	0.9969	0.9969	0.9969	0.9969
179	0.9964	0.9964	0.9965	0.9965	0.9965	0.9965	0.9965	0.9965
291	0.9956	0.9956	0.9957	0.9957	0.9957	0.9957	0.9957	0.9957
292	0.9956	0.9956	0.9957	0.9957	0.9957	0.9957	0.9957	0.9957
312	0.9957	0.9957	0.9957	0.9957	0.9957	0.9957	0.9957	0.9957
346	0.9994	0.9994	0.9994	0.9994	0.9994	0.9994	0.9994	0.9994
461	0.9945	0.9945	0.9945	0.9945	0.9945	0.9945	0.9945	0.9945
462	0.9993	0.9993	0.9993	0.9993	0.9993	0.9993	0.9993	0.9993
463	0.9992	0.9992	0.9992	0.9992	0.9992	0.9992	0.9992	0.9992
643	0.9945	0.9946	0.9946	0.9946	0.9946	0.9946	0.9946	0.9946
644	0.9950	0.9950	0.9951	0.9951	0.9951	0.9951	0.9951	0.9951
651	0.9992	0.9992	0.9992	0.9992	0.9992	0.9992	0.9992	0.9992
695	0.9953	0.9953	0.9953	0.9953	0.9953	0.9953	0.9953	0.9953
702	0.9986	0.9986	0.9986	0.9986	0.9986	0.9986	0.9986	0.9986
703	0.9985	0.9985	0.9985	0.9985	0.9985	0.9985	0.9985	0.9985
744	0.9952	0.9952	0.9953	0.9953	0.9953	0.9953	0.9953	0.9953
820	0.9996	0.9996	0.9996	0.9996	0.9996	0.9996	0.9996	0.9996
821	0.9993	0.9993	0.9993	0.9993	0.9993	0.9993	0.9993	0.9993
873	0.9965	0.9965	0.9965	0.9965	0.9965	0.9965	0.9965	0.9965
874	0.9951	0.9951	0.9951	0.9951	0.9951	0.9951	0.9951	0.9951

CIM = Current Injection Method; PM = Proposed Method

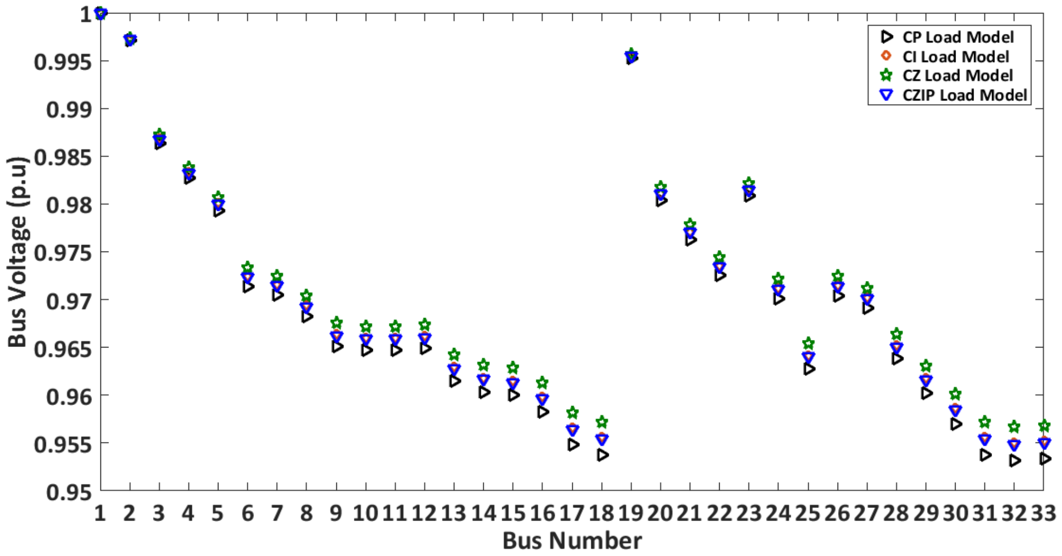

Figure 2.9 Voltage profile of the IEEE 33-bus *WMDN* for different Load models

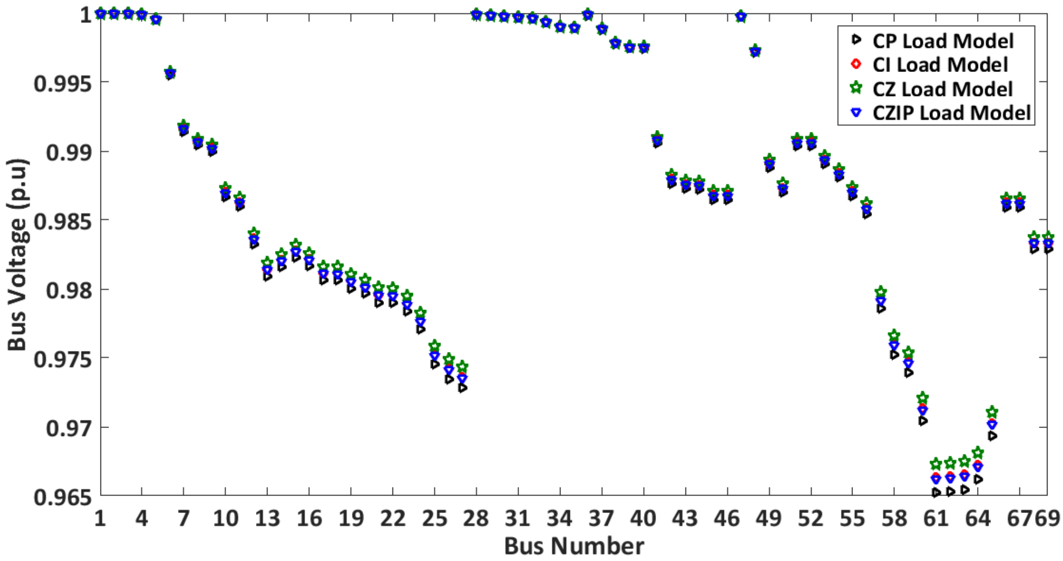

Figure 2.10 Voltage profile of the IEEE 69-bus *WMDN* for different Load models

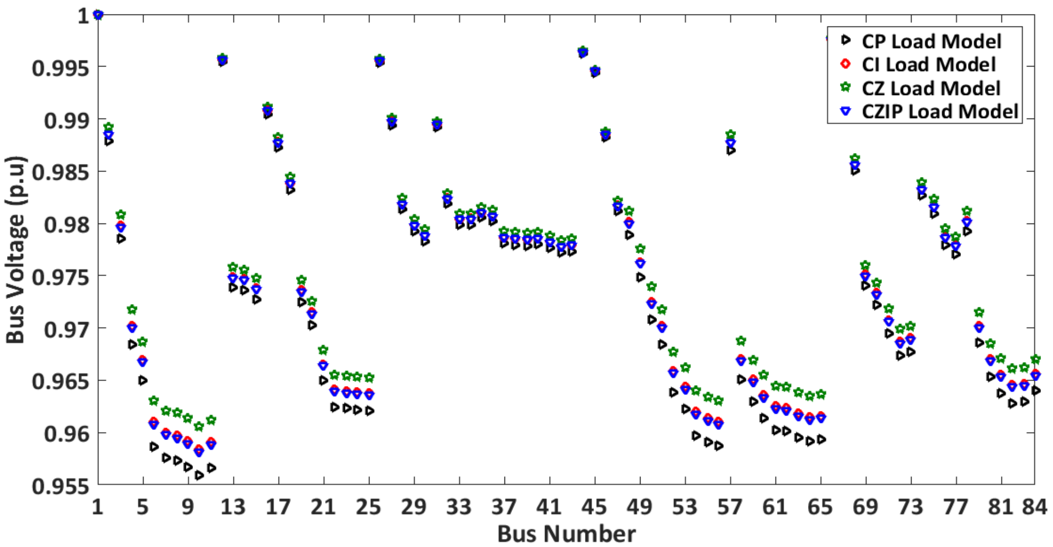

Figure 2.11 Voltage profile of the TPC 84-bus *WMDN* for different Load models

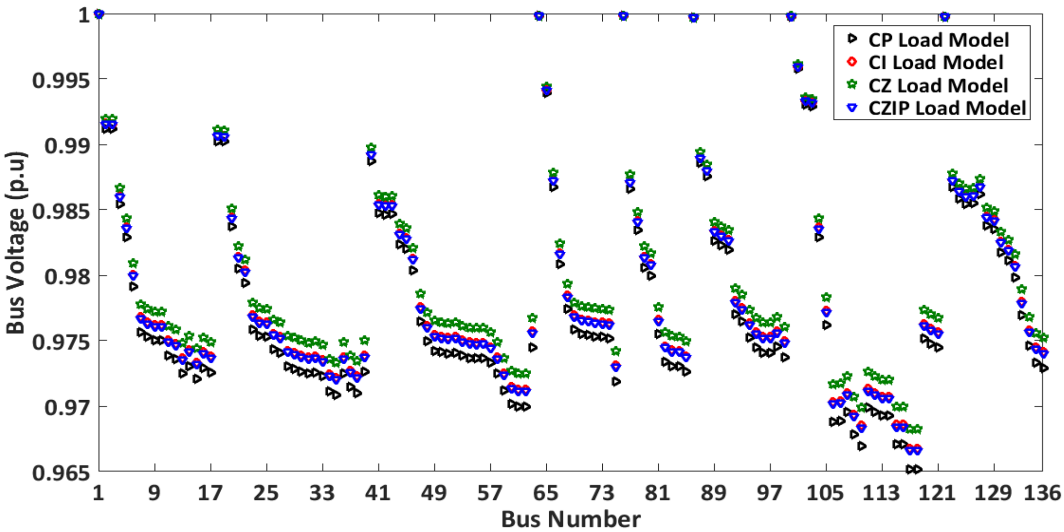

Figure 2.12 Voltage profile of the 136-bus *WMDN* for different Load models

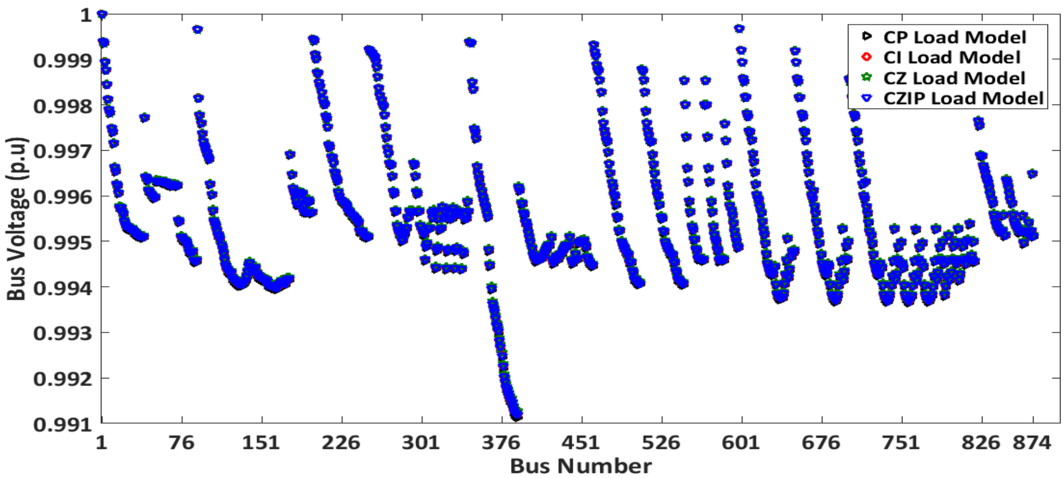

Figure 2.13 Voltage profile of the 874-bus *WMDN* for different Load models

Table 2.17 Comparison of real & reactive power losses and minimum voltage magnitude for different Load models of IEEE 33-bus *WMDN*

Type of Load	CIM [18]			PM		
	Ploss (kW)	Qloss (kVAR)	Vmin @ bus	Ploss (kW)	Qloss (kVAR)	Vmin @ bus
CP	123.37	88.34	0.9532@32	123.35	88.33	0.9532@32
CI	114.47	81.91	0.9550@32	114.41	81.86	0.9550@32
CZ	106.81	76.37	0.9566@32	106.71	76.30	0.9566@32
CZIP	115.41	82.59	0.9548@32	115.36	82.55	0.9548@32

CIM = Current Injection Method; PM = Proposed Method

Table 2.18 Comparison of real & reactive power losses and minimum voltage magnitude for different Load models of IEEE 69-bus *WMDN*

Type of Load	CIM [18]			PM		
	Ploss (kW)	Qloss (kVAR)	Vmin @ bus	Ploss (kW)	Qloss (kVAR)	Vmin @ bus
CP	82.69	65.27	0.9653@61	82.69	65.27	0.9652@61
CI	77.98	61.87	0.9663@61	77.98	61.87	0.9663@61
CZ	73.80	58.83	0.9672@61	73.81	58.83	0.9672@61
CZIP	78.48	62.22	0.9662@61	78.48	62.22	0.9661@61

CIM = Current Injection Method; PM = Proposed Method

Table 2.19 Comparison of real & reactive power losses and minimum voltage magnitude for different Load models of TPC 84-bus *WMDN*

Type of Load	CIM [18]			PM		
	Ploss (kW)	Qloss (kVAR)	Vmin @ bus	Ploss (kW)	Qloss (kVAR)	Vmin @ bus
CP	462.68	1164.02	0.9559@10	462.67	1164.01	0.9558@10
CI	433.55	1090.36	0.9577@10	433.55	1090.36	0.9583@10
CZ	408.07	1025.98	0.9592@10	408.73	1027.65	0.9605@10
CZIP	436.60	1098.09	0.9575@10	436.42	1097.63	0.9580@10

CIM = Current Injection Method; PM = Proposed Method

Table 2.20 Comparison of real & reactive power losses and minimum voltage magnitude for different Load models of 136-bus *WMDN*

Type of Load	CIM [18]			PM		
	Ploss (kW)	**Qloss (kVAR)**	**Vmin @ bus**	**Ploss (kW)**	**Qloss (kVAR)**	**Vmin @ bus**
CP	271.76	588.48	0.9652@117 & 118	271.75	588.45	0.9651@117 & 118
CI	258.03	558.98	0.9662@117 & 118	258.03	558.97	0.9667@117 & 118
CZ	245.65	532.37	0.9671@117 & 118	246.13	533.40	0.9682@117 & 118
CZIP	259.46	562.04	0.9661@117 & 118	259.34	561.78	0.9666@117 & 118

CIM = Current Injection Method; PM = Proposed Method

Table 2.21 Comparison of real & reactive power losses and minimum voltage magnitude for different Load models of 874-bus *WMDN*

Type of Load	CIM [18]			PM		
	Ploss (kW)	**Qloss (kVAR)**	**Vmin @ bus**	**Ploss (kW)**	**Qloss (kVAR)**	**Vmin @ bus**
CP	463.56	548.79	0.9911@391	463.54	548.76	0.9911@391
CI	458.84	543.24	0.9912@391	458.84	543.24	0.9912@391
CZ	454.21	537.81	0.9913@391	454.19	537.78	0.9912@391
CZIP	459.31	543.80	0.9912@391	459.31	543.80	0.9911@391

CIM = Current Injection Method; PM = Proposed Method

From the above discussion, it may be concluded that as compared to the *RDN*, the *WMDN* provides the lower system losses and better voltage profile due to the presence of the loops. The results reported in Table 2.7 and 2.17 confirm this observation. In these tables, for *CP load model*, the real power loss is reduced from 210.98 kW to 123.35 kW, reactive power loss from 143.02 kVAR to 88.33 kVAR and the 'minimum node voltage' has been improved from 0.9037 p.u to 0.9532 p.u. Similar kind of improvements can be noticed in all the case studies.

2.7 Iteration Count and CPU Time

The strength of any effective algorithm is measured in terms of accuracy of the results, number iterations, promised convergency for all operating conditions, and required solution time. The accuracy aspect of the results produced by the proposed DLF method has been analyzed in the above discussion. To assess the total solution time, the following tables have been reported.

Table 2.22 and Table 2.23 show the number of iterations and CPU time taken by the proposed DLF method and Current Injection Method (CIM) [18] for *CP load model*. From these Tables 2.22 and 2.23, it is observed that the proposed method is much faster than CIM and the proposed method converges within a few iterations (2 to 4) even for bigger size system of 874 bus system. In all the case studies, the proposed method has shown superior performance. The proposed method is 4 to 10 times faster than the method in [18] for all case studies except for 874 bus system. For 874 bus RDN, proposed method is 130.52 times faster than the CIM and for weakly meshed network it is only 39.01 times faster due to the presence of loops.

The proposed DLF method is simple, accurate, and very effective for small to large size Radial and Weakly Meshed Distribution System studies. This goes as significant new contribution and can be used as supporting powerful tool in distribution network studies.

Table 2.22 Number of Iterations and CPU time comparison for *RDN*

RDN Test Systems	**CIM [18]**		**PM**		**Ratio = t_1/t_2**
	Itr	**CPU time (s), t_1**	**Itr**	**CPU time (s), t_2**	
IEEE 33 Bus	4	0.657155	4	0.118755	5.53
IEEE 69 Bus	4	0.926907	4	0.151645	6.11
TPC 84 Bus	4	1.076354	4	0.173748	6.19
136 Bus System	4	2.566460	4	0.235871	10.88
874 Bus System	4	693.8026	3	5.315800	130.52

CIM = Current Injection Method; PM = Proposed Method; Itr = Number of iterations

Table 2.23 Number of Iterations and CPU time comparison for *WMDN*

WNDN Test Systems	CIM [18]		PM		Ratio = t_1/t_2
	Itr	CPU time (s), t_1	Itr	CPU time (s), t_2	
IEEE 33 Bus	3	0.658372	3	0.132299	4.98
IEEE 69 Bus	3	0.843850	3	0.179944	4.69
TPC 84 Bus	4	1.114831	4	0.274654	4.06
136 Bus System	4	2.580557	3	0.545324	4.73
874 Bus System	3	576.7975	2	14.785645	39.01

CIM = Current Injection Method; PM = Proposed Method; Itr = Number of iterations

2.8 Test Results on Simulated Ill conditioned system

Many of the algorithms may exhibit good convergence characteristics for normal Distribution Networks. But they exhibit poor convergence under ill-conditioned cases. Any good algorithm should have promised convergence characteristics for both normal and ill-conditioned systems. To address this aspect also, the proposed DLF is tested on ill-conditioned networks. The power distribution network sometimes may face the following practical situations leading to ill-conditioned system operation.

(1) The X/R ratio of the network may be too low.

(2) Some of the elements (distribution transformers, lines, *etc*.,) of the Distribution Network may be over loaded (more than full load).

Table 2.24 and 2.25 report the performance of the proposed DLF method on *RDN* and *WMDN* test systems, respectively. The investigation is carried out under *CP load model*. The performance of DLF is evaluated with respect to different tolerance values for convergence, several X/R ratios, and various loading conditions. From the tables 2.24 and 2.25, it may be pointed out that the proposed method is not having any divergence problem for the variation of tolerance values (0.01 to 0.00001 p.u), increase of system resistance (1.5r to 4r, to simulate low X/R condition), and rise of load (1 to 3 times the original load, to simulate overload condition). However, the number of the iterations are getting increased for the increase of accuracy level, resistance, and loading values. The results presented in Table 2.22, 2.23, 2.24, and 2.25 are clearly establishing the promised convergence of the proposed DLF with reduced CPU burden for both *RDN* and *WMDN* systems.

Table 2.24 Variation of Iteration Count for ill conditioned *RDN*

Tolerance Value	No. of iterations				
	IEEE 33 bus	**IEEE 69 bus**	**TPC 84 bus**	**136 - bus**	**874 - bus**
0.01	2	2	2	2	2
0.001	3	3	3	3	3
0.0001	4	4	4	4	3
0.00001	5	5	5	5	5
X/R ratio at 0.0001 tolerance level					
1.5r+jx	5	5	4	4	4
2r+jx	5	6	4	5	4
2.5r+jx	6	7	5	5	4
3r+jx	8	10	5	5	5
3.5r+jx	9	17	5	6	5
4r+jx	14	19	6	6	5
Loading factor at 0.0001 tolerance level					
1.0	4	4	4	4	4
1.5	5	5	5	5	4
2.0	6	6	6	6	4
2.5	8	8	7	7	5
3.0	11	14	9	10	5

Table 2.25 Variation of Iteration Count for ill conditioned *WMDN*

Tolerance Value	No. of iterations				
	IEEE 33 bus	IEEE 69 bus	TPC 84 bus	136 - bus	874 - bus
0.01	2	2	2	2	1
0.001	3	3	3	3	2
0.0001	3	3	4	3	2
0.00001	4	4	4	4	3
X/R ratio at 0.0001 tolerance level					
1.5r+jx	4	3	4	3	3
2r+jx	4	4	4	4	3
2.5r+jx	4	4	4	4	3
3r+jx	5	4	4	4	3
3.5r+jx	5	4	4	4	3
4r+jx	5	5	4	4	3
Loading factor at 0.0001 tolerance level					
1.0	3	3	4	3	2
1.5	4	4	4	4	3
2.0	4	4	5	4	3
2.5	5	4	5	4	3
3.0	5	5	6	5	3

This part of the work was presented as "An efficient Power Flow Method for Distribution System Studies under various load models," *13th International IEEE India Conference INDICON 2016*, 16-18 Dec 2016. IISc Banglore, Page(s):1-6. DOI:10.1109/INDICON.2016.7838992.

2.9 Summary

This chapter has discussed the development and implementation of the proposed effective Distribution Load Flow (DLF) method for both Radial and Weakly meshed distribution systems. The strength of the proposed method is demonstrated on five benchmark distribution systems *viz*., IEEE 33-, IEEE 69-, TPC 84-, 136, and 874 bus (both Radial and Weakly meshed) for different load models. The Constant Power (CP), Constant Current (CI), Constant Impedance (CZ), and Composite (CZIP) load models are considered to analyze their impact on the voltage profile of the tests systems. Furthermore, it is investigated the performance of the proposed DLF on simulated ill-conditioned network.

As the proposed DLF method has shown excellent convergence characteristics with reduced CPU burden even on large size test systems for *RDN* and *WMDN*, it can act as major supporting tool in all optimization studies where large number of load flow studies are indispensable.

The next stage of the investigation is focused on the Optimal Placement and Sizing of the Distributed Generation (DG) units. An Analytical Method is developed for solving the Optimal Deployment of Distributed Generation (ODDG) problem by considering the four objective functions subjected to different constraints and same is reported in Chapter-3.

CHAPTER-3

Analytical Approach for Multi-objective Optimal Accommodation of DG Unit

3.1 Introduction

Unlike, the traditional and conventional centralized generation, Distributed Generation (DG) is a modular, decentralized, and more flexible technology that directly connected to the distribution network where the generated power from the DG unit is consumed by the end users locally. Integration of DG units into the traditional power distribution network has increased rapidly in recent years. This rampant increase of DG penetration is due to the technical, economical, and environmental benefits offered by the DG units. In order to get these benefits, the DG units should be optimally placed and sized.

Optimal placement and sizing of DG units in distribution network is a complex, combinatorial, and mixed integer non linear problem. To solve this complex problem, numerous analytical and meta-heuristic methods have been proposed with various objective functions subjected to different operational system constraints. These methods have shown some merits and demerits while solving the DG placement and sizing problem. In this Chapter, a simple but more effective Analytical approach is proposed to solve the Optimal Deployment of Distributed Generation (ODDG) problem aiming at single and multi-objective cases.

3.2 Methodology to find the optimal location for the placement of DG unit

Normally, DG units are accommodated in the distribution system to optimize certain objectives that include real power loss minimization, reduction of reactive power losses, enhancement of voltage stability margin, improvement of voltage profile, increasing of system reliability, reduction of gas emissions, increase of annual savings, *etc*. In order to attain these objective functions, the DG units should be placed at candidate locations. In this thesis, an analytical method called *Branch Loss Bus Injection Index (BLBII)* is proposed to identify the candidate location for the placement of DG unit. This method is explained in the following section.

3.2.1 Proposed Branch Loss Bus Injection Index (BLBII) method

In this section, mathematical model of the proposed *BLBII* method has been presented to find the optimal location for the placement of DG unit. A simple radial distribution system is shown in Figure 3.1. The line has V_m and V_n as voltage magnitudes at nodes m and n, respectively. δ_m and δ_n indicate the phase angles of voltages at nodes m and n, respectively. z_k and y_k represent primitive impedance and admittance of a k^{th} - line, respectively. r_k and x_k are the primitive resistance and reactance of the k^{th}-line, respectively. I_k is the current flowing in the line-k.

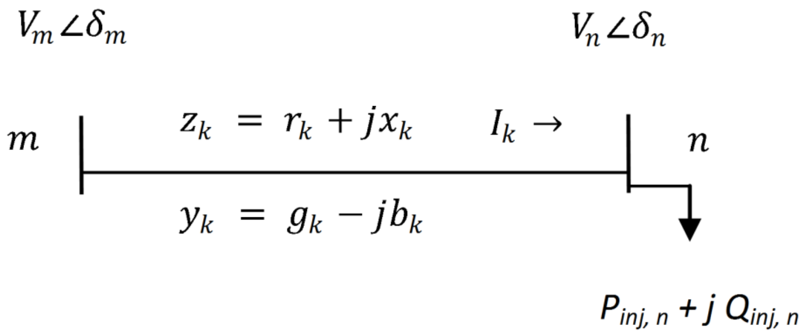

Figure 3.1 Typical representation of Power Distribution Network

The loss in the k^{th}-branch may be expressed in terms of complex power flows S_{mn} & S_{nm} as in Eq. (3.1):

$$\left.\begin{aligned} Sloss_k &= S_{mn} + S_{nm} = V_m I_{mn}^{*} + V_n I_{nm}^{*}; \\ I_{mn} &= I_k; \\ I_{nm} &= -I_k; \end{aligned}\right\} \qquad (3.1)$$

where I_{mn} = the branch current flowing from node-m to node-n;

I_{nm} = the branch current flowing from node-n to node-m;

I_k = current flowing through the k^{th}-line.

On manipulating Eq. (3.1), the complex power loss of the k^{th}-line can be represented as Eq. (3.2)

$$Sloss_k = (V_m - V_n) I_k^* \;; \tag{3.2}$$

Further, the branch current I_k can be expressed as in Eq. (3.3)

$$I_k = (V_m - V_n) y_k \;; \tag{3.3}$$

Substitute Eq. (3.3) in Eq. (3.2). Then, the final expression for complex power loss of line-*k* is as follows:

$$Sloss_k = (V_m - V_n)\left((V_m - V_n) y_k\right)^* \tag{3.4}$$

The performance equation of any Radial Distribution System with *NB* buses can be expressed in terms of bus voltages V_{bus}, bus injections I_{bus}, and network matrix Z_{bus} and is shown in Eq. (3.5).

$$[V_{bus}]_{NBx1} = [Z_{bus}]_{NBxNB} [I_{bus}]_{NBx1} \tag{3.5}$$

The complex power loss of a line in terms of Z_{bus} elements may be derived as below:

On expanding Eq. (3.5), the node voltage V_m and V_n in terms of Z_{bus} elements may be expressed as in Eq. (3.6) and Eq. (3.7), respectively.

$$V_m = \sum_{i=1}^{NB} Z_{mi} I_{\mathrm{i}} \tag{3.6}$$

$$V_n = \sum_{i=1}^{NB} Z_{ni} I_{\mathrm{i}} \tag{3.7}$$

where Z_{mi} and Z_{ni}, are the elements of Z_{bus} that belong to the m^{th} row and i^{th} column and n^{th} row and i^{th} column, respectively. I_i represents the current injection at bus-*i*.

The current injection at i^{th}-bus may be expressed as in Eq. (3.8).

$$I_i = \frac{(P_{inj,i} + jQ_{inj,i})^*}{V_i^*} \tag{3.8}$$

where $P_{inj,i}$ and $Q_{inj,i}$ indicate the real and reactive power injections at bus-*i*.

Substitute Eq. (3.8) in Eq. (3.6) and Eq. (3.7). Then, the bus voltages V_m and V_n are given through Eqs. (3.9) - (3.10).

$$V_m = \sum_{i=1}^{NB} \frac{Z_{mi}(P_{inj,i} + jQ_{inj,i})^*}{V_i^*} \tag{3.9}$$

$$V_n = \sum_{i=1}^{NB} \frac{Z_{ni}(P_{inj,i} + jQ_{inj,i})^*}{V_i^*} \tag{3.10}$$

Now, substitute Eq. (3.9) and Eq. (3.10) in Eq. (3.4). Then, Eq. (3.11) represents the power loss of the *k*-line in terms of Z_{bus} elements, power injections and voltage magnitudes.

$$Sloss_k = (V_m - V_n)\left(\frac{\sum_{i=1}^{NB}(Z_{mi} - Z_{ni})\,(P_{inj,i} + jQ_{inj,i})^*(\,y_k\,)}{V_i^*} \right)^* \tag{3.11}$$

Then,

$$Sloss_k = (V_m - V_n)\left(\frac{\sum_{i=1}^{NB}(Z_{mi} - Z_{ni})\,(y_k)}{V_i^*} \right)^* (P_{inj,i} + jQ_{inj,i}) \tag{3.12}$$

For a system with *NL* as number of lines, the branch complex loss, BL_k may be written as Eq. (3.13).

$$BL_k = \sum_{i=1}^{NB} \left[\frac{(V_m - V_n)(Z_{mi} - Z_{ni})^* \, y_k{}^*}{V_i} \right] S_{inj,i} \tag{3.13}$$

where $BL_k = Sloss_k$; represents loss of branch-*k.*

$Sinj,i = [P_{inj,i} + jQ_{inj,i}]$; indicates complex power injection at bus-*i*,

and k represents the line number.

In compact matrix form, Eq. (3.13) can be expressed as shown in Eq. (3.14).

$$[BL]_k = \sum_{i=1}^{NB} [LIF_{ki}] [S_{inj,i}] \; ; \quad k = 1 \; to \; NL \tag{3.14}$$

where LIF_{ki} = Load Index Factor of the k^{th}-line due to complex power injection at bus-*i* and is given in Eq. (3.15).

$$LIF_{ki} = \left[\frac{(V_m - V_n)(Z_{mi} - Z_{ni})^* \, y_k^*}{V_i} \right] \tag{3.15}$$

The Load Index Factor (LIF_{ki}) of the k^{th}-line can be derived from i^{th}-bus voltage, Z_{bus} elements, voltage drop, and primitive admittance of k^{th}-line. The term LIF_{ki}, helps in identifying the optimal location for the accommodation of DG unit. The numerical value of LIF_{ki} of k^{th}-line depends on whether the k^{th}-line is in the path of i^{th}-bus to the source node or not. It has a non zero value if the k^{th}-line is present in the path or else its value is zero. Further, multiplication of LIF_{ki} and $S_{inj,i}$ offers in power loss of k^{th}-line due to i^{th}-bus complex power injection.

$$LIF_{ki} = \begin{cases} \text{non-zero;} & \text{if } k^{th}\text{-line is in the path of } i^{th}\text{-bus to the source node} \\ 0; & \text{Else} \end{cases}$$

***Illustration**:* Consider a simple radial distribution system of size 6-bus and 5-branches as shown in Figure 3.2. It has power injections (i.e. $S_{inj,i}$) at all buses except at source node. The branches are numbered as *L1 - L5*.

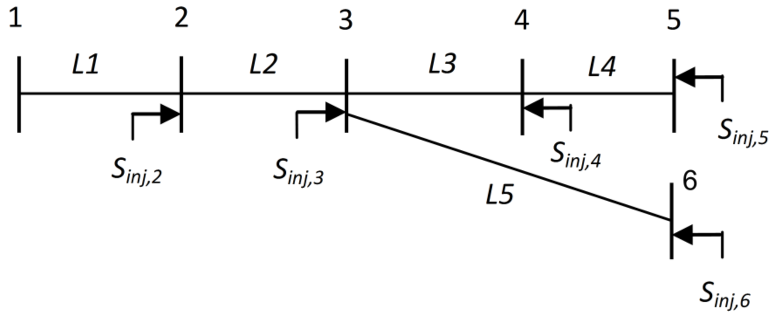

Figure 3.2 A simple 6-bus Radial Distribution System

The expansion of Eq. (3.14) for Figure 3.2 is illustrated below and is described by Eq. (3.16).

$$\begin{bmatrix} BL_1 \\ BL_2 \\ BL_3 \\ BL_4 \\ BL_5 \end{bmatrix}_{5\times1} = \begin{bmatrix} LIF_{11} & LIF_{12} & LIF_{13} & LIF_{14} & LIF_{15} & LIF_{16} \\ LIF_{21} & LIF_{22} & LIF_{23} & LIF_{24} & LIF_{25} & LIF_{26} \\ LIF_{31} & LIF_{32} & LIF_{33} & LIF_{34} & LIF_{35} & LIF_{36} \\ LIF_{41} & LIF_{42} & LIF_{43} & LIF_{44} & LIF_{45} & LIF_{46} \\ LIF_{51} & LIF_{52} & LIF_{53} & LIF_{54} & LIF_{55} & LIF_{56} \end{bmatrix}_{5\times6} \begin{bmatrix} S_{inj,1} \\ S_{inj,2} \\ S_{inj,3} \\ S_{inj,4} \\ S_{inj,5} \\ S_{inj,6} \end{bmatrix}_{6\times1} \quad (3.16)$$

The compact form of Eq. (3.16) would be as below:

$[BLM]_{5x1} = [LIFM]_{5x6}\ [SM]_{6x1}$

where *BLM*, *LIFM*, and *SM* represent the Branch Loss Matrix, Load Index Factor Matrix, and Complex Power Injection Matrix, respectively.

Some of the elements of *LIFM* matrix are zero due to the insignificant impact of power injections on the branches. For example, the influence of $S_{inj,2}$ is only on branch *L1* as this is the only line available in the path from node-2 to node-1. Hence, all the elements of column-2 of *LIFM* matrix are zero except LIF_{12}. Likewise, the $S_{inj,6}$ injection has the effect on the lines *L1*, *L2* and *L5*. Therefore, in column-6 of *LIFM* matrix, the factors LIF_{16}, LIF_{26} and LIF_{56} will be of non-zero values whereas LIF_{36} and LIF_{46} are zeros.

Based on the above discussion and similar explanation can be extended to other buses ($S_{inj,3}$, $S_{inj,4}$, *and* $S_{inj,5}$). The structure of Eq. (3.16) is reduced to Eq. (3.17) as below.

$$\begin{bmatrix} BL_1 \\ BL_2 \\ BL_3 \\ BL_4 \\ BL_5 \end{bmatrix}_{5\times1} = \begin{bmatrix} 0 & LIF_{12} & LIF_{13} & LIF_{14} & LIF_{15} & LIF_{16} \\ 0 & 0 & LIF_{23} & LIF_{24} & LIF_{25} & LIF_{26} \\ 0 & 0 & 0 & LIF_{34} & LIF_{35} & 0 \\ 0 & 0 & 0 & 0 & LIF_{45} & 0 \\ 0 & 0 & 0 & 0 & 0 & LIF_{56} \end{bmatrix}_{5\times6} \begin{bmatrix} S_{inj,1} \\ S_{inj,2} \\ S_{inj,3} \\ S_{inj,4} \\ S_{inj,5} \\ S_{inj,6} \end{bmatrix}_{6\times1} \quad (3.17)$$

Now, a term M_i for any i^{th}-bus is proposed as in Eq. (3.18). This term can be determined using either the summation of elements corresponding to the i^{th}-column of *LIFM* matrix or the addition of *LIF*s of the lines that are in the path of the i^{th}-bus to the source node. Here, M_i plays a significant role in identifying the DG location along with the term $S_{eff}(i)$ given in Eq. (3.19).

$$M_i = \sum_{k=1}^{NL} LIF_{ki} \quad (3.18)$$

As initial line losses are not available, calculate the effective complex power injection at each bus by ignoring the line losses for the radial distribution system shown in Figure 3.2. Then, the effective power injection at various buses may be computed as expressed in Eq. (3.19):

$$\left.\begin{aligned} &S_{eff}(6) = S_{inj}(6); \\ &S_{eff}(5) = S_{inj}(5); \\ &S_{eff}(4) = S_{inj}(4) + S_{eff}(5); \\ &S_{eff}(3) = S_{inj}(3) + S_{eff}(4) + S_{eff}(6); \\ &S_{eff}(2) = S_{inj}(2) + S_{eff}(3); \\ &S_{eff}(1) = S_{inj}(1) + S_{eff}(2); \end{aligned}\right\} \quad (3.19)$$

In general, the effective complex power injection at i^{th}-bus may be designated as $S_{eff}(i)$. Further, the product of magnitude of $S_{eff}(i)$ and magnitude of M_i term may be used to identify the candidate location of DG unit, and is expressed as Eq. (3.20).

$$BLBII_i = |M_i| * |S_{eff}(i)|, \qquad i = 1,2.......NB \quad (3.20)$$

The term *Branch Loss Bus Injection Index*, $BLBII_i$ of Eq. (3.20) is a product of $|M_i|$ and $|S_{eff}(i)|$ which can be used as the index for finding the optimal location of DG unit. In fact, the term $|M_i|$ given in Eq. (3.18) is fully depends on the sum of *LIF* (Load Index Factor) values of *all the lines connected between i^{th}-bus and the reference bus* (substation node). The nearness of a bus-*i* from the reference node is clearly reflected in the analytical equation of LIF_{ki} shown in Eq. (3.15). If the bus-*i* is faraway, the number of branches between bus-*i* and reference node would be more in number and the corresponding Z_{mi}, Z_{ni}, and y_k parameters will automatically account the role of these branches in loss component. Further, it is clear that the value of LIF_{ki} is also depends on V_i (voltage magnitude of bus-*i*). If V_i is more, the value of LIF_{ki} will be low and vice versa is also observed. The equation of $BLBII_i = |M_i| * |S_{eff}(i)|$ will also account the effective complex power $S_{eff}(i)$ supplied by the node-*i*. The term $BLBII_i$ will be high only when both the terms $|M_i|$ and $|S_{eff}(i)|$ are high. Further, if either one of these components is high and other is low, then the value of $BLBII_i$ would be low only. The value of $BLBII_i$ signifies its contribution in total loss component. In view of this, the $BLBII_i$ value will act as measure of identifying the potential location for DG placement.

The bus with highest *BLBII* value among all other buses is selected as the candidate location to accommodate the DG unit. If the *BLBII* values of all the buses are arranged in descending order, they clearly guide the operator in identifying the list of potential buses for DG units placement. The *BLBII* values for different benchmark test systems such as IEEE 33-bus and INDIAN 85-bus are depicted in Figure 3.3 and Figure 3.4, respectively. From figure 3.3 and figure 3.4, it may be observed that higher *BLBII* values are occurred at bus number 6 and 8 for IEEE 33-bus and INDIAN 85-bus systems, respectively. Thus, these are the potential locations to accommodate a DG unit in the power distribution system.

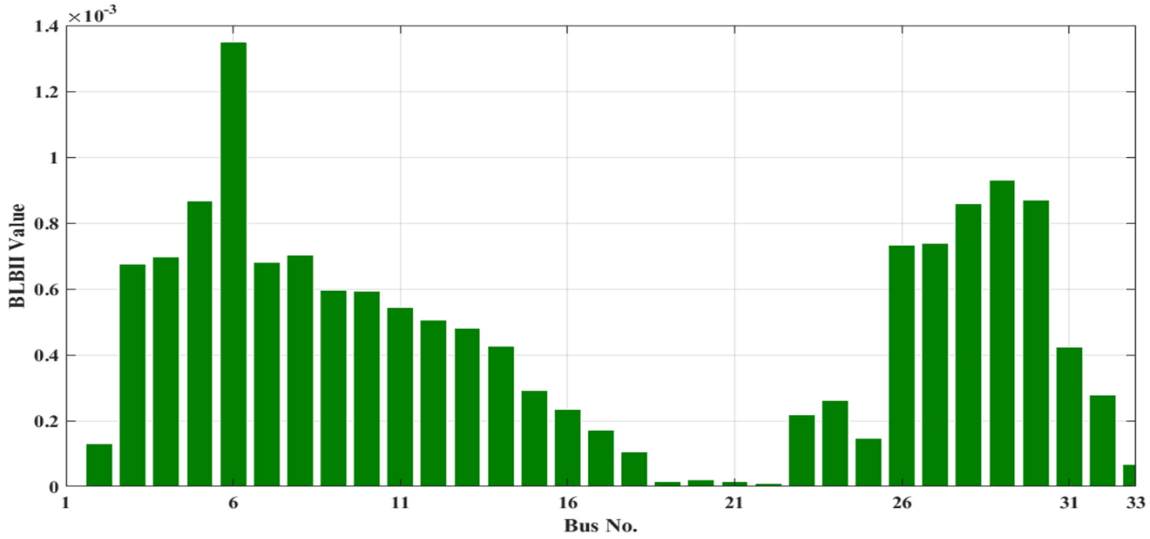

Figure 3.3 *BLBII* values for IEEE 33-bus Study System

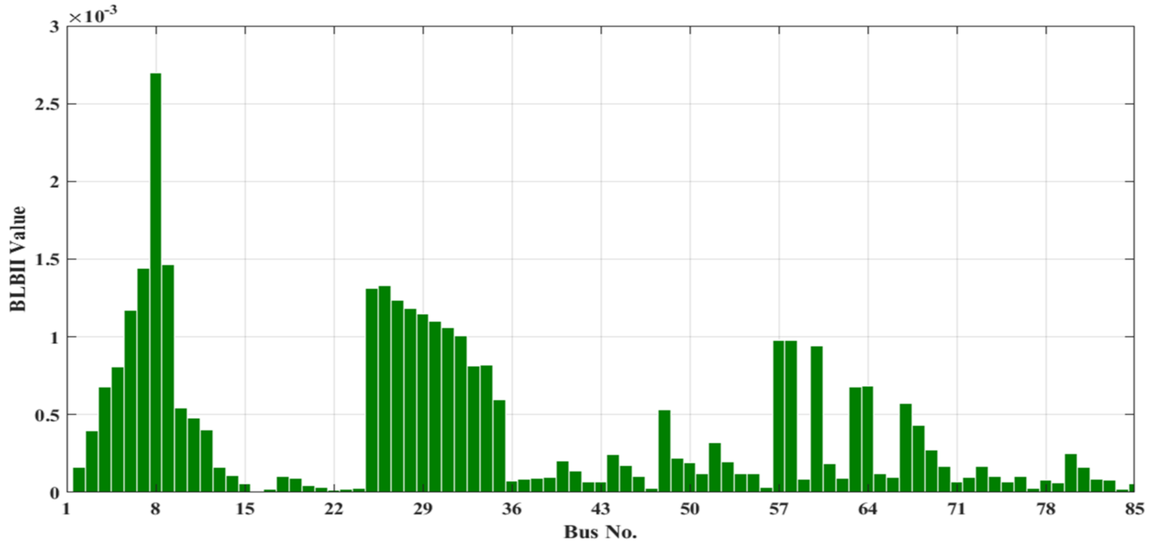

Figure 3.4 *BLBII* values for INDIAN 85-bus Study System

3.3 Objective functions

In this chapter, *four objectives* are considered to address an Optimal Deployment of DG (ODDG) problem: (i) Minimization of electrical energy losses (f_1), (ii) Minimization of overall bus voltage deviation (f_2), (iii) Maximization of overall voltage stability margin (f_3), and (iv) Minimization of Energy Not Served (f_4). These objective functions can be optimized only when the DGs are optimally placed and sized. Hence, DG locations and DG sizes are considered as the decision variables which are of discrete type in nature. The overall-objective-function that should be minimized is expressed in Eq. (3.21):

$$\min FF = \xi_1 f_1 + \xi_2 f_2 + \xi_3 f_3^{-1} + \xi_4 f_4 + \sum_{i=1}^{NC} \alpha_i C_i \qquad (3.21)$$

where ξ_1 to ξ_4 are the weight coefficients assigned to each objective and their summation should be equal to unity. For third objective function, f_3^{-1} is employed to treat the Eq. (3.21) as minimization function. The weights associated with the individual objectives are estimated by using an *Analytical Hierarchy Process* (*AHP*) [84] method which will be discussed in the **Section 3.5**. The above α_i (constant) is a i^{th}-penalty function value, imposed on the i^{th}-operational constraint (C_i) to account its violation. For minimization problem, α carries a very high numeral value to include the violation, and is zero otherwise. *NC* indicates the number of operational constraints.

Here, the individual objective functions f_1 to f_4 are made dimensionless quantities which are to be obtained from the ratio of '*with DG presence*' to the '*without DG presence*' of the respective objective function.

3.3.1 Minimization of Electrical Energy Losses

During the transmission and distribution of electrical energy to the end customers, a considerable amount of energy loss occurs in the distribution systems that may affect the annual revenue of Distribution Companies (DISCOs). Reducing electrical energy losses is the primary objective of DISCOs. This objective is expressed in Eq. (3.22):

$$\min f_1 = \sum_{k=1}^{NL} g_k \left[V_{k,m}^2 + V_{k,n}^2 - 2V_{k,m}V_{k,n}\cos\left(\delta_{k,m} - \delta_{k,n}\right)\right] * TH_k \qquad (3.22)$$

where $V_{k,m}$ and $V_{k,n}$ represent the voltage magnitudes at buses *m* (sending) and *n* (receiving) of k^{th}-line. The $\delta_{k,m}$ and $\delta_{k,n}$. indicate the phase angles of voltage at buses *m* and *n* of k^{th}-line. TH_k and g_k represent the total working hours (8760 hrs) and conductance, respectively, of that line-*k*. *NL* indicates the system total number of lines/branches.

3.3.2 Minimization of overall bus Voltage Deviation (VD)

Modern power systems operate under stressed conditions due to increased load demand that affects the system node voltages. The voltage magnitude of a bus may be used as a tool to estimate system safety and quality power. Utilities have considered the bus voltage deviation as an objective to improve the system voltage profile. Voltage deviation can be defined as the deviation of an individual bus voltage from source node voltage (substation node). Substation bus voltage is maintained at 1 p.u. (i.e., V_1 = 1). This objective can be expressed as Eq. (3.23).

$$\min f_2 = \sum_{m=1}^{NB} \left(\frac{V_1 - V_m}{V_m^{\max} - V_m^{\min}} \right)^2 \tag{3.23}$$

where V_1 and V_m indicate the voltage magnitudes of substation node and bus-m, respectively. The $V_m^{\max}$ (1.05 p.u) and $V_m^{\min}$ (0.95 p.u) are the voltage boundaries of m^{th}-bus. *NB* is the number of buses in a system.

3.3.3 Maximization of overall Voltage Stability Margin (VSM)

The voltage stability margin can be used as a yard-stick to measure the security level of the distribution system. It can be estimated from the voltage stability index (VSI) [40] determined at each bus except the source node and summation of all these *VSI*s yields the overall voltage stability margin. If this value is low, the system is said to be near to unstable condition, and vice versa. The formula to find the overall voltage stability margin may be expressed as Eq. (3.24).

$$\left. \begin{aligned} &\max\ f_3 = \sum_{n=2}^{NB} VSI_n \\ &VSI_n = \left[V_m^4 - 4\left(P_n X_{mn} - Q_n R_{mn}\right)^2 - 4\left(P_n R_{mn} + Q_n X_{mn}\right) V_m^2 \right] \end{aligned} \right\} \tag{3.24}$$

where P_n, and Q_n indicate the effective active- and reactive load demand, respectively, at n^{th}-bus. R_{mn} / X_{mn} represents the resistance / reactance of the distribution line available between buses m and n, respectively. The details of Eq. (3.24) are presented in APPENDIX-8.

3.3.4 Minimization of Energy Not Served (ENS)

Evaluating Energy Not Served (ENS) enables the power system utilities to estimate the acceptable degree of reliability to be maintained at the customers end, identify vulnerable points in a system, develop appropriate operation policies, *etc.*, [83]. *ENS* of the system can be computed as shown in Eq. (3.25).

$$\min\ f_4 = \sum_{i=1}^{NB} P_{DL,i}\, U_i \tag{3.25}$$

where $P_{DL,i}$ and U_i indicate the load demand and annual outage time, respectively, at the i^{th}-bus.

Usually, reliability of a system is computed based on the following three parameters expressed as in Eq. (3.26) [83].

$$\left.\begin{aligned} \lambda_S &= \sum_{i=1}^{n} \lambda_i \ ; \\ U_S &= \sum_{i=1}^{n} \lambda_i r_i \ ; \\ r_S &= \frac{U_S}{\lambda_S} = \frac{\sum_{i=1}^{n} \lambda_i r_i}{\sum_{i=1}^{n} \lambda_i} \end{aligned}\right\} \tag{3.26}$$

where λ_i, U_i, and r_i indicate the average failure rate, annual outage time, and average outage time, respectively, of i^{th}- component and the corresponding terms for distribution network are represented by λ_S, U_S, and r_S, respectively. n represents the total number of line sections in the distribution network.

Reliability of the Power Distribution Network (PDN) can be increased by reducing the failure-rates of overhead lines. The failure-rate of a line is in proportionate to the amount of current passing through the line. Very large current leads to higher resistive losses which raise the temperature of a line, may increase the chances of occurring electric break (failure). If the DG unit is placed at the optimal location, it can reduce the magnitude of the branch current. The DG which injects only the real power will influence the real component of the branch current (I_k^{DG}). Further, if the DG supplies both active and reactive power to the network they can influence both the real and reactive components of the branch current (I_k^{DG}). Before the deployment of DG unit, any k^{th}-line has an uncompensated failure rate of λ_k^{uncomp}. If the magnitude of branch current is fully compensated, the failure rate will be reduced to λ_k^{comp}. The new failure-rate (λ_k^{DG}) of a line is computed after the appropriate accommodation of DG in the distribution system as it can reduce the branch current flows and may be expressed in Eq. (3.27) [83].

$$\lambda_k^{DG} = \frac{\left|I_k^{DG}\right|}{\left|I_k^{NODG}\right|}\left(\lambda_k^{uncomp} - \lambda_k^{comp}\right) + \lambda_k^{comp} \tag{3.27}$$

where I_k^{NODG} and I_k^{DG} represent the current passing through the k^{th}-line before and after the accommodation of DG unit, respectively. The λ_k^{comp} is taken as 85% of λ_k^{uncomp} for the branch-*k* [83].

3.4 Operational Constraints

For the distribution system with a deployed DG unit, the optimization problem considers the following operational constraints.

3.4.1 Power balance

At each bus, the following power balance equations must be satisfied.

$$NetP_n = P_{DG,n} - P_{DL,n} = V_n \sum_{m=1}^{NB} V_m y_{n,m} \cos(\delta_n - \delta_m - \theta_n + \theta_m) \tag{3.28}$$

$$NetQ_n = Q_{DG,n} - Q_{DL,n} = V_n \sum_{m=1}^{NB} V_m y_{n,m} \sin(\delta_n - \delta_m - \theta_n + \theta_m) \tag{3.29}$$

Here $NetP_n$ and $NetQ_n$ represent the net active and reactive power injection at n^{th}- node, and it should be satisfied at any operating condition.

3.4.2 DG Capacity limits

The DG output power should be well within the specified limits and is expressed through Eq. (3.30) and Eq. (3.31).

$$P_{DG,\min,n} \leq P_{DG,n} \leq P_{DG,\max,n} \tag{3.30}$$

$$Q_{DG,\min,n} \leq Q_{DG,n} \leq Q_{DG,\max,n} \tag{3.31}$$

where $P_{DG,n}$, $P_{DG,min,n}$, and $P_{DG,max,n}$ indicate the active power generation, minimum, and maximum real power generation limits of the DG unit placed at n^{th}-node. Similarly, $Q_{DG,n}$, $Q_{DG,min,n}$, and $Q_{DG,max,n}$ indicate the reactive power generation, minimum, and maximum reactive power generation limits of the DG unit placed at n^{th}-node.

3.4.3 Bus Voltage limits

The voltage magnitude at each bus should be maintained within the operational limits as shown in Eq. (3.32).

$$V_{\min,n} \leq V_n \leq V_{\max,n} \tag{3.32}$$

where V_n is the voltage magnitude at n^{th}-bus. $V_{\min,n}$ and $V_{max,n}$ represent the minimum- and maximum voltages at n^{th}- bus.

3.4.4 Line flow limits

The current flowing through the overhead line should not overreach the acceptable limits as given in Eq. (3.33).

$$I_k \leq I_{\max,k} \tag{3.33}$$

where I_k and $I_{max,k}$ indicate the operating and permissible current of k^{th}-line, respectively.

3.5 Analytical Hierarchy Process for determination of Optimal Weights

The weight coefficient assigned to the each objective of Eq. (3.21) may play vital role in improving the overall system performance. An *Analytical Hierarchy Process* (*AHP*) [84] approach is employed to determine the suitable weight coefficients for the objectives. AHP is used to deal with problems of complex in nature (decision-making) and can support the decision-maker to give the best compromised solution. The procedure involved in the AHP method is summarized in the following steps:

Step-1 [Formation of reciprocal 'or' *pairwise comparison matrix[A]]*:

The pair-wise comparison matrix 'or' reciprocal matrix [A], is built for the selected objective functions according to the choice of the decision maker's with pair wise comparison in the ratio scale of 1 (equal) to 9 (extreme). The values of the elements of the matrix *A* are selected subjectively by comparing the importance of each of the two objectives [84]. The size of the square matrix is equal to that of the number of selected objective functions (*NF*). Any row represents a particular objective function, and higher value of an element in that row indicates the amount of importance given to this objective function compared to other objective function. The reciprocal matrix [A], is given in Eq. (3.34).

$$A = \begin{bmatrix} a_{ii} & a_{ij} & . & . & a_{iNF} \\ 1/a_{ij} & a_{jj} & . & . & a_{jNF} \\ . & . & . & . & . \\ . & . & . & . & . \\ 1/a_{iNF} & 1/a_{jNF} & . & . & a_{NFNF} \end{bmatrix} \tag{3.34}$$

where $a_{ii,}$=1, the self-value given to i^{th}- objective; a_{ij} represents mutual-value allocated to i^{th}-objective against the j^{th}- objective. Then, the reciprocal is $a_{ji} = 1/a_{ij}$.

Step-2 [Computation of weight coefficient]:

The weight coefficient value for i^{th}- objective is determined as shown in Eq. (3.35) [65].

$$W_i = \frac{\sqrt[NF]{\prod_{j=1}^{NF} a_{ij}}}{\sum_{i=1}^{NF} \sqrt[NF]{\prod_{j=1}^{NF} a_{ij}}} \qquad (i = 1, 2, \ldots.. NF) \tag{3.35}$$

The weight coefficients can be expressed in the vector notation as shown in Eq. (3.36).

$$W = [W_1, W_2, \ \ldots \ W_{NF}]^T \tag{3.36}$$

Step-3 [Check for matrix consistency]: The consistency of the matrix [A] is obtained only if the Index Consistency ratio (I_{CR}) is less than 0.1.

$$\left.\begin{aligned} I_{CR} &= \frac{I_{CI}}{I_{RI}} < 0.1 \\ I_{CI} &= \frac{(\lambda_{\max} - NF)}{(NF-1)} \end{aligned}\right\} \tag{3.37}$$

Here, I_{CI} indicates index-consistency and I_{RI} is the random-index. If $I_{CR} < 0.1$, the weight of each objective estimated by Eq. (3.36) is rational (reasonable). The general numerical values of the random index (I_{RI}) corresponding to the number of assumed objectives are reported in Table 3.1 [84]. $\lambda_{\max}$ is the maximum eigenvalue of matrix A and is proved that the relationship $[A][W] = \lambda_{\max} [W]$ must be satisfied [84].

Based on the above procedure, the optimal weight coefficients for the objectives of Eq. (3.22), Eq. (3.23), Eq. (3.24), and Eq. (3.25) are obtained as 0.3940, 0.2593, 0.1970, and 0.1497, respectively, with the I_{CR} of 0.0530. Furthermore, the *reciprocal matrix* [A] is given in Eq. (3.38).

$$A = \begin{bmatrix} 1 & 8 & 1 & 1 \\ 1/8 & 1 & 6 & 2 \\ 1 & 1/6 & 1 & 3 \\ 1 & 1/2 & 1/3 & 1 \end{bmatrix} \tag{3.38}$$

Table 3.1 Random Consistency Index (I_{RI}) values

NF	1	2	3	4
I_{RI}	0.00	0.00	0.58	0.90

3.6 Implementation Steps of Proposed Algorithm and Flow Chart for Multi-Objective Optimal Deployment of Distribution Generation

This section presents the step by step procedure of the proposed method to solve the *Multi-Objective Optimal Deployment of Distribution Generation* (*MOODDG*) problem of power distribution networks.

Step-1: Read the test system data.

Step-2: Find the *optimal weight coefficients* for the objectives using *Analytical Hierarchy Process* (*AHP*) approach (Section 3.5).

Step-3: Identify the *optimal DG location* based on the *BLBII* method (Section 3.2.1).

Set $P_{DG} = 0$.

Step-4: // Identification of Optimal DG Size //

A: Run the load flow by injecting the power from DG unit at an *optimal DG location* and evaluate the *overall objective function* as expressed in Eq. (3.21).

B: Update $P_{DG} = P_{DG} + \Delta P_{DG}$. Where ΔP_{DG} = 0.00005 p.u (step increment of DG injection). Repeat the **Step-4A** with this updated power from DG unit. Continue this process until P_{DG} value reaches the maximum P_{DG}. Now, identify and designate the *minimum overall objective function* value as *best value*.

C: The DG size corresponding to the *best value* of the objective is treated as an *optimal DG size*.

Step-5: STOP.

Furthermore, the flowchart of the proposed method is also shown in Figure 3.5 for better understanding purpose.

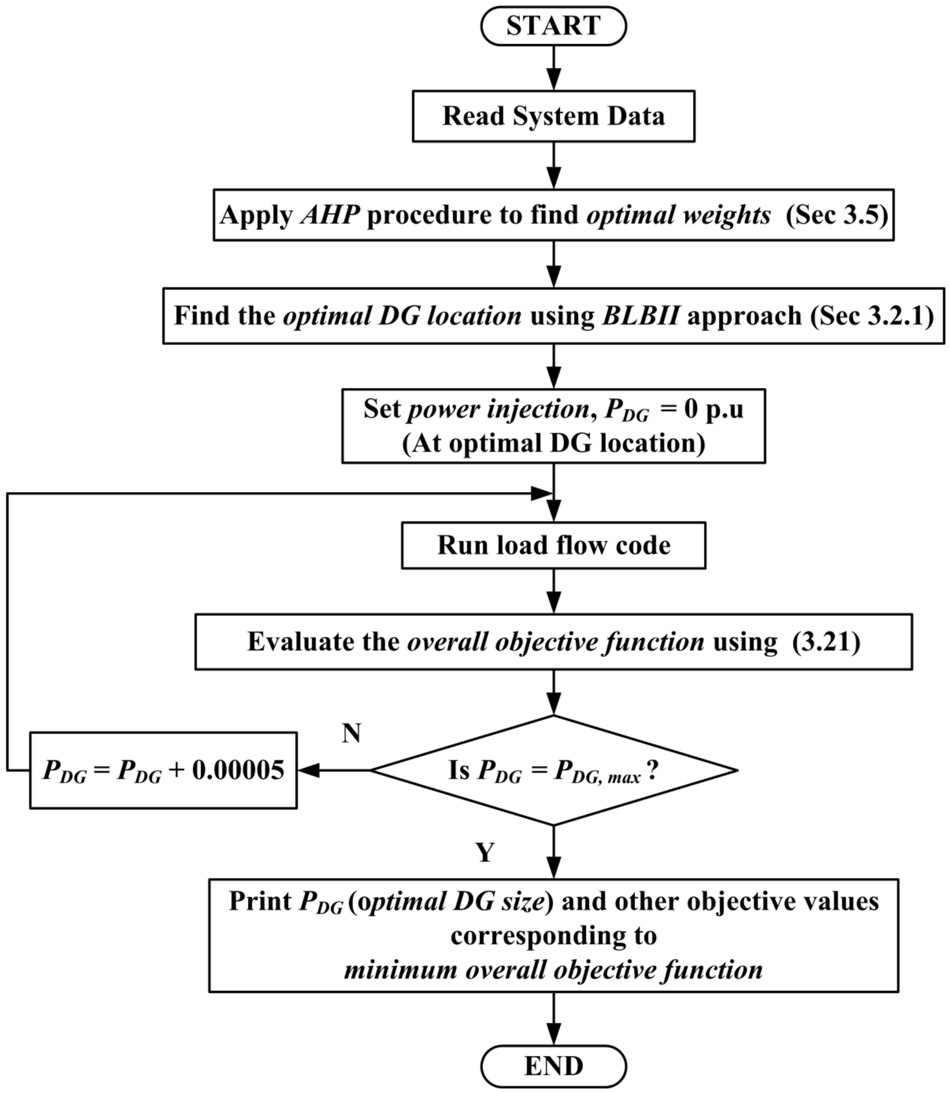

Figure 3.5 Flowchart of the proposed Analytical approach

3.7 Test Results and Discussion

The proposed *Branch Loss Bus Injection Index* (*BLBII*) is implemented in MATLAB software on a Windows 7, Intel Core i7-3770 processor with CPU speed 3.40GHz, and 8GB RAM. Two test systems such as IEEE 33-bus and INDIAN 85-bus Radial Distribution Systems are considered to illustrate the applicability of the proposed method. The following aspects are taken into account in the above implementation for the solution of Multi-Objective Optimal Deployment of Distribution Generation (MOODDG) problem.

1. The shunt admittance of overhead lines is ignored.

2. For simplicity, the DG is modelled as negative load.

3. For the distribution system, a longest line has the highest impedance with biggest failure-rate (0.5 f/year) and shortest line has the smallest impedance with the least failure-rate (0.1 f/year). The failure-rates of the other branches/lines are estimated based on these two ranges and their respective impedances, using principle of proportionality [83].

4. The feeder-line has a main circuit breaker.

5. Each line is equipped with a sectionaliser at the beginning of the line. [83].

6. The repair and switching times are assumed as 8 h and 0.5 h, respectively [83].

7. To compute the cost of energy saving, the net energy loss is multiplied by 60 $/MWh [28].

   [Cost of the energy saving = (Energy loss before DG - Energy loss after DG)*60 $/MWh].

3.7.1 Case study on IEEE 33-bus Radial Distribution Network

The applicability of the proposed *BLBII* method is tested on benchmark IEEE 33-bus Radial Distribution Network. The test system is operating at 12.66 kV with 100 kVA base, having 33 nodes and 32 line sections. The data pertaining to the lines and buses of the study system is presented in APPENDIX -1 [78]. The network total real and reactive power loads are 3715 kW and 2300 kVAR, respectively. The overall-objective function of Eq. (3.21) can be minimized with the deployment of DG unit at the optimal location (i.e. 6^{th}-bus) obtained by the proposed *BLBII* method. The impact of the DG unit on IEEE 33-bus Radial Distribution System is investigated under two different scenarios.

3.7.1.1 Single DG operating with Unity Power Factor – First Scenario

In this case, one DG operating at *unity power factor* is considered to solve the MOODDG problem. Here, the goal is, simultaneously, *reduce the energy losses, overall bus voltage deviation minimization, maximization of overall voltage stability margin, and minimization of Energy Not Served (ENS).* The results offered by the proposed method under this scenario are tabulated in Table 3.2. From the close observation of the results in

Table 3.2, it is noticed that the proposed *BLBII* method has significantly improved all the objective functions due to the presence of optimal DG at potential location (i.e. 6th-bus). The improvement with respect to the cost of energy saving is about 48,540 US $ per annum and nearly 43.77% reduction has been observed in energy loss through the optimal placement. Furthermore, about 83.39% reduction in overall bus voltage deviation and 14.24% improvement in the overall voltage stability margin have been realized. Therefore, it is concluded that the bus voltage magnitudes and security level of the system have improved from the base case to DG case. The voltage profile of this test case is shown in Figure 3.6. From Figure 3.6, it may be observed that there is significant improvement in voltage profile due to the deployment of DG unit at potential location. The minimum voltage magnitude occurring at bus-18 is enhanced from 0.9038 p.u. to 0.9529 p.u. after placement of DG unit.

Table 3.2 Results offered by the Proposed *BLBII* method for IEEE 33-bus *RDN*

Cases	**DG loc**	**DG Size (kVA)**	f_1	f_2	f_3	f_4	**Cost of Energy loss Saving (US $)**	**Reduction of Eloss, %**	**Vmin @bus**	**CPU Time (s)**
Base Case	-	-	1848.2	13.37	26.05	5.7733	-	-	0.9038 @18	-
First Scenario	6	3340	1039.2	2.22	29.76	5.3941	48,540	43.77	0.9529 @18	3.8518
Second Scenario	6	3639	657.4	0.92	30.87	5.5393	71,446	64.63	0.9667 @18	3.8826

f_1 = Energy loss (MWh); f_2 = Overall node Voltage Deviation; f_3 = Overall Voltage Stability Margin;

f_4 = Energy Not Served (10^4 kWh/year)

3.7.1.2 Single DG operating with 0.9 Lagging Power Factor – Second Scenario

This case considers a single DG unit operating at 0.9 lagging power factor (LPF) that can deliver both the reactive and real power to the power distribution network. The simulation results obtained by proposed method for this scenario are also reported in Table 3.2. The proposed method *BLBII* have exhibited proven quality of optimal values for all the four objectives of Eq. (3.21). The improvement with respect to the cost of energy saving is about 71,446 US $ per annum and a notable 64.63% reduction in energy loss has been achieved through the optimal DG placement. Besides, nearly 93.11% reduction in overall bus voltage deviation and 18.50% improvement in the overall voltage stability margin have been realized. Therefore, it is concluded that the bus voltage magnitudes and security level of the system have improved from the base case to DG case. The voltage magnitude at each bus of the test system under this case (scenario) is also presented in Figure 3.6. The minimum voltage magnitude at bus-18 is enhanced from 0.9038 p.u. to 0.9667 p.u. after placement of DG unit.

From the above discussion, it may be concluded that the cost of energy saving, reduction of energy loss, and voltage profile of the *second scenario* are much better than the *first scenario* and *base case scenario*. It is mainly due to the provision of active and reactive powers support by the DG unit locally.

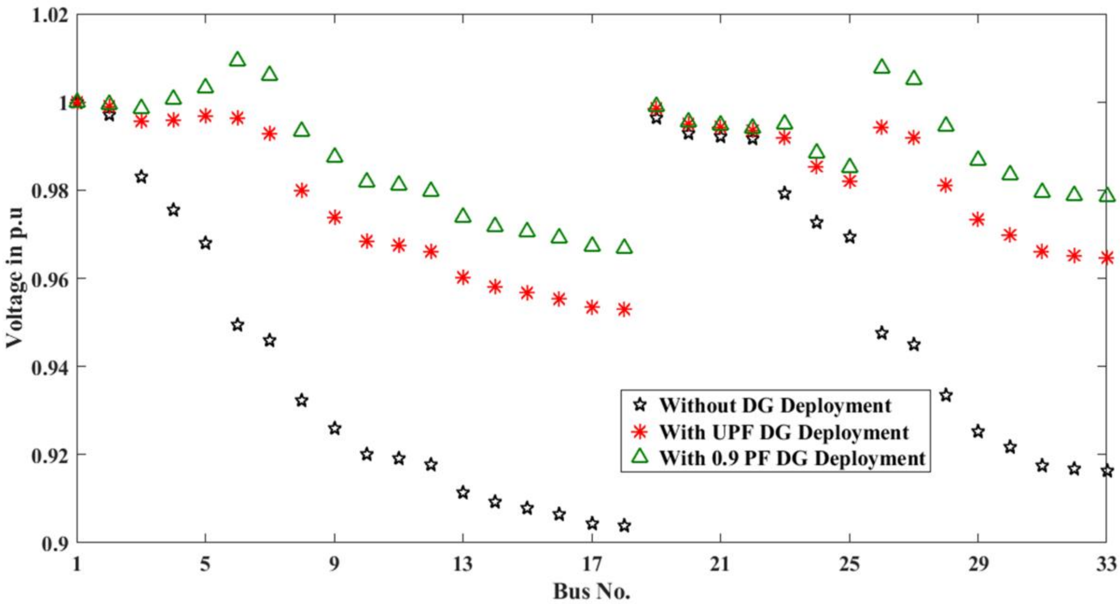

Figure 3.6 Node voltages of IEEE 33-bus *RDN* without and with DG deployment

3.7.2 Case study on INDIAN 85-bus Radial Distribution Network

The effectiveness of *BLBII* approach is also demonstrated on INDIAN 85-bus benchmark study system. This system is operating with 11 kV, 100 kVA base, and having 85-buses and 84-lines. The line data and bus data of this test system is reported in APPENDIX - 4 [82]. The network total real and reactive loads are 2569.28 kW and 2621.18 kVAR, respectively. The objective function of Eq. (3.21) can be minimized with the incorporation of DG unit at the optimal location (i.e. 8^{th}-bus) obtained by the proposed

BLBII method. The impact of the DG unit on INDIAN 85-bus RDN is investigated under two different scenarios.

3.7.2.1 Single DG operating with Unity Power Factor – First Scenario

The results of the *BLBII*, proposed method for this case are summarized in Table 3.3. From the test results reported in Table 3.3, it may be observed that the proposed *BLBII* method has significantly improved all the objective functions due to the placement of DG unit at candidate location. Furthermore, the improvement with respect to the cost of energy saving is about 62,598 US $ per annum and an energy loss reduction of 37.72% has been realized through the optimal placement of DG unit. On top of them, closely 90.90% reduction and 30.92% improvement have been achieved in the case of overall bus voltage deviation and overall voltage stability margin, respectively. Therefore, to sum up the node voltages and security level of the distribution system has improved from the base case to DG case. The node voltage profile of this test case is depicted in Figure 3.7. From Figure 3.7, it may be observed that there is a notable improvement in voltage profile due to the deployment of DG unit at potential location. The minimum voltage magnitude at bus-54 is enhanced from 0.8714 p.u. to 0.9500 p.u. after the emplacement of DG unit at optimal location .

Table 3.3 Results offered by the Proposed *BLBII* method for INDIAN 85-bus *RDN*

Cases	DG loc	DG Size (kVA)	f_1	f_2	f_3	f_4	Cost of Energy loss Saving (US $)	Reduction of Eloss , %	Vmin @bus	CPU Time (s)
Base Case	-	-	2765.6	82.02	58.01	7.0172	-	-	0.8714 @54	-
First Scenario	8	3375	1722.3	7.46	75.95	6.5399	62,598	37.72	0.9500 @54	5.1521
Second Scenario	8	3522	787.1	1.72	81.24	6.7381	1,18,709	71.53	0.9700 @54	5.2016

f_1 = Energy loss (MWh); f_2 = Overall node Voltage Deviation; f_3 = Overall Voltage Stability Margin;
f_4 = Energy Not Served (10^4 kWh/year)

3.7.2.2 Single DG operating with 0.9 Lagging Power Factor – Second Scenario

The results offered by the proposed method for the second scenario are also reported in Table 3.3. From this table, it is observed that the *BLBII* method has yielded the optimum results for the objective functions *viz* minimum energy loss, minimum overall VD, maximum overall VSM, and minimum ENS. The improvement with respect to the cost of energy saving is about 1,18,709 US $ per annum and an energy loss reduction of 71.53% has been achieved through the optimal accommodation of DG unit. In addition to this, about 97.90% reduction in overall bus voltage deviation and 40.04% improvement in the overall voltage stability margin have been obtained. Therefore, in summary, the voltage profile and security level of the radial distribution system have improved from the base case to DG case. The voltage magnitudes of this test system under the second scenario are also shown in Figure 3.7. From Figure 3.7, it may be observed that bus voltage profile of all the buses are improved significantly due to the deployment of DG unit at the candidate location. The minimum voltage magnitude at bus-54 is raised from 0.8714 p.u. to 0.9700 p.u.

From the above discussion, it may be concluded that the cost of energy saving, reduction of energy loss, and voltage profile under *second scenario* are much better compared to *first scenario* and *base case scenario*. This is mainly due to the provision of active and reactive power supply within the distribution system by means of DG unit.

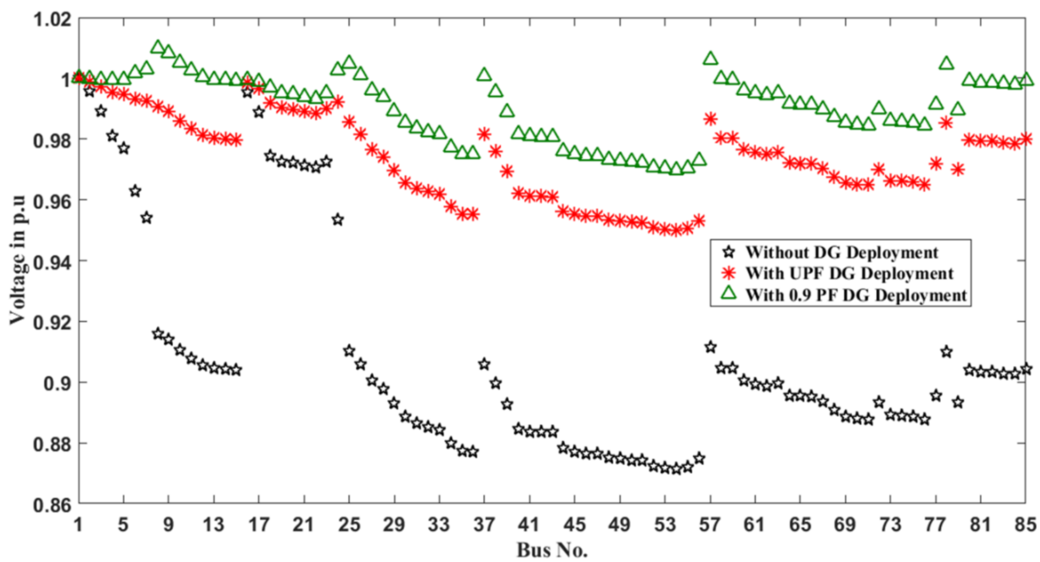

Figure 3.7 Node voltages of INDIAN 85-bus *RDN* without and with DG deployment

3.8 Comparison with works reported in Literature

In this section, a comparative study of the various methods for *real power loss minimization* of *IEEE* 33-*bus Radial Distribution Network* for both the scenarios has been presented. The results offered by the proposed *BLBII* approach along with the results of other methods available in literature are tabulated in Table 3.4. This table compares the DG location, DG Size, Ploss, %Ploss reduction, and minimum voltage magnitude@bus obtained by the distinct methods.

Table 3.4 Comparison of the results of different approaches available in Literature

Cases	DG loc	DG Size (kVA)	Ploss (kW)	Ploss Reduction, %	Vmin@bus
Base Case	-	-	210.98	-	0.9037@18
First Scenario					
Modified Novel Method [25]	6	2494	111.14	47.32	0.9412@18
Combined Method [25]	8	1800	118.12	44.01	0.9433@18
Index Vector [25]	30	1550	125.15	40.68	0.9275@18
Voltage Sensitivity [25]	16	1000	136.75	35.18	0.9318@18
Loss Sensitivity [23]	10	1400	123.82	41.31	-
Repeated Load Flow [23]	6	2600	111.10	47.34	-
Mithulananthan [23]	6	2490	111.24	47.27	-
LSF [26]	18	0743	146.82	30.48	-
IA [26]	6	2601	111.10	47.39	0.9425@18
ELF [26]	6	2601	111.10	47.39	-
MINLP [30]	6	2590	111.01	47.39	-
GA+AE [38]	6	2380	132.64	38.59	-
Proposed *BLBII*	6	2590	111.02	47.39	0.9521@18
Second Scenario					
Modified Novel Method [25]	6	3011	70.90	66.39	0.9566@18
Combined Method [25]	8	2100	84.47	59.96	0.9534@18
Index Vector [25]	30	1950	78.41	62.84	0.9391@18
Voltage Sensitivity [25]	16	1200	112.78	46.54	0.9378@18
Proposed *BLBII*	6	3072	70.86	66.41	0.9573@18

From Table 3.4, for the *First Scenario*: it may be pointed out that all the methods have improved the system performance by reducing the system losses. However, more loss reduction of 47.39% is obtained by proposed *BLBII*, Improved Analytical (IA) [26], Exhaustive Load Flow (ELF) [26], and Mixed Integer Non-linear Problem (MINLP) [30] methods as compared to remaining methods, Modified Novel Method [25], Repeated Load

Flow [23], Mithulananthan [23], and Genetic Algorithm along with Analytical Expression (GA+AE) [38] methods though they identified the same optimal DG location (i.e. 6^{th}-bus). Moreover, the optimal DG size obtained by the *BLBII* approach is less than IA [26], and ELF [26] methods for the same %loss reduction. This may depend on the system parameters and step increment of DG size considered in the search process to find the optimal DG size. Also, the %loss reduction obtained by Combined Method [25], Index Vector [25], Voltage Sensitivity [25], Loss Sensitivity [23], and Loss Sensitivity Factor (LSF) [26] method is low as compared to proposed *BLBII* method due to the inappropriate DG location for these methods.

The inappropriate DG location obtained by these methods can be observed in the Table 3.4. The minimum voltage magnitude at 18-bus is raised from 0.9037 p.u (base case) to 0.9521 p.u (DG case) in the case of proposed *BLBII* method which is *highest* among all the reported methods. This improved voltage profile at other buses will lead to reduced real power losses. Similarly, for *Second Scenario*: higher %loss reduction of the order 66.41% and enhanced voltage magnitude of 0.9573 p.u at bus-18 has been obtained by the proposed *BLBII* method.

This part of the work was published as "A solution to Multi-objective Optimal Accommodation of Distributed Generation Problem of Power Distribution Networks: An Analytical approach," *International Transactions on Electrical and Energy Systems*, vol. 29, no. 10, October 2019, e12093. https://doi.org/10.1002/2050-7038.12093. (Indexed in SCIE)

3.9 Summary

In this Chapter, an analytical method, *Branch Loss Bus Injection Index (BLBII)* has been proposed to find the optimal location for the emplacement of DG unit. By accommodating the DG at identified optimal location, a new multi-objective problem of the power distribution network has been investigated by considering: *minimization of electrical energy losses, minimization of overall bus voltage deviation, maximization of overall voltage stability margin, and minimization of energy not served* to find the optimal DG size. An unique *Analytical Hierarchy Process* (*AHP*) approach has been proposed to estimate the optimal weights for the individual objectives of the multi-objective function. The applicability of the proposed method was validated on *IEEE* 33-bus and *INDIAN* 85-

bus benchmark radial test systems under two different scenarios. Furthermore, a comparative study with the established algorithms was conducted aiming at the minimization of power loss.

Up to this part of the research work, Multi-Objective Optimal Deployment of Distributed Generation (MOODDG) problem has been solved using an Analytical method by placing the *Single DG unit* at the optimal location. Analytical methods are often easily implementable, ensure the convergence of the DG planning solution and short computation time.

The next stage of the investigation is focused on the implementation of a *Hybrid Multi-Verse Optimization* (*MHVO*) meta-heuristic algorithm for solving the MOODDG problem with the placement of *multiple DG units*. The same is presented in Chapter-4.

CHAPTER-4

New Hybrid Multi-Verse Optimization Approach for Optimal Accommodation of DG units in Power Distribution Networks

4.1 Introduction

Nature inspired algorithms are in forefront to solve the real-life optimization problems, which may be very difficult or sometimes impossible to be addressed using Analytical methods [35]. The source of inspiration to develop such a nature inspired algorithms is the behavioral aspects of particles, ant, fishes, bees, cats, monkey, firefly, cuckoos, bats, krill herd, grey wolf, elephant, ant lion, crow, dragonfly, *etc.*, as mentioned in [36]. The wide application of these methods can be found in the area of electrical power systems optimization particularly to the power distribution network optimization problems that include network reconfiguration, capacitor placement, distributed generation placement and sizing, optimal design of distribution lines, network reinforcement, *etc*.

In recent years, the application of numerous meta-heuristic/nature inspired algorithms for solving the optimal placement and sizing of the DG have been increased. Some of them are Particle Swarm Optimization (PSO) [37], Genetic Algorithm (GA) [38], Imperialistic Competitive Algorithm (ICA) [40], Simulated Annealing (SA) [42], Teaching Learning Based Optimization (TLBO) [45], Quasi-Oppositional Teaching Learning Based Optimization (QOTLBO) [46], Chaos Symbiotic Organisms Search (CSOS) [47], Comprehensive Teaching Learning Based Optimization (CTLBO) [48], Whale Optimization Algorithm (WOA) [49], Non-dominated Sorting Genetic Algorithm-II (NSGA-II) [50], Hybrid Immune Genetic Algorithm (HIGA) [51], Bacterial Foraging Optimization Algorithm (BFOA) [52], Shuffled Bat Algorithm (ShBAT) [54], Chaotic Artificial Bee Colony (CABC) [57], Salp Swarm Algorithm (SSA) [61], and Combined Harmony Search Firefly Algorithm (CHSFA) [76]. These methods have shown some merits and demerits while solving the DG deployment problem. For example, PSO [37] is easy to implement, requires less parameters to tune, and quick convergence but suffers from the difficulty of describing initial design parameters, possibility of premature convergence, and getting trapped into local optimum value. Genetic Algorithm (GA) [38] is suitable to solve discrete and continuous optimization problems but computationally inefficient for large problems and offers the local optimum value. Imperialistic Competitive Algorithm (ICA) [40], effective and capable of handling Mixed Integer Non-linear Optimization problems in DGs but suffers from the slow convergence. The Simulated Annealing (SA) [42] is computationally accurate for several combinatorial problems but need large number of iterations and excessive computation time to get the solution.

Teaching Learning Based Optimization (TLBO) [45], reliable, accurate, and robust for optimization problems but slow convergence for multi-objective problems. Bacterial Foraging Optimization Algorithm (BFOA) [52], efficient to find the results in less computational time but requires tuning of great number of parameters. Chaotic Artificial Bee Colony (CABC) [57], fast converging and capable of handling complex optimization problems but performance of this method depends on the type of the constraints handling.

In the light of the above discussion, there is a need to propose an efficient optimization technique to attain the global optimum value for the case of Optimal DG Deployment problem. Hence, in this Chapter, an improved meta-heuristic algorithm called Hybrid Multi-Verse Optimization (HMVO) is proposed to solve the Multi-objective Optimal Deployment of Distributed Generation (MOODDG) problem of Distribution Network.

4.2 Proposed Hybrid Multi -Verse Optimization (HMVO) Method

The Multi-Verse Optimizer is recently formulated nature-inspired algorithm introduced by Seyedali Mirjalili *et al*. in 2016 [85]. The algorithm was developed based on the concept of Big-Bang theory and Multi-Verse theory. The first theory states that the Big-Bang is the origin for existence of everything in our universe and is limited to the one universe only, where as the later one deals with the existence of more than one universe. According to the Multi-Verse theory, each universe might have different physical laws and they interact, and collide with each other [85].

There are three central concepts in Multi-Verse theory:

(1) White hole: It is the replica of Big-Bang and used for exploration purpose.

(2) Black hole: Due to its high gravitational force, they attract everything, and used in exploration phase.

(3) Wormhole: Acts as a bridge either for different universes or for distinct parts of the same universe and is used for exploitation purpose.

4.2.1 Basic Multi-Verse Optimizer (MVO)

The mathematical model of the basic MVO is split into different steps and are arranged as below [85].

Step-1: (*Initialisation Phase*)

Let, U_{ij} stands for j^{th} - variable of i^{th} - universe.

LB_j and UB_j are the lower and upper boundaries of the j^{th} - variable.

Popsize indicates the number of universes.

D_{size} represents the number of variables to be optimized.

rand is the random number generated between 0 to 1.

Then, generate a population randomly using the Eq. (4.1).

$$U_{ij} = LB_j + rand*(UB_j - LB_j) \ ; \quad i = 1,2,...Popsize; \quad j = 1,2,...Dsize \tag{4.1}$$

Each solution generated using Eq. (4.1) is analogous to a universe and each variable-*j* in the solution is an object in that universe.

The randomly generated population is to be evaluated to find the fitness (inflation rates) and are normalised by dividing with highest fit value. These normalised values are to be sorted in descending order to identify the *Best Universe*. Then, set this *Best Universe* to *old Best Universe.*

Step-2: *(Exploration Phase - Roulette Wheel mechanism for white/black hole tunnel formation)*

The Roulette Wheel technique is applied on the sorted normalised inflation rates to create the white/black hole tunnel which is used for the exchange of objects between the universes and may be represented as Eq. (4.2).

$$U_{ij} = \begin{cases} U_{kj} & if \ rand_1 < U_i^{NI} \\ U_{ij} & if \ rand_1 > U_i^{NI} \end{cases} \tag{4.2}$$

Here, U_{kj} indicates the j^{th}- variable of k^{th}- universe (k^{th}- universe is selected from *Roulette Wheel*). The U_i^{NI} is the normalised inflation rate of i^{th} - universe. The $rand_1$ is the random number generated in the range of [0, 1].

Step-3: *(Exploitation Phase - based on Wormhole Existence Probability (WEP) and Travelling Distance Rate (TDR))*

Two parameters such as *Wormhole Existence Probability* (*WEP*) and *Travelling Distance Rate* (*TDR*) are employed to operate around the *Best Universe*. The *WEP* represents the probability of existence of *Wormhole* in the universes. It is required to increase linearly over the iterations. The numerical value of *WEP* is made to vary between 0.2 to 1. The *TDR* is used to define the distance rate (variation) that an object/variable can be teleported by a *Wormhole* around the so far obtained *Best Universe*. In contrast to *WEP*, *TDR* is decreased over the iterations to have more precise exploitation/local search around the *Best Universe*.

The adaptive formulae for *WEP* and *TDR* are given in Eq. (4.3).

$$WEP = WEP_{\min} + iter \times \left(\frac{WEP_{\max} - WEP_{\min}}{iterma} \right) \; ; \quad TDR = 1 - \frac{iter^{1/p}}{iterma^{1/p}} \qquad (4.3)$$

where WEP_{min} and WEP_{max} are the minimum and maximum values of *Wormhole Existence Probability* (*WEP*). *iter* indicates the current iteration, whereas *iterma* represents the maximum iterations. Here, *p* is a parametric value which defines the exploitation accuracy over the iterations. The higher value of *p* leads to faster and better accurate exploitation/local search process.

Now, conduct the local search around the *Best Universe* using *WEP* and *TDR* as expressed in Eq. (4.4).

$$U_{ij} = \begin{cases} \left. \begin{cases} U_j^{best} + \mathrm{TDR} \times (LB_j + rand_4 * (UB_j - LB_j)) & if\ rand_3 < 0.5 \\ U_j^{best} - \mathrm{TDR} \times (LB_j + rand_4 * (UB_j - LB_j)) & if\ rand_3 \geq 0.5 \end{cases} \right\} & if\ \ rand_2 < WEP \\ U_{ij} & if\ \ rand_2 \geq WEP \end{cases} \qquad (4.4)$$

where U_j^{best} is the j^{th}- variable of the *Best Universe*. The $rand_2$, $rand_3$, and $rand_4$ are the random numbers generated in the range of 0 - 1.

Step-4: *(Convergence)*

Now, find the fitness values (i.e. inflation rates) for the *updated universes* obtained using the Eq. (4.4) and arrange them in descending order, after the normalization process, to get the *Best Universe*. Replace the *old Best Universe* if better universe is found from the *updated universes.* Repeat the *Steps* 2 - 3 until the convergence is attained. Here, the convergence criterion is the maximum iterations/generations used in the optimization algorithm.

4.2.2 Hybrid Multi-Verse Optimizer

The basic MVO is suffering from poor convergence and provides the solution near to the local optimum value. This snag can be alleviated with the incorporation of the following two effective strategies.

4.2.2.1 Space Transformation Search (STS) Method

The *STS* is an evolutionary algorithm, proposed by Wang H., *et al*. [86]. In STS, solutions are found simultaneously in the two search spaces such as current search space and transformed search space and the best values from these two search spaces are separated.

The advantages of *Space Transformation Search (STS) Method*:

(1) avoids the premature convergence

(2) increases the probability to find the solutions near to the global solution

The mathematical model of *STS* is given through Eqs. (4.5) - (4.6).

Let $x \in [Lb \;\; Ub]$, is a solution in the current search domain *S* and its new solution, $\bar{x}$ in the transformed search domain $\bar{S}$ is expressed as follows.

$$\bar{x} = k(Lb + Ub) - x \tag{4.5}$$

where, Lb and Ub represent the lower and upper limits of a variable *x*. The *k* denotes the random number in the range of 0 - 1.

Now, for *Dsize* space (number of variables), the above equation can be extended to multi-variables as Eq. (4.6).

$$\overline{x_{ij}} = k(Lb_j + Ub_j) - x_{ij}, i = 1, 2, \ldots Popsize, \quad j = 1, 2, \ldots Dsize \tag{4.6}$$

where,

x_{ij} = j^{th} - variable of i^{th} - solution;

Lb_j = min (x_{ij}); i = 1, 2,........ *Popsize*

Ub_j = max (x_{ij}); i = 1, 2,........ *Popsize*

k = random number generated in the range of 0-1.

If any solution of Eq. (4.6) in the transformed search space is violates its bounds, then it has to be re-initialised within [Lb_j Ub_j].

4.2.2.2 Piecewise Linear Chaotic Map (PLCM) Method

Chaos means a randomness which is generated by simple deterministic model and is extremely sensitive to its initial values. Chaos is associated with stochasticity, complex, and irregular motion. The properties of chaos such as non-periodicity, ergodicity, and stochasticity are motivating its application towards the optimization in recent research. In the literature, numerous chaotic maps are proposed but this work employs the *Piecewise Linear Chaotic Map* (*PLCM*) as a chaos operator due to its better chaotic behaviour as well as higher speed [87].

From the basic *MVO*, it is evident that the transition from exploration phase to exploitation phase depends on the value of '*p*' being used in Eq. (4.3) of Travelling Distance Rate (*TDR*). For solving the benchmark functions, the authors of [85], have suggested the optimal value for '*p*' as 6. However, to solve the real world problem like DG deployment in a distribution system, this value is not suitable. It is observed that the higher *p*-value is required to get the global optimum result. Finding the optimal value for '*p*' is tedious as trial and error method has to be followed. In this situation, chaotic optimization may be the viable solution to address the problem. The chaotic variable is more effective in the range of 0-1. Here, the chaotic variable '*cy*' is defined as a random number Eq. (4.7) in place of the inverse of '*p*' (i.e., $cy = 1/p$).

In order to apply the *PLCM* chaos on *TDR* of Eq. (4.9), generate a variable of the chaotic sequence in k^{th}-iteration using Eq. (4.7) and the new chaotic sequence in $(k+1)^{th}$ iteration can be obtained using Eq. (4.8).

$$cy_k = rand(0,1) \tag{4.7}$$

$$cy_{k+1} = \begin{cases} \dfrac{cy_k}{m} & \text{if } cy_k \in (0,m) \\ \dfrac{(1-cy_k)}{(1-m)} & \text{if } cy_k \in (m,1) \end{cases} \tag{4.8}$$

where m and cy_k are representing the control parameter with 0.5 value and chaotic variable with 0-1 range, respectively.

Now, redefine the *TDR* of Eq. (4.3) in $(k+1)^{th}$ iteration as in Eq. (4.9):

$$TDR^{cy_{k+1}} = 1 - \frac{iter^{cy_{k+1}}}{iter\max^{cy}{}_{k+1}} \tag{4.9}$$

The $TDR^{cy_{k+1}}$ is mapped back to search around the *Best Universe*, U_j^{best} of Eq. (4.4) based on the *WEP* value.

4.3 Implementation Steps of Proposed Hybrid Multi-Verse Optimization Method and Flow Chart

To implement the Proposed *HMVO* algorithm, the objective functions and operational constraints reported in *Chapter-3* are considered. They include (i) *minimization of electrical energy losses*, (ii) *minimization of overall node voltage deviation*, (iii) *maximization of overall voltage stability margin*, and (iv) *minimization of Energy Not Served* (*ENS*). The operational constraints comprises of (i) power balance equation, (ii) DG capacity limits, (iii) bus voltage limits, and (iv) line flow limits.

The step by step procedure of the proposed *HMVO* methodology for the Optimal Deployment of DG (ODDG) problem is given below as:

Step-1: Read the System Data (line data and bus data);

Popsize = Size of the population (Solutions);

$Dsize$ = Number of the variables;

Iter$kmax$ = maximum number of iterations for Chaotic phase (Phase -II);

WEP_{min} = minimum wormhole existence probability (0.2);

WEP_{max} = maximum wormhole existence probability (1.0);

Iter$HMVO$max = maximum number of iterations;

Step-2: Obtain the *optimal weights* for the objective functions using *AHP approach* (Section 3.5).

Step-3: Generate an initial solution vector U_{ij} using Eq. (4.1) within their lower and upper bounds with the size of (*Popsize*) *X* (*Dsize*) and is given as Eq. (4.10).

$$U_{ij} = \left[LC_{i1,} \;\; LC_{i2,} \;\; \ldots \; LC_{in} \;\; , P_{i1}^{DG} , \; P_{i2}^{DG} \ldots \; P_{in}^{DG} \; , \quad Q_{i1}^{DG} , \quad Q_{i2}^{DG} \ldots \; Q_{in}^{DG} \right] \quad (4.10)$$

where LC, P^{DG}, and Q^{DG} are indicate the location, real power generation, and reactive power generation of the DGs to be installed. Each DG needs LC, P^{DG}, and Q^{DG} variables. For this reason, *Dsize* is made equal to three times the DGs to be deployed.

Step-4: Now convert the *Current Search Space solution* of Eq. (4.10) into the *Space Transformation Search* (*STS*) domain using Eqs. (4.5-4.6).

Step-5: Run the load flows on these *two search spaces simultaneously*, and evaluate the overall objective function value *FF* governed by Eq. (3.21). Then, compare the one to one *FF's* of both the searches and pick up the minimum values. Further, identify the *best solution* from this solution set. (Phase-I: Step-4 & Step-5)

Step-6: Set $k = 0$. Initialise the chaotic variable cy_k by using Eq. (4.7).

Step-7: Based on Eq. (4.8), calculate cy_{k+1}. Now, map cy_{k+1} back to the *TDR* of Eq. (4.9) and apply on the exploitation phase Eq. (4.4) to evaluate fitness value related to cy_{k+1}.

Step-8: If a better solution is found, update the *best solution* and go to *Step - 9*. Otherwise, go back to the *Step-7*.

Step-9: Stop the procedure if Iter$kmax$ is reached.

Step-10: Identify the *Best Universe* from Phase-II (Step-6 to Step-9).

Step-11: If the maximum number of generations/iterations, *IterHMVOmax,* is reached, the algorithm stops the simulation. Otherwise, it goes back to *Step - 4*.

For better understanding of the algorithm, the flowchart of the proposed *HMVO* is also shown in Figure 4.1.

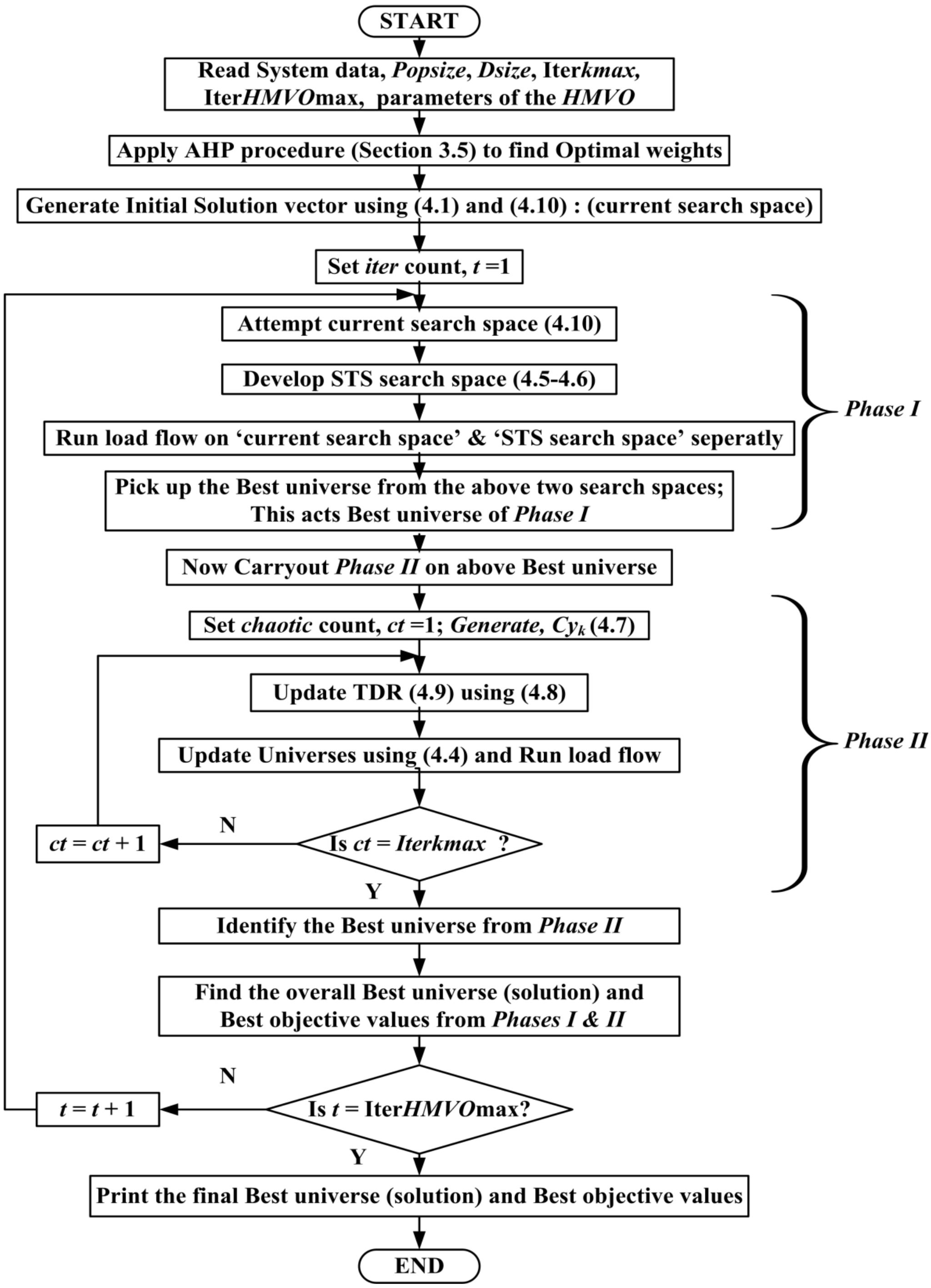

Figure 4.1 Flowchart of the proposed *HMVO* algorithm

4.4 Case studies and Discussion

To implement the proposed *HMVO* algorithm, the objective functions, operational constraints, and other aspects which were discussed in the *Chapter-3* are considered to solve the Multi-objective Optimal Deployment of DG (MOODDG) problem with *multi DG unit* placement. The objective functions under consideration are: *(i) minimization of electrical energy losses, (ii) minimization of overall node voltage deviation, (iii) maximization of overall voltage stability margin, and (iv) minimization of Energy Not Served* (*ENS*). The operational constraints such as *power balance equation, DG capacity limits, bus voltage limits, and line flow limits* are also incorporated.

The proposed Hybrid MVO (*HMVO*) algorithm is implemented in MATLAB environment on a Windows 7 based DELL desktop with Intel Core i7-3770, CPU@3.40GHz and 8GB Random Access Memory. Two test systems are considered to illustrate the effectiveness of the method. To validate the results obtained by the proposed approach, these test results are compared with the results offered by the (a) Particle Swarm Optimization (PSO) [37], (b) Adaptive Harmony Search Optimization (AHS) [88], (c) Salp Search Algorithm (SSA) [89], (d) basic MVO algorithm [85], (e) Space Transformation Search based MVO (SMVO), and (f) Chaotic map embedded MVO (ChMVO). The methods indicated in (e) and (f) are proposed to observe the effectiveness of these versions and then tried to propose the Hybrid MVO algorithm. To implement these algorithms, MATLAB codes are developed *by us* as per the basic steps given in their papers. Furthermore, in order to extract the best possible optimal solutions of these attempted algorithms, the following approach is employed.

a) Generate a random population of *Popsize* and feed this population as same initial search domain for all the above listed algorithms and identify the best optimal solution after 100 iterations. This portion is taken as 1st run.
b) Again generate another random population and go for 2nd run similar to step (a). Identify second best optimal solution related to 2nd run.
c) Complete the above process for 50 runs. *Among the best 50 optimal solutions, select the final best solution of individual algorithms*.

The parametric values and other essential quantities of above referred algorithms are given in Table 4.1.

Table 4.1 Parameters of the algorithms used

Parameter	PSO [Stud]	AHS [Stud]	SSA [Stud]	Basic MVO [Stud]	SMVO [Stud]	ChMVO [Stud]	HMVO [Prop]
Population Size	20	20	20	20	20	20	20
Max Iter	100	100	100	100	100	100	100
Choas IterkMax	-	-	-	-	-	20	20
Max runs 'or' trials	50	50	50	50	50	50	50
Algorithm Parameter	Wmax = 0.9	HMCR = 0.9	-	WEP_Max = 1.0	WEP_Max = 1.0	WEP_Max = 1.0	WEP_Max = 1.0
	Wmin = 0.4	PARmin = 0.4	-	WEP_Min = 0.2	WEP_Min = 0.2	WEP_Min = 0.2	WEP_Min = 0.2
	$C_1 = 2$	PARmax = 0.9	-	p=6	p=6	m = 0.5	m = 0.5
	$C_2 = 2$	bwmin = 0.0001	-	-	-	-	-
	-	bwmax = 1.0	-	-	-	-	-

4.4.1 Case study on IEEE 33-bus Radial Distribution Network

The competency of the proposed HMVO is tested on well known *IEEE* 33-bus Radial Distribution Network. The test system is operating at 12.66 kV with 100 kVA base, having 33 buses and 32 line sections. The line data and bus data of the test system are delineated in APPENDIX-1 [78]. The system has total active and reactive power demands of 3715 kW and 2300 kVAR, respectively. The overall objective function governed by Eq. (3.21) can be minimized by appropriately accommodating the *multiple DG units* for two different scenarios of the test system.

4.4.1.1 Three DGs operating with Unity Power Factor – First Scenario

In this scenario, three numbers of DG units operating with *Unity Power Factor* (*UPF*) are considered to solve the optimal DG accommodation problem. The goal here is to, simultaneously, *minimize the electrical energy losses, minimize the overall node voltage deviation, maximize the overall voltage stability margin*, and *minimize the energy not served*.

The simulation results of the proposed *HMVO* method for this scenario are summarized in Table 4.2 and compared with the results obtained by the attempted algorithms such as PSO, AHS, SSA, basic MVO, SMVO, and ChMVO. From Table 4.2, it may be pointed out that the proposed HMVO method has the capability to provide the optimum values for energy losses, overall VD, overall VSM, and ENS compared to the other algorithms. Also, it is observed that 62.64% of energy loss reduction has been realized using proposed *HMVO* approach, which is *highest* among the attempted algorithms. Furthermore, almost 96.10% reduction and 17.81% improvement have been realized in the case of overall bus voltage deviation and overall voltage stability margin, respectively. Therefore, it may be concluded that the system performance in terms of voltage magnitudes and security margin has been enhanced from the base case to DG case (first scenario). The best values offered by the algorithms are boldfaced in the Table 4.2. The system node voltage magnitudes attained by the proposed approach under this scenario are depicted in Figure 4.2. This figure indicates that the voltage profile has improved remarkably from *'without DG accommodation case'* to *'with DG accommodation case'*. Furthermore, the comparative convergence characteristics of various algorithms are illustrated in Figure 4.3. The Figure 4.3 reveals that the proposed *HMVO* provides the faster convergence and better solution in terms of *minimum FF* value over the PSO, AHS, SSA, basic MVO, SMVO, and ChMVO algorithms.

Table 4.2 Comparative results of the *studied algorithms* for IEEE 33-bus *RDN*

Cases	Optimizer	DG loc (DG Size in kVA)	f_1	f_2	f_3	f_4	*Eloss reduction* (%)
Base Case	-	-	1848.20	13.3784	26.05	5.7733	-
First Scenario	**PSO [Stud]**	02 (2220) 13 (1065) 30 (1360)	798.40	0.6276	30.55	4.9405	56.80
	AHS [Stud]	11 (1220) 21 (0395) 30 (1358)	807.44	0.6935	30.52	4.9533	56.31
	SSA [Stud]	08 (0797) 12 (0772) 30 (1167)	783.70	0.6369	30.59	5.0372	57.59
	Basic MVO [Stud]	10 (1155) 24 (1157) 28 (1390)	732.93	0.6774	30.67	5.0321	60.34
	SMVO [Stud]	03 (1910) 14 (0920) 30 (1236)	727.73	0.5718	30.65	4.9566	60.62
	ChMVO [Stud]	11 (1195) 24 (1160) 30 (1210)	699.71	0.5714	30.69	4.9489	62.14
	HMVO [Prop]	13 (1030) 24 (1185) 30 (1270)	**690.31**	**0.5213**	**30.69**	**4.8797**	**62.64**
Second Scenario	**PSO [Stud]**	06 (1247) 14 (0745) 30 (1122)	235.85	0.0721	31.84	5.2989	87.23
	AHS[Stud]	06 (1443) 10 (0921) 31 (0762)	270.95	0.1236	31.66	5.3392	85.33
	SSA [Stud]	13 (0932) 24 (1700) 28 (2388)	437.40	0.5088	**33.32**	5.3830	76.33
	Basic MVO [Stud]	03 (1860) 12 (1018) 30 (1341)	231.12	0.0604	31.79	5.3178	87.49
	SMVO [Stud]	03 (1923) 14 (0868) 30 (1395)	221.94	0.0515	31.79	5.3020	87.99
	ChMVO [Stud]	03 (1930) 14 (0865) 30 (1395)	221.95	0.0513	31.79	5.3019	87.99
	HMVO [Prop]	13 (0950) 24 (1198) 30 (1450)	**164.72**	**0.0303**	**32.97**	**5.2491**	**91.08**

f_1 = Energy loss (MWh); f_2 = Overall VD; f_3 = Overall VSM; f_4 = Energy Not Served (10^4 kWh/year)

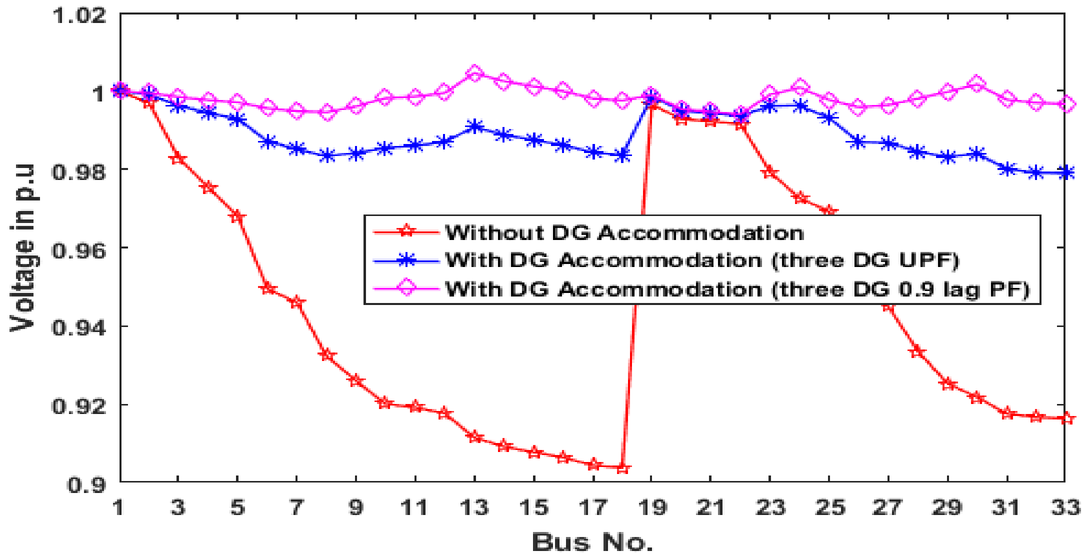

Figure 4.2 Node voltage of IEEE 33-bus *RDN* without and with DG accommodation

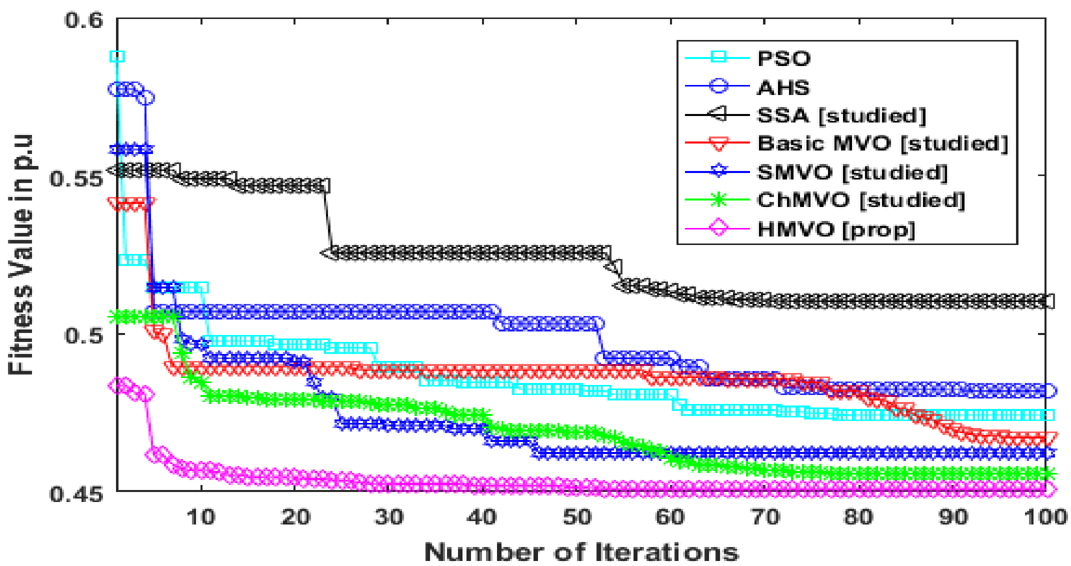

Figure 4.3 First Scenario - convergence profiles of *min FF* offered by different optimizers for IEEE 33-bus *RDN*

4.4.1.2 Three DGs operating with 0.9 Lagging Power Factor – Second Scenario

This scenario considers the three DG units operating with 0.9 *Lagging Power Factor* (*LPF*) which can deliver both real- and reactive powers to the power distribution system. The comparison of the test results of the various optimization methods are also presented in Table 4.2. From this table, it may be noticed that the proposed method outperforms the other methods in terms of energy losses, overall VD, and ENS but the

VSM obtained by the SSA algorithm is high among the all the methods. However, it is near to the value of VSM obtained by the proposed algorithm. The voltage profile of the system for this scenario is also depicted in Figure 4.2. Furthermore, the convergence curve for all the optimization methods is illustrated through Figure 4.4. This figure indicates that the proposed method has shown faster convergence curve and least *minimum FF* values.

From the above discussion on the IEEE 33-bus *RDN* Test System for two scenarios, it may be concluded that the proposed *HMVO* optimizer can provide the maximum benefits in terms of minimizing the energy losses, minimizing the VD, maximizing the VSM, and minimizing the energy not served upon the optimal accommodation of DG units. Further, it is observed that the proposed method has furnished the better *minimum FF* values and faster convergence characteristics. The voltage profile of the test system is enhanced from '*without DG case*' to '*with DG case*'. Furthermore, the voltage profile is best for the *second scenario* as compared with the *first scenario*, as the second scenario can provide both real and reactive powers to the distribution system.

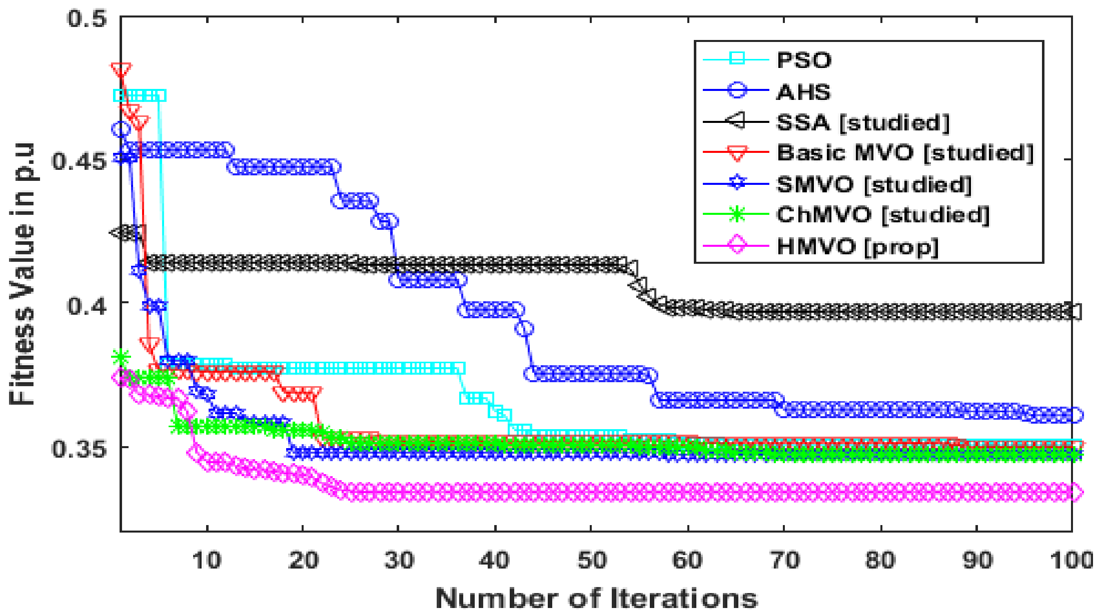

Figure 4.4 Second Scenario - convergence profiles of *min FF* offered by different optimizers for IEEE 33-bus *RDN*

4.4.2 Case study on INDIAN 85-bus Radial Distribution Network

The effectiveness of the proposed *HMVO* method is also tested on large size INDIAN 85-bus *RDN* Test System. This system is operating with 11 kV, 100 kVA base, and having 85-buses, and 84-lines. The line data and bus data of this test system are reported in APPENDIX-4 [82]. The system has total active and reactive power demand of 2569.28 kW and 2621.18 kVAR, respectively.

4.4.2.1 Three DGs operating with Unity Power Factor – First Scenario

In this scenario, three DG units operating with *unity power factor* are considered to get the maximum benefits from DG accommodation in a 85 -bus distribution system. The test results of the proposed method along with the other optimizers are reported in Table 4.3. From this table, it may be pointed out that the proposed algorithm is competent to dispense the better results of the other methods. The voltage profile of the test system for this scenario is shown in Figure 4.5. The convergence profiles of *minimum FF* offered by different optimizers are shown in Figure 4.6. From this figure one can observe that the proposed *HMVO* method provides the faster convergence.

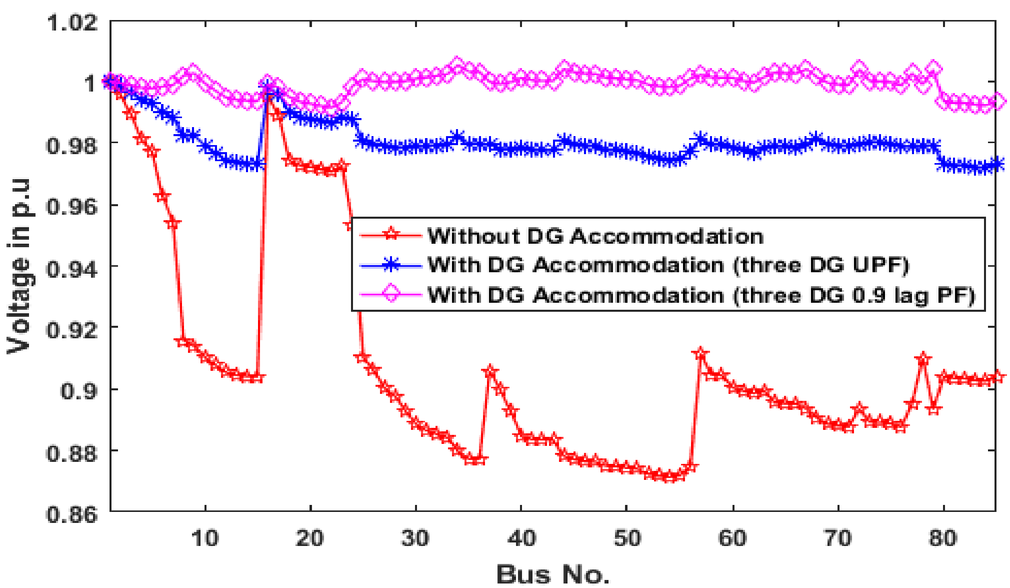

Figure 4.5 Node voltage of INDIAN 85-bus *RDN* without and with DG accommodation

Table 4.3 Comparative results of the *studied algorithms* for INDIAN 85-bus *RDN*

Cases	Optimizer	DG loc (DG Size in kVA)	f_1	f_2	f_3	f_4	*Eloss reduction (%)*
Base Case	-	-	2765.5	82.0256	58.01	7.0172	-
First Scenario	**PSO [Stud]**	27 (1082) 48 (0466) 60 (1288)	1452.2	3.9673	77.53	6.2489	47.48
	AHS [Stud]	10 (0910) 32 (1140) 67 (0735)	1406.3	4.1099	77.36	6.2215	49.14
	SSA [Stud]	25 (0730) 34 (0975) 60 (1122)	1440.5	3.8240	77.66	6.2417	47.91
	Basic MVO [Stud]	25 (1366) 35 (0741) 67 (0790)	1431.5	3.5732	77.82	6.2090	48.23
	SMVO [Stud]	12 (0624) 32 (1210) 64 (0938)	1429.4	3.5836	77.76	6.1704	48.31
	ChMVO [Stud]	09 (1665) 35 (0757) 68 (0567)	1407.6	3.6513	77.75	6.2136	49.10
	HMVO [Prop]	09 (1392) 34 (0920) 68 (0620)	**1405.8**	**3.5394**	**77.82**	**6.2028**	**49.16**
Second Scenario	**PSO [Stud]**	34 (1081) 60 (1340) 80 (0510)	413.2	0.1218	83.41	6.5982	85.05
	AHS[Stud]	08 (1560) 35 (0855) 67 (0770)	391.8	0.1115	83.93	6.5808	85.83
	SSA [Stud]	26 (0725) 34 (0995) 60 (1380)	444.3	0.2934	**84.46**	6.6153	83.93
	Basic MVO [Stud]	11 (0770) 32 (1335) 64 (0900)	412.1	0.1256	83.93	6.6013	85.09
	SMVO [Stud]	11 (0965) 34 (1072) 67 (0914)	396.6	0.1012	83.68	6.5941	85.65
	ChMVO [Stud]	09 (1430) 34 (0935) 67 (0770)	387.1	0.1057	83.86	6.5824	86.00
	HMVO [Prop]	09 (1480) 34 (0950) 67 (0740)	**381.2**	**0.0891**	**84.01**	**6.5801**	**86.21**

f_1 = Energy loss (MWh); f_2 = Overall VD; f_3 = Overall VSM; f_4 = Energy Not Served (10^4 kWh/year)

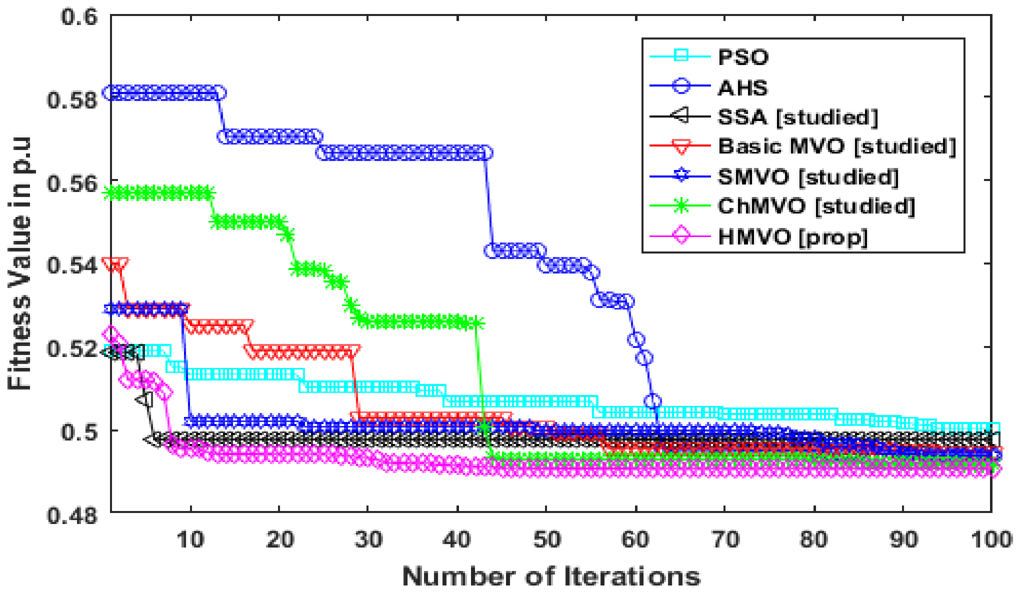

Figure 4.6 First Scenario - convergence profiles of *min FF* offered by different optimizers for INDIAN 85-bus *RDN*

4.4.2.2 Three DGs operating with 0.9 Lagging Power Factor – Second Scenario

The simulation results of the proposed algorithm along with the other optimizers are also tabulated in Table 4.3 for this scenario. Here also, the *HMVO* method has yielded the better solutions compared to the other optimization methods. The voltage profile of the test system for this case is also represented in Figure 4.5. Also, the comparative convergence characteristics of the different optimizers are shown in Figure 4.7. The proposed *HMVO* optimization method has offered the best *minimum FF* values than the other methods.

From the above discussion of the two scenarios of the *INDIAN* 85-bus *RDN*, it may be concluded that the proposed *HMVO* optimizer is capable to dispense the maximum benefits in terms of minimizing the energy losses, minimizing the VD, maximizing the VSM, and minimizing the energy not served (ENS) due to the optimal accommodation of DG's. Faster convergence characteristics with best *minimum FF* values are always promised by proposed method. The voltage profile of the test system is improved significantly due to the optimal placement and sizing of DG units. Furthermore, the node voltages of the test system with 0.9 *lagging power factor* DG's are much better than the voltages of the case of DG's with *unity power factor* as the real and reactive powers are supported locally in the case of 0.9 *lagging power factor* DG's.

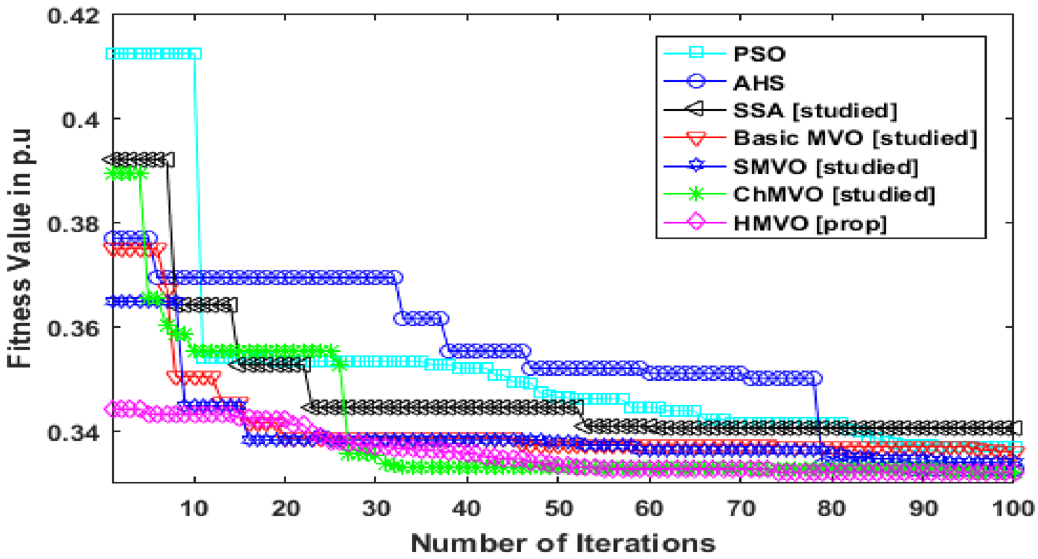

Figure 4.7 Second Scenario - convergence profiles of *minFF* offered by different optimizers for INDIAN 85-bus *RDN*

4.5 Statistical Analysis of Proposed HMVO algorithm

In order to validate the performance of any meta-heuristic optimization algorithm, it has to undergo through some statistical measures. In this work, the following three statistical measures are considered for the proposed *HMVO* method to endorse its capability to solve the optimal accommodation of DG problem .

Statistical Mean: It is an average of the solutions that are generated by executing the optimizer for *Maxiter* generations of M runs and is given by Eq. (4.11).

$$S\_Mean = \frac{1}{M}\sum_{i=1}^{M}\left(\frac{1}{MaxIter}\sum_{j=1}^{MaxIter} S_{ij}\right) \tag{4.11}$$

where S_{ij} is the solution obtained for j^{th}-iteration of i^{th}-run.

Statistical Standard Deviation: It is an indicator of the variation of the best fitness values found when running the optimizer for *M* runs. Additionally, it represents the robustness and stability of the algorithm and it is governed by Eq. (4.12).

$$S\_Std = \sqrt{\frac{1}{M-1}\sum_{i=1}^{M}\left(\left(\frac{1}{MaxIter}\sum_{j=1}^{MaxIter} S_{ij}\right) - S\_Mean\right)^2} \tag{4.12}$$

t-test method: The *t-test* method is a statistical assessment to measure the considerable variation between two algorithms and is expressed as in Eq. (4.13) [90].

$$t = \frac{S\_Mean_2 - S\_Mean_1}{\sqrt{(S\_Std_2^2 + S\_Std_1^2)/(\beta+1)}} \tag{4.13}$$

where S_Mean_1 and S_Mean_2 are the statistical mean values of the algorithm-1 and algorithm-2, respectively. S_Std_1 and S_Std_2 are the statistical standard deviation of the algorithm-1 and algorithm-2, respectively. β is the value of degree of freedom.

The positive value for "*t*" indicates that the first algorithm is superior over the second algorithm. If the value of *t* is greater than 1.645 with β (=49), there is a huge contrast established between two algorithms with a 95% confidence interval level [90].

The proposed HMVO algorithm and other optimizers have been tested upon these three statistical measures for the two test systems and the results are tabulated in Table 4.4 and Table 4.5. From Table 4.4, for the first scenario, it may be observed that the lowest *S_mean*, *S_Std*, and *t-test* values are secured by the proposed *HMVO* method and their values are reported as 0.463, 0.010, and 0, respectively. Also, for the second scenario, the *S_mean*, *S_Std*, and *t-test* values are shown as 0.343, 0.007, and 0, respectively. Additionally, the *t-value* for the other algorithms is obtained as more than 3.45 with confidence interval level of 98%, implies that the significant difference has been established between the proposed and other algorithms. Furthermore, the proposed *HMVO* approach holds the Rank-1 position in both the scenarios and this implies that it can provide the optimal solutions as compared to the other methods. Thus, from the statistical analysis conducted on the two bench-mark radial power distribution systems, it is evident that the proposed *HMVO* based optimization approach offers robust and promising results. The proposed method produces the quality solutions for the planning problem due to its two level inbuilt characteristics with some additional computational requirement. This additional requirement plays insignificant influence as the ODDG problem is a planning problem where quality solution occupies top priority.

Table 4.4 Statistical measures of IEEE 33-bus *RDN*

Cases	Method	*S_mean*	*S_Std*	*t-test value @Rank*	*CPU Time (s)*
First scenario	**PSO**	0.507	0.055	5.619@4	16.8
	AHS	0.519	0.050	7.842@6	25.5
	SSA	0.625	0.259	4.451@3	23.7
	***B*- MVO**	0.515	0.044	8.177@7	14.0
	SMVO	0.473	0.014	4.274@2	25.3
	ChMVO	0.491	0.030	6.331@5	50.2
	HMVO	**0.463**	**0.010**	**0/1**	59.4
Second scenario	**PSO**	0.380	0.022	10.97@6	15.9
	AHS	0.389	0.021	14.47@7	23.8
	SSA	0.443	0.158	4.513@3	21.3
	***B*- MVO**	0.410	0.138	3.456@2	12.9
	SMVO	0.354	0.010	5.749@4	23.8
	ChMVO	0.364	0.019	6.979@5	45.1
	HMVO	**0.343**	**0.007**	**0/1**	55.2

Table 4.5 Statistical measures of INDIAN 85-bus *RDN*

Cases	Method	*S_mean*	*S_Std*	*t-test value @Rank*	*CPU Time (s)*
First scenario	**PSO**	0.600	0.300	2.551@4	47.4
	AHS	0.504	0.006	11.40@7	91.5
	SSA	0.785	0.451	4.612@5	48.2
	***B*- MVO**	0.864	0.481	5.503@6	47.0
	SMVO	0.516	0.140	3.663@2	55.8
	ChMVO	0.520	0.141	3.966@3	73.4
	HMVO	**0.493**	**0.002**	**0/1**	84.1
Second scenario	**PSO**	0.432	0.089	6.635@6	46.5
	AHS	0.411	0.054	7.969@7	89.2
	SSA	0.483	0.177	5.453@5	46.1
	***B*- MVO**	0.462	0.194	4.168@3	46.2
	SMVO	0.359	0.014	3.983@2	52.4
	ChMVO	0.383	0.044	5.451@4	69.8
	HMVO	**0.348**	**0.013**	**0/1**	76.3

4.6 Comparison with the works reported in Literature

Furthermore, in order to verify the superiority of the proposed *HMVO* method, it is compared with the results of algorithms available in the literature such as Genetic Algorithm (GA) [44], Particle Swarm Optimization (PSO) [44], GAPSO [44], QTLBO

[46], TLBO [45], and LFSSA [43]. The objectives considered are same as that of [43, 44 45, 46] which are (i) minimization of real power losses (Ob_1), (ii) Voltage profile improvement (Ob_2), and (iii) maximization of voltage stability index (Ob_3). The algorithm has been tested in two cases: (I) *three DGs operating at unity power factor*, (II) *three DGs operating at 0.85 lagging power factor.*

Table 4.6 Comparison of results offered by the proposed method and algorithms available in the literature for IEEE 33-bus *RDN*

Cases	Method	Optimal DG loc (DG Size in kVA)	Ob_1 (MW)	Ob_2 (p.u)	Ob_3 (p.u)	Loss reduct -ion (%)	No. Iter
Base Case		-	0.2109	0.1338	0.6690	-	-
I	**GA [44]**	11(1500) 29(0422) 30(1071)	0.1063	0.0407	0.9490	49.62	-
	PSO [44]	08(1176) 13(0981) 32(0829)	0.1053	0.0335	0.9256	50.09	-
	GAPSO [44]	11(0925) 16(0863) 32(1200)	0.1034	0.0124	0.9508	50.99	-
	TLBO [46]	12(1182) 28(1191) 30(1186)	0.1246	0.0011	0.9503	40.94	73
	QTLBO [46]	13(1083) 26(1187) 30(1199)	0.1034	0.0011	0.9530	50.99	62
	TLBO [45]	09(0884) 18(0895) 31(1195)	0.1040	0.0295	0.9547	50.68	-
	HMVO	13(1120) 24(1168) 30(1684)	**0.0959**	**0.0008**	**0.9640**	**54.43**	**17**
II	**LSFSA [43]**	06(1383) 18(0552) 30(1063)	0.0267	0.0013	0.9323	86.83	-
	HMVO	13(0918) 24(1210) 30(1454)	**0.0148**	**0.0002**	**0.9789**	**92.98**	**24**

Ob_1 = minimization of losses; Ob_2 = Voltage profile improvement; Ob_3 = maxi. of Voltage stability index

The test results are presented in the Table 4.6. From this table, it may be pointed out that the proposed method is outperforms the existing algorithms in terms of the values corresponding to the objective functions with better convergence features (number of iterations).

This part of the work was published as "New Hybrid Multiverse Optimization Approach for Optimal Accommodation of DGs in Power Distribution Networks," *IET Generation, Transmission & Distribution*, vol. 13, no. 13, pp. 2673-2685, July 2019. DOI: 10.1049/iet-gtd.2018.5763 (*Indexed in SCI*) and a primitive portion of this work was presented as "An Optimal Accommodation of Distributed Generation in Power Distribution Systems," *20th National Power Systems Conference (NPSC), 14-16 Dec 2018. Tiruchirappalli, India,* DOI: 10.1109/NPSC.2018.8771743.

4.7 Summary

This chapter has covered the implementation of proposed Hybrid Multi-Verse Optimization (HMVO) algorithm for optimal DG accommodation problem in Radial Distribution Systems. The Hybrid Multi-Verse Optimization method has been formulated by integrating the Space Transformation Search (STS) method and Piecewise Linear Chaotic Map (PLCM) based optimization method. The proposed method is illustrated on the two bench-mark radial systems under two scenarios and the test results are presented in this chapter. These test results revealed that the proposed method has outperformed its basic counterpart as well as other algorithms in terms of quality solutions and better convergence characteristics. To check the quality of the solutions, it has been tested on three statistical measures and these measures indicated that the proposed method has provided better solutions as compared to other optimization techniques. The proposed method may serve as promising tool for multi-objective DG accommodation in distribution systems.

Up to this part of the research work, the multi-objective optimization problem is solved by converting it in to single objective optimization problem (i.e. Weighted Sum Approach). Further, the uncertainty associated with the load demand and power output of the DG units has not incorporated in the optimization problem. The next stage of the investigation is focused on system studies under uncertainty environment with *Multi-Objective Jaya Algorithm* (*MOJA*) and the same is reported in Chapter-5.

CHAPTER-5

Long term Mixed DG units optimal deployment with the incorporation of uncertainty and DG degradation effect

5.1 Introduction

The future distribution system is no more passive but active with the widespread deployment of Renewable Energy Sources (RESs) technologies such as Solar Photo Voltaic (SPV), Wind Turbines (WTs), Bio-mass, Geo-thermal, Tidal, and Hydro-power units. These energy resources seem to be the only option to a sustainable energy supply infrastructure since they are neither exhaustible nor polluting. However, most of renewable energy based Distributed Generations (DGs) are with intermittent power output. So, while considering renewable DGs, the stochastic nature of load demand has also to be taken into account.

In this Chapter, the optimal deployment of DGs (ODDGs) problem have been solved by considering the uncertainty associated with the load demand, WT and SPV. Furthermore, *DG degradation effect* is also incorporated in the optimization model which was ignored by majority of the works in literature. To create the uncertainty in load demand (real and reactive) of different customers and resources (Power output of WT and PV), a Self-adaptive Polyhedral Deterministic Uncertainty Set (SPDUS) [75] has been used. In the next section, the concept of SPDUS is explained in detail.

5.2 Modelling of Uncertainty using Self-adaptive Polyhedral Deterministic Uncertainty Set (SPDUS) [75]

The optimal accommodation of DGs under uncertain environmental condition primarily depends on the uncertainty of load demand, power output from DGs, and the number of states of the system being considered. Usually, DGs are expected to operate for 20-25 years. Therefore, the system states which are selected should represent this total planning horizon while solving the optimal DG accommodation problem. Also, special attention must be paid for the accurate modeling of load demand and DGs generation profiles under uncertainty environment. To model the randomness of variables (load, WT power, PV output power, load growth, fuel prices), Probability Distribution Function (PDF) [65, 67, 69, 70, 72, 73], Point Estimation Method (PEM) [66, 68], Fuzzy Approach (FA) [71], Self-adaptive Polyhedral Deterministic Uncertainty Set (SPDUS) [75], and Robust Optimization (RO) [76] have been employed. The PDF method suffers from computational effort, whereas Fuzzy needs the suitable membership function, PEM requires the solution on interval basis and RO is difficult to employ for nonlinear optimization problems. However, SPDUS needs only the mean and standard deviation of the historical data which can be easily determined from the stored data base. The SPDUS approach has resulted in an uncertainty pattern which has close relevance with practical data.

In this thesis, the more efficient method for uncertainty treatment, *Self-adaptive Polyhedral Deterministic Uncertainty Set* (SPDUS) [75] is employed. This method handles the uncertain data that inherently considers most probable data set for the adequate number of system states with seasonal variations. The SPDUS requires only the basic information such as the mean and standard deviation of the historical data. The mean and standard deviation are used to determine the (i) data spread (DS), and (ii) budget of uncertainty (BOU). These are two essential parameters that play a crucial role while generating the synthetic data. In the work of [75], data has been generated on hourly basis. Unlike [75], the quarter-hourly (i.e. 15 minutes) available data has been used to generate synthetic data *in order to not to miss* the opportunity to identify the high load factor or power generation that may be ignored in the hourly historical data. This available quarter-hourly annual historical data is divided into 12 segments (each segment represents a month). Further, for each month data, quarter-hourly mean and standard deviation are determined to generate the synthetic data (using polyhedral deterministic sets) for the WT, PV, and different load customers. The historical data of years 2017 and 2018 related to load, Wind power, and PV power is collected from Elia, an ISO of Belgium of Europe on 03.01.2019 [91] and then the synthetic data is generated using SPDUS.

To generate the synthetic data, the following terms and notation have been used.

Let, Ψ represents the value of synthetic data;

$\mu_{y,ms,t,i}^{PDL,R,C,I}$ denotes the historical quarterly-hour (15 minutes) mean value of real power load demand of residential, commercial, and industrial customer type at time-*t*, month-*ms*, year-*y* of the planning horizon NY at i^{th}-bus;

$\sigma_{y,ms,t,i}^{PDL,R,C,I}$ describes the historical quarterly-hour (15 minutes) standard-deviation value of real power load demand of residential, commercial, and industrial customer type at time-*t*, month-*ms*, year-*y* of the planning horizon NY at i^{th}-bus;

$\underline{\mu}_{y,ms,t,i}^{PDL,R,C,I}$ represents the lower boundary: *i.e.* ($\mu_{y,ms,t,i}^{PDL,R,C,I} - \zeta\sigma_{y,ms,t,i}^{PDL,R,C,I}$);

$\overline{\mu}_{y,ms,t,i}^{PDL,R,C,I}$ indicates the upper boundary: *i.e.* ($\mu_{y,ms,t,i}^{PDL,R,C,I} + \zeta\sigma_{y,ms,t,i}^{PDL,R,C,I}$);

$\underline{\mu}_{y,ms,t,i}^{PDL,R,C,I}$ and $\overline{\mu}_{y,ms,t,i}^{PDL,R,C,I}$ cover the Data Spread (DS);

$\hat{\mu}_{y,ms,i}^{PDL,R,C,I}$ is the average of all the mean values of $\mu_{y,ms,t,i}^{PDL,R,C,I}$ terms; (*t* =1,2,..*NT*; *NT* = Total number of time stamps in a day (i.e. 96));

$\hat{\sigma}_{y,ms,i}^{PDL,R,C,I}$ represents the average of all the standard-deviation values of $\sigma_{y,ms,t,i}^{PDL,R,C,I}$ terms; (*t* =1,2,..*NT*; *NT* = Total number of time stamps in a day (i.e. 96));

($\hat{\mu}_{y,ms,i}^{PDL,R,C,I} - \zeta \hat{\sigma}_{y,ms,i}^{PDL,R,C,I}$) and ($\hat{\mu}_{y,ms,i}^{PDL,R,C,I} + \zeta \hat{\sigma}_{y,ms,i}^{PDL,R,C,I}$) are the lower and upper boundaries which constitute the Budget of Uncertainty (BOU);

$\hat{\Psi}_{y,ms,i}^{PDL,R,C,I}$ indicates the average of all the synthetic data values of $\Psi_{y,ms,t,i}^{PDL,R,C,I}$ terms; (*t* =1,2,..*NT*; *NT* = Total number of time stamps in a day (i.e. 96));

ζ is a constant set to 1;

NB represents the total number of buses in the distribution system;

NWT indicates the total number of WT units;

NPV is the total number of PV units;

Then, the polyhedral deterministic uncertainty set, $W_{y,ms,t}^{PDL,R,C,I}$ for *active power load demand* of residential, commercial, and industrial customers at time-*t*, month-*ms*, year-*y* over the planning horizon *NY* is expressed in Eq. (5.1) [75].

$$\left.\begin{array}{l} W_{y,ms,t,i}^{PDL,R,C,I} = \left\{ \Psi_{y,ms,t,i}^{PDL,R,C,I} \in R^n : \underline{\mu}_{y,ms,t,i}^{PDL,R,C,I} \le \Psi_{y,ms,t,i}^{PDL,R,C,I} \le \overline{\mu}_{y,ms,t,i}^{PDL,R,C,I} \right\}; \forall i \in NB \\ \underline{\mu}_{y,ms,t,i}^{PDL,R,C,I} = \mu_{y,ms,t,i}^{PDL,R,C,I} - \zeta\sigma_{y,ms,t,i}^{PDL,R,C,I} \quad ; \quad \overline{\mu}_{y,ms,t,i}^{PDL,R,C,I} = \mu_{y,ms,t,i}^{PDL,R,C,I} + \zeta\sigma_{y,ms,t,i}^{PDL,R,C,I} \\ s.t. \quad \hat{\mu}_{y,ms,i}^{PDL,R,C,I} - \zeta \hat{\sigma}_{y,ms,i}^{PDL,R,C,I} \le \hat{\Psi}_{y,ms,i}^{PDL,R,C,I} \le \hat{\mu}_{y,ms,i}^{PDL,R,C,I} + \zeta \hat{\sigma}_{y,ms,i}^{PDL,R,C,I} \end{array}\right\} \tag{5.1}$$

Similarly, the polyhedral deterministic uncertainty set, $W_{y,ms,t}^{QDL,R,C,I}$ for *reactive power load demand* of residential, commercial, and industrial customers at time-*t*, month-*ms,* year-*y* over the planning horizon *NY* is expressed in Eq. (5.2).

$$\left.\begin{array}{l} W_{y,ms,t,i}^{QDL,R,C,I} = \left\{ \Psi_{y,ms,t,i}^{QDL,R,C,I} \in R^n : \underline{\mu}_{y,ms,t,i}^{QDL,R,C,I} \le \Psi_{y,ms,t,i}^{QDL,R,C,I} \le \overline{\mu}_{y,ms,t,i}^{QDL,R,C,I} \right\}; \forall i \in NB \\ \underline{\mu}_{y,ms,t,i}^{QDL,R,C,I} = \mu_{y,ms,t,i}^{QDL,R,C,I} - \zeta \sigma_{y,ms,t,i}^{QDL,R,C,I} \quad ; \quad \overline{\mu}_{y,ms,t,i}^{QDL,R,C,I} = \mu_{y,ms,t,i}^{QDL,R,C,I} + \zeta \sigma_{y,ms,t,i}^{QDL,R,C,I} \\ s.t. \quad \hat{\mu}_{y,ms,i}^{QDL,R,C,I} - \zeta \hat{\sigma}_{y,ms,i}^{QDL,R,C,I} \le \hat{\Psi}_{y,ms,i}^{QDL,R,C,I} \le \hat{\mu}_{y,ms,i}^{QDL,R,C,I} + \zeta \hat{\sigma}_{y,ms,i}^{QDL,R,C,I} \end{array} \right\} \tag{5.2}$$

Here, $\Psi_{y,ms,t,i}^{QDL,R,C,I}$, $\mu_{y,ms,t,i}^{QDL,R,C,I}$, and $\sigma_{y,ms,t,i}^{QDL,R,C,I}$ denote the synthetic data, mean value, and standard deviation values of *reactive power demand* of residential, commercial, and industrial customers at time-*t*, month-*ms*, year-*y* of i^{th}-bus. The $\hat{\mu}_{y,ms,i}^{QDL,R,C,I}$ and $\hat{\sigma}_{y,ms,i}^{QDL,R,C,I}$ represent the average of mean and standard deviation values of *reactive power demand* of residential, commercial, and industrial customers for the month-*ms* of year-*y* at i^{th}-bus. The average values for mean and standard deviations are calculated using 96 time stamps.

Also, the polyhedral deterministic uncertainty sets for Wind Turbine's real power output and SPV's real power output are represented by using Eq. (5.3) and Eq. (5.4), respectively.

$$\left.\begin{array}{l} W_{y,ms,t,i}^{WT} = \left\{ \Psi_{y,ms,t,i}^{WT} \in R^n : \underline{\mu}_{y,ms,t,i}^{WT} \le \Psi_{y,ms,t,i}^{WT} \le \overline{\mu}_{y,ms,t,i}^{WT} \right\}; \forall n \in NWT \\ \underline{\mu}_{y,ms,t,i}^{WT} = \mu_{y,ms,t,i}^{WT} - \zeta \sigma_{y,ms,t,i}^{WT} \quad ; \quad \overline{\mu}_{y,ms,t,i}^{WT} = \mu_{y,ms,t,i}^{WT} + \zeta \sigma_{y,ms,t,i}^{WT} \\ s.t. \quad \hat{\mu}_{y,ms,i}^{WT} - \zeta \hat{\sigma}_{y,ms,i}^{WT} \le \hat{\Psi}_{y,ms,i}^{WT} \le \hat{\mu}_{y,ms,i}^{WT} + \zeta \hat{\sigma}_{y,ms,i}^{WT} \end{array} \right\} \tag{5.3}$$

$$\left.\begin{array}{l} W_{y,ms,t,i}^{PV} = \left\{ \Psi_{y,ms,t,i}^{PV} \in R^n : \underline{\mu}_{y,ms,t,i}^{PV} \le \Psi_{y,ms,t,i}^{PV} \le \overline{\mu}_{y,ms,t,i}^{PV} \right\}; \forall n \in NPV \\ \underline{\mu}_{y,ms,t,i}^{PV} = \mu_{y,ms,t,i}^{PV} - \zeta \sigma_{y,ms,t,i}^{PV} \quad ; \quad \overline{\mu}_{y,ms,t,i}^{PV} = \mu_{y,ms,t,i}^{PV} + \zeta \sigma_{y,ms,t,i}^{PV} \\ s.t. \quad \hat{\mu}_{y,ms,i}^{PV} - \zeta \hat{\sigma}_{y,ms,i}^{PV} \le \hat{\Psi}_{y,ms,i}^{PV} \le \hat{\mu}_{y,ms,i}^{PV} + \zeta \hat{\sigma}_{y,ms,i}^{PV} \end{array} \right\} \tag{5.4}$$

In this work, the renewable DG units such as WT and PV are treated to operate at 0.85 *lagging power factor* [44]. Therefore, *the synthetic data corresponding to the* ***Reactive***

Power generation *of both WT and PV unit is calculated by multiplying their "real power output" with the term* "$\tan\left(\cos^{-1}(PF)\right)$". Here, *PF* is the power factor of DG unit. Also, a non-renewable DG unit (constant power output) of Micro Turbine (MT) operating with 0.85 *lagging power factor* is chosen to participate along with the renewable DGs (WT and PV) to address the unavailability and intermittent nature of the renewable DGs.

5.3 Generation of Synthetic Data

The synthetic data generated for the *real power demand of Residential customer* is shown in Figure 5.1 for the month of (i) January of the beginning (1st year) and (ii) January of the last year (20th year) of the planning horizon. This data is generated on the basis of quarter-hourly time stamp historical load data [91]. For the annual historical data, the attention is paid to the 96 samples (each sample equal to 15 minutes) of each day of selected two months (like January 2017 and January 2018). There will be a total 62 days with 96 samples per day. Then, mean and standard deviation of 62 data entries related to first time interval are calculated. These mean and standard deviations are also calculated for remaining 95 time intervals. The Data Spread (DS) for each time interval is determined by using the estimated mean and standard deviation values. The arithmetic addition of standard deviation and mean with some arbitrary constant represents the upper bound of DS. On the other hand the lower bound is the subtraction of standard deviation from the mean value. Once the lower and upper bounds of DS values for all time intervals are calculated, the synthetic data which will be generated must be within these limits. Further, the synthetic data is constrained by the Budget of Uncertainty (BOU). To arrive at the BOU values, the average of 96 mean values and the average of 96 standard deviations are predetermined. Then, this (average of mean values + ζ*average of standard deviations) will act as upper boundary of BOU and (average of mean values - ζ*average of standard deviations) governing the lower boundary of BOU. Here, ζ is a constant taken as 1.

From the Figure 5.1, it is observed that the states of the synthetic data generated are not constant but have shown some variation for the beginning and end of the planning horizon. Further, it is bounded by the limits of DS. The generated synthetic data is kept as constant throughout the planning horizon (20 years). Before generating the synthetic data, the annual load growth of 3% has been imposed on the original load to include the load growth effect.

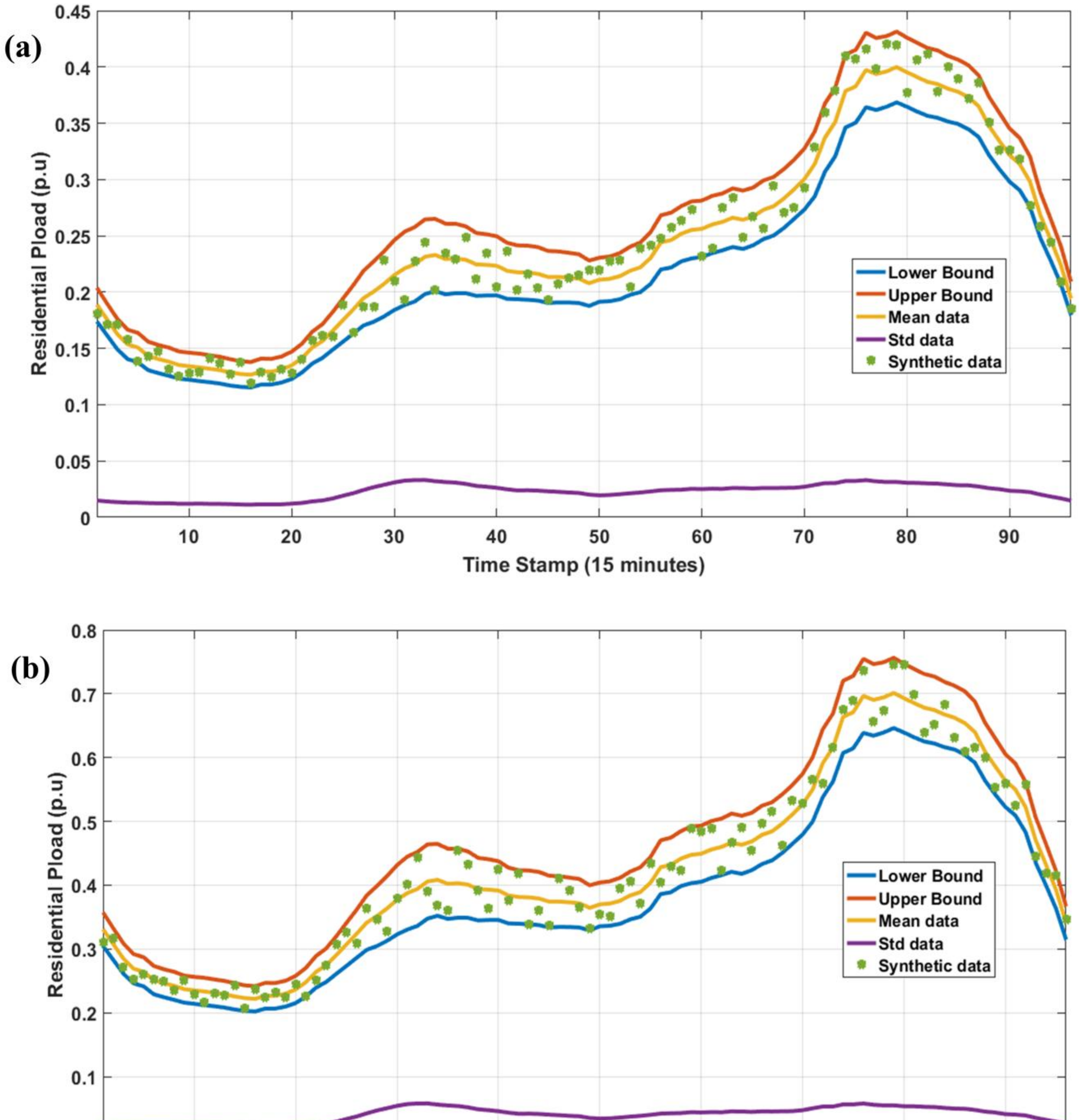

Figure 5.1 Synthetic Data profile for Real power demand of Residential customer for the (a) January month of the beginning (1st year) of planning horizon (b) January month of the last year (20th year) of the planning horizon.

In the similar way, the quarter-hourly synthetic data for *reactive power demand of Residential* customers is generated. Further, the *procedure adopted for the generation of synthetic data for real and reactive power demand of Residential customers* will be used to *generate the synthetic data for real and reactive power demands of commercial customer and industrial customers* using Eqs. (5.1)-(5.4). Also, the synthetic data for *real power generation* of both WT and PV is generated using the above steps. Then, the synthetic data for *reactive power generation* of WT and PV is determined by multiplying the generated real power synthetic data with term "$\tan\left(\cos^{-1}(PF)\right)$". Here, *PF* is the power factor of DG unit and is considered as *0.85 lagging power factor* [44].

5.4 DG degradation

Ageing is a fact of life. Just as with conventional power generation units, the energy produced by renewable sources like WT and SPV and non-renewable Micro Turbine (MT) gradually decreases over the planning horizon. This phenomenon is called *DG degradation*. It may be due to improper operation, falling aerodynamic performance, failure to take up preventive maintenance, unable to monitor the equipment *etc*. Understanding of these factors has lead to observation that there is an annual degradation of 0.2%, 0.25%, and 0.3% for Wind Turbine, SPV and MT, respectively [93]. Majority of the literature have not considered the effect of DG degradation for optimal placement and sizing problem especially under uncertainty environment. Planning of DG without considering the degradation effect is not near to the reality. Therefore, in this thesis, the annual DG degradation aspect is also considered for optimal planning of mixed DGs. The following expressions Eq. (5.5)-(5.7) are proposed to account the degradation effect.

$$P_{DG,y,ms,t,i}^{WT} = W_{y,ms,t,i}^{WT} \; P_{DG,i}^{WT} \left(1-\Delta^{WT}\right)^{y} \tag{5.5}$$

$$P_{DG,y,ms,t,i}^{PV} = W_{y,ms,t,i}^{PV} \; P_{DG,i}^{PV} \left(1-\Delta^{PV}\right)^{y} \tag{5.6}$$

$$P_{DG,y,ms,t,i}^{MT} = P_{DG,i}^{MT} \left(1-\Delta^{MT}\right)^{y} \tag{5.7}$$

where $P_{DG,y,ms,t,i}^{WT}$, $P_{DG,y,ms,t,i}^{PV}$, and $P_{DG,y,ms,t,i}^{WT}$ are the actual power produced by WT, SPV, and MT units at bus-*i* time-*t* month-*ms* of year-*y*, respectively. The $W_{y,ms,t,i}^{WT}$ and $W_{y,ms,t,i}^{PV}$ are the synthetic data values. The $P_{DG,i}^{WT}$, $P_{DG,i}^{PV}$, and $P_{DG,i}^{MT}$ are the maximum DG capacities installed at bus-i. The Δ^{WT} , Δ^{PV} , and Δ^{MT} represent the degradation rates of WT, SPV and MT, respectively. Finally, y represents the year.

5.5 Variability and diversity of load demand

In practical scenario, power distribution network supplies different types of customers such as residential, commercial, and industrial loads through various dedicated feeders namely residential feeders, commercial feeders, and industrial feeders, respectively. Further, the load of a particular type of customer at any node of the distribution system is not constant but depends on the *time and season.* Therefore, the optimal DG planning requires the accurate modelling of electrical loads that accounts the seasonality, variability, and diversity of the loads along with uncertainty. In this thesis, the variability of the loads at different buses is considered as that of [92] which is depicted in Figure 5.2. The seasonality in the load is accounted through the practical data as discussed in section 5.3 [91]. The diversity in the load is considered by dividing the system loads into different types of loads such as residential, commercial, and industrial loads. The mathematical model for real and reactive load of different customers is given as below Eqs. (5.8) - (5.9).

$$P_{y,ms,t,i}^{DL,R,C,I} = P_{y,ms,t,i}^{DL0,R,C,I} \left(\frac{V_{y,ms,t,i}}{V_0} \right)^{\eta_{R,C,I}} W_{y,ms,t,i}^{PDL,R,C,I} \tag{5.8}$$

$$Q_{y,ms,t,i}^{DL,R,C,I} = Q_{y,ms,t,i}^{DL0,R,C,I} \left(\frac{V_{y,ms,t,i}}{V_0} \right)^{l_{R,C,I}} W_{y,ms,t,i}^{QDL,R,C,I} \tag{5.9}$$

where $P_{y,ms,t,i}^{DL,R,C,I}$ and $Q_{y,ms,t,i}^{DL,R,C,I}$ are the active and reactive load demands of different customers at bus-i, time-t, month-ms of year-y. The $P_{y,ms,t,i}^{DL0,R,C,I}$ and $Q_{y,ms,t,i}^{DL0,R,C,I}$ are the real- and reactive- demands of various customers at base operating point for bus-i, time-t, month-ms in the year y. The $V_{y,ms,t,i}$ is the node voltage magnitude of i^{th}-bus at time-t, month-ms of year-y. The V_o is the base operating point voltage magnitude and $\eta_{R,C,I}$ and $\ell_{R,C,I}$ are the real- and reactive- power exponents for residential, commercial and industrial load models and are tabulated in Table 5.1 [92]. The $W_{y,ms,t,i}^{PDL,R,C,I}$ and $W_{y,ms,t,i}^{QDL,R,C,I}$ are the synthetic data corresponding to real and reactive power loads of various customers at bus-i, time-t, month-ms of year-y.

Table 5.1 Load Exponent Values for different Customers

Load model	Exponent value	
Residential	$\eta_R = 0.92$	$l_R = 4.04$
Commercial	$\eta_C = 1.51$	$l_C = 3.4$
Industrial	$\eta_I = 0.18$	$l_I = 6.0$

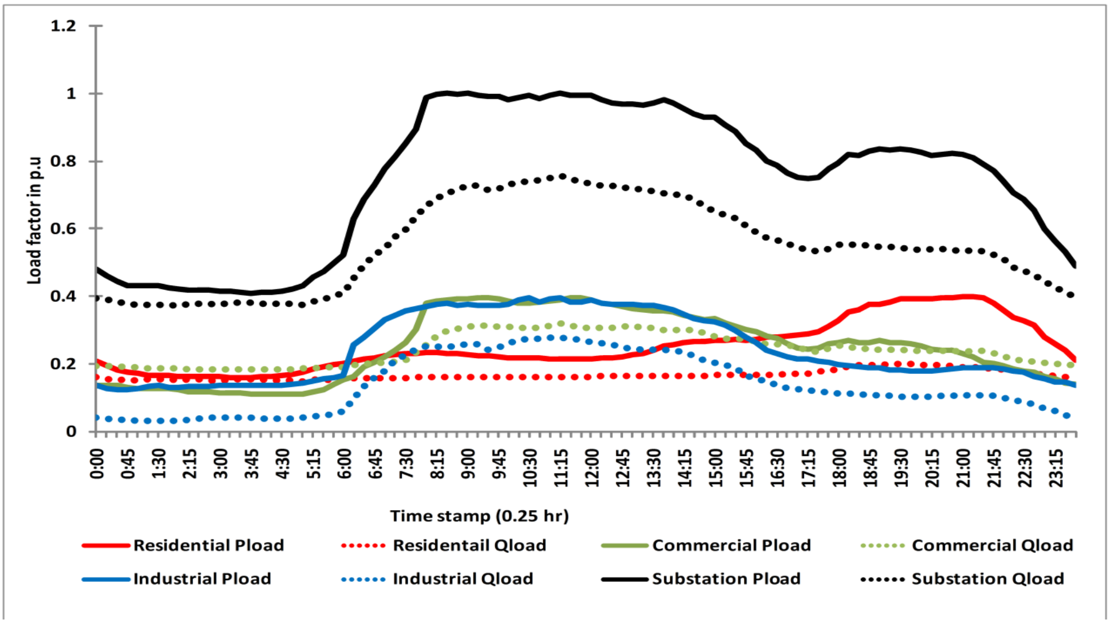

Figure 5.2 Quarter-hourly (15 minutes) load factors of different customers

5.6 Objective functions

Primary aim of any Distribution Company, DISCO, is to provide an uninterrupted quality power to the customers. Under deregulated environment, the ownership of DG can be either private party or DISCO itself. In this thesis, it is assumed that DISCO is the owner of the DG units. Further, the long-term DG planning problem has been considered to find the optimal place and size of mixed DG (WT, PV, and MT) units to optimize several techno-economical and environmental objectives without violating the operational constraints of the network.

In this Chapter, two prime objective functions, (i) *Maximization* of *DISCOs Profit* (*maxF1*) and (ii) *Distribution Network Technical Improvement* (*minF2*) have been formulated for optimal emplacement and sizing of Distributed Generation (DG) units under uncertainty environment by employing: (a) without DG degradation aspect.

(b) with DG degradation effect.

5.6.1 Maximization of DISCO Profit

As DISCO is the owner of the DGs, to calculate its net profit, the cost associated with DGs (investment, operation, maintenance, fuel and emissions) is to be subtracted from the Net Revenue. The Net Revenue of a DISCO refers to: (Revenue from different customers)+(Revenue from grid related to the surplus energy supplied to the grid)-(Amount paid to the grid for the energy drawn from the grid). The profit maximization function is defined as in Eq. (5.10). The proposed cost function is different from [75] in terms of Emission cost.

$$\max \ F_1 = \left[COST_{Rev} - COST_{Inv} - COST_{Op} - COST_{Ma} - COST_{Fu} - COST_{Emi} \right] \tag{5.10}$$

where $COST_{Rev}$ = Net revenue generation;

$COST_{Inv}$ = Investment cost of DG units (WT, PV, and MT);

$COST_{Op}$ = Operating cost of DGs;

$COST_{Ma}$ = Maintenance cost towards DG units;

$COST_{Fu}$ = Fuel cost;

$COST_{Emi}$ = Cost of Emissions;

5.6.1.1 Amount of Revenue

For any DISCO, the net revenue is generated by selling the power to customers and grid (if surplus power available). The deficit power of the DISCO can be met by the grid. The following Eq. (5.11) is used to determine the Net Revenue of DISCO.

$$COST_{\mathrm{Rev}} = \sum_{y=1}^{NY} \lambda^{y} \left[\sum_{ms=1}^{NM} ND_{ms,y} \sum_{t=1}^{NT} \left(C_y^{sg} P_{y,ms,t}^{excess} H_{y,ms,t} - C_y^{bg} P_{y,ms,t}^{defi} H_{y,ms,t} + C_y^{sc} \sum_{i=1}^{NB} P_{y,ms,t,i}^{LD,R,C,I} H_{y,ms,t} \right) \right] \tag{5.11 }$$

where $\lambda = \left(\frac{1+INF}{1+INR}\right)$ is the factor witch accounts the *Inflation (INF) and Interest Rates (INR)* on the various costs over the planning horizon. The indices for year, month, and time, respectively are *y*, *ms*, and *t*. Then, the *NY*, *NM*, *NT*, and *NB* are the number of years, number of months, number of time segments in a day, and number of nodes, respectively. The *i* stands for i^{th}-bus and $ND_{ms,y}$ indicates the number of days in a month- *ms* of year-*y*. The C_y^{sg} and C_y^{sc} are the selling prices to the grid and to the customers. The C_y^{bg} refers to buying price of the power from the grid. The $P_{y,ms,t}^{excess}$, $P_{y,ms,t}^{defi}$, and $P_{y,ms,t,i}^{LD,R,C,I}$ are the excess power of DISCO, deficit power of the DISCO, and load demand of various customers at time-*t* month-*ms* of year *y* at i^{th}-bus, respectively. $H_{y,ms,t}$ is the time segment (15 minutes).

5.6.1.2 Cost of DG Investment

The cost related to construction, erection, land preparation, investigation fee, labour cost, monitoring equipment *etc*., is included in the DG investment cost as expressed by Eq. (5.12).

$$COST_{Inv} = \sum_{i=1}^{NWT} P_{DG,i}^{WT} IC_{DG,i}^{WT} + \sum_{i=1}^{NPV} P_{DG,i}^{PV} IC_{DG,i}^{PV} + \sum_{i=1}^{NMT} P_{DG,i}^{MT} IC_{DG,i}^{MT} \qquad (5.12)$$

where $P_{DG,i}^{WT}$, $P_{DG,i}^{PV}$, and $P_{DG,i}^{MT}$ are the size of i^{th}-Wind generator, *PV* source, and Micro Turbine. The $IC_{DG,i}^{WT}$, $IC_{DG,i}^{PV}$, and $IC_{DG,i}^{MT}$ are the investment cost ($/kVA) of WT, PV and MT resource, respectively. The *NWT*, *NPV*, and *NMT* are the number of WT type, PV type, and MT type, respectively, to be installed in the distribution network.

5.6.1.3 Cost of DG Operation

The cost involved to produce electricity is called the operating cost of DG and is given in Eq. (5.13).

$$COST_{Op} = \sum_{y=1}^{NY} \lambda^y \left[\sum_{ms=1}^{NM} NOD_{ms,y} \sum_{t=1}^{NT} \left(OPC_y^{WT} \sum_{i=1}^{NWT} P_{y,ms,t,i}^{WT} H_{y,ms,t,i}^{WT} + OPC_y^{PV} \sum_{i=1}^{NPV} P_{y,ms,t,i}^{PV} H_{y,ms,t,i}^{PV} + OPC_y^{MT} \sum_{i=1}^{NMT} P_{y,ms,t,i}^{MT} H_{y,ms,t,i}^{MT} \right) \right] \qquad (5.13)$$

where $NOD_{ms,y}$ is the number of operating days of DG in month-*ms* of year-*y*. The OPC_y^{WT}, OPC_y^{PV}, and OPC_y^{MT} are the operating costs of WT, PV and MT, respectively. The $P_{y,ms,t,i}^{WT}$, $P_{y,ms,t,i}^{PV}$, and $P_{y,ms,t,i}^{MT}$ are the power generation from MT, PV and MT, respectively at i^{th}-bus time-*t* month-*ms* of year-*y*. The $H_{y,ms,t,i}^{WT}$, $H_{y,ms,t,i}^{PV}$, and $H_{y,ms,t,i}^{MT}$ are the operating time segments of WT, PV and MT, respectively (15 minutes).

5.6.1.4 Cost of DG Maintenance

For efficient operation of DGs, they sholud be properly maintained by yearly shut down for repaires or rennovation. Therefore, the cost associated with it is given below Eq. (5.14).

$$COST_{Ma} = \sum_{y=1}^{NY} \lambda^y \left[\sum_{ms=1}^{NM} NMD_{ms,y} \sum_{t=1}^{NT} \left(MC_y^{WT} \sum_{i=1}^{NWT} P_{y,ms,t,i}^{WT} H_{y,ms,t,i}^{WT} + MC_y^{PV} \sum_{i=1}^{NPV} P_{y,ms,t,i}^{PV} H_{y,ms,t,i}^{PV} + MC_y^{MT} \sum_{i=1}^{NMT} P_{y,ms,t,i}^{MT} H_{y,ms,t,i}^{MT} \right) \right] \quad (5.14)$$

where $NMD_{ms,y}$ is the number of maintenance days of DGs in month- *ms* of year-*y*. The MC_y^{WT}, MC_y^{PV}, and MC_y^{MT} are the maintenance costs of WT, PV, and MT, respectively.

5.6.1.5 Cost of Fuel

The power generation from MT depends on the quantity of fuel required for the power generation. The cost of fuel is given in Eq. (5.15).

$$COST_{Fu} = \sum_{y=1}^{NY} \lambda^y \left[\sum_{ms=1}^{NM} NOD_{ms,y} \sum_{t=1}^{NT} \left(FuC_y^{MT} \sum_{i=1}^{NMT} P_{y,ms,t,i}^{MT} H_{y,ms,t,i}^{MT} \right) \right] \quad (5.15)$$

where FuC_y^{MT} is the fuel cost of DG unit in year *y*. Other terms are already explained in the above subsections.

5.6.1.6 Cost of Emissions

The cost corresponding to the emissions produced by Micro Turbine and Grid should be included in the DG planning problem. The gases like, Carbon Dioxide (CO_2), Nitrogen Oxides (NO_x), and Sulphur Dioxide (SO_2) are considered as the most important pollutants. The mathematical formulation of emission cost is expressed as below Eq. (5.16) [72].

$$\left.\begin{aligned} COST_{Emi} &= \sum_{y=1}^{NY} \lambda^{y} \left[\sum_{ms=1}^{NM} NOD_{ms,y} \sum_{t=1}^{NT} \left(EMS_{y,ms,t}^{Grid} + \sum_{i=1}^{NMT} EMS_{y,ms,t,i}^{MT} \right) \right]; \\ EMS_{y,ms,t}^{Grid} &= \left(\alpha^{Grid} CO_2^{Grid} + \beta^{Grid} NOX^{Grid} + \varphi^{Grid} SO_2^{Grid} \right) P_{y,ms,t}^{Grid} H_{y,ms,t}^{Grid} \\ EMS_{y,ms,t,i}^{MT} &= \left(\alpha^{MT} CO_2^{MT} + \beta^{MT} NOX^{MT} + \varphi^{MT} SO_2^{MT} \right) P_{y,ms,t,i}^{MT} H_{y,ms,t,i}^{MT} \end{aligned}\right\} \tag{5.16}$$

where $EMS_{y,ms,t}^{Grid}$ and $EMS_{y,ms,t}^{MT}$ are the emissions due to grid and MT at time-*t* month-*ms* of year-*y*. The α, β, and φ are the emission coefficients ($/kg) associated with the gases (CO_2, NO_x, and SO_2) liberated from Grid and MT units.

5.6.2 Distribution Network Technical Objectives Improvement

Along with the profit maximization, the DISCO should also improve its technical parameters. In this study, four technical aspects are considered to enhance the performance of the distribution network. Therefore, the second objective function (F_2) which represents technical aspects should be minimized and is expressed as Eq. (5.17).

$$\min F_2 = \gamma_1 f_1 + \gamma_2 f_2 + \gamma_3 f_3^{-1} + \gamma_4 f_4 + \sum_{i=1}^{NCs} \varepsilon_i C_i \tag{5.17}$$

Here, f_1, f_2, f_3, and f_4 are the technical objective functions, discussed in ***Chapter-3***. These are explained in the following sections related to present topic. The coefficients, γ_1 to γ_4 denote the optimal weights given to the individual objectives. The sum of all these weights (γ_1, γ_2, γ_3 and γ_4) is equal to the one. As explained in ***Section 3.5***, using *Analytical Hierarchy Process* (*AHP*) [84], these weights were calculated as 0.3940, 0.2593, 0.1970, and 0.1497 for f_1, f_2, f_3, and f_4, respectively. The constant, ε_i indicates the penalty of i^{th} operational constraint C_i. *NCs* represents the total number of operational constraints. For minimization problem, ε_i will be assigned a high value when a constraint C_i violates the limit. The individual objective functions of Eq. (5.17) are made dimensionless quantities.

5.6.2.1 Minimization of Electrical Energy Losses (f_1)

The reduction in energy losses improves the efficiency of the distribution network and is expressed as Eq. (5.18). To arrive at this, the distribution network is segregated into three groups of buses to supply residential, commercial, and industrial loads.

$$\left.\begin{aligned}
f_1 &= \sum_{y=1}^{NY}\sum_{ms=1}^{NM} ND_{ms,y}\sum_{t=1}^{NT}\left[\sum_{rk=1}^{NR} Ploss_{y,ms,t,rk} + \sum_{ck=1}^{NC} Ploss_{y,ms,t,ck} + \sum_{ik=1}^{NI} Ploss_{y,ms,t,ik}\right](\Delta t)\\
Ploss_{y,ms,t,rk} &= \left[V^2_{y,ms,t,rk,p} + V^2_{y,ms,t,rk,q} - 2V_{y,ms,t,rk,p}V_{y,ms,t,rk,q}\cos\left(\delta_{y,ms,t,rk,p} - \delta_{y,ms,t,rk,q}\right)\right]g_{y,ms,t,rk}\\
Ploss_{y,ms,t,ck} &= \left[V^2_{y,ms,t,ck,p} + V^2_{y,ms,t,ck,q} - 2V_{y,ms,t,ck,p}V_{y,ms,t,ck,q}\cos\left(\delta_{y,ms,t,ck,p} - \delta_{y,ms,t,ck,q}\right)\right]g_{y,ms,t,ck}\\
Ploss_{y,ms,t,ik} &= \left[V^2_{y,ms,t,ik,p} + V^2_{y,ms,t,ik,q} - 2V_{y,ms,t,ik,p}V_{y,ms,t,ik,q}\cos\left(\delta_{y,ms,t,ik,p} - \delta_{y,ms,t,ik,q}\right)\right]g_{y,ms,t,ik}
\end{aligned}\right\} \quad (5.18)$$

where $Ploss_{y,ms,t,rk}$, $Ploss_{y,ms,t,ck}$, and $Ploss_{y,ms,t,ik}$ are the real power losses occurred in residential, commercial, and industrial branches, respectively. The subscripts y, ms, and t are already explained. The subscript 'k' denotes k^{th}-branch. The remaining subscripts r, c and i are used to indicate residential, commercial, and industrial loads. The $V_{y,ms,t,rk,p}$ and $V_{y,ms,t,rk,q}$ represent voltage magnitudes of the p^{th}-node and q^{th}-node of k^{th} line of residential area. The $\delta_{y,ms,t,rk,p}$ and $\delta_{y,ms,t,rk,q}$ are phase angles at both the nodes p and q of residential branch-rk. The $g_{y,ms,t,rk}$ is the conductance of residential line- rk and (Δt) is the time segment (15 minutes). The *NR, NC,* and *NI* indicate the total number of branches of residential, commercial, and industrial feeders, respectively.

5.6.2.2 Minimization of overall Node Voltage deviation (f_2)

The system safety and quality of power can be estimated using the voltage magnitude available at a bus. The overall voltage deviation is the sum of square of voltage differences between each node and substation voltage magnitude (i.e., V_1 = 1). This objective function is expressed in Eq. (5.19).

$$f2=\sum_{y=1}^{NY}\sum_{ms=1}^{NM}\sum_{t=1}^{NT}\left[\sum_{r=1}^{NR}\left(\frac{V_1-V_{y,ms,t,r}}{V_{y,ms,t,r}^{\max}-V_{y,ms,t,r}^{\min}}\right)^2+\sum_{c=1}^{NC}\left(\frac{V_1-V_{y,ms,t,c}}{V_{y,ms,t,c}^{\max}-V_{y,ms,t,c}^{\min}}\right)^2+\sum_{i=1}^{NI}\left(\frac{V_1-V_{y,ms,t,i}}{V_{y,ms,t,i}^{\max}-V_{y,ms,t,i}^{\min}}\right)^2\right] \quad (5.19)$$

where V_1 is the substation voltage magnitude. The $V_{y,ms,t,r}$, $V_{y,ms,t,r}^{\max}$, and $V_{y,ms,t,r}^{\min}$ are the node voltage magnitude, maximum voltage limit, and minimum voltage limit at end of residential branch *-r*. Similarly, other variables relate to commercial and individual loads can be extended.

5.6.2.3 Maximization of overall Voltage Stability Margin (f_3)

The Overall voltage stability margin maximization function (f_3) should be inverted to accommodate it in the equation (5.17). The objective function *(f_3)* can be expressed as Eq. (5.20).

$$\left.\begin{aligned}
&f3=\sum_{y=1}^{NY}\sum_{ms=1}^{NM}\sum_{t=1}^{NT}\left[\sum_{rk=1}^{NR}VSI_{y,ms,t,rk}+\sum_{ck=1}^{NC}VSI_{y,ms,t,ck}+\sum_{ik=1}^{NI}VSI_{y,ms,t,ik}\right]\\
&VSI_{y,ms,t,rk,q}=V_{y,ms,t,rk,p}^4-4\left(P_{y,ms,t,rk,q}X_{rk}-Q_{y,ms,t,rk,q}R_{rk}\right)^2-4\left(P_{y,ms,t,rk,q}R_{rk}+Q_{y,ms,t,rk,q}X_{rk}\right)V_{y,ms,t,rk,p}^2\\
&VSI_{y,ms,t,ck,q}=V_{y,ms,t,ck,p}^4-4\left(P_{y,ms,t,ck,q}X_{ck}-Q_{y,ms,t,ck,q}R_{ck}\right)^2-4\left(P_{y,ms,t,ck,q}R_{ck}+Q_{y,ms,t,ck,q}X_{ck}\right)V_{y,ms,t,ck,p}^2\\
&VSI_{y,ms,t,ik,q}=V_{y,ms,t,ik,p}^4-4\left(P_{y,ms,t,ik,q}X_{ik}-Q_{y,ms,t,ik,q}R_{ik}\right)^2-4\left(P_{y,ms,t,ik,q}R_{ik}+Q_{y,ms,t,ik,q}X_{ik}\right)V_{y,ms,t,ik,p}^2
\end{aligned}\right\}$$

(5.20)

where $P_{y,ms,t,rk,q}$, and $Q_{y,ms,t,rk,q}$ denote the effective real- and reactive- *residential load demand*, respectively, at receiving end bus-*q* of a residential branch-*rk*. Then the, R_{rk} and X_{rk} are the resistance and reactance of the residential branch- *rk*. Similar to this, terms related to commercial and industrial loads can be elaborated.

5.6.2.4 Minimization of Energy Not Served (f_4)

Estimation of *energy not served (ENS)* (f_4) enables the system utilities to determine degree of reliability that should be promised and maintained at the customers end, identify weakest points, develop suitable policies, *etc*. The *ENS* of a system can be computed using Eq. (5.21).

$$f4 = \sum_{y=1}^{NY}\sum_{ms=1}^{NM}\sum_{t=1}^{NT}\left[\sum_{r=1}^{NR} P_{y,ms,t,r}U_{y,ms,t,r} + \sum_{c=1}^{NC} P_{y,ms,t,c}U_{y,ms,t,c} + \sum_{i=1}^{NI} P_{y,ms,t,i}\right] \quad (5.21)$$

where $P_{y,ms,t,r}$ indicates *residential load demand* and $U_{y,ms,t,r}$ represents the unavailability of residential load point. Similarly, the terms related to other customer loads can be outstretched.

5.7 Operational Constraints

Optimal deployment of DGs should consider the following equality and inequality operational constraints.

5.7.1 Power balance

At each bus, the net active and reactive power injections should satisfy the equality power balance equations form of (5.22) - (5.23).

$$NetP_{y,ms,t,rk,p} = P_{DG,y,ms,t,rk,p} - P_{DL,y,ms,t,rk,p} = V_{y,ms,t,rk,p}\sum_{n=1}^{NB} V_{y,ms,t,rk,q}Y_{rk}\cos(\delta_{y,ms,t,rk,p} - \delta_{y,ms,t,rk,q} - \theta_{y,ms,t,rk,p} + \theta_{y,ms,t,rk,q}) \quad (5.22)$$

$$NetQ_{y,ms,t,rk,p} = Q_{DG,y,ms,t,rk,p} - Q_{DL,y,ms,t,rk,p} = V_{y,ms,t,rk,p}\sum_{n=1}^{NB} V_{y,ms,t,rk,q}Y_{rk}\sin(\delta_{y,ms,t,rk,p} - \delta_{y,ms,t,rk,q} - \theta_{y,ms,t,rk,p} + \theta_{y,ms,t,rk,q}) \quad (5.23)$$

where P_{DG} and Q_{DG} are the active and reactive powers generated by DG unit at a bus. The P_{DL} and Q_{DL} are the active and reactive powers of a load at the selected bus.

5.7.2 DG limits

The real and reactive power output from WT, PV, and MT DG units should not exceed the specified limits. These inequality limits are as below:

$$P_{\min,r}^{WT,PV,MT} \le P_{y,ms,t,r}^{WT,PV,MT} \le P_{\max,r}^{WT,PV,MT} \quad (5.24)$$

$$Q_{\min,r}^{WT,PV,MT} \le Q_{y,ms,t,r}^{WT,PV,MT} \le Q_{\max,r}^{WT,PV,MT} \quad (5.25)$$

where $P_{y,ms,t,r}^{WT,PV,MT}$ represents the real power generation from the DG units (WT, PV, and MT) connected to the *residential bus* at time-*t* month-*ms* of year-*y*. The terms $P_{\max,\ r}^{WT,PV,MT}$ and $P_{\min,\ r}^{WT,PV,MT}$ denote the upper and lower limits of real power generation from these DG units. Similarly, other terms related to the reactive power generation from the DGs can be elaborated.

5.7.3 Bus Voltage limits

At each bus, the voltage magnitude should be well within the specified limits.

$$V_{\min,\ r} \leq V_{y,ms,t,r} \leq V_{\max,\ r} \tag{5.26}$$

where $V_{y,ms,t,r}$ is the operating voltage at a bus for t^{th}-time, *ms*-month of y^{th}-year of *residential customer*. This can easily extended for other two types of loads (commercial and industrial loads).

5.7.4 Line Capacity limits

The operating current of the branches should not exceed the permissible maximum limits and is given in Eq. (5.27).

$$I_{y,ms,t,r} \leq I_{\max}, r \tag{5.27}$$

where $I_{y,ms,t,r}$ indicates the operating current and $I_{max,r}$ represents the maximum current limit of the *residential branch*. Then, $I_{y,ms,t,c}$ and $I_{y,ms,t,i}$ may be used for the case of commercial and industrial loads.

5.8 Solution Methodology

This section presents a solution approach for the optimal DG placement and sizing problem to obtain the techno-economical and environmental benefits under uncertainty condition while considering (a) without DG degradation and (b) with DG degradation. To solve such a large size multi-objective problem, a simple and effective meta-heuristic method is essential to provide the quality trade-off solutions. The well known meta-heuristic algorithms such as Particle Swarm Optimization (PSO), Genetic Algorithm (GA), Harmony Search (HS), Cuckoo Search Algorithm, *etc.*, require their own specific control parameters along with the *Popsize* and *maximum generations*. For example, in PSO, inertia weight, social and cognitive parameters are used. Tuning of these specific parameters is very much essential as they affect the performance of the algorithm. Improper tuning of these parameters either increases the computational effort or yields the local optimal solution. To avoid these aspects, in 2016, R.V. Rao [94] has proposed a parameter free algorithm called Jaya Algorithm (JA) for Engineering problems. Further, he has proposed an extended version of Jaya Algorithm (Multi-objective Jaya Algorithm) for multi-objective cases.

5.8.1 Jaya Algorithm

It is a single step iterative *parameter free* algorithm, which works on the concept of generating new solutions for a given minimization/maximization problem. These new solutions can be obtained by the movement of the old solutions towards the best solution and move away from the worst solution. The new i^{th}-solution in j^{th}- variable is given in Eq. (5.28).

$$X_{ij}^{new} = X_{ij}^{old} + r_1\left(X_j^{best} - \left|X_{ij}^{old}\right|\right) - r_2\left(X_j^{worst} - \left|X_{ij}^{old}\right|\right) \tag{5.28}$$

where, X_{ij}^{new} = a new i^{th}-solution in j^{th}- variable;

X_{ij}^{old} = old i^{th}-solution in j^{th}- variable;

X_j^{best} = j^{th}- variable of best solution;

X_j^{worst} = j^{th}- variable of worst solution;

r_1 and r_2 are the random variables generated in the range of [0-1].

If the *new solution* is better than the *old solution*, replace the *old solution* by the *new solution*. Otherwise, retain the *old solution*. The algorithm stops when the preset maximum generations/iterations is reached.

5.8.2 Multi-objective Jaya Algorithm (MOJA)

The multi-objective Jaya algorithm is formed by employing the *non-dominated sorting* and *crowding distance* attributes to the basic Jaya algorithm to provide the set of optimal solutions. From these set of optimal solutions a best compromised solution can be selected for a given optimization problem (minimization or maximization). The steps of the multi-objective Jaya algorithm (MOJA) is presented below [94].

Step A *(Initialization of Population)*: Initial solution of *Popsize* is generated randomly. Then, obtain the fitness values for these solutions.

Step B *(Evaluation of Best and Worst Solution Phase)*: Unlike, in basic Jaya algorithm, the superiority among the solutions is decided based on the non-dominance rank and value of the crowding distance instead of fitness value. The solution with highest rank (rank = 1) and largest value of crowding distance is chosen as the *best* solution. On the other hand the solution with the lowest rank and lowest value of crowding distance is selected as the *worst* solution.

Step C *(Updation Phase)*: Once the *best* and *worst* solutions are selected, the new solutions can be obtained from Eq. (5.28).

Step D *(Union and Separation Phase)*: The solutions obtained in Step C are combined with the initial solutions to form a set of 2*Popsize* solutions (where *Popsize* is the size of initial population). Again, the ranking process is applied on these 2*Popsize* solutions and the crowding distance for each solutions is computed. Based on the *new ranking* and *new crowding* distance value *Popsize* good solutions are chosen. Then repeat from Step B to Step D. This process will be continued till the preset maximum number of iterations are completed.

5.8.3 Fuzzy Decision Method [72]

Each solution is an optimal from a specific point of view and there is no single solution which is optimal from all points of view. Numerous methods have been proposed to select the final solution from the Pareto optimal set. In this work, a Fuzzy-rule based approach has been employed to select the best compromised solution (BCS) among the Pareto optimal solutions. According to Fuzzy Set Theory, for each objective function, a certain linear membership function should be defined. The equation (5.29) is used for generating normalized linear membership for objective functions that are to be minimized. Similarly, Eq. (5.30) is used for generating linear membership for objective functions that are to be maximized.

$$M_j^i = \frac{f_j^{\max} - f_j^i}{f_j^{\max} - f_j^{\min}} \tag{5.29}$$

$$M_j^i = \frac{f_j^i - f_j^{\min}}{f_j^{\max} - f_j^{\min}} \tag{5.30}$$

where f_j^i , $f_j^{\min}$, and $f_j^{\max}$ are the values of the j^{th}-objective function for the case of i^{th}-solution.

Therefore, the normalised membership function value for i^{th}-nondominated solution is given by Eq. (5.31).

$$NM_j^i = \frac{\sum_{j=1}^{NOF} M_j^i}{\sum_{i=1}^{Popsize} \sum_{j=1}^{NOF} M_j^i} \tag{5.31}$$

where *NOF* and *Popsize* are the number of objective functions and population size, respectively. The best compromised solution is the one which has the highest value among all the normalised values.

5.9 Implementation Steps of Proposed Multi-Objective Jaya Algorithm and Flow Chart

The step-by-step procedure, to implement the proposed *MOJA* methodology for optimal placement and sizing of mixed DG units under uncertainty environment by considering the aspect of (a) without DG degradation (b) with DG degradation, is presented below.

Step-1: Read the Distribution System Data

Popsize	=	number of solutions (Population size);
Dsize	=	number of variables (See Eq. (5.32));
Iter*MOJA*max	=	maximum number of iterations;

Step-2: Using *AHP approach* (Section 3.5), get the optimal weights ($\gamma_1, \gamma_2, \gamma_3$ and γ_4) for the individual objective functions of the overall objective function, *min F2*, Eq. (5.17).

Step-3: Generate the *Synthetic Data* using *SPDUS* approach (Eqs. 5.1-to-5.4) and keep them available.

// For different customer loads - generate both real and reactive power demands for the period of 20 Years.

// For WT and PV - generate only real power and determine the reactive power on the basis of 0.85 lagging power factor.

[Reactive Power = Real Power * $\tan\left(\cos^{-1}(PF)\right)$]; where, *PF* is the power factor.

Step-4: Select the *Scenario* (without or with DG degradation effect) for the optimal placement and sizing of mixed DG units.

Step-5: Generate an initial solution vector, X_{ij} within their *lower* and *upper* bounds with (*Popsize*) *X* (*Dsize*) as given by Eq. (5.32).

$$X_{ij} = \left[LC_{i1},\ \ LC_{i2},\ \ \ldots\ LC_{in}\ \ , P_{i1}^{DG},\ P_{i2}^{DG} \ldots\ P_{in}^{DG},\ \ Q_{i1}^{DG},\ \ Q_{i2}^{DG} \ldots\ Q_{in}^{DG} \right] \qquad (5.32)$$

where *LC*, P^{DG}, and Q^{DG} are used to indicate the location, real power generation and reactive power generation of the DGs to be installed. It may be noted that each DG needs *LC*, P^{DG}, and Q^{DG} variables. For this reason, *Dsize* is taken as three times the DG units that are to be deployed.

Step-6: Run the Load Flow and Evaluate the objective functions, *max* F_1 (5.10) and *min* F_2 (5.17). Treat these solutions as the *old Solutions.*

Step-7: Identify the *Best* and *Worst* solutions based on the *Step - B* of *MOJA* algorithm (Section 5.8.2).

Step-8: Update the solutions using Eq. (5.28). Again, Evaluate the objective functions *max* F_1 (5.10) and *min* F_2 (5.17).

Step-9: Add the *updated solutions* (Step-8) to the *old solution* to get twice of *Popsize* solutions. Then, apply *Step-D* of *MOJA* algorithm and get the **only *Popsize good solutions***. Process these good solutions by moving them to *Step - 8*. Now, treat these *Popsize good solutions* as the *old solutions*.

If the algorithm reaches the preset maximum number of iterations (i.e. *IterMOJAmax*), the algorithm ***STOPS*** the simulation.

Else repeat the Step-8 & Step-9 until the maximum number of iterations is reached.

Step-10: Apply Fuzzy Decision Method to select the *Best Compromised Solution* (*BCS*) using Eqs. (5.29) - (5.31) and Print out this Solution. This completes the work for the selected '*Scenario*'.

Now, go to *Step - 4* for *another Scenario*.

For better understanding of the algorithm, the flowchart of the proposed *MOJA* is also shown in Figure 5.3.

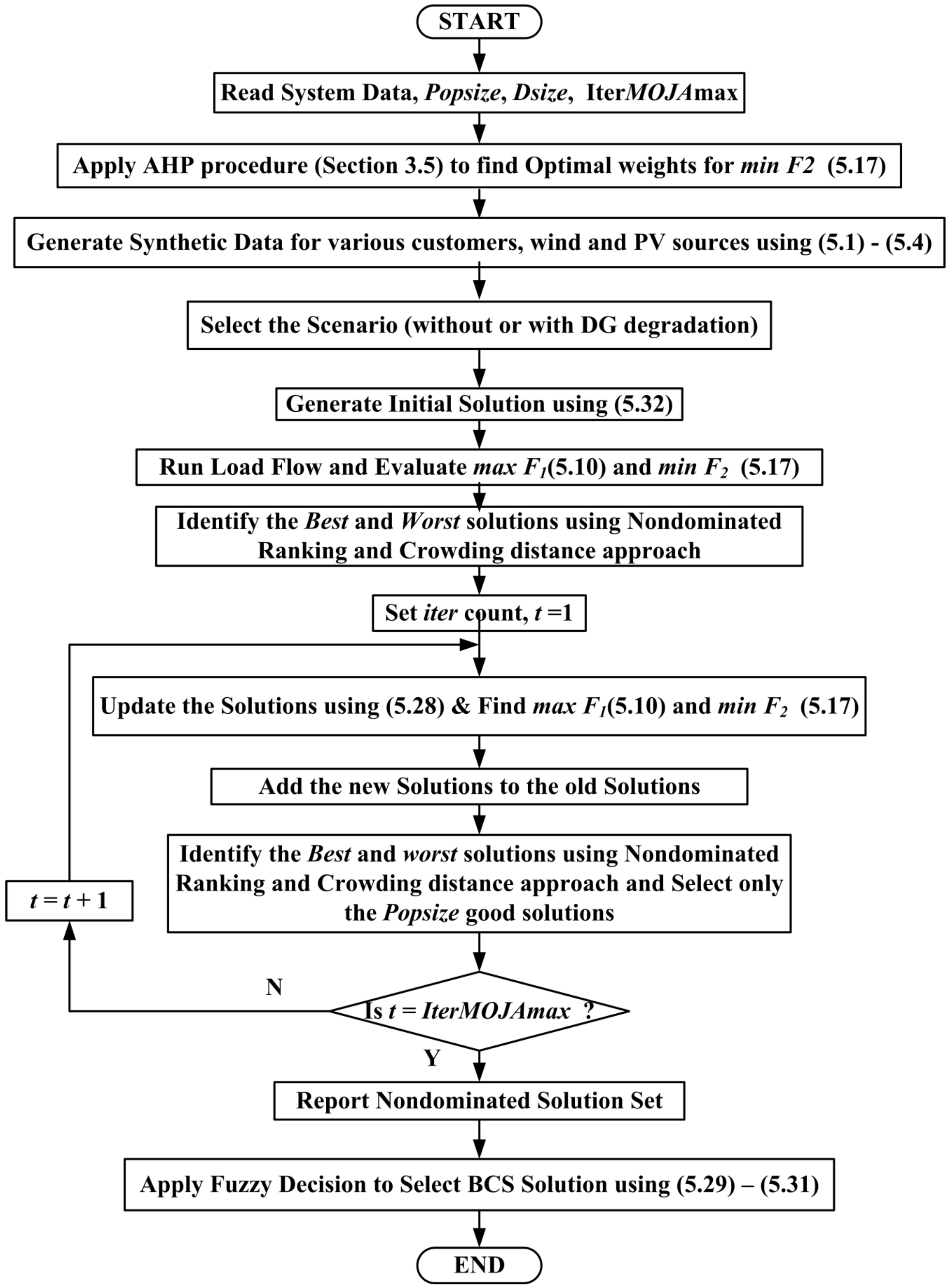

Figure 5.3 Flowchart of the proposed *MOJA* algorithm

5.10 Case Studies and Discussion

The *Multi-Objective Jaya Algorithm* (*MOJA*) for optimal deployment of mixed DG units under uncertainty environment is implemented in MATLAB environment on a Windows 7 based DELL desktop with Intel Core i7-3770, CPU@3.40GHz and 8GB Random Access Memory.

5.10.1 Case study on IEEE 33-bus Radial Distribution Network

The effectiveness and applicability of proposed *MOJA* algorithm have been investigated on modified IEEE 33-bus Radial Test System. This modified test system is shown in Figure 5.4. It has been divided into three feeders such as residential, commercial, and industrial feeders. The loads alongside these feeders are treated as residential, commercial, and industrial loads (customers). The line data and bus data of original IEEE 33-bus Radial Test System is reported APPENDIX-1 [78].

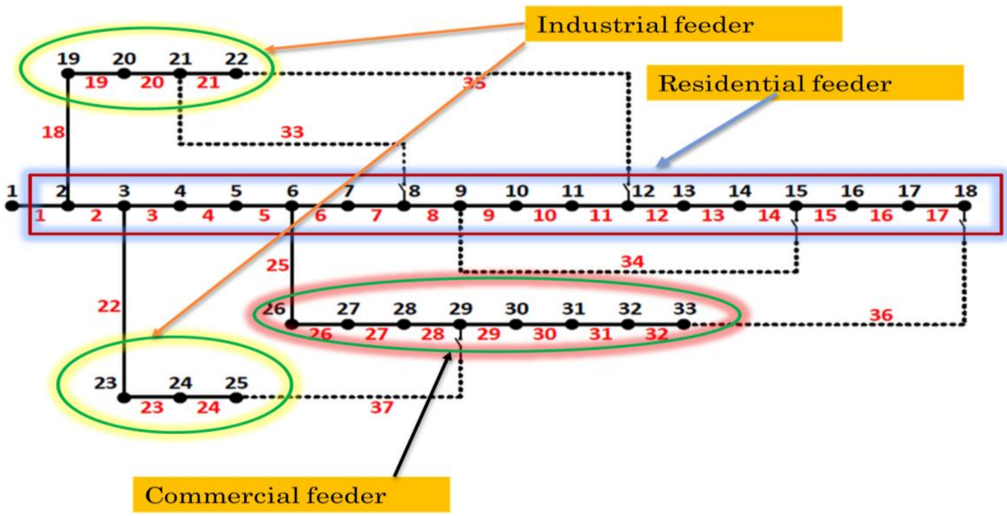

Figure 5.4 Modified IEEE 33-bus Radial Test System with various customers

The test results offered by the MOJA have been compared with the results of Nondominated Sorting Genetic Algorithm - II (NAGA-II). The parametric values for the proposed MOJA algorithm and NSGA-II are as below:

For *MOJA*: Population size = 20, maximum number of iterations = 100;

For *NSGA-II*: Population size = 20, maximum number of iterations = 100, crossover probability = 0.9, mutation probability = 0.01;

Each algorithm is run for 50 independent trails and the resulting best values are presented.

The following *two scenarios* have been considered for the optimal planning of mixed DGs in uncertainty environment over the planning period of 20 years.

Scenario - I : Mixed DG accommodation without DG unit degradation effect

Scenario - II : Mixed DG accommodation with DG unit degradation effect

The data related to technical, environment, and the cost associated with different DGs are presented in Table 5.2. An incremental size (discrete) of 40 kVA power generation from each DG unit is considered while attempting the optimization problem.

Table 5.2 Different Costs of DG units and design parameters

Parameter	**Value**	**Parameter**	**Value**
NY (years)	20	$\alpha^{Grid} / \alpha^{MT}$ ($/kg)	0.002/0.003
MS (months)	12	$\beta^{Grid} / \beta^{MT}$ ($/kg)	0.018/0.003
NT (15 minutes)	96	$\varphi^{Grid} / \varphi^{MT}$ ($/kg)	0.002/0.003
IC_i^{WT} ($/kVA)	1882	CO_2^{Grid} / CO_2^{MT} (kg/kWh)	0.9212/0.72
IC_i^{PV} ($/kVA)	2125	NOX^{Grid} / NOX^{MT} (kg/kWh)	0.02/0.091
IC_i^{MT} ($/kVA)	2293	SO_2^{Grid} / SO_2^{MT} (kg/kWh)	0.003/0.002
OPC_y^{WT} ($/kWh)	0.001	C_y^{sg} / C_y^{sc} ($/kWh)	0.06/0.06
OPC_y^{PV} ($/kWh)	0.001	C_y^{bg} ($/kWh)	0.055
OPC_y^{MT} ($/kWh)	0.022	*INF* (%)	6
MC_y^{WT} ($/kWh)	0.01	*INR* (%)	5
MC_y^{PV} ($/kWh)	0.01	Δ^{WT} (%)	0.2
MC_y^{MT} ($/kWh)	0.012	Δ^{PV} (%)	0.25
FuC_y^{MT} ($/kWh)	0.0335	Δ^{MT} (%)	0.3

The objective functions governed by Eq. (5.10) and Eq. (5.17) can be optimized by optimally placing the mixed DG units for different scenarios. The mixed opted DGs are Wind Turbine (WT), Solar Photo Voltaic (SPV), and Micro Turbine (MT). These DG units are assumed to be operated at *0.85 lagging power factor* [44]. Since, the DGs are operating at lagging power they can supply both real- and reactive- power to the Distribution System. The mixed DG accommodation problem under the above *two scenarios* has been solved and results are presented below.

Scenario - I : *Mixed DG accommodation without DG unit degradation effect*

The Pareto Optimal Solutions offered by the proposed MOJA and NSGA-II for the case of without DG degradation (i.e. *Scenario-I*) have been depicted in Figure 5.5. From this figure, it is evident that the solutions provided by the *MOJA* are superior over the NAGA-II. Using Fuzzy Decision Method (Section 5.8.3), the Best Compromised Solution (BCS) is determined from the set of Pareto Optimal Solutions dispensed by the both algorithms. The BCS solution of MOJA and NSGA-II are also depicted in the same Figure 5.5. Further, the solution corresponding to BCS in terms of various costs and technical improvement has been reported in Table 5.3.

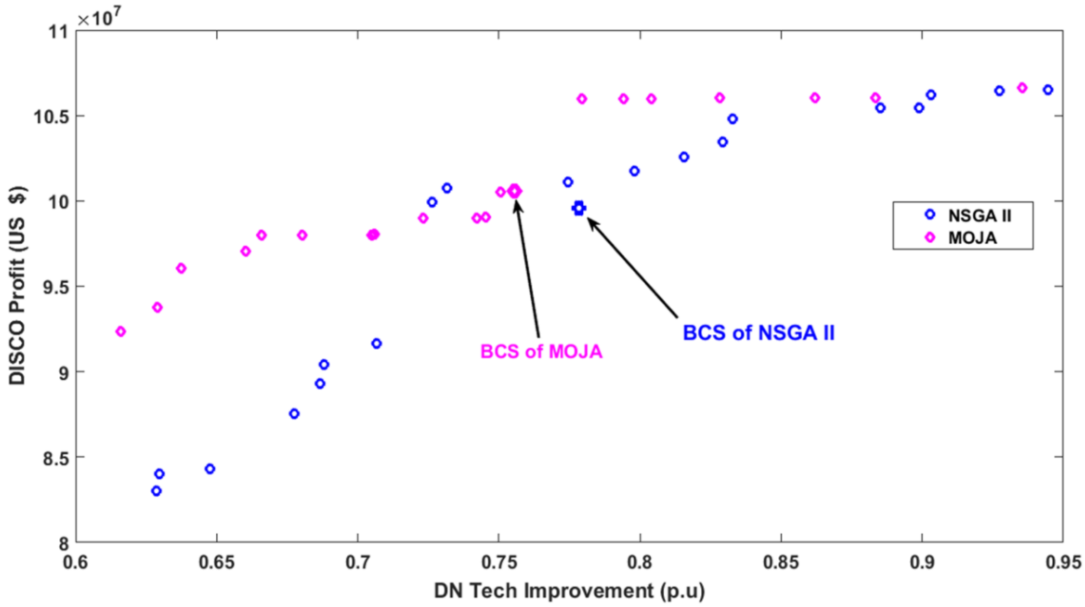

Figure 5.5 Pareto front when DG degradation effect is not considered

From Table 5.3, for the case of *Scenario - I*, without DG degradation effect, the DISCO profit (*max* F_1) and Distribution Network Technical Improvement (*min* F_2) are 100.55 US million \$ and 0.7554 p.u., respectively for the proposed *MOJA* algorithm. These values are better than the values offered by NSGA-II algorithm. The above quantities for the NSGA-II algorithm are 99.57 US million \$ and 0.7782 p.u. Further, the combined size (kVA) of three DGs determined by MOJA (7980 = 3250+3250+1480) is less than the NSGA-II (8300 = 3250+3250+1800) algorithm. The optimal locations for DG units are different for both the algorithms. These locations might have played a crucial role in achieving the higher profit and better technical improvement for the proposed *MOJA* algorithm. The individual costs of DISCO profit and individual technical improvements of Distribution Network are reported in Table 5.4.

Table 5.3 Comparison of BCS results obtained by MOJA and NSGA-II

Cases	**Parameter**	**NSGA - II [Stud]**	**MOJA [Prop]**
Scenario - I	*DISCO Profit (in US million $)* (max F_1 Eq.(5.10))	99.57	100.55
	Distribution Network Technical Improvement (min F_2 Eq.(5.17))	0.7782	0.7554
	DG loc (Size in kVA) DG Type	33 (3250) WT 32 (3250) PV 15 (1800) MT	30 (3250) WT 13 (3250) PV 18 (1480) MT
Scenario - II	*DISCO Profit (in US million $)* (max F_1 Eq.(5.10))	101.93	101.99
	Distribution Network Technical Improvement (min F_2 Eq.(5.17))	0.7813	0.7536
	DG loc (Size in kVA) DG Type	24 (3250) WT 22 (3250) PV 11 (0890) MT	30 (3250) WT 12 (3250) PV 17 (1080) MT

In Table 5.4, for *Scenario - I*, the individual costs and technical improvements obtained by the both algorithms are found to be different. It may be noted that the individual technical objective functions such as energy loss, voltage deviation, ENS should be *less than unity*. Lower values for these functions are always helpful in realizing better technical improvement. However, VSM should be more than the unity for better stability margin. The Distribution Network Technical improvement achieved by the *MOJA* algorithm is superior over the NSGA-II approach.

Also, the transactions between (i) grid & DISCO and (ii) customer & DISCO are depicted in Figure 5.6. This figure shows the revenue collected from grid and customers during the January month of *first year* and *last year* of the planning horizon. The negative sign in the grid revenue denotes that the grid is re-paying to the DISCO. Further, it may be noted that the transactions related to the *last year* are higher as compared to the *first year*. This variation is due to consideration of 6% annual increment rate for the costs that are to be calculated.

Table 5.4 Individual results of DISCO profit and Distribution Network Improvement for BCS of both MOJA and NSGA-II

Cases	**Objective Function**	**Parameter**	**NSGA - II [Stud]**	**MOJA [Prop]**
Scenario - I	*DISCO Profit (in US million $)* (max F_1 Eq.(5.10))	*DISCO Profit*	99.57	100.55
		Revenue from Customers	233.43	229.46
		Revenue from Grid	30.92	46.08
		DG Investment Cost	14.56	13.93
		DG Operation Cost	34.27	26.65
		DG Maintenance Cost	0.11	0.1
		DG Fuel Cost	49.14	37.53
		Grid Emission Cost	1.24	1.85
		MT Emission Cost	3.57	2.73
	Distribution Network Technical Improvement (min F_2 Eq.(5.17))	*Overall DN Improvement*	0.7782	0.7554
		Energy Loss	0.7081	0.7008
		Voltage deviation	0.7547	0.7054
		VSM	1.2642	1.3028
		ENS	0.9866	0.9699
Scenario - II	*DISCO Profit (in US million $)* (max F_1 Eq.(5.10))	*DISCO Profit*	101.93	101.99
		Revenue from Customers	222.18	229.42
		Revenue from Grid	74.91	70.42
		DG Investment Cost	12.8	13.17
		DG Operation Cost	12.39	16.74
		DG Maintenance Cost	0.07	0.08
		DG Fuel Cost	15.88	22.52
		Grid Emission Cost	3	2.82
		MT Emission Cost	1.15	1.63
	Distribution Network Technical Improvement (min F_2 Eq.(5.17))	*Overall DN Improvement*	0.7813	0.7536
		Energy Loss	0.6951	0.6714
		Voltage deviation	0.7162	0.6797
		VSM	1.1147	1.1957
		ENS	0.9687	0.9889

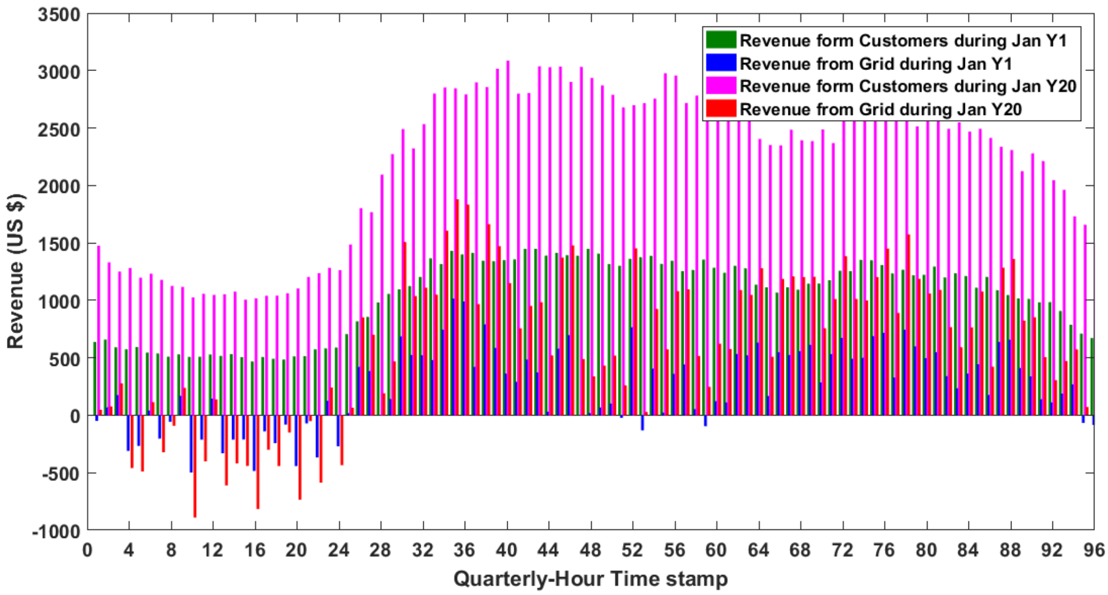

Figure 5.6 Revenue generation when DG degradation effect is not considered

Scenario - II : Mixed DG accommodation with DG unit degradation effect

The Pareto Optimal Set of this scenario is shown in Figure 5.7. From the Figure 5.7, it is evident that the solutions provided by the MOJA is superior over the NAGA-II. The Best Compromised Solution (BCS) of these two algorithms have been shown in the same Figure 5.7. The solution corresponding to the BCS of the both the algorithms is also reported in Table 5.3. From this table, it may be pointed out that the MOJA produces the optimal results in comparison with the NAGA-II. Further, its individual costs and technical components are summarized in the Table 5.4. It is interesting to note that the DG planning solution of *Scenario-II* is better than that of the *Scenario-I*. This gives new opportunity for the DG planning problem to consider the realistic DG degradation effect to realize the better profits and technical improvement.

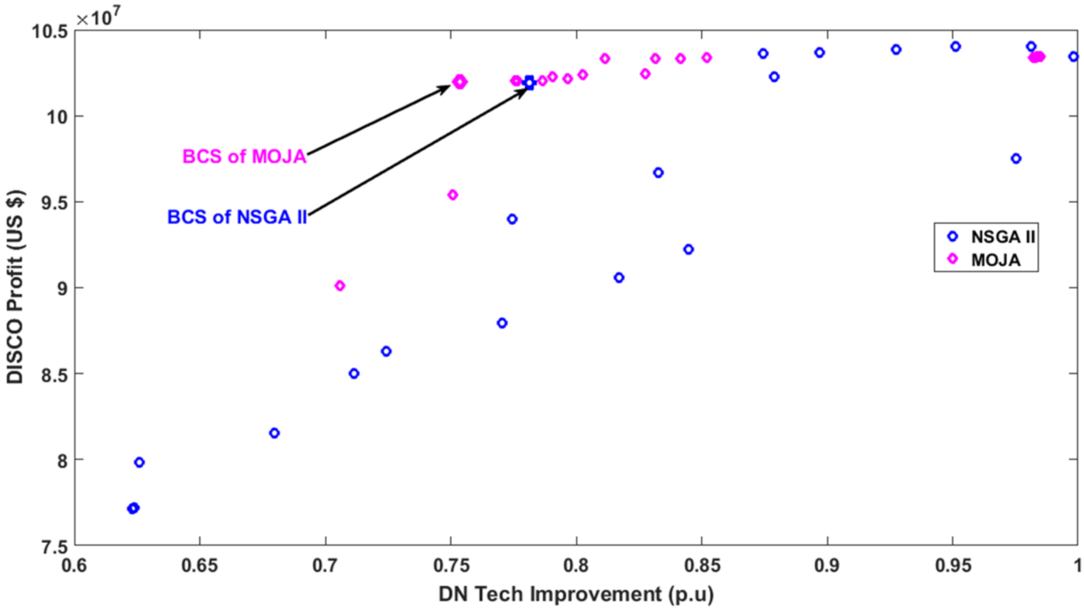

Figure 5.7 Pareto front when DG degradation effect is considered

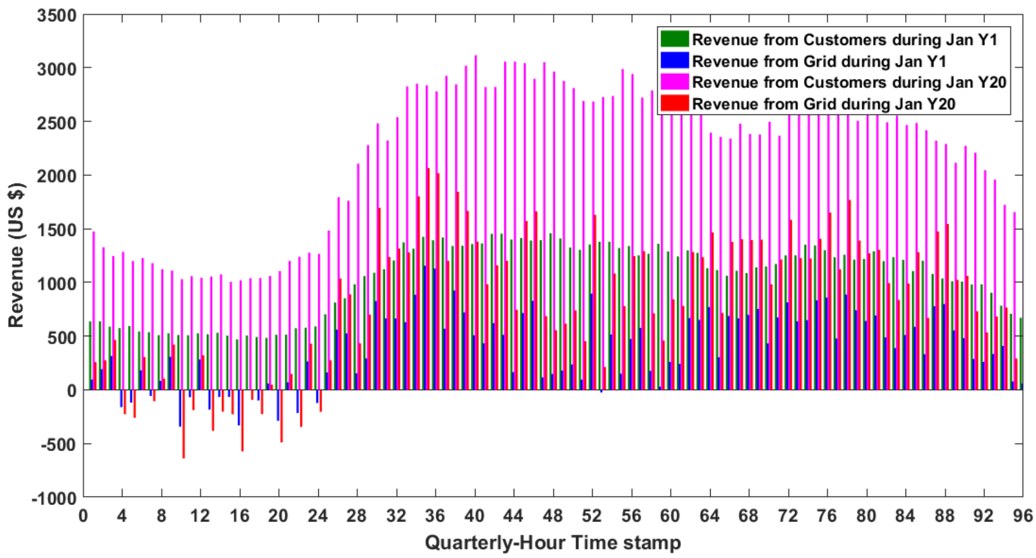

Figure 5.8 Revenue generation when DG degradation effect is considered

Also, the revenues between (i) grid & DISCO and (ii) customer & DISCO are depicted in Figure 5.8. This figure shows the revenue collected from grid and customers during the January month of *first year* and *last year* of the planning horizon. The negative sign in the grid revenue represents that the grid is re-paying to the DISCO.

Finally, for *Scenario - I and II*, the yearly minimum voltages of MOJA are shown in Figure 5.9. The voltages of both scenarios are improved form the base case. However, Scenario-I voltage magnitudes are better than that of Scenario-II due to its more power injection from the optimally placed DGs. In the planning model, the minimum and maximum voltage limits are taken as 0.90 p.u and 1.05 p.u, respectively [30].

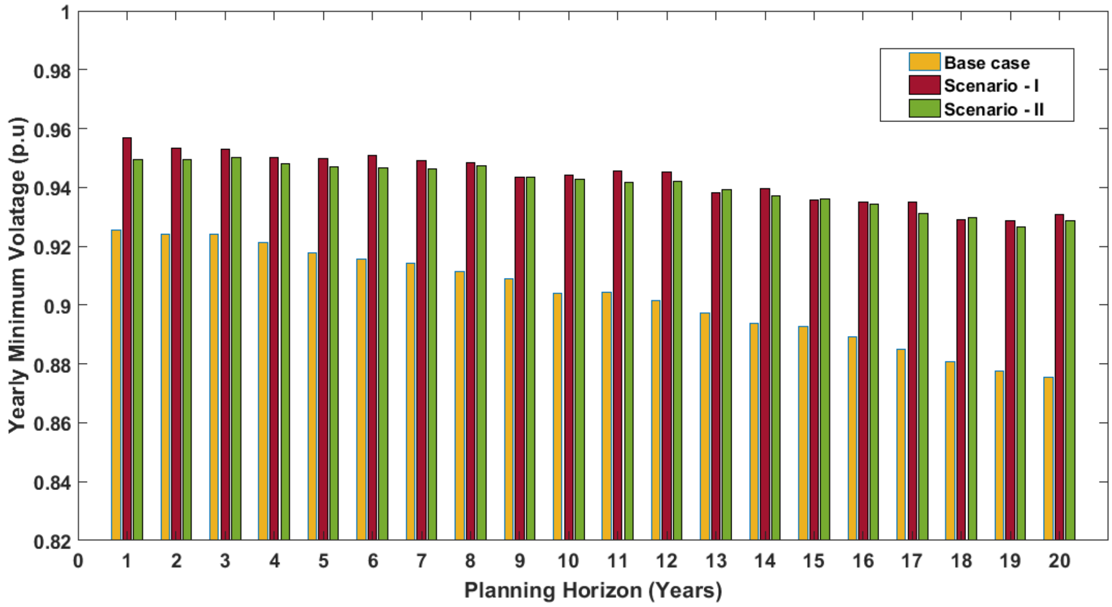

Figure 5.9 Yearly minimum voltage profile of proposed MOJA algorithm

This part of the work has been communicated to *Energy* journal as "Long Term Mixed DG Deployment Considering Uncertainty and DG Equipment Degradation," (Indexed in SCI)

5.11 Summary

In this Chapter, a *Multi-objective Jaya Algorithm (MOJA)* embedded with *Fuzzy Satisfaction Method* is presented for the case of long-term optimal deployment of mixed DGs under *uncertainty environment* incorporated with the *DG degradation effect*. The optimization problem is formulated with two objective functions: (i) Maxi. of DISCO profit (ii) Distribution Network Technical objectives optimization. Uncertainty associated with realistic customer load demand, WT power, and PV power is modelled using *Self-adaptive Polyhedral Deterministic Uncertainty Set* (*SPDUS*). Further, quarterly-hour (15 minutes) time stamp data has been used to generate the synthetic data required for different types of customer loads, WT, and PV resources. The case studies were conducted on modified IEEE 33-bus Radial Distribution Network. Test results revealed that the proposed *MOJA* is found to be promising over the NSGA-II algorithm.

The conclusions of this research work and scope for future work are presented in Chapter-6.

CHAPTER-6

Conclusions and Scope for Future Work

6.1 Conclusions

The salient features of this thesis work and conclusions drawn from the investigations carried out at various stages are presented in this Chapter.

The performance of the power distribution network under normal and abnormal operating conditions can be improved by the optimal deployment of the Distributed Generation (DG) units. Optimal placement and sizing of DGs is a complex, combinatorial, mixed-integer non linear optimization problem with various non-linear objectives subjected to the equality and inequality operational constraints. The objectives can be considered are of active power loss minimization, reactive power loss minimization, node voltage deviation minimization, maximization of voltage stability margin, reliability improvement, investment and operational cost minimization, reduction of emissions from pollutant gases, *etc*. These objective functions can be categorised as technical, economical, and environmental benefits. In order to attain the aforementioned benefits, the DG units should be optimally placed and sized.

Optimal Deployment of DGs (ODDGs) is a planning problem where the quality of solutions (optimal location and size of DGs) is more important than the solution time. However, the time incurred for getting the optimal solution cannot be given less importance. The solution time to get the optimum values for ODDG problem depends on the planning horizon, optimizer being used, and an employed Distribution Load Flow (DLF) method. The planning horizon on long-term basis can demand more solution time as it involves the execution of several load flows and update of various optimizer steps and vice-versa. For an optimizer, the steps and time for the execution of these steps remains constant. Therefore, the solution time purely depends on the planning horizon and DLF. The DLF that offers the solution in less time can be adopted to reduce the overall solution time of ODDGs problem. Also, the optimizer which is easy to understand, implement and takes less time to produce the required results can also be selected. Therefore, in this direction, investigation has been carried out to propose an efficient and fast DLF algorithm and optimizer for optimal deployment of DGs problem.

In Chapter-1, the basic introduction and requirement of Distributed Load Flow (DLF) and optimal DG deployment are briefly reported along with the discussion on the necessity of Multi-objective optimization approaches. The detailed literature survey on

DLF and optimal placement and sizing of DGs was conducted. Furthermore, a critical review has been presented on the optimal deployment of DGs using an analytical and meta-heuristic methods for single and multi-objective cases under normal and uncertainty environment condition.

In Chapter-2, an efficient DLF method has been proposed that works *equally well* for both Radial and Weakly meshed systems under different load models. The load models being considered were Constant Power (CP), Constant Current (CI), Constant Impedance (CZ), and combination of these three (CZIP). Impact of these load models on the voltage profile of the test systems was investigated. The proposed DLF method was tested on five benchmark IEEE 33-, IEEE 69-, Taiwan Power Company (TPC) 84-, Test system of 136-, and Test system of 874- buses with radial and weakly meshed distribution systems. The results offered by the proposed DLF are compared with Current Injection Method (CIM) and concluded that proposed DLF is time efficient, robust, and divergence free over the CIM method. Furthermore, the robustness of the algorithm has been tested by simulating different scenarios. These scenarios include different tolerance values, X/R ratio, and loading (kVA) conditions.

Optimal accommodation of DGs can be solved for Single and Multi-objective cases using Analytical methods. Analytical methods are often easily implementable, ensure the convergence of the DG planning solution and short computation time. In Chapter-3, an analytical method, *Branch Loss Bus Injection Index (BLBII)* has been proposed to find the optimal location for the emplacement of DG unit. The capability of this analytical method in finding the potential DG location lies in the proposed term *BLBII* as it accounts the complex losses in terms of *Loss Index Factor* (*LIF)* and effective complex power injections. By accommodating the DG at identified optimal location, a new multi-objective problem of the power distribution network has been investigated by considering: *(i) minimization of electrical energy losses, (ii) minimization of overall bus voltage deviation, (iii) maximization of overall voltage stability margin, and (iv) minimization of energy not served* to find the optimal DG size. A Weighted Sum Approach was employed to address these multi-objectives. An unique *Analytical Hierarchy Process* (*AHP*) approach has been proposed to estimate the optimal weights for the individual objectives of the multi-objective function. The applicability of the proposed method has been validated on IEEE 33-bus and INDIAN 85-bus benchmark Radial test systems under two scenarios. The

Scenario-I: Single DG unit operating at Unity Power Factor (UPF) and Scenario-II: Single DG unit operating at 0.9 Lagging Power Factor (LPF). From the test results it was observed that the solution of 'Scenario-II' offers the significant improvement in terms of voltage profile and energy loss cost saving along with the improvement of proposed multi-objectives as compared to 'Scenario-I'. This is due to the DG unit of 'Scenario-II' supplies both real and reactive power locally. Furthermore, by considering the minimization of real power losses as mono-objective, the results of the proposed method are compared with that of the algorithms presented in the literature. The study reveals that the proposed method provides the better loss reduction and improved node voltages.

Meta-heuristic techniques are more popular to solve the complex combinatorial optimization problems where the analytical methods have failed to offer the solution. In Chapter-4, Multi-Verse Optimization (MVO), a recently introduced nature inspired algorithm was implemented for ODDG problem. The basic MVO is suffering from poor convergence and provides the solutions near to the local optima when applied to the real life problem like optimal DG accommodation. Hence, a hybrid version of algorithm (HMVO) has been developed by combining the best features of Space Transformation Search (STS) and Piecewise Linear Chaotic Map (PLCM) algorithms. To implement the HMVO algorithm, the multi-objective problem of Chapter-3 was adopted. The capability and applicability of the HMVO algorithm was demonstrated on IEEE 33-bus and INDIAN 85-bus Radial Distribution Network under two scenarios. The 'Scenario-I': Optimal Accommodation of Three DG units operating with UPF and 'Scenario-II': Optimal Accommodation of Three DG units operating with 0.9 LPF. The results produced by proposed HMVO algorithm are compared with various algorithms and works already reported in the literature and the test results found to be superior. Furthermore, the HMVO algorithm was tested with the statistical measurements such as statistical mean, statistical standard deviation and *t-test* values to establish its suitability for the DG planning problem. From these statistical values, it was observed that HMVO out performs the algorithms used for comparison purpose.

The future distribution system is no more passive but active with the widespread deployment of Renewable Energy Sources (RESs) technologies such as Solar Photo Voltaic (SPV), Wind Turbines (WTs), Bio-mass, Geo-thermal, Tidal, and hydro-power units. These energy resources are neither exhaustible nor polluting. Hence, they seem to be the only option to a sustainable energy supply. However, most of the RES DGs are with intermittent power output. So, while considering the renewable DGs, the stochastic nature of load demand has also to be taken into account. In Chapter-5, the long-term mixed DG deployment problem has been solved under *uncertainty environment condition* along with *DG degradation effect*. The DGs such as WT, SPV, and MT were chosen for the placement. The power output from the MT is constant. Hence, it was used along with the intermittent power sources such as WT and SPV. The randomness associated with the different customers loads (residential, commercial, and industrial), WT, and SPV was modeled using *Self-adaptive Polyhedral Deterministic Uncertainty Set* (*SPDUS*). Furthermore, quarterly-hour (15 minutes) time stamp historical data has been used to generate the synthetic data required for different types of customer loads, WT, and PV resources. The optimization problem was formulated with two objective functions: *(i) Maximization of DISCO profit (ii) Distribution Network Technical Objectives Improvement*. A parameter free algorithm such as *Multi-objective Jaya Algorithm (MOJA)* embedded with *Fuzzy Decision Method* was attempted. The case studies were conducted on modified IEEE 33-bus Radial Distribution Network for the case of long-term optimal deployment of mixed DGs under *uncertainty environment* incorporated with the *DG degradation effect*. Test results revealed that the proposed MOJA was found to be promising over the NSGA-II algorithm.

To summarize, the major contributions of this thesis are

- The proposed new Distribution Load Flow (DLF) method is time efficient, robust and with no divergence problems and it could work very effectively for both Radial and Weakly meshed Distribution Systems. The method converges in 2 to 4 iterations irrespective of the size of the system and is 4 to 10 times faster than the Current Injection method (CIM).
- The effect of single DG unit operating at unity and 0.9 lagging power factor was analyzed on single objective and newly formulated Multi-objective optimization model by placing the DG unit at an optimal location identified by proposed Analytical method, *Branch Loss Bus Injection Index* (*BLBII*). Furthermore, a Multi Criteria decision making method such as *Analytical Hierarchy Process* (*AHP*), has been proposed to obtain the optimal weights of the individual objectives of the Weighted Sum Multi-objective optimization. The investigation was carried out on two standard Radial test systems, IEEE 33- and INDIAN 85-bus systems.

- The *Hybrid Multi-Verse Optimizer* (*HMVO*) method has been proposed to address the ODDG problem. The investigation was carried out on two standard Radial test systems, IEEE 33- and INDIAN 85-bus systems, under two scenarios (i) three DGs operating with unity power factor and (ii) three DGs operating with 0.9 lagging power factor. The study reveals that the second scenario offers the optimal values and better voltage profiles when compared to the base case and the first scenario, due to the support of both real and reactive power locally.
- The impact of techno-economic and environment issues are analyzed using proposed *Multi-objective Jaya Algorithm* (*MOJA*) incorporated with *Fuzzy Decision Method* for the case of *long-term optimal deployment of mixed DGs* problem under *uncertainty environment* along with the *DG degradation effect*. The uncertainty associated with the different customers loads (residential, commercial, industrial), WT and SPV was modeled using *Self-adaptive Polyhedral Deterministic Uncertainty Set* (*SPDUS*). The investigation was carried out on modified IEEE 33-bus Radial Distribution Network. From the results of the case studies, it was observed that the DG accommodation with the incorporation of DG degradation effect earns more profit than the case of without DG degradation effect.

Based on the above studies, the Distribution Network can be *planned* and *operated* in an efficient manner by placing the DG units at potential locations with appropriate sizes.

6.2 Scope for the future work

Further, the research work in the area of optimal DG deployment in the distribution system can be extended in the following directions.

1. Uncertainties in Fuel pricing, Energy pricing, and future Load growth can be considered in DG planning problem.
2. Simultaneous optimal allocation of DGs, Protective Devices, and Electric Vehicle/ Plug-in Hybrid Electric Vehicle charging stations can be investigated.
3. The investigation can be extended for the Optimal placement of DGs, Phasor Measurement Units (PMUs) and Intelligent Electronic Devices (IEDs) in Distribution Network.

List of Publications based on this Research Work

International Journals (Published)

[1] Kiran Babu B and Sydulu Maheswarapu, "New Hybrid Multiverse Optimisation Approach for Optimal Accommodation of DGs in Power Distribution Networks," *IET Generation, Transmission & Distribution*, vol. 13, no. 13, pp. 2673-2685, July 2019. DOI: 10.1049/iet-gtd.2018.5763. (**Indexed in SCI**)

[2] Kiran Babu B and Sydulu Maheswarapu, "A solution to Multi-objective Optimal Accommodation of Distributed Generation Problem of Power Distribution Networks: An analytical approach," *International Transactions on Electrical and Energy Systems*, vol. 29, no. 10, October 2019, e12093. https://doi.org/10.1002/2050-7038.12093. (**Indexed in SCIE**)

Manuscripts Communicated

[1] Kiran Babu B and Sydulu Maheswarapu, "Long Term Mixed DG Deployment Considering Uncertainty and DG Equipment Degradation," *Energy* journal.

National/International Conferences

[1] Kiran Babu B and Sydulu Maheswarapu, "An efficient Power Flow Method for Distribution System Studies under various load models," 13th International IEEE India Conference INDICON 2016, 16-18 Dec 2016. IISc Banglore, DOI:10.1109/INDICON.2016.7838992.

[2] Kiran Babu B and Sydulu Maheswarapu, "An Optimal Accommodation of Distributed Generation in Power Distribution Systems," 20th National Power Systems Conference (NPSC), 14-16 Dec 2018. Tiruchirappalli, India, DOI: 10.1109/NPSC.2018.8771743.

References

[1] William H. Kersting, *Distribution System Modeling and Analysis*, Third Edition, CRC Press, 2012, p. 455.

[2] Eltantawy AB and Salama MM, "A novel zooming algorithm for distribution load flow analysis for smart grid," *IEEE Transactions on Smart Grid*, vol. 5, no. 4, pp.1704-1711, 2014.

[3] Tinney WG and Hart CE, "Power flow solutions by Newton's method," *IEEE Transactions on Power Apparatus and Systems*, vol. PAS-86, no. 11, pp.1449-1460, 1967.

[4] Stott B and Alsaç O, "Fast decoupled load flow," *IEEE Transactions on Power Apparatus and Systems*, vol. PAS-93, no. 3, pp. 859–869, 1974.

[5] Da Costa VM, Martins N and Pereira JRL, "Developments in the Newton Raphson power flow formulation based on current injections," *IEEE Transactions on Power Systems*, vol. 14, no. 4, pp. 1320–1326, 1999.

[6] Rajicic D and Tamura Y, "A modification to fast decoupled power flow for networks with high R/X ratio," *IEEE Transactions on Power Systems*, vol. 3, no. 2, pp. 1320-1326, 1988.

[7] Available at https://go.frost.com/NA_PR_EE_JBrinkley_MF1A_DistributedEnergy_Apr20 [accessed on 02-07-2020].

[8] W. El-Khattam and M. M. A. Salama, "Distributed generation technologies, definitions and benefits," *Electric Power System Research*, vol. 71, no.2, pp.119-128, 2004.

[9] P. Aravindhababu, S. Ganapathy and K.R. Nayar, "A novel technique for the analysis of radial distribution systems," *International Journal of Electrical Power & Energy Systems*, vol. 23, no. 3, pp. 167–171, 2001.

[10] S. F. Mekhamer, S.A Soliman, M.A Moustafa and M.E El-Hawary, "Load flow solution of radial distribution feeders: a new contribution," *International Journal of Electrical Power & Energy Systems*, vol. 24. no. 9, pp. 701–707, 2002.

[11] R Ranjan and Das, "Simple and Efficient Computer Algorithm to Solve Radial Distribution Networks," *Electric Power Components and Systems*, vol. 31, no.1, pp. 95-107, 2003.

[12] G. Chang, S. Chu and H. Wang, "An improved backward/forward sweep load flow algorithm for radial distribution systems," *IEEE Transactions on Power Systems*, vol. 22, no. 2, pp. 882–884, 2007.

[13] S. Ghosh and K. S. Sherpa, "An efficient method for load-flow solution of radial distribution networks," *International Journal of Electrical and Computer Engineering*, vol. 2, no. 9, pp. 2094–2101, 2008.

[14] K. Nagaraju, S. Sivanagaraju, T. Ramana and P. V. Prasad, "A Novel Load Flow Method for Radial distribution Systems for Realistic Loads," *Electric Power Components and Systems*, vol. 39, no. 2, pp. 128–141, 2011.

[15] Ahmed R. Abul'Wafa, "A network-topology-based load flow for radial distribution networks with composite and exponential load," *Electric Power Systems Research*, vol. 91, pp. 37–43, 2012.

[16] S. Singh and T.Ghose, "Improved radial load flow method," *International Journal of Electrical Power & Energy Systems*, vol. 44, pp. 721–727, 2013.

[17] V. V. S. N. Murty, B. Ravi Teja and Ashwani Kumar, "A Contribution to Load Flow in Radial Distribution system and Comparison of Different Load Flow Methods," in: *International Conference on Power, Signals, Controls and Computation (EPSCICON)*, 8 – 10 Jan 2014, 2014.

[18] Paulo A. N. Garcia, Jose Luiz R. Pereira, Sandoval Carneiro Jr, Vander M. da Costa and Nelson Martins, "Three phase power flow calculations using the current injection Method," *IEEE Transactions on Power Systems*, vol. 15, no. 2, pp. 508–514, 2000.

[19] Jen-Hao Teng, "A Direct Approach for Distribution System Load Flow Solutions," *IEEE Transactions on Power Delivery*, vol. 18, no. 3, pp. 882-887, 2003.

[20] Chang G, Chu S Y, Hsu M F, Chuang C S and Wang H L, "An efficient power flow algorithm for weakly meshed distribution system," *Electric Power System Research*, vol. 84, no. 1, pp. 90-99, 2012.

[21] Ravi Teja Bhimarasetti and Ashwani Kumar, "A New Contribution to Distribution Load Flow Analysis for Radial and Mesh Distribution Systems," *International Conference on Computational Intelligence and Communication Networks*, Bhopal, India, 14-16 Nov 2014.

[22] Ali Ehsan and Qiang Yang, "Optimal integration and planning of renewable distributed generation in the power distribution networks: A review of analytical techniques," *Applied Energy*, vol. 210, pp. 44-50, 2018.

[23] Acharya N, Mahat P and Mithulananthan N, "An analytical approach for DG allocation in primary distribution network," *International Journal of Electrical Power & Energy Systems*, vol. 28, no. 10, pp. 669–678, 2006.

[24] Aman MM, Jasmon GB, Mokhlis H and Bakar AHA, "Optimal placement and sizing of a DG based on a new power stability index and line losses," *International Journal of Electrical Power & Energy Systems*, vol. 43, pp. 1296-1304, 2012.

[25] Murthy VVSN and Ashwani Kumar, "Comparison of optimal DG allocation methods in radial distribution systems based on sensitivity approaches," *International Journal of Electrical Power & Energy Systems*, vol. 53, pp. 450–467, 2013.

[26] Hung DQ and Mithulananthan N, "Multiple Distributed Generator Placement in Primary Distribution Networks for Loss Reduction," *IEEE Transactions on Industrial Electronics*, vol. 60, no. 4, pp. 1700-1708, 2013.

[27] Hung DQ, Mithulananthan N and Bansal RC, "Analytical strategies for renewable distributed generation integration considering energy loss minimization," *Applied Energy*, vol. 105, pp. 75–85, 2013.

[28] Murthy VVSN and Ashwani Kumar, "Optimal placement of DG in radial distribution systems based on new voltage stability index under load growth," *International Journal of Electrical Power & Energy Systems*, vol 69, pp. 246–256, 2015.

[29] Viral R and Khatod DK, "An analytical approach for sizing and siting of DGs in balanced radial distribution networks for loss minimization," *International Journal of Electrical Power & Energy Systems*, vol. 67, pp. 191–201, 2015.

[30] Sandeep Kaur, Ganesh Kumbhar and Jaydev Sharma, "A MINLP technique for optimal placement of multiple DG units in distribution systems," *International Journal of Electrical Power & Energy Systems*, vol. 63, pp. 609–617, 2014.

[31] Elsaiah S, Benidris M and Mitra J, "Analytical approach for placement and sizing of distributed generation on distribution systems," *IET Generation, Transmission and Distribution*, vol. 8, no. 6, pp. 1039–1049, 2014.

[32] Gopiya Naik SN, Khatod DK and Sharma MP, "Analytical approach for optimal siting and sizing of distributed generation in radial distribution networks," *IET Generation, Transmission & Distribution*, vol. 9, no. 3, pp. 209-220, 2015.

[33] Hung DQ and Mithulananthan N, "Loss reduction and loadability enhancement with DG: A dual-index analytical approach," *Applied Energy*, vol. 115, pp. 233–241, 2014.

[34] Hung DQ, Mithulananthan N and Lee KY, "Determining PV Penetration for Distribution Systems With Time-Varying Load Models," *IEEE Transactions on Power Systems*, vol. 29, no. 6, pp. 3048-3057, 2014.

[35] Prem Prakash and Dheeraj K Khatod, "Optimal sizing and siting techniques for distributed generation in distribution systems: A review," *Renewable and Sustainable Energy Reviews*, vol. 57, pp. 111–130, 2016.

[36] Mahmoud Pesaran HA, Huya PD and Ramachandaramurthy VK, "A review of the optimal allocation of distributed generation: Objectives, constraints, methods, and algorithms," *Renewable and Sustainable Energy Reviews*, vol. 75, pp. 293–312, 2017.

[37] Satish K, Vishal K and Barjeev T, "Optimal placement of different type of DG sources in distribution networks," *International Journal of Electrical Power & Energy Systems*, vol. 53, pp. 752–760, 2013.

[38] Shukla TN, Singh SP, Srinivasarao V and Naik KB, "Optimal Sizing of Distributed Generation Placed on Radial Distribution Systems," *Electric Power Components and Systems*, vol. 38, no. 3, pp. 260-274, 2010.

[39] Komail Nekooei, Malihe M. Farsangi, Hossein Nezamabadi-Pour and Kwang Y. Lee, "An Improved Multi-Objective Harmony Search for Optimal Placement of DGs in Distribution Systems," *IEEE Transactions on Smart Grid*, vol. 4, no. 1, pp. 557-567, 2013.

[40] Bahram P, Peyman K, Gharehpetian GB and M Abedi, "Optimal allocation and sizing of DG units considering voltage stability, losses and load variations," *International Journal of Electrical Power & Energy Systems*, vol. 79, pp. 42-52, 2016.

[41] Aman M M, Jasmon GB, Bakar AHA and Mokhlis H, "A new approach for optimum DG placement and sizing based on voltage stability maximization and minimization of power losses," *Energy Conversion and Management*, vol. 70, pp.202–210, 2013.

[42] Joydeep Mitra, Mallikarjuna R. Vallem and Chanan Singh, "Optimal Deployment of Distributed Generation Using a Reliability Criterion," *IEEE Transactions on Industry Applications*, vol. 52, no. 3, pp.1989-1997, 2016.

[43] Satish Kumar I and Prema Kumar N, "A novel approach to identify optimal access point and capacity of multiple DGs in a small, medium and large scale radial distribution systems," *International Journal of Electrical Power & Energy Systems*, vol. 45, pp. 142–151, 2013.

[44] Moradi MH and Abedini M, "A combination of genetic algorithm and particle swarm optimization for optimal DG location and sizing in distribution systems," *International Journal of Electrical Power & Energy Systems*, vol. 34, pp. 66-74, 2012.

[45] Mohanty B and Tripathy S, "A teaching learning based optimization technique for optimal location and size of DG in distribution network," *Journal of Electrical Systems and Information Technology*, vol. 3, pp. 33–44, 2016.
[46] Sneha S and Roy PK, "Multi-objective quasi-oppositional teaching learning based optimization for optimal location of distributed generator in radial distribution systems," *International Journal of Electrical Power & Energy Systems*, vol. 63, pp. 534-545, 2014.
[47] Subhodip Saha and Vivekananda Mukherjee, "Optimal placement and sizing of DGs in RDS using chaos embedded SOS algorithm," *IET Generation, Transmission & Distribution*, vol. 10, no. 14, pp. 3671 - 3680, 2016.
[48] Quadri IA, Bhowmick S and Joshi D, "A comprehensive technique for optimal allocation of distributed energy resources in radial distribution systems," *Applied Energy*, vol. 211, pp. 1245–1260, 2018.
[49] D.B. Prakash and C. Lakshminarayana, "Multiple DG placements in radial distribution system for multi objectives using Whale Optimization Algorithm," *Alexandria Engineering Journal*, vol. 57, pp. 2797–2806, 2018.
[50] Wanxing Sheng, Ke-Yan Liu, Yuan Liu, Xiaoli Meng and Yunhua Li, "Optimal Placement and Sizing of Distributed Generation via an Improved Nondominated Sorting Genetic Algorithm II," *IEEE Transactions on Power Delivery*, vol. 30, no. 2, pp. 569 - 578, 2015.
[51] Alireza Soroudi, Mehdi Ehsan and Hamidreza Zareipour, "A practical eco-environmental distribution network planning model including fuel cells and non-renewable distributed energy resources," *Renewable Energy*, vol. 36, pp. 179-188, 2011.
[52] I. A. Mohamed and M. Kowsalya, "Optimal size and siting of multiple distributed generators in distribution system using bacterial foraging optimization," *Swarm and Evolutionary Computation*, vol. 15, pp. 58–65, 2014.
[53] Aashish Kumar Bohre, Ganga Agnihotri and Manisha Dubey, "Optimal sizing and sitting of DG with load models using soft computing techniques in practical distribution system," *IET Generation, Transmission & Distribution*, vol. 10, no. 11, pp. 2606 - 2621,2016.
[54] Chandrasekhar Y, Sydulu M and Sailaja Kumari M, "Optimal placement and sizing of distributed generations using shuffled bat algorithm with future load enhancement," *International Transactions on Electrical Energy Systems*, vol. 26, pp. 274–292, 2016.
[55] Ameli A, Bahrami S, Khazaeli F and Haghifam MR, "A multi objective particle swarm optimization for sizing and placement of DGs from DG owner's and distribution company's view points," *IEEE Transactions on Power Delivery*, vol. 29, no. 4, pp. 1831–1840, 2014.
[56] Srinivasa Rao G and Das D, "Optimum placement and sizing of DGs considering average hourly variations of load," *International Journal of Electrical Power & Energy Systems*, vol. 66, pp. 25–40, 2015.
[57] N. Mohandas, R. Balamurugan and L. Lakshminarasimman, "Optimal location and sizing of real power DG units to improve the voltage stability in the distribution system using ABC algorithm united with chaos," *International Journal of Electrical Power & Energy Systems*, vol. 66, pp. 41–52, 2015.

[58] Sh. Abdi and K. Afshar, "Application of IPSO-Monte Carlo for optimal distributed generation allocation and sizing," *International Journal of Electrical Power & Energy Systems*, vol. 44, no. 1, pp. 786-797, 2013.
[59] Surender Singh Tanwar and D.K. Khatod, "Techno-economic and environmental approach for optimal placement and sizing of renewable DGs in distribution system," *Energy*, vol. 127, pp. 52-67, 2017.
[60] Nand K. Meena, Anil Swarnkar, Nikhil Gupta and Khaleequr R. Niazi, "Multi-objective Taguchi approach for optimal DG integration in distribution systems," *IET Generation, Transmission & Distribution*, vol. 11, no. 9, pp. 2418-2428, 2017.
[61] Tolba M, Rezk H, Diab A and Al-Dhaifallah M.A, "Novel Robust Methodology Based Salp Swarm Algorithm for Allocation and Capacity of Renewable Distributed Generators on Distribution Grids," *Energies*, vol. 11, 2556, 2018.
[62] S. Arabi Nowdeh, I. Faraji Davoudkhani, M.J. Hadidian Moghaddam, E. Seifi Najmi, A.Y. Abdelaziz, A. Ahmadi, S.E. Razavi and F.H. Gandoman, "Fuzzy multi-objective placement of renewable energy sources in distribution system with objective of loss reduction and reliability improvement using a novel hybrid method," *Applied Soft Computing Journal*, vol. 77, pp. 761–779, 2019.
[63] Sajjan Kumar, Kamal K. Mandal and Niladri Chakraborty, "Optimal DG placement by multi-objective opposition based chaotic differential evolution for techno-economic analysis," *Applied Soft Computing Journal*, vol. 78, pp. 70–83, 2019.
[64] Zubo R.H.A, Mokryani G, Rajamani H.S, Jamshid A, Taher N and Prashant P, "Operation and planning of distribution networks with integration of renewable distributed generators considering uncertainties: a review," *Renewable and Sustainable Energy Reviews*, vol. 72, pp. 1177–1198, 2017.
[65] Zhipeng L, Fushuan W and Gerard L, "Optimal Siting and Sizing of Distributed Generators in Distribution Systems Considering Uncertainties," *IEEE Transactions on Power Delivery*, vol. 26, no. 4, pp. 2541-2551, 2011.
[66] Soroudi A, Ehsan M and Caire R, "Hybrid immune-genetic algorithm method for benefit maximisation of distribution network operators and distributed generation owners in a deregulated environment," *IET Generation, Transmission & Distribution*, vol. 5, no. 9, pp. 961-972, 2011.
[67] Jain N, Singh S N and Srivastava S C, "PSO based placement of multiple wind DGs and capacitors using probabilistic load flow model," *Swarm and Evolutionary Computation*, vol. 19, pp. 15-24, 2014.
[68] Vasileios A. Evangelopoulos and Pavlos S. Georgilakis, "Optimal distributed generation placement under uncertainties based on point estimate method embedded genetic algorithm," *IET Generation, Transmission & Distribution*, vol. 8, no. 3, pp. 389–400, 2014.
[69] Partha Kayal and C.K. Chanda, "Optimal mix of solar and wind distributed generations considering performance improvement of electrical distribution network," *Renewable Energy*, vol. 75, pp. 173-186, 2015.
[70] M. Kefayat, A. L. Ara and S. A. N. Niaki, "A hybrid of ant colony optimization and artificial bee colony algorithm for probabilistic optimal placement and sizing of distributed energy resources," *Energy Conversion and Management*, vol. 92, pp. 149–161, 2015.

[71] Sanjib Ganguly and Dipanjan Samajpati, "Distributed Generation Allocation on Radial Distribution Networks Under Uncertainties of Load and Generation Using Genetic Algorithm," *IEEE Transactions on Sustainable Energy*, vol. 6 , no. 3, pp. 688 - 697, 2015.

[72] Amir Ameli, Mohammad-Reza Farrokhifard, Ehsan Davari-nejad, Hashem Oraee and Mahmoud-Reza Haghifam, "Profit-Based DG Planning Considering Environmental and Operational Issues: A Multiobjective Approach," *IEEE Systems Journal*, vol. 11, no. 4, pp. 1959 - 1970, 2017.

[73] Javad Salehi and Mohammad Reza Jannati Oskuee, "Optimal planning of distributed generation from the DisCo and the DGO viewpoints considering the uncertainties in future demand and electricity price," *International Journal of Ambient Energy*, vol. 39, no. 8, pp. 863–872, 2018.

[74] Hamid H and Alireza J, "Optimal sizing and location of renewable energy based DG units in distribution systems considering load growth," *International Journal of Electrical Power & Energy Systems*, vol. 101, pp. 356-370, 2018.

[75] Kanwar N, Gupta N, Niazi KR and Swarnkar, "Optimal distributed resource planning for microgrids under uncertain environment," *IET Renewable Power Generation*, vol. 12, no. 2, pp. 244–251, 2018.

[76] Babak Jeddi, Vahid Vahidinasab, Parviz Ramezanpour, Jamshid Aghaei, Miadreza Shafie-khah and João P.S. Catalão, "Robust optimization framework for dynamic distributed energy resources planning in distribution networks," *International Journal of Electrical Power & Energy Systems*, vol. 110, pp. 419–433, 2019.

[77] Stagg GW and El-Abiad AH, *Computer Methods in Power System Analysis*, McGraw Hill, New York, 1968, p.427.

[78] M A Kashem, V. Ganapathy, G. B. Jasmon and M. I. Buhari, "A novel method for loss minimization in distribution networks," In *Proceedings of IEEE International Conference on Electric Utility Deregulation and Restructuring and Power Technologies*, London, UK, 2000. pp. 251-256, 2000.

[79] M.A. Kashem, A. Mohamed and G. B. Jasmon, "Loss Reduction in distribution networks using new network reconfiguration algorithm," *Electric Machines & Power Systems*, vol. 26, no. 8, pp. 815-829, 1998.

[80] Ji-Pyng Chiou, Chung-Fu Chang and Ching-Tzong Su, "Variable Scaling Hybrid Differential Evolution for Solving Network Reconfiguration of Distribution Systems," *IEEE Transactions on Power Systems*, vol. 20, no. 2, pp. 668-674, 2005.

[81] Rajesh Kavasseri and Cristinel Ababei, "REDS: REpository of Distribution Systems," Available online (http://www.dejazzer.com/reds.html).

[82] D Das, Kothari DP and Kalam A, "Simple and efficient method for load flow solution of radial distribution networks," *International Journal of Electrical Power & Energy Systems*, vol. 17, no. 5, pp. 335-346, 1995.

[83] Etemadi AH and Fotuhi-Firuzabad M, "Distribution system reliability enhancement using optimal capacitor placement," *IET Generation, Transmission & Distribution*, vol. 2, no. 5, pp. 621-631, 2008.

[84] Jeonghwan J, Rothrock L, Mcdermott PL and Barnes M, "Using the Analytic Hierarchy Process to Examine Judgment Consistency in a Complex Multiattribute Task," *IEEE Transactions on Systems, Man, and Cybernetics - Part A: Systems and Humans*, vol. 40, no. 5, pp. 1105-1115, 2010.

[85] Seyedali M, Seyed M.M and Abdolreza H, "Multi-Verse Optimizer: a nature-inspired algorithm for global optimization," *Neural Computing and Applications*, vol. 27, no. 2, pp. 495–513, 2016.

[86] Wang H, Zhijian W, Yong L, Jing Wang, Dazhi Jiang and Lili Chen, "Space transformation search : A new evolutionary technique," *Proc. World Summit on Genetic and Evolutionary Computation, Shanghai, China*, pp. 537–544, 12 - 14 June 2009.

[87] Xiang T, Xiaofeng L and Kwok-wo W, "An improved particle swarm optimisation algorithm combined with piecewise linear chaotic map," *Applied Mathematics and Computation*, vol. 190, no. 2, pp. 1637-1645, 2007.

[88] Mahdavi M, Fesanghary M and Damangir E, "An improved harmony search algorithm for solving optimization problems," *Applied Mathematics and Computation*, vol. 188, no. 2, pp. 1567-1579, 2007.

[89] Seyedali Mirjalili, Amir H. Gandomi, Seyedeh Zahra Mirjalili, Shahrzad Saremi, Hossam Faris and Seyed Mohammad Mirjalili, "Salp Swarm Algorithm: A bio-inspired optimizer for engineering design problems," *Advances in Engineering Software*, vol. 114, pp. 163–191, 2017.

[90] Chatterjee A, Ghoshal S.P and Mukherjee V, "Transient performance improvement of grid connected hydro system using distributed generation and capacitive energy storage unit," *International Journal of Electrical Power & Energy Systems*, vol. 43, no. 1, pp. 210–221, 2012.

[91] http://www.elia.be/en/grid-data. [accessed on 03.01.19].

[92] H. R. Esmaeilian and R. Fadaeinedjad, "Energy Loss Minimization in Distribution Systems Utilizing an Enhanced Reconfiguration Method Integrating Distributed Generation," *IEEE Systems Journal*, vol. 9, no. 4, pp. 1430-1439, 2015.

[93] Iain Staffell and Richard Green, "How does wind farm performance decline with age?," *Renewable Energy*, vol. 66, pp. 775-786, 2014.

[94] Rao R.V, Rai D.P, Ramkumar J and Balic J, "A new multi-objective Jaya algorithm for optimization of modern machining processes," *Advances in Production Engineering & Management*, vol. 11, no. 4, pp. 271–286, 2016.

APPENDIX - 1 [78]

IEEE 33-bus Distribution System

Number of buses: 33

Number of lines: 32

Number of Tie-lines: 5

Base Voltage: 12.66 kV

Tie-lines: 33, 34, 35, 36 and 37

Total Active Power Load: 3715 kW

Total Reactive Power Load: 2300 kVAR

System Real Power Losses: 210.98 kW (For RDN) / 123.35 kW (For WMDN)

System Reactive Power Losses: 143.02 kVAR (For RDN) / 88.33 kVAR (For WMDN)

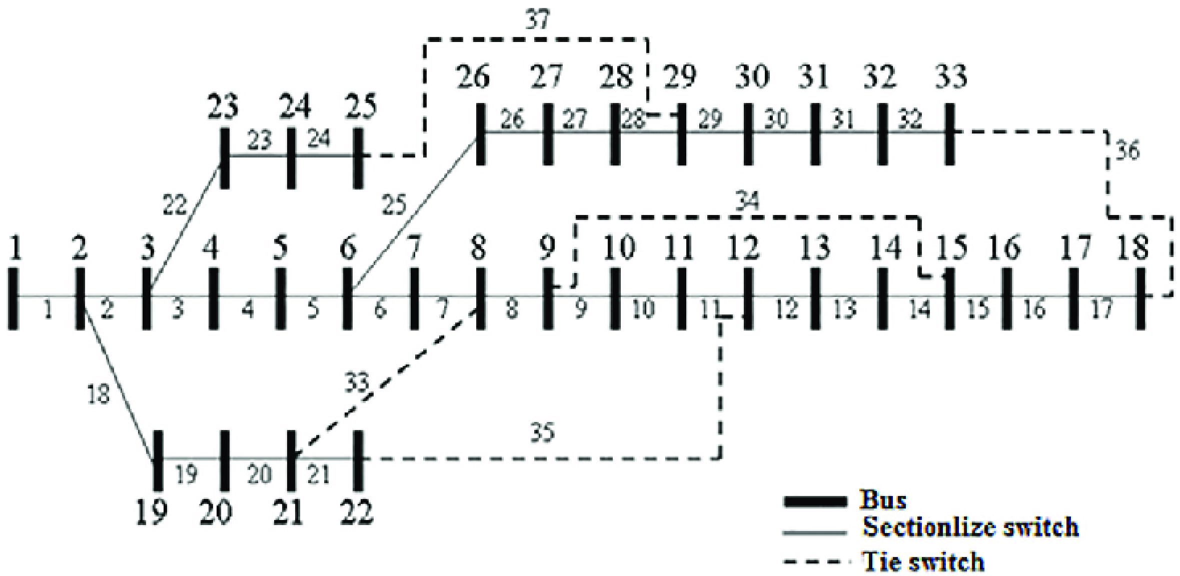

IEEE 33-bus Distribution System Single line diagram

Line and Load Data of IEEE 33-bus Distribution System

Line number	From Bus	To Bus	Resistance (Ω)	Reactance (Ω)	Active Load (kW) @ To Bus	Reactive Load (kVAR) @ To Bus
1	1	2	0.0922	0.0470	100	60
2	2	3	0.4930	0.2511	90	40
3	3	4	0.3660	0.1864	120	80
4	4	5	0.3811	0.1941	60	30
5	5	6	0.8190	0.7070	60	20

6	6	7	0.1872	0.6188	200	100
7	7	8	1.7114	1.2351	200	100
8	8	9	1.0300	0.7400	60	20
9	9	10	1.0440	0.7400	60	20
10	10	11	0.1966	0.0650	45	30
11	11	12	0.3744	0.1238	60	35
12	12	13	1.4680	1.1550	60	35
13	13	14	0.5416	0.7129	120	80
14	14	15	0.5910	0.5260	60	10
15	15	16	0.7463	0.5450	60	20
16	16	17	1.2890	1.7210	60	20
17	17	18	0.7320	0.5740	90	40
18	2	19	0.1640	0.1565	90	40
19	19	20	1.5042	1.3554	90	40
20	20	21	0.4095	0.4784	90	40
21	21	22	0.7089	0.9373	90	40
22	3	23	0.4512	0.3083	90	50
23	23	24	0.8980	0.7091	420	200
24	24	25	0.8960	0.7011	420	200
25	6	26	0.2030	0.1034	60	25
26	26	27	0.2842	0.1447	60	25
27	27	28	1.0590	0.9337	60	20
28	28	29	0.8042	0.7006	120	70
29	29	30	0.5075	0.2585	200	600
30	30	31	0.9744	0.9630	150	70
31	31	32	0.3105	0.3619	210	100
32	32	33	0.3410	0.5302	60	40

Tie-line Data of IEEE 33-bus Distribution System

Line number	From Bus	To Bus	Resistance (Ω)	Reactance (Ω)
33	8	21	2.0000	2.0000
34	9	15	2.0000	2.0000
35	12	22	2.0000	2.0000
36	18	33	0.5000	0.5000
37	25	29	0.5000	0.5000

APPENDIX - 2 [79]

IEEE 69-bus Distribution System

Number of buses: 69

Number of lines: 68

Number of Tie-lines: 5

Base Voltage: 12.66 kV

Tie-lines: 69, 70, 71, 72 and 73

Total Active Power Load: 3801.89 kW

Total Reactive Power Load: 2694.10 kVAR

System Real Power Losses: 224.93 kW (For RDN) / 82.69 kW (For WMDN)

System Reactive Power Losses: 102.13 kVAR (For RDN) / 65.27 kVAR (For WMDN)

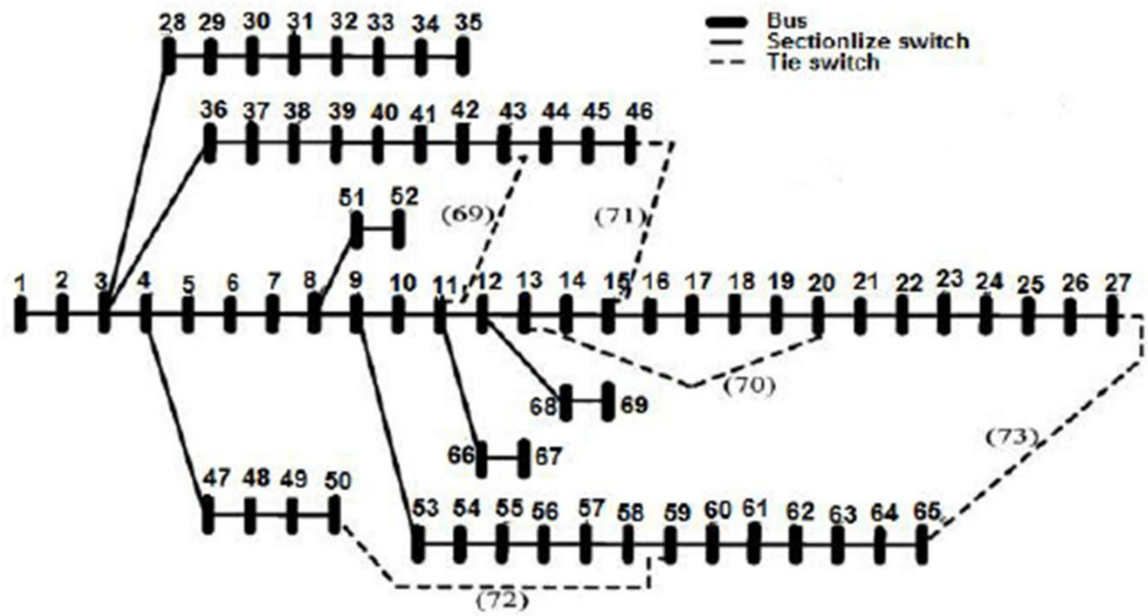

IEEE 69-bus Distribution System Single line diagram

Line and Load Data of IEEE 69-bus Distribution System

Line number	From Bus	To Bus	Resistance (Ω)	Reactance (Ω)	Active Load (kW) @ To Bus	Reactive Load (kVAR) @ To Bus
1	1	2	0.0005	0.0012	0.00	0.00
2	2	3	0.0005	0.0012	0.00	0.00
3	3	4	0.0015	0.0036	0.00	0.00

4	4	5	0.0251	0.0294	0.00	0.00
5	5	6	0.3660	0.1864	2.60	2.20
6	6	7	0.3811	0.1941	40.40	30.00
7	7	8	0.0922	0.0470	75.00	54.00
8	8	9	0.0493	0.0251	30.00	22.00
9	9	10	0.8190	0.2707	28.00	19.00
10	10	11	0.1872	0.0619	145.00	104.00
11	11	12	0.7114	0.2351	145.00	104.00
12	12	13	1.0300	0.3400	8.00	5.00
13	13	14	1.0440	0.3450	8.00	5.50
14	14	15	1.0580	0.3496	0.00	0.00
15	15	16	0.1966	0.0650	45.50	30.00
16	16	17	0.3744	0.1238	60.00	35.00
17	17	18	0.0047	0.0016	60.00	35.00
18	18	19	0.3276	0.1083	0.00	0.00
19	19	20	0.2106	0.0690	1.00	0.60
20	20	21	0.3416	0.1129	114.00	81.00
21	21	22	0.0140	0.0046	5.00	3.50
22	22	23	0.1591	0.0526	0.00	0.00
23	23	24	0.3463	0.1145	28.00	20.00
24	24	25	0.7488	0.2475	0.00	0.00
25	25	26	0.3089	0.1021	14.00	10.00
26	26	27	0.1732	0.0572	14.00	10.00
27	3	28	0.0044	0.0108	26.00	18.60
28	28	29	0.0640	0.1565	26.00	18.60
29	29	30	0.3978	0.1315	0.00	0.00
30	30	31	0.0702	0.0232	0.00	0.00
31	31	32	0.3510	0.1160	0.00	0.00
32	32	33	0.8390	0.2816	14.00	10.00
33	33	34	1.7080	0.5646	19.50	14.00
34	34	35	1.4740	0.4873	6.00	4.00
35	3	36	0.0044	0.0108	26.00	18.55
36	36	37	0.0640	0.1565	26.00	18.55
37	37	38	0.1053	0.1230	0.00	0.00
38	38	39	0.0304	0.0355	24.00	17.00
39	39	40	0.0018	0.0021	24.00	17.00
40	40	41	0.7283	0.8509	1.20	1.00
41	41	42	0.3100	0.3623	0.00	0.00
42	42	43	0.0410	0.0478	6.00	4.30
43	43	44	0.0092	0.0116	0.00	0.00
44	44	45	0.1089	0.1373	39.22	26.30

45	45	46	0.0009	0.0012	39.22	26.30
46	4	47	0.0034	0.0084	0.00	0.00
47	47	48	0.0851	0.2083	79.00	56.40
48	48	49	0.2898	0.7091	384.70	274.50
49	49	50	0.0822	0.2011	384.70	274.50
50	8	51	0.0928	0.0473	40.50	28.30
51	51	52	0.3319	0.1114	3.60	2.70
52	9	53	0.1740	0.0886	4.35	3.50
53	53	54	0.2030	0.1034	26.40	19.00
54	54	55	0.2842	0.1447	24.00	17.20
55	55	56	0.2813	0.1433	0.00	0.00
56	56	57	1.5900	0.5337	0.00	0.00
57	57	58	0.7837	0.2630	0.00	0.00
58	58	59	0.3042	0.1006	100.00	72.00
59	59	60	0.3861	0.1172	0.00	0.00
60	60	61	0.5075	0.2585	1244.00	888.00
61	61	62	0.0974	0.0496	32.00	23.00
62	62	63	0.1450	0.0738	0.00	0.00
63	63	64	0.7105	0.3619	227.00	162.00
64	64	65	1.0410	0.5302	59.00	42.00
65	11	66	0.2012	0.0611	18.00	13.00
66	66	67	0.0047	0.0014	18.00	13.00
67	12	68	0.7394	0.2444	28.00	20.00
68	68	69	0.0047	0.0016	28.00	20.00

Tie-line Data of IEEE 69-bus Distribution System

Line number	From Bus	To Bus	Resistance (Ω)	Reactance (Ω)
69	11	43	0.5000	0.5000
70	13	20	0.5000	0.5000
71	15	46	1.0000	0.5000
72	50	59	2.0000	1.0000
73	27	65	1.0000	0.5000

APPENDIX - 3 [80]

Taiwan Power Company (TPC) 84-bus Distribution System

Number of buses: 84

Number of lines: 83

Number of Tie-lines: 13

Base Voltage: 11.4 kV

Tie-lines: 84, 85, 86, 87, 88, 89, 90, 91, 92, 93, 94, 95 and 96

Total Active Power Load: 28350 kW

Total Reactive Power Load: 20700 kVAR

System Real Power Losses: 531.97 kW (For RDN) / 462.67 kW (For WMDN)

System Reactive Power Losses: 1374.28 kVAR (For RDN) / 1164.01 kVAR (For WMDN)

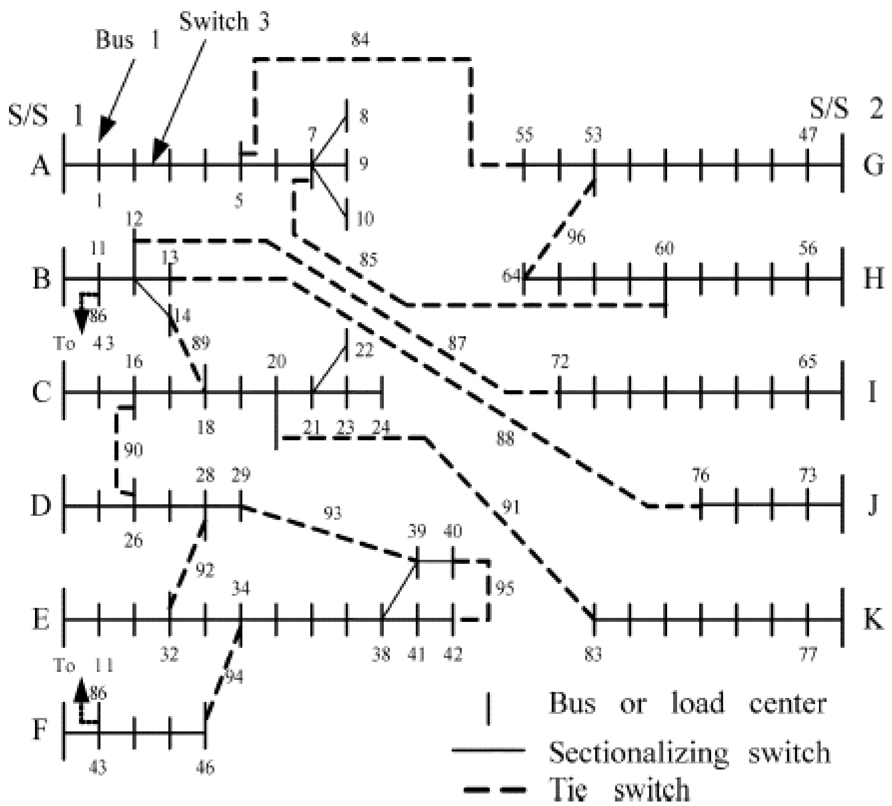

Taiwan Power Company (TPC) 84-bus Distribution System Single line diagram

Line and Load Data of TPC 84-bus Distribution System

Line number	From Bus	To Bus	Resistance (Ω)	Reactance (Ω)	Active Load (kW) @ To Bus	Reactive Load (kVAR) @ To Bus
1	A	1	0.1944	0.6624	0	0
2	1	2	0.2096	0.4304	100	50
3	2	3	0.2358	0.4842	300	200
4	3	4	0.0917	0.1883	350	250
5	4	5	0.2096	0.4304	220	100
6	5	6	0.0393	0.0807	1100	800
7	6	7	0.0405	0.1380	400	320
8	7	8	0.1048	0.2152	300	200
9	7	9	0.2358	0.4842	300	230
10	7	10	0.1048	0.2152	300	260
11	B	11	0.0786	0.1614	0	0
12	11	12	0.3406	0.6944	1200	800
13	12	13	0.0262	0.0538	800	600
14	12	14	0.0786	0.1614	700	500
15	C	15	0.1134	0.3864	0	0
16	15	16	0.0524	0.1076	300	150
17	16	17	0.0524	0.1076	500	350
18	17	18	0.1572	0.3228	700	400
19	18	19	0.0393	0.0807	1200	1000
20	19	20	0.1703	0.3497	300	300
21	20	21	0.2358	0.4842	400	350
22	21	22	0.1572	0.3228	50	20
23	21	23	0.1965	0.4035	50	20
24	23	24	0.1310	0.2690	50	10
25	D	25	0.0567	0.1932	50	30
26	25	26	0.1048	0.2152	100	60
27	26	27	0.2489	0.5111	100	70
28	27	28	0.0486	0.1656	1800	1300
29	28	29	0.1310	0.2690	200	120
30	E	30	0.1965	0.3960	0	0
31	30	31	0.1310	0.2690	1800	1600
32	31	32	0.1310	0.2690	200	150
33	32	33	0.0262	0.0538	200	100
34	33	34	0.1703	0.3497	800	600
35	34	35	0.0524	0.1076	100	60
36	35	36	0.4978	1.0222	100	60
37	36	37	0.0393	0.0807	20	10

38	37	38	0.0393	0.0807	20	10
39	38	39	0.0786	0.1614	20	10
40	39	40	0.2096	0.4304	20	10
41	38	41	0.1965	0.4035	200	160
42	41	42	0.2096	0.4304	50	30
43	F	43	0.0486	0.1656	0	0
44	43	44	0.0393	0.0807	30	20
45	44	45	0.1310	0.2690	800	700
46	45	46	0.2358	0.4842	200	150
47	G	47	0.2430	0.8280	0	0
48	47	48	0.0655	0.1345	0	0
49	48	49	0.0655	0.1345	0	0
50	49	50	0.0393	0.0807	200	160
51	50	51	0.0786	0.1614	800	600
52	51	52	0.0393	0.0807	500	300
53	52	53	0.0786	0.1614	500	350
54	53	54	0.0524	0.1076	500	300
55	54	55	0.1310	0.2690	200	80
56	H	56	0.2268	0.7728	0	0
57	56	57	0.5371	1.1029	30	20
58	57	58	0.0524	0.1076	600	420
59	58	59	0.0405	0.1380	0	0
60	59	60	0.0393	0.0807	20	10
61	60	61	0.0262	0.0538	20	10
62	61	62	0.1048	0.2152	200	130
63	62	63	0.2358	0.4842	300	240
64	63	64	0.0243	0.0828	300	200
65	I	65	0.0486	0.1656	0	0
66	65	66	0.1703	0.3497	50	30
67	66	67	0.1215	0.4140	0	0
68	67	68	0.2187	0.7452	400	360
69	68	69	0.0486	0.1656	0	0
70	69	70	0.0729	0.2484	0	0
71	70	71	0.0567	0.1932	2000	1500
72	71	72	0.0262	0.0528	200	150
73	J	73	0.3240	1.1040	0	0
74	73	74	0.0324	0.1104	0	0
75	74	75	0.0567	0.1932	1200	950
76	75	76	0.0486	0.1656	300	180
77	K	77	0.2511	0.8556	0	0
78	77	78	0.1296	0.4416	400	360

79	78	79	0.0486	0.1656	2000	1300
80	79	80	0.1310	0.2640	200	140
81	80	81	0.1310	0.2640	500	360
82	81	82	0.0917	0.1883	100	30
83	82	83	0.3144	0.6456	400	360

Tie-line Data of TPC 84-bus Distribution System

Line number	**From Bus**	**To Bus**	**Resistance (Ω)**	**Reactance (Ω)**
84	5	55	0.1310	0.2690
85	7	60	0.1310	0.2690
86	11	43	0.1310	0.2690
87	12	72	0.3406	0.6994
88	13	76	0.4585	0.9415
89	14	18	0.5371	1.0824
90	16	26	0.0917	0.1883
91	20	83	0.0786	0.1614
92	28	32	0.0524	0.1076
93	29	39	0.0786	0.1614
94	34	46	0.0262	0.0538
95	40	42	0.1965	0.4035
96	53	64	0.0393	0.0807

APPENDIX - 4 [82]

INDIAN 85-bus Radial Distribution System

Number of buses: 85

Number of lines: 84

Base Voltage: 11 kV

Total Active Power Load: 2569.28 kW

Total Reactive Power Load: 2621.18 kVAR

System Real Power Losses: 315.70 kW (For RDN)

System Reactive Power Losses: 198.35 kVAR (For RDN)

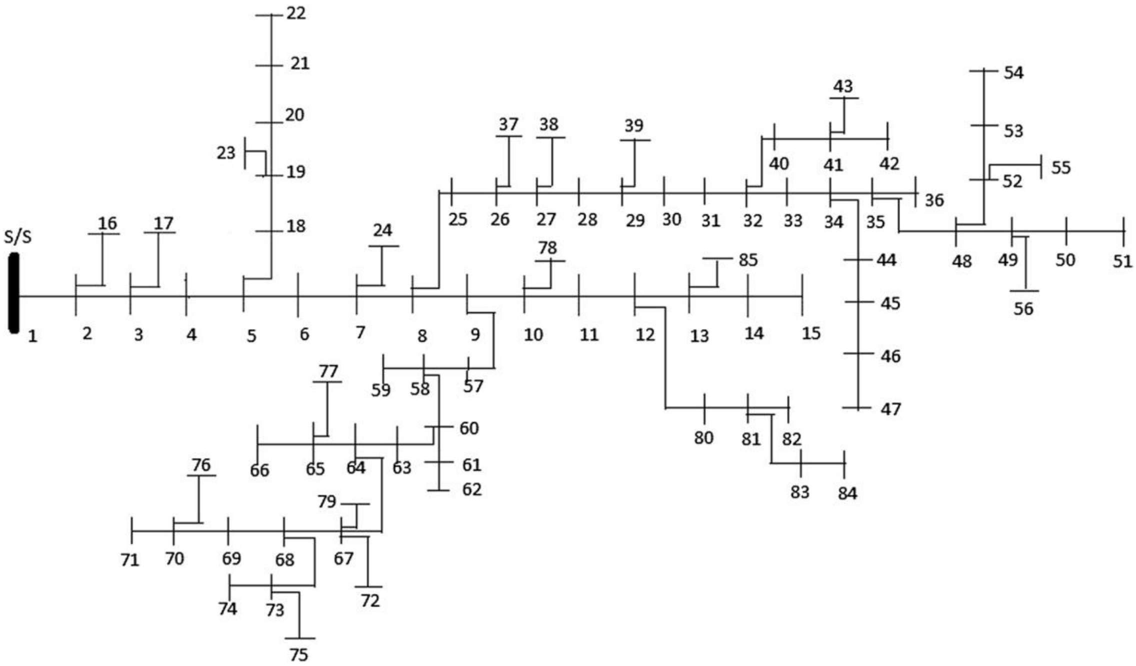

INDIAN 85-bus Radial Distribution System Single line diagram

Line and Load Data of INDIAN 85-bus Distribution System

Line number	From Bus	To Bus	Resistance (Ω)	Reactance (Ω)	Active Load (kW) @ To Bus	Reactive Load (kVAR) @ To Bus
1	1	2	0.1080	0.0750	0.00	0.00
2	2	3	0.1630	0.1120	0.00	0.00
3	3	4	0.2170	0.1490	56.00	57.13
4	4	5	0.1080	0.0740	0.00	0.00
5	5	6	0.4350	0.2980	35.28	35.99

6	6	7	0.2720	0.1860	0.00	0.00
7	7	8	1.1970	0.8200	35.28	35.99
8	8	9	0.1080	0.0740	0.00	0.00
9	9	10	0.5980	0.4100	0.00	0.00
10	10	11	0.5440	0.3730	56.00	57.13
11	11	12	0.5440	0.3730	0.00	0.00
12	12	13	0.5980	0.4100	0.00	0.00
13	13	14	0.2720	0.1860	35.28	35.99
14	14	15	0.3260	0.2230	35.28	35.99
15	2	16	0.7280	0.3020	35.28	35.99
16	3	17	0.4550	0.1890	112.00	114.26
17	5	18	0.8200	0.3400	56.00	57.13
18	18	19	0.6370	0.2640	56.00	57.13
19	19	20	0.4550	0.1890	35.28	35.99
20	20	21	0.8190	0.3400	35.28	35.99
21	21	22	1.5480	0.6420	35.28	35.99
22	19	23	0.1820	0.0750	56.00	57.13
23	7	24	0.9100	0.3780	35.28	35.99
24	8	25	0.4550	0.1890	35.28	35.99
25	25	26	0.3640	0.1510	56.00	57.13
26	26	27	0.5460	0.2260	0.00	0.00
27	27	28	0.2730	0.1130	56.00	57.13
28	28	29	0.5460	0.2260	0.00	0.00
29	29	30	0.5460	0.2260	35.28	35.99
30	30	31	0.2730	0.1130	35.28	35.99
31	31	32	0.1820	0.0750	0.00	0.00
32	32	33	0.1820	0.0750	14.00	14.28
33	33	34	0.8190	0.3400	0.00	0.00
34	34	35	0.6370	0.2640	0.00	0.00
35	35	36	0.1820	0.0750	35.28	35.99
36	26	37	0.3640	0.1510	56.00	57.13
37	27	38	1.0020	0.4160	56.00	57.13
38	29	39	0.5460	0.2260	56.00	57.13
39	32	40	0.4550	0.1890	35.28	35.99
40	40	41	1.0020	0.4160	0.00	0.00
41	41	42	0.2730	0.1130	35.28	35.99
42	41	43	0.4550	0.1890	35.28	35.99
43	34	44	1.0020	0.4160	35.28	35.99
44	44	45	0.9110	0.3780	35.28	35.99
45	45	46	0.9110	0.3780	35.28	35.99
46	46	47	0.5460	0.2260	14.00	14.28

47	35	48	0.6370	0.2640	0.00	0.00
48	48	49	0.1820	0.0750	0.00	0.00
49	49	50	0.3640	0.1510	35.28	35.99
50	50	51	0.4550	0.1890	56.00	57.13
51	48	52	1.3660	0.5670	0.00	0.00
52	52	53	0.4550	0.1890	35.28	35.99
53	53	54	0.5460	0.2260	56.00	57.13
54	52	55	0.5460	0.2260	56.00	57.13
55	49	56	0.5460	0.2260	14.00	14.28
56	9	57	0.2730	0.1130	56.00	57.13
57	57	58	0.8190	0.3400	0.00	0.00
58	58	59	0.1820	0.0750	56.00	57.13
59	58	60	0.5460	0.2260	56.00	57.13
60	60	61	0.7280	0.3020	56.00	57.13
61	61	62	1.0020	0.4150	56.00	57.13
62	60	63	0.1820	0.0750	14.00	14.28
63	63	64	0.7280	0.3020	0.00	0.00
64	64	65	0.1820	0.0750	0.00	0.00
65	65	66	0.1820	0.0750	56.00	57.13
66	64	67	0.4550	0.1890	0.00	0.00
67	67	68	0.9100	0.3780	0.00	0.00
68	68	69	1.0920	0.4530	56.00	57.13
69	69	70	0.4550	0.1890	0.00	0.00
70	70	71	0.5460	0.2260	35.28	35.99
71	67	72	0.1820	0.0750	56.00	57.13
72	68	73	1.1840	0.4910	0.00	0.00
73	73	74	0.2730	0.1130	56.00	57.13
74	73	75	1.0020	0.4160	35.28	35.99
75	70	76	0.5460	0.2260	56.00	57.13
76	65	77	0.0910	0.0370	14.00	14.28
77	10	78	0.6370	0.2640	56.00	57.13
78	67	79	0.5460	0.2260	35.28	35.99
79	12	80	0.7280	0.3020	56.00	57.13
80	80	81	0.3640	0.1510	0.00	0.00
81	81	82	0.0910	0.0370	56.00	57.13
82	81	83	1.0920	0.4530	35.28	35.99
83	83	84	1.0020	0.4160	14.00	14.28
84	13	85	0.8190	0.3400	35.28	35.99

APPENDIX - 5 [81]

136-bus Distribution System

Number of buses: 136

Number of lines: 135

Number of Tie-lines: 21

Base Voltage: 13.8 kV

Tie-lines: 136, 137, 138, 139, 140, 141, 142, 143, 144, 145, 146, 147, 148, 149, 150, 151, 152, 153, 154, 155 and 156

Total Active Power Load: 18312.81 kW

Total Reactive Power Load: 7930.26 kVAR

System Real Power Losses: 320.25 kW (For RDN) / 271.75 kW (For WMDN)

System Reactive Power Losses: 702.62 kVAR (For RDN) / 588.45 kVAR (For WMDN)

Line and Load Data of 136-bus Distribution System

Line number	From Bus	To Bus	Resistance (Ω)	Reactance (Ω)	Active Load (kW) @ To Bus	Reactive Load (kVAR) @ To Bus
1	1	2	0.3320	0.7665	0	0
2	2	3	0.0018	0.0043	47.78	19.01
3	3	4	0.2234	0.5153	42.55	16.93
4	4	5	0.0994	0.2295	87.02	34.62
5	5	6	0.1557	0.3594	311.31	123.85
6	6	7	0.1632	0.3767	148.87	59.22
7	7	8	0.1144	0.2641	238.67	94.95
8	7	9	0.0567	0.0566	62.29	24.78
9	9	10	0.5212	0.2741	124.59	49.57
10	9	11	0.1087	0.1086	140.17	55.76
11	11	12	0.3980	0.2093	116.81	46.47
12	11	13	0.9174	0.3146	249.20	99.14
13	11	14	0.1182	0.1180	291.44	115.59
14	14	15	0.5022	0.2642	303.72	120.83
15	14	16	0.0567	0.0566	215.39	85.69
16	16	17	0.2937	0.1545	198.58	79.00
17	1	18	0.3320	0.7665	0	0

18	18	19	0.0018	0.0043	0	0
19	19	20	0.2232	0.5153	0	0
20	20	21	0.1088	0.2511	30.12	14.72
21	21	22	0.7107	0.3738	230.97	112.92
22	21	23	0.1819	0.4200	60.25	29.45
23	23	24	0.3032	0.1595	230.97	112.92
24	23	25	0.0243	0.0563	120.50	58.91
25	25	26	0.0450	0.1039	0	0
26	26	27	0.0187	0.0433	56.98	27.85
27	27	28	0.1182	0.1123	364.66	178.28
28	28	29	0.0236	0.0236	0	0
29	29	30	0.1895	0.0997	124.64	60.93
30	30	31	0.3980	0.2093	56.98	27.85
31	29	32	0.0567	0.0566	0	0
32	32	33	0.0947	0.0498	85.47	41.78
33	33	34	0.4169	0.2193	0	0
34	34	35	0.1137	0.0598	396.73	193.96
35	32	36	0.0756	0.0755	0	0
36	36	37	0.3696	0.1944	181.15	88.56
37	37	38	0.2653	0.1395	242.17	118.39
38	36	39	0.0567	0.0566	75.31	36.82
39	1	40	0.3320	0.7665	0	0
40	40	41	0.1181	0.2728	1.25	0.53
41	41	42	2.9628	1.0162	6.27	2.66
42	41	43	0.0018	0.0043	0	0
43	43	44	0.0694	0.1602	117.88	49.97
44	44	45	0.8150	0.4287	62.66	25.56
45	44	46	0.0637	0.1472	172.28	73.03
46	46	47	0.1313	0.3031	458.55	194.38
47	47	48	0.0619	0.1429	262.96	111.47
48	48	49	0.1144	0.2641	235.76	99.94
49	49	50	0.2837	0.2833	0	0
50	50	51	0.2837	0.2832	109.21	46.29
51	49	52	0.0450	0.1039	0	0
52	52	53	0.0262	0.0606	72.81	30.86
53	53	54	0.0600	0.1385	258.47	109.57
54	54	55	0.0300	0.0692	69.17	29.32
55	55	56	0.0206	0.0476	21.84	9.26
56	53	57	0.1088	0.2511	0	0
57	57	58	0.2558	0.1346	20.53	8.70
58	58	59	0.4169	0.2193	150.55	63.82

59	59	60	0.5022	0.2642	220.68	93.55
60	60	61	0.3317	0.1744	92.38	39.16
61	61	62	0.2084	0.1096	0	0
62	48	63	0.1388	0.3204	226.69	96.09
63	1	64	0.0075	0.0173	0	0
64	64	65	0.2701	0.6236	294.02	116.97
65	65	66	0.3827	0.8834	83.01	33.02
66	66	67	0.3301	0.7622	83.01	33.02
67	67	68	0.3283	0.7578	103.77	41.28
68	68	69	0.1707	0.3940	176.41	70.18
69	69	70	0.5591	0.2941	83.01	33.02
70	69	71	0.0581	0.1342	217.92	86.69
71	71	72	0.7013	0.3689	23.29	9.26
72	72	73	1.0235	0.5383	5.07	2.02
73	71	74	0.0675	0.1559	72.63	28.89
74	74	75	1.3235	0.4539	405.99	161.52
75	1	76	0.0112	0.0259	0	0
76	76	77	0.7297	1.6846	100.18	42.47
77	77	78	0.2251	0.5196	142.52	60.42
78	78	79	0.2082	0.4807	96.04	40.71
79	79	80	0.0469	0.1082	300.45	127.36
80	80	81	0.6195	0.6185	141.24	59.87
81	81	82	0.3404	0.3399	279.85	118.63
82	82	83	0.5686	0.2991	87.31	37.01
83	82	84	0.1087	0.1086	243.85	103.37
84	84	85	0.5686	0.2991	247.75	105.02
85	1	86	0.0112	0.0259	0	0
86	86	87	0.4183	0.9657	89.87	38.10
87	87	88	0.1049	0.1364	1137.28	482.10
88	87	89	0.4389	1.0133	458.34	194.29
89	89	90	0.0752	0.0257	385.19	163.29
90	90	91	0.0769	0.1775	0	0
91	91	92	0.3320	0.7665	79.61	33.74
92	92	93	0.0844	0.1948	87.31	37.01
93	93	94	0.1332	0.3074	0	0
94	94	95	0.2932	0.2927	74.00	31.37
95	95	96	0.2175	0.2172	232.05	98.36
96	96	97	0.2648	0.2644	141.82	60.11
97	94	98	0.1031	0.2381	0	0
98	98	99	0.1350	0.3118	76.45	32.40
99	1	100	0.0093	0.0216	0	0

100	100	101	0.1688	0.3897	51.32	21.75
101	101	102	0.1181	0.2728	59.87	25.38
102	102	103	2.2860	0.7841	9.06	3.84
103	102	104	0.4558	1.0523	2.09	0.88
104	104	105	0.6960	1.6066	16.73	7.09
105	105	106	0.4577	1.0566	1506.52	638.63
106	106	107	0.2029	0.2637	313.02	132.69
107	107	108	0.2134	0.2773	79.83	33.84
108	108	109	0.5496	0.2891	51.32	21.75
109	109	110	0.5401	0.2841	0	0
110	108	111	0.0455	0.0591	202.43	85.81
111	111	112	0.4738	0.2492	60.82	25.87
112	112	113	0.8624	0.4536	45.62	19.33
113	113	114	0.5686	0.2991	0	0
114	109	115	0.7771	0.4087	157.07	66.58
115	115	116	1.0803	0.5683	0	0
116	110	117	1.0663	0.5782	250.15	106.04
117	117	118	0.4738	0.2492	0	0
118	105	119	0.3226	0.7448	68.81	28.59
119	119	120	0.1463	0.3377	32.07	13.59
120	120	121	0.1238	0.2858	61.08	25.89
121	1	122	0.0112	0.0259	0	0
122	122	123	0.6491	1.4984	94.62	46.26
123	123	124	0.0450	0.1039	49.85	24.37
124	124	125	0.5264	0.1805	123.16	60.21
125	124	126	0.0206	0.0476	78.35	38.30
126	126	127	0.5307	0.2791	145.47	71.12
127	126	128	0.0975	0.2252	21.37	10.44
128	128	129	0.1181	0.2728	74.79	36.56
129	128	130	0.1388	0.3204	227.92	111.43
130	130	131	0.0431	0.0996	35.61	17.41
131	131	132	0.0919	0.2122	249.29	121.87
132	132	133	0.1613	0.3724	316.72	154.84
133	133	134	0.3783	0.3777	333.81	163.19
134	134	135	0.3972	0.3966	249.29	121.87
135	135	136	0.2932	0.2927	0	0

Tie-line Data of 136-bus Distribution System

Line number	From Bus	To Bus	Resistance (Ω)	Reactance (Ω)
136	8	74	0.1313	0.3031
137	10	25	0.2653	0.1395
138	16	84	0.1418	0.1416
139	39	136	0.0851	0.0849
140	26	52	0.0450	0.1039
141	51	97	0.1418	0.1416
142	56	99	0.1418	0.1416
143	63	121	0.0394	0.0909
144	67	80	0.1294	0.2988
145	80	132	0.0168	0.0389
146	85	136	0.3317	0.1744
147	92	105	0.1418	0.1716
148	91	130	0.0769	0.1775
149	91	104	0.0769	0.1775
150	93	105	0.0769	0.1775
151	93	133	0.0769	0.1775
152	97	121	0.2648	0.2644
153	111	48	0.4969	0.6456
154	127	77	0.1705	0.0897
155	129	78	0.0525	0.1212
156	136	99	0.2932	0.2927

APPENDIX - 6 [81]

874-bus Distribution System

Number of buses: 874

Number of lines: 873

Number of Tie-lines: 27

Base Voltage: 130.8 kV

Tie-lines: 874, 875, 876, 877, 878, 879, 880, 881, 882, 883, 884, 885, 886, 887, 888, 889, 890, 891, 892, 893, 894, 895, 896, 897, 898, 899 and 900

Total Active Power Load: 124871.61 kW

Total Reactive Power Load: 75262.22 kVAR

System Real Power Losses: 1502.62 kW (For RDN) / 463.54 kW (For WMDN)

System Reactive Power Losses: 1404.30 kVAR (For RDN) / 548.76 kVAR (For WMDN)

Line and Load Data of 874-bus Distribution System

Line number	From Bus	To Bus	Resistance (Ω)	Reactance (Ω)	Active Load (kW) @ To Bus	Reactive Load (kVAR) @ To Bus
1	1	2	0.3320	0.7665	100.00	100.00
2	2	3	0.0188	0.0433	47.78	19.01
3	3	4	0.2234	0.5153	42.55	16.93
4	4	5	0.0994	0.2295	87.02	34.62
5	5	6	0.1557	0.3594	311.31	123.86
6	6	7	0.1632	0.3767	148.87	59.23
7	7	8	0.1144	0.2641	238.67	94.96
8	8	9	0.0567	0.0566	62.30	24.79
9	9	10	0.5212	0.2741	124.60	49.57
10	10	11	0.1087	0.1086	140.18	55.77
11	11	12	0.3980	0.2093	116.81	46.47
12	12	13	0.9174	0.3146	249.20	99.15
13	13	14	0.1182	0.1180	291.45	115.59
14	14	15	0.5022	0.2642	303.72	120.84
15	15	16	0.0567	0.0566	215.40	85.70
16	16	17	0.2937	0.1545	198.59	79.01
17	17	18	0.3320	0.7665	100.00	100.00

18	18	19	0.0188	0.0433	100.00	100.00
19	19	20	0.2232	0.5153	100.00	100.00
20	20	21	0.1088	0.2511	30.13	14.73
21	21	22	0.7107	0.3738	230.97	112.92
22	22	23	0.1819	0.4200	60.26	29.46
23	23	24	0.3032	0.1595	230.97	112.92
24	24	25	0.0243	0.0563	120.51	58.92
25	25	26	0.0450	0.1039	100.00	100.00
26	26	27	0.0187	0.0433	56.98	27.86
27	27	28	0.1182	0.1123	364.67	178.28
28	28	29	0.0236	0.0236	100.00	100.00
29	29	30	0.1895	0.0997	124.65	60.94
30	30	31	0.3980	0.2093	56.98	27.86
31	31	32	0.0567	0.0566	100.00	100.00
32	32	33	0.0947	0.0498	85.47	41.79
33	33	34	0.4169	0.2193	100.00	100.00
34	34	35	0.1137	0.0598	396.74	193.96
35	35	36	0.0756	0.0755	100.00	100.00
36	36	37	0.3696	0.1944	181.15	88.56
37	37	38	0.2653	0.1395	242.17	118.40
38	38	39	0.0567	0.0566	75.32	36.82
39	39	40	0.3320	0.7665	100.00	100.00
40	9	41	0.1181	0.2728	1.25	0.53
41	41	42	2.9628	1.0162	6.27	2.66
42	42	43	0.0188	0.0433	100.00	100.00
43	43	44	0.0694	0.1602	117.88	49.97
44	44	45	0.8150	0.4287	62.67	25.57
45	45	46	0.0637	0.1472	172.29	73.03
46	46	47	0.1313	0.3031	458.56	194.39
47	47	48	0.0619	0.1429	262.96	111.47
48	48	49	0.1144	0.2641	235.76	99.94
49	49	50	0.2837	0.2833	100.00	100.00
50	50	51	0.2837	0.2832	109.22	46.30
51	44	52	0.0450	0.1039	100.00	100.00
52	52	53	0.0262	0.0606	72.81	30.87
53	53	54	0.0600	0.1385	258.47	109.57
54	54	55	0.0300	0.0692	69.17	29.32
55	55	56	0.0206	0.0476	21.84	9.26
56	56	57	0.1088	0.2511	100.00	100.00
57	57	58	0.2558	0.1346	20.53	8.70
58	58	59	0.4169	0.2193	150.55	63.82

59	59	60	0.5022	0.2642	220.69	93.55
60	44	61	0.3317	0.1744	92.38	39.16
61	61	62	0.2084	0.1096	100.00	100.00
62	62	63	0.1388	0.3204	226.69	96.10
63	63	64	0.0750	0.0173	100.00	100.00
64	64	65	0.2701	0.6236	294.02	116.97
65	65	66	0.3827	0.8834	83.02	33.03
66	63	67	0.3301	0.7622	83.02	33.03
67	67	68	0.3283	0.7578	103.77	41.29
68	64	69	0.1707	0.3940	176.41	70.18
69	69	70	0.5591	0.2941	83.02	33.03
70	65	71	0.0581	0.1342	217.92	86.70
71	71	72	0.7013	0.3689	23.29	9.27
72	18	73	1.0235	0.5383	5.08	2.02
73	73	74	0.0675	0.1559	72.64	28.90
74	74	75	1.3235	0.4539	405.99	161.52
75	75	76	0.0112	0.0259	100.00	100.00
76	76	77	0.7297	1.6846	100.18	42.47
77	77	78	0.2251	0.5196	142.52	60.42
78	78	79	0.2082	0.4807	96.04	40.71
79	79	80	0.0469	0.1082	300.45	127.37
80	75	81	0.6195	0.6185	141.24	59.87
81	81	82	0.3404	0.3399	279.85	118.63
82	82	83	0.5686	0.2991	87.31	37.01
83	83	84	0.1087	0.1086	243.85	103.37
84	84	85	0.5686	0.2991	247.75	105.03
85	85	86	0.0112	0.0259	100.00	100.00
86	86	87	0.4183	0.9657	89.88	38.10
87	87	88	0.1049	0.1364	137.28	482.11
88	88	89	0.4389	1.0133	458.34	194.30
89	87	90	0.0752	0.0257	385.20	163.29
90	1	91	0.0769	0.1775	100.00	100.00
91	91	92	0.3320	0.7665	79.61	33.75
92	92	93	0.0844	0.1948	87.31	37.01
93	93	94	0.1332	0.3074	100.00	100.00
94	94	95	0.2932	0.2927	74.00	31.37
95	95	96	0.2175	0.2172	232.05	98.37
96	96	97	0.2648	0.2644	141.82	60.12
97	97	98	0.1031	0.2381	100.00	100.00
98	98	99	0.1350	0.3118	76.45	32.41
99	99	100	0.0938	0.0216	100.00	100.00

100	100	101	0.1688	0.3897	51.32	21.76
101	101	102	0.1181	0.2728	59.87	25.38
102	102	103	2.2860	0.7841	9.07	3.84
103	103	104	0.4558	1.0523	2.09	0.89
104	104	105	0.6960	1.6066	16.74	7.09
105	105	106	0.4577	1.0566	506.52	638.63
106	106	107	0.2029	0.2637	313.02	132.69
107	107	108	0.2134	0.2773	79.83	33.84
108	108	109	0.5496	0.2891	51.32	21.76
109	109	110	0.5401	0.2841	100.00	100.00
110	110	111	0.0455	0.0591	202.44	85.82
111	111	112	0.4738	0.2492	60.82	25.87
112	112	113	0.8624	0.4536	45.62	19.34
113	113	114	0.5686	0.2991	100.00	100.00
114	114	115	0.7771	0.4087	157.07	66.58
115	115	116	1.0803	0.5683	100.00	100.00
116	116	117	1.0663	0.5782	250.15	106.04
117	117	118	0.4738	0.2492	100.00	100.00
118	118	119	0.3226	0.7448	68.81	28.59
119	119	120	0.1463	0.3377	32.07	13.60
120	120	121	0.1238	0.2858	61.08	25.89
121	121	122	0.0112	0.0259	100.00	100.00
122	122	123	0.6491	1.4984	94.62	46.26
123	123	124	0.0450	0.1039	49.86	24.38
124	124	125	0.5264	0.1805	123.16	60.21
125	125	126	0.0206	0.0476	78.35	38.30
126	126	127	0.5307	0.2791	145.48	71.12
127	127	128	0.0975	0.2252	21.37	10.45
128	128	129	0.1181	0.2728	74.79	36.56
129	129	130	0.1388	0.3204	227.93	111.43
130	130	131	0.0431	0.0996	35.61	17.41
131	131	132	0.0919	0.2122	249.30	121.88
132	132	133	0.1613	0.3724	316.72	154.84
133	133	134	0.3783	0.3777	333.82	163.20
134	134	135	0.3972	0.3966	249.30	121.88
135	135	136	0.2932	0.2927	100.00	100.00
136	136	137	0.7771	0.4087	157.07	66.58
137	137	138	1.0803	0.5683	100.00	100.00
138	138	139	1.0663	0.5782	250.15	106.04
139	139	140	0.4738	0.2492	100.00	100.00
140	120	141	0.1144	0.2641	238.67	94.96

141	141	142	0.0567	0.0566	62.30	24.79
142	142	143	0.5212	0.2741	124.60	49.57
143	143	144	0.1087	0.1086	140.18	55.77
144	144	145	0.3980	0.2093	116.81	46.47
145	145	146	0.9174	0.3146	249.20	99.15
146	146	147	0.1182	0.1180	291.45	115.59
147	147	148	0.5022	0.2642	303.72	120.84
148	148	149	0.0567	0.0566	215.40	85.70
149	149	150	0.2937	0.1545	198.59	79.01
150	150	151	0.3320	0.7665	100.00	100.00
151	151	152	0.0188	0.0433	100.00	100.00
152	152	153	0.2232	0.5153	100.00	100.00
153	153	154	0.1088	0.2511	30.13	14.73
154	154	155	0.7107	0.3738	230.97	112.92
155	155	156	0.1819	0.4200	60.26	29.46
156	130	157	0.3032	0.1595	230.97	112.92
157	157	158	0.0243	0.0563	120.51	58.92
158	158	159	0.5264	0.1805	123.16	60.21
159	159	160	0.0206	0.0476	78.35	38.30
160	160	161	0.5307	0.2791	145.48	71.12
161	161	162	0.0975	0.2252	21.37	10.45
162	162	163	0.1181	0.2728	74.79	36.56
163	163	164	0.1388	0.3204	227.93	111.43
164	164	165	0.0431	0.0996	35.61	17.41
165	165	166	0.0919	0.2122	249.30	121.88
166	160	167	0.1613	0.3724	316.72	154.84
167	167	168	0.3783	0.3777	333.82	163.20
168	168	169	0.3972	0.3966	249.30	121.88
169	169	170	0.2932	0.2927	100.00	100.00
170	170	171	0.7771	0.4087	157.07	66.58
171	171	172	1.0803	0.5683	100.00	100.00
172	172	173	0.1350	0.3118	76.45	32.41
173	169	174	0.0938	0.0216	100.00	100.00
174	174	175	0.1688	0.3897	51.32	21.76
175	175	176	0.1181	0.2728	59.87	25.38
176	176	177	2.2860	0.7841	9.07	3.84
177	96	178	0.4558	1.0523	2.09	0.89
178	178	179	0.6960	1.6066	16.74	7.09
179	179	180	0.4577	1.0566	506.52	638.63
180	180	181	0.2029	0.2637	313.02	132.69
181	181	182	0.2134	0.2773	79.83	33.84

182	182	183	0.5496	0.2891	51.32	21.76
183	183	184	0.5401	0.2841	100.00	100.00
184	184	185	0.0455	0.0591	202.44	85.82
185	185	186	0.4738	0.2492	60.82	25.87
186	181	187	0.8624	0.4536	45.62	19.34
187	187	188	0.5686	0.2991	100.00	100.00
188	188	189	0.7771	0.4087	157.07	66.58
189	184	190	1.0800	0.5683	100.00	100.00
190	190	191	1.0663	0.5782	250.15	106.04
191	190	192	0.4738	0.2492	100.00	100.00
192	191	193	0.3226	0.7448	68.81	28.59
193	192	194	0.1463	0.3377	32.07	13.60
194	193	195	0.1238	0.2858	61.08	25.89
195	193	196	0.0112	0.0259	100.00	100.00
196	194	197	0.6491	1.4984	94.62	46.26
197	194	198	0.0450	0.1039	49.86	24.38
198	1	199	0.5264	0.1805	123.16	60.21
199	199	200	0.0206	0.0476	78.35	38.30
200	200	201	0.5307	0.2791	145.48	71.12
201	201	202	0.0975	0.2252	21.37	10.45
202	202	203	0.3320	0.7665	100.00	100.00
203	203	204	0.0188	0.0433	47.78	19.01
204	204	205	0.2234	0.5153	42.55	16.93
205	205	206	0.0994	0.2295	87.02	34.62
206	206	207	0.1557	0.3594	311.31	123.86
207	207	208	0.1632	0.3767	148.87	59.23
208	208	209	0.1144	0.2641	238.67	94.96
209	209	210	0.0567	0.0566	62.30	24.79
210	210	211	0.5212	0.2741	124.60	49.57
211	211	212	0.1087	0.1086	140.18	55.77
212	212	213	0.3980	0.2093	116.81	46.47
213	213	214	0.9174	0.3146	249.20	99.15
214	214	215	0.1182	0.1180	291.45	115.59
215	215	216	0.5022	0.2642	303.72	120.84
216	216	217	0.0567	0.0566	215.40	85.70
217	217	218	0.2937	0.1545	198.59	79.01
218	218	219	0.3320	0.7665	100.00	100.00
219	219	220	0.0188	0.0433	100.00	100.00
220	220	221	0.2232	0.5153	100.00	100.00
221	221	222	0.1088	0.2511	30.13	14.73
222	222	223	0.7107	0.3738	230.97	112.92

223	223	224	0.1819	0.4200	60.26	29.46
224	224	225	0.3032	0.1595	230.97	112.92
225	225	226	0.0243	0.0563	120.51	58.92
226	226	227	0.0450	0.1039	100.00	100.00
227	227	228	0.0187	0.0433	56.98	27.86
228	228	229	0.11823	0.1123	364.67	178.28
229	229	230	0.0236	0.0236	100.00	100.00
230	230	231	0.1895	0.0997	124.65	60.94
231	231	232	0.3980	0.2093	56.98	27.86
232	232	233	0.0567	0.0566	100.00	100.00
233	233	234	0.0947	0.0498	85.47	41.79
234	234	235	0.4169	0.2193	100.00	100.00
235	235	236	0.1137	0.0598	396.74	193.96
236	236	237	0.0756	0.0755	100.00	100.00
237	237	238	0.3696	0.1944	181.15	88.56
238	238	239	0.2653	0.1395	242.17	118.40
239	239	240	0.0567	0.0566	75.32	36.82
240	240	241	0.3320	0.7665	100.00	100.00
241	241	242	0.1181	0.2728	1.25	0.53
242	242	243	2.9628	1.0162	6.27	2.66
243	243	244	0.0188	0.0433	100.00	100.00
244	244	245	0.0694	0.1602	117.88	49.97
245	245	246	0.8150	0.4287	62.67	25.57
246	246	247	0.0637	0.1472	172.29	73.03
247	247	248	0.1313	0.3031	458.56	194.39
248	248	249	0.0619	0.1429	262.96	111.47
249	249	250	0.1144	0.2641	235.76	99.94
250	250	251	0.2837	0.2833	100.00	100.00
251	200	252	0.2837	0.2832	109.22	46.30
252	252	253	0.0450	0.1039	100.00	100.00
253	253	254	0.0262	0.0606	72.81	30.87
254	254	255	0.0600	0.1385	258.47	109.57
255	255	256	0.0300	0.0692	69.17	29.32
256	256	257	0.0206	0.0476	21.84	9.26
257	257	258	0.1088	0.2511	100.00	100.00
258	258	259	0.2558	0.1346	20.53	8.70
259	259	260	0.4169	0.2193	150.55	63.82
260	260	261	0.5022	0.2642	220.69	93.55
261	261	262	0.3317	0.1744	92.38	39.16
262	262	263	0.2084	0.1096	100.00	100.00
263	263	264	0.1388	0.3204	226.69	96.10

264	264	265	0.0700	0.0173	100.00	100.00
265	265	266	0.2701	0.6236	294.02	116.97
266	266	267	0.3827	0.8834	83.02	33.03
267	267	268	0.3301	0.7620	83.02	33.03
268	268	269	0.3283	0.7578	103.77	41.29
269	269	270	0.1707	0.3940	176.41	70.18
270	270	271	0.5591	0.2941	83.02	33.03
271	271	272	0.0581	0.1342	217.92	86.70
272	272	273	0.7013	0.3689	23.29	9.27
273	273	274	1.0235	0.5383	5.08	2.02
274	274	275	0.0675	0.1559	72.64	28.90
275	275	276	1.3235	0.4539	405.99	161.52
276	276	277	0.0112	0.0259	100.00	100.00
277	277	278	0.7297	1.6846	100.18	42.47
278	278	279	0.2251	0.5196	142.52	60.42
279	279	280	0.2082	0.4807	96.04	40.71
280	280	281	0.0469	0.1082	300.45	127.37
281	281	282	0.6195	0.6185	141.24	59.87
282	282	283	0.3404	0.3399	279.85	118.63
283	283	284	0.5686	0.2991	87.31	37.01
284	284	285	0.1087	0.1086	243.85	103.37
285	285	286	0.5686	0.2991	247.75	105.03
286	286	287	0.0112	0.0259	100.00	100.00
287	287	288	0.4183	0.9657	89.88	38.10
288	288	289	0.1049	0.1364	137.28	482.11
289	289	290	0.4389	1.0133	458.34	194.30
290	290	291	0.0752	0.0257	385.20	163.29
291	233	292	0.0769	0.1775	100.00	100.00
292	271	293	0.3320	0.7665	79.61	33.75
293	272	294	0.0844	0.1948	87.31	37.01
294	273	295	0.1332	0.3074	100.00	100.00
295	274	296	0.2932	0.2927	74.00	31.37
296	275	297	0.2175	0.2172	232.05	98.37
297	276	298	0.2648	0.2644	141.82	60.12
298	277	299	0.1031	0.2381	100.00	100.00
299	278	300	0.1350	0.3118	76.45	32.41
300	279	301	0.0938	0.0216	100.00	100.00
301	280	302	0.1688	0.3897	51.32	21.76
302	281	303	0.1181	0.2728	59.87	25.38
303	282	304	2.2860	0.7841	9.07	3.84
304	283	305	0.4558	1.0523	2.09	0.89

305	284	306	0.6960	1.6066	16.74	7.09
306	285	307	0.4577	1.0566	506.52	638.63
307	286	308	0.2029	0.2637	313.02	132.69
308	287	309	0.2134	0.2773	79.83	33.84
309	288	310	0.5496	0.2891	51.32	21.76
310	289	311	0.5401	0.2841	100.00	100.00
311	290	312	0.0455	0.0591	202.44	85.82
312	233	313	0.4738	0.2492	60.82	25.87
313	304	314	0.8624	0.4536	45.62	19.34
314	305	315	0.5686	0.2991	100.00	100.00
315	306	316	0.7771	0.4087	157.07	66.58
316	307	317	1.0803	0.5683	100.00	100.00
317	308	318	1.0663	0.5782	250.15	106.04
318	309	319	0.4738	0.2492	100.00	100.00
319	310	320	0.3226	0.7448	68.81	28.59
320	311	321	0.1463	0.3377	32.07	13.60
321	312	322	0.1238	0.2858	61.08	25.89
322	313	323	0.0112	0.0259	100.00	100.00
323	314	324	0.6491	1.4984	94.62	46.26
324	315	325	0.0450	0.1039	49.86	24.38
325	316	326	0.5264	0.1805	123.16	60.21
326	317	327	0.0206	0.0476	78.35	38.30
327	310	328	0.5307	0.2791	145.48	71.12
328	311	329	0.0975	0.2252	21.37	10.45
329	312	330	0.1181	0.2728	74.79	36.56
330	313	331	0.1388	0.3204	227.93	111.43
331	314	332	0.0431	0.0996	35.61	17.41
332	315	333	0.0919	0.2122	249.30	121.88
333	316	334	0.1613	0.3724	316.72	154.84
334	317	335	0.3783	0.3777	333.82	163.20
335	322	336	0.3972	0.3966	249.30	121.88
336	323	337	0.2932	0.2927	100.00	100.00
337	324	338	0.7771	0.4087	157.07	66.58
338	325	339	1.0803	0.5683	100.00	100.00
339	326	340	1.0663	0.5782	250.15	106.04
340	327	341	0.4738	0.2492	100.00	100.00
341	328	342	0.6195	0.6185	141.24	59.87
342	329	343	0.3404	0.3399	279.85	118.63
343	330	344	0.5686	0.2991	87.31	37.01
344	331	345	0.1087	0.1086	243.85	103.37
345	1	346	0.5686	0.2991	247.75	105.03

346	346	347	0.0112	0.0259	100.00	100.00
347	347	348	0.4183	0.9657	89.88	38.10
348	348	349	0.1049	0.1364	137.28	482.11
349	349	350	0.4389	1.0133	458.34	194.30
350	350	351	0.0752	0.0257	385.20	163.29
351	351	352	0.0769	0.1775	100.00	100.00
352	352	353	0.3320	0.7665	79.61	33.75
353	353	354	0.0844	0.1948	87.31	37.01
354	354	355	0.1332	0.3074	100.00	100.00
355	355	356	0.2932	0.2927	74.00	31.37
356	356	357	0.2175	0.2172	232.05	98.37
357	357	358	0.2648	0.2644	141.82	60.12
358	358	359	0.1031	0.2381	100.00	100.00
359	359	360	0.1350	0.3118	76.45	32.41
360	360	361	0.0938	0.0216	100.00	100.00
361	361	362	0.1688	0.3897	51.32	21.76
362	362	363	0.1181	0.2728	59.87	25.38
363	363	364	2.2860	0.7841	9.07	3.84
364	364	365	0.4558	1.0523	2.09	0.89
365	365	366	0.6960	1.6066	16.74	7.09
366	366	367	0.4577	1.0566	506.52	638.63
367	367	368	0.2029	0.2637	313.02	132.69
368	368	369	0.2134	0.2773	79.83	33.84
369	369	370	0.5496	0.2891	51.32	21.76
370	370	371	0.5401	0.2841	100.00	100.00
371	371	372	0.0455	0.0591	202.44	85.82
372	372	373	0.4738	0.2492	60.82	25.87
373	373	374	0.8624	0.4536	45.62	19.34
374	374	375	0.5686	0.2991	100.00	100.00
375	375	376	0.7771	0.4087	157.07	66.58
376	376	377	1.0803	0.5683	100.00	100.00
377	377	378	1.0663	0.5782	250.15	106.04
378	378	379	0.4738	0.2492	100.00	100.00
379	379	380	0.3226	0.7448	68.81	28.59
380	380	381	0.1463	0.3377	32.07	13.60
381	381	382	0.1613	0.3724	316.72	154.84
382	382	383	0.3783	0.3777	333.82	163.20
383	383	384	0.3972	0.3966	249.30	121.88
384	384	385	0.2932	0.2927	100.00	100.00
385	385	386	0.7771	0.4087	157.07	66.58
386	386	387	1.0803	0.5683	100.00	1000.00

387	387	388	1.0663	0.5782	250.15	106.04
388	388	389	0.4738	0.2492	100.00	100.00
389	389	390	0.6195	0.6185	141.24	59.87
390	390	391	0.3404	0.3399	279.85	118.63
391	354	392	0.5686	0.2991	87.31	37.01
392	392	393	0.1087	0.1086	243.85	103.37
393	393	394	0.5686	0.2991	247.75	105.03
394	394	395	0.0112	0.0259	100.00	100.00
395	395	396	0.4183	0.9657	89.88	38.10
396	396	397	0.1049	0.1364	137.28	482.11
397	397	398	0.4389	1.0133	458.34	194.30
398	398	399	0.0455	0.0591	202.44	85.82
399	399	400	0.4738	0.2492	60.82	25.87
400	400	401	0.8624	0.4536	45.62	19.34
401	401	402	0.5686	0.2991	100.00	100.00
402	402	403	0.7771	0.4087	157.07	66.58
403	403	404	1.0803	0.5683	100.00	100.00
404	404	405	1.0663	0.5782	250.15	106.04
405	405	406	0.4738	0.2492	100.00	100.00
406	406	407	0.3226	0.7448	68.81	28.59
407	407	408	0.1463	0.3377	32.07	13.60
408	408	409	0.1613	0.3724	316.72	154.84
409	409	410	0.3783	0.3777	333.82	163.20
410	410	411	0.3972	0.3966	249.30	121.88
411	411	412	0.2932	0.2927	100.00	100.00
412	412	413	0.7771	0.4087	157.07	66.58
413	413	414	1.0803	0.5683	100.00	100.00
414	414	415	1.0663	0.5782	250.15	106.04
415	415	416	0.4738	0.2492	100.00	100.00
416	416	417	0.6195	0.6185	141.24	59.87
417	417	418	0.3404	0.3399	279.85	118.63
418	418	419	0.1688	0.3897	51.32	21.76
419	419	420	0.1181	0.2728	59.87	25.38
420	420	421	2.2860	0.7841	9.07	3.84
421	402	422	0.4558	1.0523	2.09	0.89
422	407	423	0.696	1.6066	16.74	7.09
423	408	424	0.4577	1.0566	506.52	638.63
424	409	425	0.2029	0.2637	313.02	132.69
425	410	426	0.2134	0.2773	79.83	33.84
426	411	427	0.5496	0.2891	51.32	21.76
427	412	428	0.5401	0.2841	100.00	100.00

428	413	429	0.0455	0.0591	202.44	85.82
429	414	430	0.4738	0.2492	60.82	25.87
430	415	431	0.8624	0.4536	45.62	19.34
431	416	432	0.5686	0.2991	100.00	100.00
432	417	433	0.7771	0.4087	157.07	66.58
433	418	434	1.0803	0.5683	100.00	100.00
434	419	435	1.0663	0.5782	250.15	106.04
435	420	436	0.4738	0.2492	100.00	100.00
436	419	437	0.3226	0.7448	68.81	28.59
437	420	438	0.1463	0.3377	32.07	13.60
438	421	439	0.1238	0.2858	61.08	25.89
439	422	440	0.0112	0.0259	100.00	100.00
440	423	441	0.6491	1.4984	94.62	46.26
441	424	442	0.0450	0.1039	49.86	24.38
442	425	443	0.5264	0.1805	123.16	60.21
443	426	444	0.0206	0.0476	78.35	38.30
444	427	445	0.5307	0.2791	145.48	71.12
445	428	446	0.0975	0.2252	21.37	10.45
446	429	447	0.1181	0.2728	74.79	36.56
447	420	448	0.1388	0.3204	227.93	111.43
448	448	449	0.0431	0.0996	35.61	17.41
449	449	450	0.0919	0.2122	249.30	121.88
450	450	451	0.1613	0.3724	316.72	154.84
451	451	452	0.3783	0.3777	333.82	163.20
452	452	453	0.3972	0.3966	249.30	121.88
453	453	454	0.2932	0.2927	100.00	100.00
454	454	455	0.0694	0.1602	117.88	49.97
455	455	456	0.8150	0.4287	62.67	25.57
456	456	457	0.0637	0.1472	172.29	73.03
457	457	458	0.1313	0.3031	458.56	194.39
458	458	459	0.0619	0.1429	262.96	111.47
459	459	460	0.1144	0.2641	235.76	99.94
460	460	461	0.2837	0.2833	100.00	100.00
461	1	462	0.2837	0.2832	109.22	46.30
462	462	463	0.0450	0.1039	100.00	100.00
463	463	464	0.0262	0.0606	72.81	30.87
464	464	465	0.0600	0.1385	258.47	109.57
465	465	466	0.0300	0.0692	69.17	29.32
466	466	467	0.0206	0.0476	21.84	9.26
467	467	468	0.1088	0.2511	100.00	100.00
468	468	469	0.2558	0.1346	20.53	8.70

469	469	470	0.4169	0.2193	150.55	63.82
470	470	471	0.5022	0.2642	220.69	93.55
471	471	472	0.3317	0.1744	92.38	39.16
472	472	473	0.2084	0.1096	100.00	100.00
473	473	474	0.1388	0.3204	226.69	96.10
474	474	475	0.0750	0.0173	100.00	100.00
475	475	476	0.2701	0.6236	294.02	116.97
476	476	477	0.3827	0.8834	83.02	33.03
477	477	478	0.3301	0.7622	83.02	33.03
478	478	479	0.3283	0.7578	103.77	41.29
479	479	480	0.1707	0.3940	176.41	70.18
480	480	481	0.5591	0.2941	83.02	33.03
481	481	482	0.0581	0.1342	217.92	86.70
482	482	483	0.7013	0.3689	23.29	9.27
483	483	484	1.0235	0.5383	5.08	2.02
484	484	485	0.0675	0.1559	72.64	28.90
485	485	486	1.3235	0.4539	405.99	161.52
486	486	487	0.0112	0.0259	100.00	100.00
487	487	488	0.7297	1.6846	100.18	42.47
488	488	489	0.2251	0.5196	142.52	60.42
489	489	490	0.2082	0.4807	96.04	40.71
490	490	491	0.0469	0.1082	300.45	127.37
491	491	492	0.6195	0.6185	141.24	59.87
492	492	493	0.3404	0.3399	279.85	118.63
493	493	494	0.5686	0.2991	87.31	37.01
494	494	495	0.1087	0.1086	243.85	103.37
495	495	496	0.5686	0.2991	247.75	105.03
496	496	497	0.0112	0.0259	100.00	100.00
497	497	498	0.4183	0.9657	89.88	38.10
498	498	499	0.1049	0.1364	137.28	482.11
499	499	500	0.4389	1.0133	458.34	194.30
500	500	501	0.0752	0.0257	385.20	163.29
501	501	502	0.0769	0.1775	100.00	100.00
502	502	503	0.3320	0.7665	79.61	33.75
503	503	504	0.0844	0.1948	87.31	37.01
504	504	505	0.1332	0.3074	100.00	100.00
505	505	506	0.2932	0.2927	74.00	31.37
506	466	507	0.2175	0.2172	232.05	98.37
507	467	508	0.2648	0.2644	141.82	60.12
508	468	509	0.1031	0.2381	100.00	100.00
509	469	510	0.1350	0.3118	76.45	32.41

510	470	511	0.0938	0.0216	100.00	100.00
511	471	512	0.1688	0.3897	51.32	21.76
512	472	513	0.1181	0.2728	59.87	25.38
513	473	514	2.2860	0.7841	9.07	3.84
514	474	515	0.4558	1.0523	2.09	0.89
515	475	516	0.6960	1.6066	16.74	7.09
516	476	517	0.4577	1.0566	506.52	638.63
517	477	518	0.2029	0.2637	313.02	132.69
518	478	519	0.2134	0.2773	79.83	33.84
519	479	520	0.5496	0.2891	51.32	21.76
520	480	521	0.5401	0.2841	100.00	100.00
521	481	522	0.0455	0.0591	202.44	85.82
522	482	523	0.4738	0.2492	60.82	25.87
523	483	524	0.8624	0.4536	45.62	19.34
524	484	525	0.5686	0.2991	100.00	100.00
525	485	526	0.7771	0.4087	157.07	66.58
526	486	527	1.0803	0.5683	100.00	100.00
527	487	528	1.0663	0.5782	250.15	106.04
528	488	529	0.4738	0.2492	100.00	100.00
529	489	530	0.3226	0.7448	68.81	28.59
530	490	531	0.1463	0.3377	32.07	13.60
531	491	532	0.1238	0.2858	61.08	25.89
532	492	533	0.0112	0.0259	100.00	100.00
533	493	534	0.6491	1.4984	94.62	46.26
534	494	535	0.0450	0.1039	49.86	24.38
535	495	536	0.5264	0.1805	123.16	60.21
536	496	537	0.0206	0.0476	78.35	38.30
537	497	538	0.5307	0.27917	145.48	71.12
538	498	539	0.0975	0.2252	21.37	10.45
539	499	540	0.1182	0.2728	74.79	36.56
540	500	541	0.1388	0.3204	227.93	111.43
541	501	542	0.0431	0.0996	35.61	17.41
542	502	543	0.0919	0.2122	249.30	121.88
543	503	544	0.1613	0.3724	316.72	154.84
544	504	545	0.3783	0.3777	333.82	163.20
545	505	546	0.3972	0.3966	249.30	121.88
546	466	547	0.2932	0.2927	100.00	100.00
547	547	548	0.7771	0.4087	157.07	66.58
548	548	549	1.0803	0.5683	100.00	100.00
549	549	550	1.0663	0.5782	250.15	106.04
550	550	551	0.4738	0.2492	100.00	100.00

551	551	552	0.6195	0.6185	141.24	59.87
552	552	553	0.3404	0.3399	279.85	118.63
553	553	554	0.5686	0.2991	87.31	37.01
554	554	555	0.1087	0.1086	243.85	103.37
555	555	556	0.5686	0.2991	247.75	105.03
556	556	557	0.0112	0.0259	100.00	100.00
557	557	558	0.4183	0.9657	89.88	38.10
558	558	559	0.1049	0.1364	137.28	482.11
559	559	560	0.4389	1.0133	458.34	194.30
560	560	561	0.0752	0.0257	385.20	163.29
561	561	562	0.0769	0.1775	100.00	100.00
562	562	563	0.3320	0.7665	79.61	33.75
563	563	564	0.0844	0.1948	87.31	37.01
564	564	565	0.1332	0.3074	100.00	100.00
565	548	566	0.2932	0.2927	74.00	31.37
566	547	567	0.2175	0.2172	232.05	98.37
567	548	568	0.2648	0.2644	141.82	60.12
568	549	569	0.1031	0.2381	100.00	100.00
569	550	570	0.1350	0.3118	76.45	32.41
570	551	571	0.0938	0.0216	100.00	100.00
571	552	572	0.1688	0.3897	51.32	21.76
572	553	573	0.1181	0.2728	59.87	25.38
573	554	574	2.2860	0.7841	9.07	3.84
574	555	575	0.4558	1.0523	2.09	0.89
575	556	576	0.6960	1.6066	16.74	7.09
576	557	577	0.4577	1.0566	506.52	638.63
577	558	578	0.2029	0.2637	313.02	132.69
578	559	579	0.2134	0.2773	79.83	33.84
579	560	580	0.5496	0.2891	51.32	21.76
580	561	581	0.5401	0.2841	100.00	100.00
581	562	582	0.0455	0.0591	202.44	85.82
582	563	583	0.4738	0.2492	60.82	25.87
583	564	584	0.8624	0.4536	45.62	19.34
584	470	585	0.5686	0.2991	100.00	100.00
585	585	586	0.7771	0.4087	157.07	66.58
586	586	587	1.0803	0.5683	100.00	100.00
587	587	588	1.0663	0.5782	250.15	106.04
588	588	589	0.4738	0.2492	100.00	100.00
589	589	590	0.3226	0.7448	68.81	28.59
590	590	591	0.1463	0.3377	32.07	13.60
591	591	592	0.1613	0.3724	316.72	154.84

592	592	593	0.3783	0.3777	333.82	163.20
593	593	594	0.3972	0.3966	249.30	121.88
594	594	595	0.2932	0.2927	100.00	100.00
595	595	596	0.7771	0.4087	157.07	66.58
596	596	597	1.0803	0.5683	100.00	100.00
597	597	598	1.0663	0.5782	250.15	106.04
598	1	599	0.4738	0.2492	100.00	100.00
599	599	600	0.6195	0.6185	141.24	59.87
600	600	601	0.3404	0.3399	279.85	118.63
601	601	602	0.5686	0.2991	87.31	37.01
602	602	603	0.1087	0.1086	243.85	103.37
603	603	604	0.5686	0.2991	247.75	105.03
604	604	605	0.0112	0.0259	100.00	100.00
605	605	606	0.4183	0.9657	89.88	38.10
606	606	607	0.1049	0.1364	137.28	482.11
607	607	608	0.4389	1.0133	458.34	194.30
608	608	609	0.0455	0.0591	202.44	85.82
609	609	610	0.4738	0.2492	60.82	25.87
610	610	611	0.8624	0.4536	45.62	19.34
611	611	612	0.5686	0.2991	100.00	100.00
612	612	613	0.7771	0.4087	157.07	66.58
613	613	614	1.0803	0.5683	100.00	100.00
614	614	615	1.0663	0.5782	250.15	106.04
615	615	616	0.4738	0.2492	100.00	100.00
616	616	617	0.3226	0.7448	68.81	28.59
617	617	618	0.1463	0.3377	32.07	13.60
618	618	619	0.1613	0.3724	316.72	154.84
619	619	620	0.3783	0.3777	333.82	163.20
620	620	621	0.3972	0.3966	249.30	121.88
621	621	622	0.2932	0.2927	100.00	100.00
622	622	623	0.7771	0.4087	157.07	66.58
623	623	624	1.0803	0.5683	100.00	100.00
624	624	625	1.0663	0.5782	250.15	106.04
625	625	626	0.4738	0.2492	100.00	100.00
626	626	627	0.6195	0.6185	141.24	59.87
627	627	628	0.3404	0.3399	279.85	118.63
628	628	629	0.1688	0.3897	51.32	21.76
629	629	630	0.1181	0.2728	59.87	25.38
630	630	631	2.2860	0.7841	9.07	3.84
631	631	632	0.4558	1.0523	2.09	0.89
632	632	633	0.6960	1.6066	16.74	7.09

633	633	634	0.4577	1.0566	506.52	638.63
634	634	635	0.2029	0.2637	313.02	132.69
635	635	636	0.2134	0.2773	79.83	33.84
636	636	637	0.5496	0.2891	51.32	21.76
637	637	638	0.5401	0.2841	100.00	100.00
638	638	639	0.0455	0.0591	202.44	85.82
639	639	640	0.4738	0.2492	60.82	25.87
640	640	641	0.8624	0.4536	45.62	19.34
641	641	642	0.5686	0.2991	100.00	100.00
642	642	643	0.7771	0.4087	157.07	66.58
643	643	644	1.0803	0.5683	100.00	100.00
644	630	645	1.0663	0.5782	250.15	106.04
645	631	646	0.4738	0.2492	100.00	100.00
646	632	647	0.3226	0.7448	68.81	28.59
647	647	648	0.1463	0.3377	32.07	13.60
648	648	649	0.1238	0.2858	61.08	25.89
649	648	650	0.0112	0.0259	100.00	100.00
650	600	651	0.6491	1.4984	94.62	46.26
651	601	652	0.0450	0.1039	49.86	24.38
652	602	653	0.5264	0.1805	123.16	60.21
653	603	654	0.0206	0.0476	78.35	38.30
654	604	655	0.5307	0.2791	145.48	71.12
655	605	656	0.0975	0.2252	21.37	10.45
656	606	657	0.1181	0.2728	74.79	36.56
657	607	658	0.1388	0.3204	227.93	111.43
658	608	659	0.0431	0.0996	35.61	17.41
659	609	660	0.0919	0.2122	249.30	121.88
660	610	661	0.1613	0.3724	316.72	154.84
661	611	662	0.3783	0.3777	333.82	163.20
662	612	663	0.3972	0.3966	249.30	121.88
663	613	664	0.2932	0.2927	100.00	100.00
664	614	665	0.3404	0.3399	279.85	118.63
665	615	666	0.5686	0.2991	87.31	37.01
666	616	667	0.1087	0.1086	243.85	103.37
667	617	668	0.5686	0.2991	247.75	105.03
668	618	669	0.0112	0.0259	100.00	100.00
669	619	670	0.4183	0.9657	89.88	38.10
670	620	671	0.1049	0.1364	137.28	482.11
671	621	672	0.4389	1.0133	458.34	194.30
672	622	673	0.0752	0.0257	385.20	163.29
673	623	674	0.0769	0.1775	100.00	100.00

674	624	675	0.3320	0.7665	79.61	33.75
675	625	676	0.0844	0.1948	87.31	37.01
676	626	677	0.1332	0.3074	100.00	100.00
677	627	678	0.2932	0.2927	74.00	31.37
678	628	679	0.2175	0.2172	232.05	98.37
679	629	680	0.2648	0.2644	141.82	60.12
680	630	681	0.1031	0.2381	100.00	100.00
681	631	682	0.1350	0.3118	76.45	32.41
682	632	683	0.0938	0.0216	100.00	100.00
683	633	684	0.1688	0.3897	51.32	21.76
684	634	685	0.1181	0.2728	59.87	25.38
685	635	686	2.2860	0.7841	9.07	3.84
686	636	687	0.4558	1.0523	2.09	0.89
687	637	688	0.6960	1.6066	16.74	7.09
688	638	689	0.4577	1.0566	506.52	638.63
689	639	690	0.2029	0.2637	313.02	132.69
690	640	691	0.2134	0.2773	79.83	33.84
691	641	692	0.5496	0.2891	51.32	21.76
692	642	693	0.5401	0.2841	100.00	100.00
693	643	694	0.0455	0.0591	202.44	85.82
694	644	695	0.4738	0.2492	60.82	25.87
695	645	696	0.8624	0.4536	45.62	19.34
696	646	697	0.5686	0.2991	100.00	100.00
697	647	698	0.7771	0.4087	157.07	66.58
698	648	699	1.0803	0.5683	100.00	100.00
699	649	700	1.0663	0.5782	250.15	106.04
700	650	701	0.4738	0.2492	100.00	100.00
701	653	702	0.3226	0.7448	68.81	28.59
702	654	703	0.1463	0.3377	32.07	13.60
703	655	704	0.1238	0.2858	61.08	25.89
704	656	705	0.0112	0.0259	100.00	100.00
705	657	706	0.6491	1.4984	94.62	46.26
706	658	707	0.0450	0.1039	49.86	24.38
707	659	708	0.5264	0.1805	123.16	60.21
708	660	709	0.0206	0.0476	78.35	38.30
709	661	710	0.5307	0.2791	145.48	71.12
710	662	711	0.0975	0.2252	21.37	10.45
711	663	712	0.1181	0.2728	74.79	36.56
712	664	713	0.1388	0.3204	227.93	111.43
713	665	714	0.0431	0.0996	35.61	17.41
714	666	715	0.0919	0.2122	249.30	121.88

715	667	716	0.1613	0.3724	316.72	154.84
716	668	717	0.3783	0.3777	333.82	163.20
717	669	718	0.3972	0.3966	249.30	121.88
718	670	719	0.2932	0.2927	100.00	100.00
719	671	720	0.7771	0.4087	157.07	66.58
720	672	721	1.0803	0.5683	100.00	100.00
721	673	722	1.0663	0.5782	250.15	106.04
722	674	723	0.4738	0.2492	100.00	100.00
723	675	724	0.6195	0.6185	141.24	59.87
724	676	725	0.3404	0.3399	279.85	118.63
725	677	726	0.5686	0.2991	87.31	37.01
726	678	727	0.1087	0.1086	243.85	103.37
727	679	728	0.5686	0.2991	247.75	105.03
728	680	729	0.0112	0.0259	100.00	100.00
729	681	730	0.4183	0.9657	89.88	38.10
730	682	731	0.1049	0.1364	137.28	482.11
731	683	732	0.4389	1.0133	458.34	194.30
732	684	733	0.0752	0.0257	385.20	163.29
733	685	734	0.0769	0.1775	100.00	100.00
734	686	735	0.3320	0.7665	79.61	33.75
735	687	736	0.0844	0.1948	87.31	37.01
736	688	737	0.1332	0.3074	100.00	100.00
737	689	738	0.2932	0.2927	74.00	31.37
738	690	739	0.2175	0.2172	232.05	98.37
739	691	740	0.2648	0.2644	141.82	60.12
740	692	741	0.1031	0.2381	100.00	100.00
741	693	742	0.1350	0.3118	76.45	32.41
742	694	743	0.0938	0.0216	100.00	100.00
743	695	744	0.1688	0.3897	51.32	21.76
744	696	745	0.1181	0.2728	59.87	25.38
745	697	746	2.2860	0.7841	9.07	3.84
746	698	747	0.4558	1.0523	2.09	0.89
747	699	748	0.6960	1.6066	16.74	7.09
748	700	749	0.4577	1.0566	506.52	638.63
749	701	750	0.2029	0.2637	313.02	132.69
750	731	751	0.2134	0.2773	79.83	33.84
751	732	752	0.5496	0.2891	51.32	21.76
752	733	753	0.5401	0.2841	51.32	21.76
753	734	754	0.0455	0.0591	202.44	85.82
754	735	755	0.4738	0.2492	60.82	25.87
755	736	756	0.8624	0.4536	45.62	19.34

756	737	757	0.5686	0.2991	100.00	100.00
757	738	758	0.7771	0.4087	157.07	66.58
758	739	759	1.0803	0.5683	100.00	100.00
759	740	760	1.0663	0.5782	250.15	106.04
760	741	761	0.4738	0.2492	100.00	100.00
761	742	762	0.3226	0.7448	68.81	28.59
762	743	763	0.1463	0.3377	32.07	13.60
763	744	764	0.1613	0.3724	316.72	154.84
764	745	765	0.3783	0.3777	333.82	163.20
765	746	766	0.3972	0.3966	249.30	121.88
766	747	767	0.2932	0.2927	100.00	100.00
767	748	768	0.7771	0.4087	157.07	66.58
768	749	769	1.0803	0.5683	100.00	100.00
769	750	770	1.0663	0.5782	250.15	106.04
770	683	771	0.4738	0.2492	100.00	100.00
771	684	772	0.6195	0.6185	141.24	59.87
772	685	773	0.3404	0.3399	279.85	118.63
773	686	774	0.5686	0.2991	87.31	37.01
774	687	775	0.1087	0.1086	243.85	103.37
775	688	776	0.5686	0.2991	247.75	105.03
776	689	777	0.0112	0.0259	100.00	100.00
777	690	778	0.4183	0.9657	89.88	38.10
778	691	779	0.1049	0.1364	137.28	482.11
779	692	780	0.4389	1.0133	458.34	194.30
780	693	781	0.0455	0.0591	202.44	85.82
781	694	782	0.4738	0.2492	60.82	25.87
782	695	783	0.8624	0.4536	45.62	19.34
783	696	784	0.5686	0.2991	100.00	100.00
784	697	785	0.7771	0.4087	157.07	66.58
785	698	786	1.0803	0.5683	100.00	100.00
786	699	787	1.0663	0.5782	250.15	106.04
787	700	788	0.4738	0.2492	100.00	100.00
788	701	789	0.3226	0.7448	68.81	28.59
789	731	790	0.1463	0.3377	32.07	13.60
790	691	791	0.1613	0.3724	316.72	154.84
791	692	792	0.3783	0.3777	333.82	163.20
792	693	793	0.3972	0.3966	249.30	121.88
793	694	794	0.2932	0.2927	100.00	100.00
794	695	795	0.7771	0.4087	157.07	66.58
795	696	796	1.0803	0.5683	100.00	100.00
796	697	797	1.0663	0.5782	250.15	106.04

797	698	798	0.4738	0.2492	100.00	100.00
798	699	799	0.6195	0.6185	141.24	59.87
799	700	800	0.3404	0.3399	279.85	118.63
800	701	801	0.1688	0.3897	51.32	21.76
801	731	802	0.1181	0.2728	59.87	25.38
802	694	803	2.2860	0.7841	9.07	3.84
803	695	804	0.4558	1.0523	2.09	0.89
804	696	805	0.6960	1.6066	16.74	7.09
805	697	806	0.4577	1.0566	506.52	638.63
806	698	807	0.2029	0.2637	313.02	132.69
807	699	808	0.2134	0.2773	79.83	33.84
808	700	809	0.5496	0.2891	51.32	21.76
809	701	810	0.5401	0.2841	100.00	100.00
810	731	811	0.0455	0.0591	202.44	85.82
811	698	812	0.4738	0.2492	60.82	25.87
812	699	813	0.8624	0.4536	45.62	19.34
813	700	814	0.5686	0.2991	100.00	100.00
814	701	815	0.7771	0.4087	157.07	66.58
815	731	816	1.0803	0.5683	100.00	100.00
816	700	817	1.0663	0.5782	250.15	106.04
817	701	818	0.4738	0.2492	100.00	100.00
818	731	819	0.3226	0.7448	68.81	28.59
819	1	820	0.1463	0.3377	32.07	13.60
820	820	821	0.1238	0.2858	61.08	25.89
821	821	822	0.0112	0.0259	100.00	100.00
822	822	823	0.6491	1.4984	94.62	46.26
823	823	824	0.0450	0.1039	49.86	24.38
824	824	825	0.5264	0.1805	123.16	60.21
825	825	826	0.0206	0.0476	78.35	38.30
826	826	827	0.5307	0.2791	145.48	71.12
827	827	828	0.0975	0.2252	21.37	10.45
828	828	829	0.1181	0.2728	74.79	36.56
829	829	830	0.1388	0.3204	227.93	111.43
830	830	831	0.0431	0.0996	35.61	17.41
831	831	832	0.0919	0.2122	249.30	121.88
832	832	833	0.1613	0.3724	316.72	154.84
833	833	834	0.3783	0.3777	333.82	163.20
834	834	835	0.3972	0.3966	249.30	121.88
835	835	836	0.2932	0.2927	100.00	100.00
836	836	837	1.0663	0.5782	250.15	106.04
837	837	838	0.4738	0.2492	100.00	100.00

838	838	839	0.3226	0.7448	68.81	28.59
839	839	840	0.1463	0.3377	32.07	13.60
840	840	841	0.1613	0.3724	316.72	154.84
841	841	842	0.3783	0.3777	333.82	163.20
842	842	843	0.3972	0.3966	249.30	121.88
843	843	844	0.2932	0.2927	100.00	100.00
844	844	845	0.7771	0.4087	157.07	66.58
845	845	846	1.0803	0.5683	100.00	100.00
846	846	847	1.0663	0.5782	250.15	106.04
847	847	848	0.4738	0.2492	100.00	100.00
848	831	849	0.6195	0.6185	141.24	59.87
849	832	850	0.3404	0.3399	279.85	118.63
850	833	851	0.1688	0.3897	51.32	21.76
851	834	852	0.1181	0.2728	59.87	25.38
852	835	853	2.2860	0.7841	9.07	3.84
853	836	854	0.4558	1.0523	2.09	0.89
854	837	855	0.6960	1.6066	16.74	7.09
855	838	856	0.4577	1.0566	506.52	638.63
856	839	857	0.2029	0.2637	313.02	132.69
857	840	858	0.2134	0.2773	79.83	33.84
858	841	859	0.5496	0.2891	51.32	21.76
859	842	860	0.5401	0.2841	51.32	21.76
860	843	861	0.0455	0.0591	202.44	85.82
861	844	862	0.4738	0.2492	60.82	25.87
862	845	863	0.8624	0.4536	45.62	19.34
863	846	864	0.5686	0.2991	100.00	100.00
864	847	865	0.7771	0.4087	157.07	66.58
865	842	866	1.0803	0.5683	157.07	66.58
866	843	867	1.0663	0.5782	250.15	106.04
867	844	868	0.4738	0.2492	100.00	100.00
868	845	869	0.3226	0.7448	68.81	28.59
869	846	870	0.1463	0.3377	32.07	13.60
870	847	871	0.1238	0.2858	61.08	25.89
871	845	872	0.0112	0.0259	100.00	100.00
872	846	873	0.6491	0.4984	94.62	46.26
873	847	874	0.0450	0.1039	49.86	24.38

Tie-line Data of 874-bus Distribution System

Line number	From Bus	To Bus	Resistance (Ω)	Reactance (Ω)
874	49	195	0.2932	0.2927
875	90	140	0.0803	0.5683
876	85	597	0.0663	0.5782
877	84	816	0.4738	0.2492
878	93	873	0.6195	0.6185
879	145	460	0.1688	0.3897
880	190	335	0.1181	0.2728
881	175	332	1.2860	0.7841
882	190	345	0.4577	0.0566
883	320	395	0.2134	0.2773
884	325	445	0.5496	0.2891
885	340	495	0.5686	0.2991
886	450	595	0.0803	0.5683
887	453	795	0.0663	0.5782
888	458	819	0.3226	0.7448
889	455	435	0.1463	0.3377
890	575	795	0.1238	0.2858
891	580	819	0.1181	0.2728
892	495	865	1.2860	0.7841
893	597	872	0.6960	1.6066
894	813	874	0.5401	0.2841
895	815	870	0.0455	0.0591
896	845	245	0.4738	0.2492
897	695	344	0.8624	0.4536
898	873	717	0.0803	0.5683
899	344	825	1.0663	0.5782
900	5	465	0.4738	0.2492

APPENDIX - 7 [77]

Step-by-Step or Building up Algorithm

In this section, the detailed concept of building up algorithm [77] to form the Z_{bus} of distribution system is presented. This method was developed based on the concept of addition of branch or link to the partial network.

Addition of uncoupled branch to partial network:

Assume, a α^{th} element with nodes p and q is added to the partial network as shown below. Further, assume that, ‘p’ is old bus and ‘q’ is new bus.

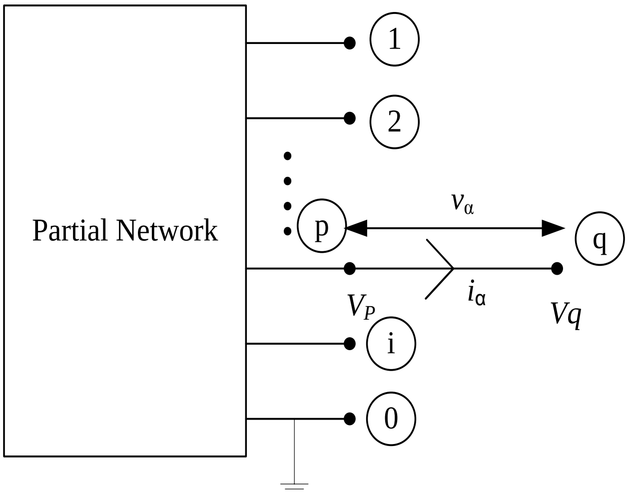

In the above figure, $i_\alpha = 0$ as there is no flow of current in the added branch (no loop formation). Further, the primitive currents flowing through the various elements of the partial network is given as below in the matrix form.

$$\begin{bmatrix} I_{old} \\ i_\alpha \end{bmatrix} = \begin{bmatrix} Y_{old} & y_{o\alpha} \\ y_{o\alpha} & y_{\alpha\alpha} \end{bmatrix} \begin{bmatrix} V_{old} \\ v_\alpha \end{bmatrix} \tag{A7.1}$$

Where, V_{old} = voltage drop across the old elements due to mutual coupling effect

v_α = voltage drop across the α^{th} element

I_{old} = currents through old elements

i_α = current through the α^{th} element

$Yold$ = primitive admittance of old elements

$y_{o\alpha}$ = mutual primitive admittance of αth element with existing elements

$y_{\alpha\alpha}$ = self primitive admittance of αth element

The expression of last row of Eq. (A7.1) can be written as below:

$$i_\alpha = y_{o\alpha}V_{old} + y_{\alpha\alpha}v_\alpha \quad \text{(A7.2)}$$

On substituting $i_\alpha = 0$, the Eq. (A7.2) yields to Eq. (A7.3).

$$v_\alpha = \frac{-(y_{o\alpha}\ V_{old})}{y_{\alpha\alpha}} \quad \text{(A7.3)}$$

But $v_\alpha = V_p - V_q$, Eq. (A7.3) is modified as below:

$$V_q = V_p + \frac{(y_{o\alpha}\ V_{old})}{y_{\alpha\alpha}} \quad \text{(A7.4)}$$

Further, the drops due to mutual coupling effect (V_{old}) is zero. This could happened due to non-presence of coupled elements in the distribution system. Therefore, the modified Eq. (A7.5) is available.

$$V_q = V_p \quad \text{(A7.5)}$$

To find the elements of Z_{qi} and $Z_{qq,}$ the concept of two port network can be applied. Therefore by definition,

$$Z_{qi} = \left.\frac{V_q}{I_i}\right|_{\text{with other ports open},\ I_i \neq 0,\ I_j = 0,\ j \neq i,\ \text{voltage sources replaced by internal impedances}} \quad \text{(A7.6)}$$

$$Z_{qq} = \left.\frac{V_q}{I_q}\right|_{\text{with other ports open},\ Iq \neq 0,\ I_j = 0,\ j \neq q,\ \text{voltage sources replaced by internal impedances}} \quad \text{(A7.7)}$$

Eq. (A7.6) and (A7.7) can easily be simulated by using the following figures.

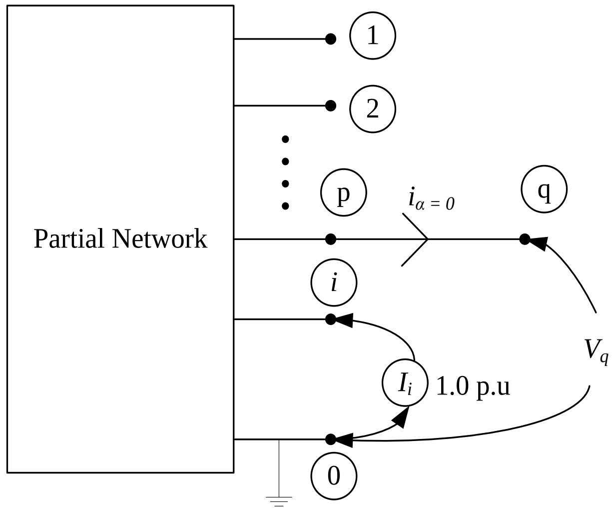

The Z_{qi} element is easily obtained from Eqs. (A7.5) and (A7.6) and is as below.

$$Z_{qi} = \frac{V_p}{I_i} = Z_{pi} \tag{A7.8}$$

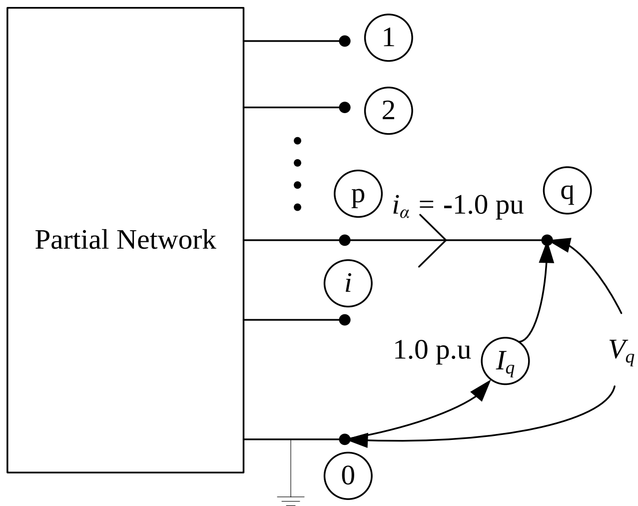

In the above figure, the current flowing through α^{th} element is –1.0 pu, the Eqs. (A7.2) - (A7.5) yields to Eq. (A7.9).

$$V_q = V_p + \frac{1}{y_{\alpha\alpha}} \tag{A7.9}$$

Further, the above equation is modified to Eq. (A7.10) and is as below.

$$V_q = V_p + z_{\alpha\alpha} \tag{A7.10}$$

The Z_{qq} element is easily obtained from Eqs. (A7.7) and (A7.10).

$$Z_{qq} = Z_{pq} + z_{\alpha\alpha} \tag{A7.11}$$

Further, if the uncoupled branch is added to the reference node, the Z_{qq} yields to Eq. (A7.12).

$$Z_{qq} = z_{\alpha\alpha} \tag{A7.12}$$

Addition of uncoupled link to partial network:

When an uncoupled link is added to the existing buses of the partial network there could be flow of some current through the added link. If we simulate $i_\alpha = 0$, the concept of addition of uncoupled branch can be utilised. This can be simulated by the addition of voltage source (E_l) in series with the uncoupled link which is connected between p – q buses of the partial network. In this process, a fictitious node l is formed and is shown in the following figure. Therefore, the elements corresponding to this fictitious node l such as Z_{li} and Z_{ll} are needs to be calculated.

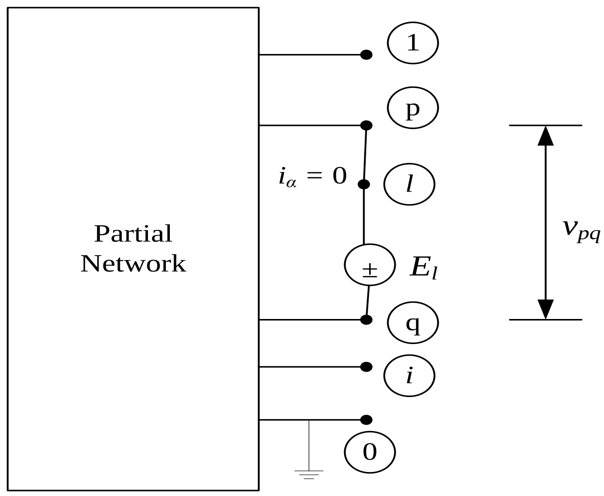

By definition,

$$Z_{li} = \left.\frac{E_l}{I_i}\right|_{\text{with other ports open}, \, I_i \neq 0, \, I_j = 0, \, j \neq i, \text{ voltage sources replaced by internal impedances}} \tag{A7.13}$$

This can be simulated easily and is shown in the figure below.

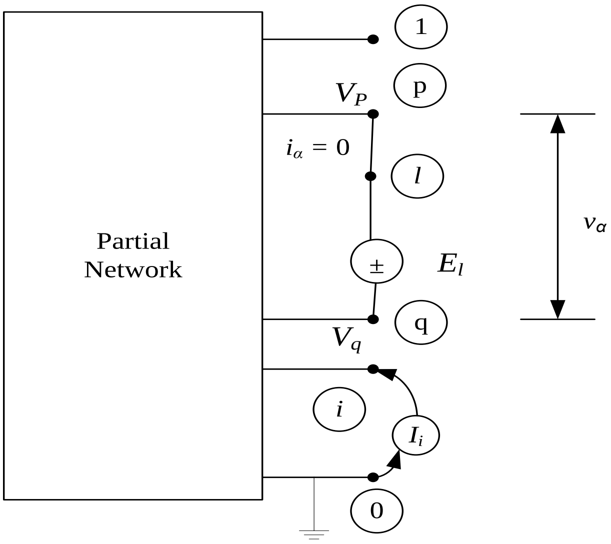

In the above figure, the voltage drop across the added link is as below.

$$v_\alpha = V_p - V_q - E_l \tag{A7.14}$$

On substituting Eq. (A7.14) in Eq. (A7.3), the expression for E_l is given by Eq. (A7.15)

$$E_l = V_p - V_q + \frac{(y_{o\alpha}\ V_{old})}{y_{\alpha\alpha}} \tag{A7.15}$$

Further, the voltage drop due to mutual effect is omitted in Eq. (A7.15). This is possible in distribution system. Hence, the reduced equation for E_l is as below.

$$E_l = V_p - V_q \tag{A7.16}$$

Substitute Eq. (A7.16) in Eq. (A7.13), the final expression for Z_{li} is given as Eq. (A7.17).

$$Z_{li} = Z_{pi} - Z_{qi} \tag{A7.17}$$

Further, if the α^{th} element (uncoupled link) is added to reference node the Eq. (A7.17) is reduced to Eq. (A7.18).

$$Z_{li} = - Z_{qi} \tag{A7.18}$$

Similarly, $Z_{ll} = \left.\dfrac{E_l}{I_l}\right|_{\text{with other ports open, } I_l \neq 0,\, I_j = 0,\, j \neq l, \text{ voltage sources replaced by internal inpedances}}$ (A7.19)

Eq. (A7.19) can easily be simulated and is shown in the figure below.

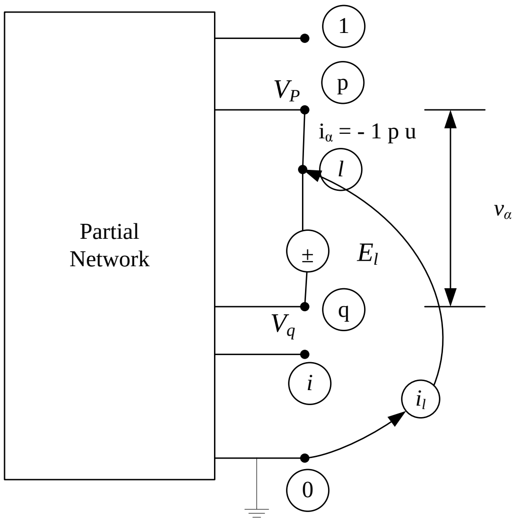

In the above figure, the current through α^th element is –1.0 pu, the Eqs. (A7.2) - (A7.3) and Eq. (A7.15) – (A7.16) yields to Eq. (A7.20).

$$E_l = V_p - V_q + \frac{1}{y_{\alpha\alpha}} \quad \text{(A7.20)}$$

Further, the above equation is modified to Eq. (A7.21) and is as below.

$$E_l = V_p - V_q + z_{\alpha\alpha} \quad \text{(A7.21)}$$

The Z_{ll} element is easily obtained from Eqs. (A7.19) and (A7.21) and is as below.

$$Z_{ll} = Z_{pl} - Z_{ql} + z_{\alpha\alpha} \quad \text{(A7.22)}$$

Further, if the uncoupled link is added to the reference node, the Z_{ll} yields to Eq. (A7.23).

$$Z_{ll} = - Z_{ql} + z_{\alpha\alpha} \quad \text{(A7.23)}$$

Look at the [Z] matrix structure,

$$\begin{bmatrix} V_{old} \\ E_l \end{bmatrix} = \begin{bmatrix} Z_{old} & Z_{il} \\ Z_{li} & Z_{ll} \end{bmatrix} \begin{bmatrix} I_{old} \\ i_l \end{bmatrix} \quad \text{(A7.24)}$$

To eliminate the fictitious node *'l'* short the E_l source, the equation corresponding to the last row of Eq. (A7.24) is as below.

$$0 = Z_{li} \; I_{old} + Z_{ll} \; i_l \tag{A7.25}$$

Now look at the first row of Eq. (A7.24) and is written in Eq. (A7.26)

$$E_{old} = Z_{old} \; I_{old} + Z_{il} \; i_l \tag{A7.26}$$

Substitute i_l from Eq. (A7.25) in Eq. (A7.26) and the modified equation for E_{old} is as below.

$$E_{old} = \left[Z_{old} - \frac{Z_{il} \; Z_{lj}}{Z_{ll}} \right] I_{old} \tag{A7.27}$$

Further, it is noticed that the new elements of $[Z]$ matrix can easily be calculated from Eq. (A7.27) and is given below.

$$Z_{ij\;new} = \left[Z_{ij\;old} - \frac{Z_{il} \; Z_{lj}}{Z_{ll}} \right] \tag{A7.28}$$

APPENDIX - 8 [40]

Derivation of Voltage Stability Index (VSI)

Voltage Stability can be defined as power system ability to maintain the voltages of all network buses within an acceptable range, after occurrence of a disturbance. In fact the main cause of instability is the weakness of the system to provide sufficient reactive power for the loads.

To derive the voltage stability index in radial distribution systems, the following power distribution network has been considered.

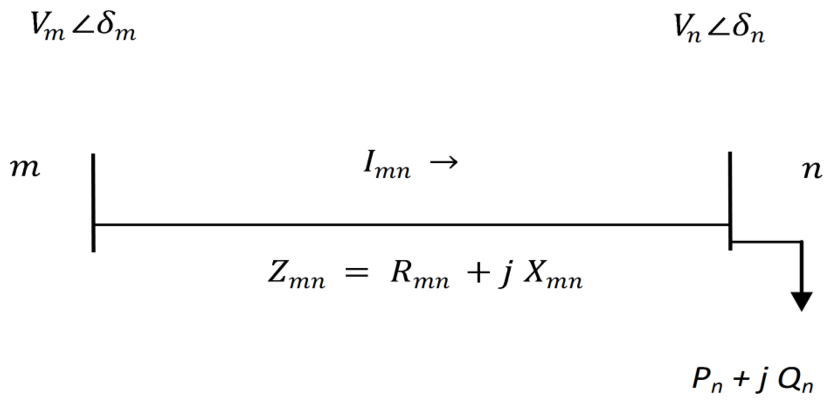

Typical representation of Power Distribution Network

Let, V_m and V_n are the voltage magnitudes at nodes *m* and *n*, respectively;

δ_m and δ_n indicate the phase angles of voltages at nodes *m* and *n*, respectively;

Z_{mn} represent primitive impedance a line connected between the nodes *m* and *n*;

R_{mn} and X_{mn} are the primitive resistance and reactance of the line connected between the nodes *m* and *n*, respectively.

I_{mn} is the current flowing in that line.

P_n and Q_n are the effective loads available at node *n*;

From the above Figure, the following equations can be written:

$$I_{mn} = \frac{[V_m \angle \delta_m - V_n \angle \delta_n]}{[R_{mn} + jX_{mn}]} \tag{A8.1}$$

$$P_n - jQ_n \quad = \quad (V_n \angle \delta_n)^* (I_{mn}) \qquad \text{(A8.2)}$$

Substitute Eq. (A8.1) in Eq. (A8.2). Then, Eq. (A8.3) is given below;

$$P_n - jQ_n \quad = \quad (V_n \angle \delta_n)^* \left(\frac{[V_m \angle \delta_m - V_n \angle \delta_n]}{[R_{mn} + jX_{mn}]} \right) \qquad \text{(A8.3)}$$

Now, manipulate the Eq. (A8.3) and get the Eq. (A8.4).

$$P_n - jQ_n \quad = \quad (V_n \angle -\delta_n) \left(\frac{[V_m \angle \delta_m - V_n \angle \delta_n]}{[R_{mn} + jX_{mn}]} \right) \qquad \text{(A8.4)}$$

Then, $P_n - jQ_n \quad = \quad \frac{[V_m V_n \angle (\delta_m - \delta_n) - V_n^2]}{[R_{mn} + jX_{mn}]}$ (A8.5)

Expand Eq. (A8.5). Then, obtain the Eq. (A8.6):

$$P_n - jQ_n \quad = \quad \frac{[V_m V_n \cos(\delta_m - \delta_n) + jV_m V_n \sin(\delta_m - \delta_n) - V_n^2]}{[R_{mn} + jX_{mn}]} \qquad \text{(A8.6)}$$

Now, cross multiply the Eq. (A8.6). Then, separate the real and imaginary terms;

$$P_n R_{mn} + Q_n X_{mn} - V_m V_n \cos(\delta_m - \delta_n) + V_n^2 \quad = 0 \qquad \text{(A8.7)}$$

$$P_n X_{mn} - Q_n R_{mn} - V_m V_n \sin(\delta_m - \delta_n) \quad = 0 \qquad \text{(A8.8)}$$

Re-arrange the above Eq. (A8.7) and Eq. (A8.8) in the form of *sin* and *cosine* terms:

$$\cos(\delta_m - \delta_n) \quad = \quad \frac{(P_n R_{mn} + Q_n X_{mn} + V_n^2)}{V_m V_n} \qquad \text{(A8.9)}$$

$$\sin(\delta_m - \delta_n) = \frac{(P_n X_{mn} - Q_n R_{mn})}{V_m V_n} \qquad \text{(A8.10)}$$

Apply, the square on both sides of the Eqs. (A8.9) and (A8.10):

$$\cos^2(\delta_m - \delta_n) = \frac{(P_n R_{mn} + Q_n X_{mn} + V_n^2)^2}{(V_m V_n)^2} \qquad \text{(A8.11)}$$

$$\sin^2(\delta_m - \delta_n) = \frac{(P_n X_{mn} - Q_n R_{mn})^2}{(V_m V_n)^2} \qquad \text{(A8.12)}$$

Add, Eq. (A8.11) and Eq. (A8.12). Then, get the Eq. (A8.13):

$$V_n^4 - V_n^2\left(V_m^2 - 2P_n R_{mn} - 2Q_n X_{mn}\right) + \left(P_n^2 + Q_n^2\right)\left(R_{mn}^2 + X_{mn}^2\right) = 0 \qquad \text{(A8.13)}$$

Now, *Let*:

$$a = 1 \qquad \text{(A8.14)}$$

$$b = V_m^2 - 2P_n R_{mn} - 2Q_n X_{mn} \qquad \text{(A8.15)}$$

$$c = \left(P_n^2 + Q_n^2\right)\left(R_{mn}^2 + X_{mn}^2\right) \qquad \text{(A8.16)}$$

From Eqs. (A8.13) - (A8.16) we get,

$$a\ V_n^4 - b\ V_n^2 + c = 0 \qquad \text{(A8.17)}$$

In Eq. (A8.17), it is obvious that the condition for load flow convergence in radial distribution systems is:

$$b^2 - 4\ a\ c \geq 0 \qquad \text{(A8.18)}$$

By substituting Eqs. (A8.14) - (A8.16) in Eq. (A8.18), after simplification we get:

$$V_m^4 - 4(P_n X_{mn} - Q_n R_{mn})^2 - 4(P_n R_{mn} + Q_n X_{mn})V_m^2 \geq 0 \qquad \text{(A8.19)}$$

Let,

VSI denotes Voltage Stability Index. Therefore, *VSI* at node *n* can be defined as below Eq. (A8.20):

$$VSI_n = V_m^4 - 4(P_n X_{mn} - Q_n R_{mn})^2 - 4(P_n R_{mn} + Q_n X_{mn})V_m^2 \qquad \text{(A8.20)}$$

ж